

Project 264
Project Record
264/1/SW

A Knowledge Based Approach to Modelling Fast Response Catchments

Department of Civil Engineering
University of Salford

R&D Project Record 264/1/SW



NRA

National Rivers Authority

A Knowledge Based Approach to Modelling Fast Response Catchments

Owen Wedgewood

Research Contractor:
Department of Civil Engineering, University of Salford

National Rivers Authority
Rivers House
Waterside Drive
Aztec West
Bristol
BS12 4UD

R&D Project Record 264/1/SW

National Rivers Authority Information Centre Head Office
Class No
Accession No AKVL

Publisher

National Rivers Authority
Rivers House
Waterside Drive
Aztec West
Bristol BS12 4UD

Tel: 0454 624400 Fax: 0454 624409

© National Rivers Authority 1994

All rights reserved. No part of this document may be produced, stored in a retrieval system or transmitted, in any form or by any means, electronic, mechanical, photocopying, recording or otherwise without the prior permission of the National Rivers Authority.

Dissemination Status

Internal: Restricted Release
External: Restricted Release

Statement of Use

The Project Record from this project will be used as information only. It is a literature review and PhD thesis produced by a Research Student at Salford University. The report will be distributed to Regional Flood Defence Managers.

Research Contractor

This document was produced under R&D Project 264 by:

Water Resources Research Group
Department of Civil Engineering
University of Salford
M5 4WT

Tel: 061 736 5843 Fax: 061 745 7808

NRA Project Leader

The NRA's Project Leader for R&D Project 264 was:

Bob Hatton - South Western Region

Additional Copies

NRA staff wishing to purchase further copies of this document should contact their Regional R&D Coordinator.

R&D Project Record 264/1/SW

TABLE OF CONTENTS

	Page
List of Figures	xiii
List of Tables	xix
List Of Abbreviations	xx
Acknowledgements	xxii
Abstract	xxiii
1. INTRODUCTION	1
1.1 Forward	1
1.2 Searching For 'Knowledge'	2
1.3 Thesis Structure	3
1.3.1 Flooding And Radar	3
1.3.2 Intensity-Duration-Frequency analysis	4
1.3.3 Rainfall Hyetograph Analysis.	5
1.3.4 Knowledge Of Model Parameter Dynamics	6
1.3.5 Case Studies	8
1.4 Conclusions And Recommendations	8
2. RAPID RESPONSE FLOODING	9
2.1 Introduction	9
2.1.1 The Scale Of The Problem	9
2.2 Causes Of Rapid Response Flooding	12
2.2.1 Rainfall	12
2.2.2 Dams	12

2.3 Flash Flood Modifying Factors	14
2.3.1 Storm Variables	14
2.3.2 Catchment Variables	16
2.3.3 The Influence of Mankind	20
2.4 Data Sources	22
2.4.1. Ground Stations	22
2.4.2 Radar	24
2.4.3 Satellites	24
2.4.4 Satellite Deficiencies	25
2.4.5 Meteorological stations	25
2.4.6 Human monitoring	26
2.5 Forecasting Techniques	27
2.5.1 Introduction	27
2.5.2 Meteorological techniques	28
2.5.3 Hydrological techniques	28
2.5.4 Meteorological - hydrological techniques	29
2.6 Warning Time	31
2.7 Non - Real Time Solutions	31
2.8 Conclusions	31
3. WEATHER RADAR	33
3.1 Introduction	33
3.2 Historical Background	33
3.3 United Kingdom Radar Networking	36
3.4 United Kingdom Radar Products	37
3.4.1 Data Resolution	37
3.4.2 FRONTIERS Data	41

3.5 International Network Co-operation	42
3.6 United Kingdom Weather Radar Hardware And Processing	44
3.6.1 Radar Hardware Characteristics	44
3.6.2 At Site Processing	45
3.7 Quantitative Rainfall Estimation using Radar	46
3.7.1 Introduction	46
3.7.2 Measurement Techniques.	46
3.7.3 Radar Reflectivity Theory	47
3.7.4 Radar Scattering	50
3.7.5 Radar Data Display	53
3.8 Radar Siting Problems	55
3.8.1 Permanent Echo	55
3.8.2 Screening	56
3.9 Radar Hardware Problems	57
3.9.1 Radar Wavelength	57
3.9.2 Dynamic Range	58
3.9.3 Beamwidth	59
3.10 Physical Factors affecting radar	60
3.10.1 The Reflectance Relationship	60
3.10.2 Beam Infilling	61
3.10.3 Curvature of the Earth	62
3.10.4 Anomalous Beam Propagation	63
3.10.5 Beam Attenuation	63
3.10.6 Bright-Band	64
3.11 Conclusions	65

4. RETURN PERIOD	66
4.1 Introduction	66
4.2 Historical Background	66
4.2.1 E.G. Bilham	67
4.2.2 The Flood Studies Report	68
4.2.3 FORGE Method	70
4.2.4 Four Parameter Model	72
4.3 Raingauge Problems	73
4.3.1 Instrumentation Errors	73
4.3.2 Influence of Site Location	73
4.3.3 Areal Representativeness	74
4.4 Rainfall-Frequency Analysis Using Radar	75
4.4.1 Introduction	75
4.4.2 Potential Advantages of Using Radar	76
4.5 Statistical Distributions and Parameter Estimation	77
4.5.1 Representation of Extreme Hydrological Data	77
4.5.2 Parameter Estimation	81
4.6 Distributed Intensity-Duration-Frequency Analysis	83
4.6.1 Rainfall Data	83
4.7 Analysis of the Rainfall Archive	84
4.7.1 Data Extraction	84
4.7.2 Data Ranking	86
4.7.3 Parameter Estimation	88
4.8 Real-Time Use	89
4.8.1 Real-Time Return Period Assessment	89
4.8.2 Database Updating	93
4.8.3 Decision Justification	94
4.9 Catchment Transposition	95

4.10	Off-Line Use	95
4.10.1	Post-Event Appraisal	96
4.10.2	Design Use	97
4.11	Discussion	99
4.12	Conclusion	101
5.	RAINFALL ANALYSIS	103
5.1	Introduction	103
5.2	Rainfall Data	105
5.2.1	Data Sources	105
5.2.2	Event Selection	106
5.2.3	Data Pre-Processing	106
5.3	Rainfall Analysis	109
5.3.1	Rainfall Intensity	112
5.3.2	Storm Duration	113
5.3.3	Gross Rainfall Volume	114
5.4	Rainfall Hyetograph Characteristics	114
5.4.1	Standardised Duration	115
5.4.2	Moments Of The Rainfall Distribution	116
5.4.3	Impulse Response Time To Peak	118
5.5	Runoff Analysis	120
5.5.1	Flow Characteristics	120
5.6	Graphical Analysis	121
5.6.1	Linear Relationships	123
5.6.2	Graphical Trends	127
5.6.3	Anomalies	132
5.7	Discussion	133
5.8	Conclusions	135

6. RAINFALL - RUNOFF MODELLING	136
6.1 Introduction	136
6.1.1 Rainfall-Runoff Representation	137
6.2 Transfer Function Models Structure	138
6.2.1 The Systems Approach	138
6.3 Simulation and Forecasting Using TF Models	140
6.3.1 Steady State Gain	141
6.3.2 Transfer Function Model Calibration	141
6.4 Transfer Function Model Adjustment	142
6.4.1 Error Prediction	142
6.4.2 State Updating	143
6.4.3 Parameter Updating	143
6.4.4 Model Gain Updating	144
6.5 The Z-Transform	145
6.5.1 Time Delay	147
6.6 Z-Transform Analysis of the TF Model	150
6.7 Problems with the Hydrological Use of Transfer Functions	152
6.7.1 Impulse Response Instability	153
6.7.2 Impulse Response Fluctuation	154
6.7.3 Negative Impulse Response	155
6.8 The Physically Realisable Transfer Function (PRTF)	156
6.8.1 Identification of a PRTF model	156
6.8.2 Adjustability of PRTF Responses	156
6.8.3 PRTF Impulse Response Adjustment	160
6.9 The MATH System	163
6.9.1 User Environment	164
6.9.2 PRTF Parameter Optimisation	164
6.10 Conclusion	166

7. KNOWLEDGE ACQUISITION	167
7.1 Introduction	167
7.2 Variables Investigated	168
7.3 The Use of Synthetic Data	169
7.4 The Kinematic Wave Model	169
7.4.1 Application to the Rainfall-Runoff Process	171
7.4.2 Finite Difference Approximations	171
7.5 Synthetic Database Creation	174
7.5.1 PRTF Model Identification	176
7.6 Rainfall Characteristics Investigated	177
7.7 Catchment Wide Rainfall	178
7.8 Static Rainfall Location	180
7.8.1 Influence of Rainfall Intensity	183
7.9 Rainfall Movement	187
7.10 Testing the Knowledge	192
7.10.1 Testing Procedure	192
7.11 Knowledge of Rainfall Runoff Percentage	196
7.11.1 Rainfall Losses	196
7.11.2 Problems with Rainfall Scaling	198
7.11.3 Rainfall Separation Reservoir	198
7.12 Antecedent Precipitation Index	201
7.12.1 Calculation of Antecedent Precipitation Index	201
7.12.2 Radar Based API	202
7.13 Conclusion	207

8. KNOWLEDGE BASED FORECASTING	208
8.1 Introduction	208
8.2 Knowledge Representation Software	208
8.2.1 Languages	208
8.2.2 Shells	209
8.3 Expert Systems In Waer Resources	210
8.3.1 Hydrological Expert Systems Applications	213
8.4 Knowledge And Expertise	215
8.4.1 KBS Architecture	216
8.5 The Knowledge Base	216
8.6 Current Status Database	218
8.7 Inference Engine	219
8.7.1 Backward Chaining	219
8.7.2 Forward Chaining	220
8.8 Rainfall Forecast Input	220
8.9 Rainfall Characteristics And Catchment Status	226
8.9.1 Catchment Division	227
8.9.2 Rainfall Areal Percentage Cover	228
8.9.3 Average Rainfall Intensity	228
8.9.4 Forecast and Actual API	229
8.10 Knowledge Base Operation	229
8.10.1 Storm Direction	231
8.10.2 Storm Movement With Flow	233
8.10.3 Storm Movement Against Flow	234
8.10.4 Storm Movement Across the Catchment	235
8.10.5 Catchment Wide Rainfall	235
8.10.6 Rainfall Concentration on the Upper Reach	236
8.10.7 Rainfall Concentration on the Middle Reach	236

8.10.8	Rainfall Concentrated on the Lower Reach	237
8.10.9	Catchment Moisture Status	237
8.11	Decision Justification	238
8.12	System Testing	239
8.12.1	Rainfall - Runoff Events	239
8.12.2	Methodology	240
8.13	Distributed Rainfall - Runoff Models	245
8.13.1	Introduction	245
8.13.2	Distributed And Semi-Distributed Models	245
8.13.3	Distributed Modelling Of Blackford Bridge	246
8.13.4	Comparison With The RAMPART System	249
8.14	Discussion	252
8.15	Conclusion	253
9.	CASE STUDIES	255
9.1	Introduction	255
9.2	Methodology	256
9.2.1	Synoptic Overview	256
9.2.2	Radar Rainfall Movement	257
9.2.3	Rainfall Return Period	257
9.2.4	Flow Forecasts	258
9.3	Event of 24th August 1982	259
9.3.1	Synoptic Conditions	259
9.3.2	Radar Data	260
9.3.3	Event Return Period	260
9.3.4	Hydrograph Forecast	263
9.4	Event of 21st November 1982	265

9.4.1 Synoptic Conditions	265
9.4.2 Radar Data	266
9.4.3 Event Return Period	266
9.4.4 Hydrograph Forecast	269
9.5 Event of 31st October 1986	270
9.5.1 Synoptic Conditions	270
9.5.2 Radar Data	271
9.5.3 Event Return Period	271
9.5.4 Hydrograph Forecast	274
9.6 Conclusions	275
10. CONCLUSIONS AND RECOMMENDATIONS	276
10.1 Introduction	276
10.2 Conclusions and Recommendations	276
10.2.1 Rapid Response Flooding	276
10.2.2 Radar	277
10.2.3 Radar Derived IDF Analysis	277
10.2.4 Rainfall	278
10.2.5 Knowledge Based Flow Forecasting	279
10.3 Summary	283
REFERENCES	284
APPENDICES	
Appendix A	301
Appendix B	309
Appendix C	316

LIST OF FIGURES

- Figure 2.1 *Floods in relation to other natural disasters, world wide.*
- Figure 2.2 *The effect of rainfall location within a drainage basin on flood hydrograph shape.*
- Figure 2.3 *The effect of Identical rainfall amounts, but with different intensities and durations.*
- Figure 2.4 *Runoff Conditions from frozen and unfrozen ground, Spring Creek Pennsylvania.*
- Figure 2.5 *The effect of drainage basin shape on the resultant flood hydrograph.*
- Figure 2.6 *Effect of urban development on flood hydrographs.*
- Figure 3.1 *U.K. Weather Radar Network*
- Figure 3.2 *Radar Ranges of 2 km and 5 km Resolution Data*
- Figure 3.3 *Diagrammatic Representation of the Electromagnetic Spectrum,*
- Figure 3.4 *The Weather Radar System*
- Figure 3.5 *Geometry of a radar pulse volume*
- Figure 3.6 *Cross-section of a radar beam from a parabolic reflector.*
- Figure 3.7 *Radar pulse reflection, scatter and attenuation following interaction with a hydrometer*
- Figure 3.8 *Radar display modes.*
- Figure 3.9 *Beam segmentation and composition for a 1.5 km Constant Altitude Plan Position Indicator (CAPPI)*
- Figure 3.10 *Screening and permanent echo (PE) in a hilly region.*
- Figure 3.11 *Influence of beamwidth on spatial resolution.*
- Figure 3.12 *Beam height against range for a 1° beamwidth radar, 0.5° elevation.*

- Figure 3.13 *A schematic example of the effect of bright-band on a weather radar system.*
- Figure 4.1 *Location of Five Storm Cells Over Southern England, 5th of June, 1983 1150 GMT.*
- Figure 4.2 *Method used to create the required number of storm events to simulate a 20 year radar archive*
- Figure 4.3 *Ranked Rainfall Intensity Matrix For Each Pixel And Duration*
- Figure 4.4 *Blackford Bridge : Storm Return Period Analysis.*
- Figure 4.5 *Blackford Bridge : Storm Return Period Analysis.*
- Figure 4.6 *Decision Justification For The 45 Minute Event Intensity-Return Period Distribution*
- Figure 4.7 *Catchment transposition to allow return period forecasting*
- Figure 4.8 *Blackford Bridge : Rainfall Return Period Examples.*
- Figure 5.1 *The North West Region, Showing Hameldon Hill Radar with 75km Quantitative Range and The Blackford Bridge Subcatchment*
- Figure 5.2 *The Blackford Bridge Subcatchment*
- Figure 5.3 *Radar Rainfall Movement.*
- Figure 5.4 *Diagrammatic Representation of the Method of Base Flow Removal from Net Runoff Volume.*
- Figure 5.5 *Finding Highest Average Rainfall Intensity For a 45 Minute Period*
- Figure 5.6 *First Moment of the Hyetograph Data - Temporal Centre of Gravity.*
- Figure 5.7 *Second Moment of the Data - Variance about the centre of gravity*
- Figure 5.8 *Third Moment of the Hyetograph Data - Temporal Skew*
- Figure 5.9 *Grouped Impulse Responses Compared with Catchment 'Average' Response Model.*
- Figure 5.10 *Effect of Hyetograph Duration on Runoff Time to Peak*

- Figure 5.11 *Effect of Gross Rainfall Volume on Runoff Time to Peak*
- Figure 5.12 *Effect of Gross Rainfall Volume / Hyetograph Centre of Gravity on Runoff Time to Peak*
- Figure 5.13 *Effect of Gross Rainfall Volume on Net Runoff Volume*
- Figure 5.14 *Effect of Rainfall Hyetograph Skew on Event Transfer Function Model Impulse Response*
- Figure 5.15 *Effect of Rainfall Hyetograph Variance on Runoff Time to Peak*
- Figure 5.16 *Effect of Hyetograph Centre of Gravity on Event TF Model Impulse Response*
- Figure 5.17 *Effect of Gross Rainfall Volume on Peak Flow*
- Figure 5.18 *Effect of Hyetograph Centre of Gravity on Runoff Time to Peak*
-
- Figure 6.1 *Representation of a typical Flood Warning System.*
- Figure 6.2 *Representation of a Single Variable Dynamic System*
- Figure 6.3 *Representation of the Z-Transform Process*
- Figure 6.4 *The Region of Convergence $|z| > R$.*
- Figure 6.5 *Typical stable and physically realisable TF model impulse response*
- Figure 6.6 *Unstable TF Model Response.*
- Figure 6.7 *Stable but Oscillatory TF Model Response*
- Figure 6.8 *Negative TF Model Response*
- Figure 6.9 *Varying Impulse Response Shape*
- Figure 6.10 *Varying Impulse Response Volume*
- Figure 6.11 *Varied Impulse Response Timing*
- Figure 6.12 *Incorrect Impulse Response Volume Error*
- Figure 6.13 *Incorrect Impulse Response Shape Error*
- Figure 6.14 *Incorrect Impulse Response Timing Error*
- Figure 6.15 *Effect of The Volumetric Adjustment Factor (α)*
- Figure 6.16 *Effect of The Shape Adjustment Factor (γ)*

- Figure 6.17 *Effect of The Timing Adjustment Factor (τ)*
- Figure 6.18 *Diagramatic Representation of MATH SCREEN*
-
- Figure 7.1 *Finite Difference Box for Numerical Solution by Finite Differences*
- Figure 7.2 *Kinematic Wave Model Simulation Catchment*
- Figure 7.3 *Kinematic Wave Model Impulse Response Function*
- Figure 7.4 *Bell Shaped Rainfall Input to KWM*
- Figure 7.5 *Effect of Varying Rainfall Intensity on Model Impulse Response, With Catchment Wide Rainfall*
- Figure 7.6 *Average Rainfall Intensity - Gamma, Catchment-Wide Rainfall*
- Figure 7.7 *Three Static Rainfall Positions Over Synthetic Catchment*
- Figure 7.8 *Impulse Responses From the Three Catchment Sections*
- Figure 7.9 *Impulse Response Transposition by Time τ*
- Figure 7.10 *Impulse Response Reformation by Shape Parameter*
- Figure 7.11 *Rainfall Intensity - Gamma Relationship, Lower Reach*
- Figure 7.12 *Rainfall Intensity - Tao Relationship, Middle Reach*
- Figure 7.13 *Rainfall Intensity - Gamma Relationship, Middle Reach*
- Figure 7.14 *Rainfall Intensity - Tao Relationship, Upper Reach*
- Figure 7.15 *Rainfall Intensity - Gamma Relationship, Upper Reach*
- Figure 7.16 *Synthetic Storm Movement In Relation To The Catchment*
- Figure 7.17 *Impulse Responses Due To Direction Of Rainfall Movement*
- Figure 7.18 *Rainfall Intensity - Gamma Relationship, Moving 'Up' Catchment*
- Figure 7.19 *Rainfall Intensity - Gamma Relationship, 'Down' Catchment*
- Figure 7.20 *Rainfall Intensity - Tao Relationship, 'Down' Catchment*
- Figure 7.21 *Stationary, Medium Intensity Rainfall, Upper Catchment Reach*
- Figure 7.22 *High Intensity Event Moving With flow*
- Figure 7.23 *Rainfall Loss Methods.*
- Figure 7.24 *RST, No Effective Rainfall Produced.*

- Figure 7.25 *RST, With Effective Rainfall Production.*
- Figure 7.26 *Schematic Diagram Of Loss And ERT Calculation*
- Figure 8.1 *Cross Correlation Forecasting Area, And Blackford Bridge Catchment*
- Figure 8.2 *Cross Correlation Surface Of North West Region*
- Figure 8.3 *'Maximum Point' Grids*
- Figure 8.4 *Parabolic Curve Fitting For P_{max}*
- Figure 8.5 *Storm Forecasting Procedure*
- Figure 8.6 *Catchment Division; Upper, Middle And Lower in Terms Of 2Km Radar Grid*
- Figure 8.7 *The Knowledge Based Parameter Tuning Procedure*
- Figure 8.8 *Direction Of Mainstream Drainage, Blackford Bridge Catchment*
- Figure 8.9 *Storm Movement Acceptance Angle With Regard To Catchment Drainage*
- Figure 8.10 *PRTF Model Impulse Response, Blackford Bridge*
- Figure 8.11 *RAMPART System, Defining Shape, Timing And Rainfall Contribution*
- Figure 8.12 *Grid Based Model Input Characteristics*
- Figure 8.13 *Event Of 18th December, 1982, Observed And Forecast Hydrographs*
- Figure 8.14 *Event Of 2nd November, 1984, Observed And Forecast Hydrographs*
- Figure 8.15 *Event Of 26th August, 1986, Observed And Forecast Hydrographs*
- Figure 8.16 *Event Of 25th October, 1986, Observed And Forecast Hydrographs*
- Figure 8.17 *Event Of 29th December, 1986, Observed And Forecast Hydrographs*
- Figure 9.1 *Five Components of an Information System*
- Figure 9.2 *Synoptic Charts for 24th August, 1982*
- Figure 9.3 *Radar Rainfall Movement*

- Figure 9.4 *Blackford Bridge Storm Return Period Analysis*
- Figure 9.5 *Comparison Forecast and Actual Hydrographs*
- Figure 9.6 *Synoptic Charts for 21st November, 1982*
- Figure 9.7 *Radar Rainfall Movement*
- Figure 9.8 *Blackford Bridge Storm Return Period Analysis*
- Figure 9.9 *Comparison Forecast and Actual Hydrographs*
- Figure 9.10 *Synoptic Charts for 31st October, 1986*
- Figure 9.11 *Radar Rainfall Movement*
- Figure 9.12 *Blackford Bridge Storm Return Period Analysis*
- Figure 9.13 *Comparison Forecast and Actual Hydrographs*

LIST OF TABLES

- Table 3.1 *United Kingdom Weather Radar Products*
- Table 3.2 *Characteristics of the Plessey Type 43-C Radar*
- Table 3.3 *Radar system characteristics and hydrometeorological applications*
- Table 3.4 *Radar beam diameter-range and reflector-wavelength relationship*
- Table 4.1 *Comparison of FSR-II and FORGE return period methods*
- Table 4.2 *Example of Radar Pixel Analysis*
- Table 5.1 *Storm Event Characteristics*
- Table 5.2 *Rainfall - Runoff R^2 Regression Coefficients*
- Table 7.1 *RMSE Values From Tuned And Static PRTF Models*
- Table 7.2 *Optimum Loss and Threshold Values For Storm Events*
- Table 8.1 *RMSE Values From Static, Tuned And Optimum PRTF Models*
- Table 8.2 *RAMPART Timing, Volume and NRA Warning Errors*
- Table 8.1 *GBDM Timing, Volume and NRA Warning Errors*

ABBREVIATIONS

Anaprop	Anomalous Propagation
API	Antecedent Precipitation Index
ARMA	Auto Regressive Moving Average
CAPPI	Constant Altitude Plan Position Indicator
CCF	Cross Corelation Forecast
CEC	Commission of the European Community
COST	Cooperation in Science and Technology
DEC	Digital Electronics Company
DIRN	Direction of Rainfall Movement (Degrees)
DWRP	Dee Weather Radar Project
ERT	Effective Rainfall Threshold
EVI	Extreme Value I - Gumbel Classification
EVII	Extreme Value II - Frechet Classification
EVIII	Extreme Value III - Weibull Classification
FAPI	Forecast Antecedent Precipitation Index
FD	Finite Difference
FE	Finite Element
FORGE	FOcused Rainfall Growth Estimation
FORTTRAN	FORmula TRANslation
FRONTIERS	Forecasting Rain Optimized using New Techniques of Interactively Enhanced Radar and Satellite data
FSR	Flood Studies Report
GANDOLF	Generating Advanced Nowcasts for Development of Operational Landsurface Flood forecasting
GEV	Generalized Extreme Value
ICE	Institute of Civil Engineers
IDF	Intensity Duration Frequency
ISO	Input Storage Output
KBS	Knowledge Based System
KWM	Kinematic Wave Model
LISP	LISt Processing language
MAFF	Ministry for Agriculture Fisheries and Food
MATH	Model Application Tool for Hydrology
METROMEX	METROpolitan Meteorological EXperiment

ML	Maximum Likelihood
MOM	Method of Moments
MORECS	Meteorological Office Rainfall and Evaporation Calculation System
NERC	National Environmental Research Council
NGR	National Grid Reference
NRA	National Rivers Authority
NWRP	North West Radar Project
NWWA	North West Water Authority
PCTCOVA/B/C	Percentage of total catchment rainfall volume on one catchment section
PDP	Primary Data Processor
PPI	Plan Position Indicator
PRTF	Physically Realisable Transfer Function
PWM	Probability Weighted Moments
Radar	RADio Detection And Ranging
RAINARK	RAINfall ARChive system
RAMPART	Real-time Automatic Model PARAmeter Tuning
RBAR	Mean annual maximum rainfall
RFINT	Average rainfall intensity
RLS	Recursive Least Squares
RMSE	Root Mean Square Error
ROC	Region of Convergence
RSAU	Radar Signal Averaging Unit
SMD	Soil Moisture Defecit
SSG	Steady State Gain
SWAT	Severe Weather Action Team
TF	Transfer Function
TFCal	Transfer Function Calculation program
UNIRAS	Graphics Driver for use with VAX
UHF	Ultra High Frequency
VAX	Virtual Architecture Extention
VHF	Very High Frequency
WRRG	Water Resources Research Group

ACKNOWLEDGMENTS

I would like to give my sincerest thanks to Ian D. Cluckie, Professor of Water Resources at the University of Salford, for all his help, encouragement and infectious enthusiasm throughout the research.

I also owe a great debt of gratitude to my friend and mentor Dr. Han Dawei, for his good humour and invaluable help and advice with all aspects of the project.

Mention must go to all the other members of the Water Resources Research Group, too numerous to name, for their contributions and bonhomie.

I am extremely grateful to the Science and Engineering Research Council for their sponsorship of my work, without which none of this would have been possible, and to the National Rivers Authority for all their assistance and supplementary funding.

Thanks go to Ian Pearse for his understanding and patience, Stuart Keeton for his help with the maths and statistics, and to all those who have wished me well.

A special word of appreciation is due to my father, for his long suffering support throughout the period of my education, study and research.

Finally, I must thank Susan for all her help, patience and support.

ABSTRACT

A Knowledge Based Approach to Modelling Fast Response Catchments

This thesis describes research into flood forecasting on rapid response catchments, using knowledge based principles. Extensive use was made of high resolution single site radar data from the radar site at Hameldon Hill in North West England.

Actual storm events and synthetic precipitation data were used in an attempt to identify 'knowledge' of the rainfall - runoff process. Modelling was carried out with the use of transfer functions, and an analysis is presented of the problems in using this type of model in hydrological forecasting. A 'physically realisable' transfer function model is outlined, and storm characteristics were analysed to establish information about model tuning. The knowledge gained was built into a knowledge based system (KBS) to enable real-time optimisation of model parameters.

A rainfall movement forecasting program was used to provide input to the system. Forecasts using the KBS tuned parameters proved better than those from a naive transfer function model in most cases. In order to further improve flow forecasts a simple catchment wetness procedure was developed and included in the system, based on antecedent precipitation index, using radar rainfall input.

A new method of intensity - duration - frequency analysis was developed using distributed radar data at a 2Km by 2Km resolution. This allowed a new application of return periods in real time, in assessing storm severity as it occurs. A catchment transposition procedure was developed allowing subjective catchment placement in front of an approaching event, to assess rainfall 'risk', in terms of catchment history, before the event reaches it.

A knowledge based approach, to work in real time, was found to be successful. The main drawback is the initial procurement of knowledge, or information about thresholds, linkages and relationships.

CHAPTER 1

INTRODUCTION

1.1 Forward

Flooding is one of the most destructive of all natural hazards, and rapid inundation, from flash floods or rapid response catchments is perhaps its most dangerous and unpredictable form. In any flood forecasting system it is essential that the warnings issued be reliable, timely and accurate. Each of these factors is vital to the success of the system, and most importantly, to those it serves, the people at risk of property damage and in some cases loss of life. Thus a system which performs perfectly in fine weather, but fails in a severe storm is useless. Similarly a forecast after the event is of no use in a real-time system, regardless of its accuracy. Finally, forecasting consistently too high will reduce peoples belief in a system which 'cries "Wolf !"', but forecasting too low may fail to warn people at all.

The key problem in forecasting rapid response flooding is the lack of lead time before the event takes place. The short duration between the rain falling on the catchment and the ensuing river rise and flooding gives the flood forecaster a minimum of time to decide what will happen, disseminate warnings and take remedial action. In this thesis assessment of rainfall risk and rapid runoff forecasting are undertaken using a knowledge based approach in an attempt to increase lead time and accuracy of warning of potential events.

In this introduction an overview is presented of the steps taken in the investigation along with a brief outline of following chapters. An underlying aim throughout the research was the use of information and development of techniques that would allow application in a real world, real-time environment. The wide-spread availability of

present day computer systems has facilitated this aim, allowing analyses and procedures to be developed that would have been almost impossible only a few years ago.

1.2 Searching For 'Knowledge'

The forecasting of floods has been of interest to mankind ever since it first began to utilize river flood plains. Increasingly, forecasting techniques have looked to complex mathematics and distributed catchment modelling in an attempt to improve forecast accuracy. In a different direction this thesis attempts to use knowledge of experienced forecasters and catchment rainfall history in order to provide improvements in forecasting accuracy and information about event risk.

Conventionally, the construction of a knowledge based or 'expert' system begins with the identification of the rules, relations and procedures carried out by the human expert, which are to be included in the system. This procedure, known technically as 'knowledge engineering', was undertaken with highly experienced flood warning officers in both the South West and North West regions of the National Rivers Authority (NRA). Unfortunately, it soon became clear that, due to the real-time nature, and large number of catchments forecast, the type of information hoped for did not exist in a detailed enough form to be built into such a knowledge based representation. The most useful aspect to emerge from the knowledge engineering process, however, was the identification of those areas perceived by the experts as being most influential in the severity of flooding in their region.

A further point which became clear was that although the radar coverage of both the South West and North West regions is displayed in the respective flood rooms, its use is mainly for visual storm identification only. In an attempt to better utilize the radar coverage from a knowledge perspective, a need was identified to allow storm 'risk'

analysis during and before a storm event arrives at a region or catchment in danger of flooding. Although no concrete rules were identified, these experiences of flood warning production and potential improvement have been used as guide lines in the investigation described here.

1.3 Thesis Structure

The thesis is divided in to five parts, covering different aspects of the rapid response problem and the research undertaken.

1.3.1 Flooding And Radar

Chapter 2 provides a definition and insight into the severity of the rapid response flooding problem. Examples are used to show the devastation which can result from large, rapidly occurring flooding. The work in this thesis concentrates on river flooding caused by rainfall, and an outline is presented of the other potential causes of fast response flooding to put this in perspective.

Also in this chapter an overview is given of the factors which modify rapid response flooding, divided into storm and catchment variables. Examples are given of the effect of rainfall direction, location and temporal distribution, as well as catchment moisture status, temperature, area, shape, topography and orientation. The influence of mankind is addressed in increasing runoff peakedness, and potentially rainfall, through the action of urbanisation.

A short review is presented of the potential sources available in the real-time forecasting of rapid response floods, radar data being discussed in more detail in Chapter 3. The techniques used in fast response forecasting are outlined, divided into

meteorological, hydrological and hydrometeorological methods. Following from this, the importance of warning timeliness is emphasised, and consideration is given to the alternative, non real-time solutions to flooding problems, such as river confinement, flood plain zoning and catchment management.

All of the research presented here is based around real-time remotely sensed precipitation data from radar. Accordingly, Chapter 3 provides an introduction to the advantages and limitations in the observation and estimation of rainfall using weather radar. The relatively short history of this remote sensing technique is explored to give an insight into the development of the United Kingdom weather radar network. In the present investigation, single site radar data was used, and the alternative remotely sensed products are reviewed with reference to spatial and temporal resolution, in the UK and internationally.

In order to give an appreciation of the operation of the radar system, the processing and assumptions behind the quantitative estimation of rainfall are outlined. Radar reflectivity theory is described, together with the display techniques used in visualising the data. Whenever information is inferred remotely about a process such as rainfall there is potential for error. These error sources are described, together with the methods used to lessen their impact. This final section provides a feel for the limitations of the data, and emphasises the fact that it should not be regarded as a perfect data source, if such exists anywhere.

1.3.2 Intensity-Duration-Frequency analysis

Return periods have long been used to assess the severity of a rainfall event of a given recurrence interval. In Chapter 4 the background to this type of analysis is outlined, followed by a critical review of the techniques used to calculate return periods. Although many problems may be identified with the procedures used to assess event

rarity, the most fundamental is the conventional basis of these assessments on point rainfall estimates from raingauges. This type of precipitation data necessitates the use of areal rainfall averaging. It also leads to the application of IDF analyses outside the area for which they were calculated, simply because of the low areal coverage of raingauge sites.

In response to these problems a new technique of rainfall frequency analysis is presented, using remotely sensed precipitation data. Parameter estimation is carried out using Probability Weighted Moments (PWM) to fit General Extreme Value (GEV) I, II and III distributions to the data record. The technique provides new applications of return periods in assessing the recurrence interval of rainfall as it takes place, using radar inputs updated every five minutes. This real-time use allows the conversion of radar 'data' into 'information' using knowledge of catchment rainfall history.

A method of storm return period forecasting is put forward, using catchment transposition, again based on knowledge past rainfall over the catchment area of interest. The radar IDF procedure allows simplified 'conventional', offline use of return period analysis and may be easily integrated into the present radar processing system. Here it may update and classify knowledge of the catchment rainfall regime automatically whilst being available for real time use.

1.3.3 Rainfall Hyetograph Analysis

Chapter 5 describes research carried out to gain knowledge of the rainfall-runoff process. The analysis concentrates on the rainfall input experienced by the catchment, using detailed investigation of the catchment rainfall hyetograph characteristics, in an attempt to relate them to subsequent catchment outflow. A short description is presented of the study area chosen for the investigation, together with the rainfall and flow data used. The catchment rainfall input through time is analysed as a

distribution. Hyetograph centre of gravity, variance and skew are calculated along with rainfall volume and the maximum average rainfall intensities sustained for different durations. These hyetograph characteristics are related to event transfer function model impulse responses, peak flow, time to peak, flow volume and event percentage runoff. The events used in the analysis are presented in Appendix A, and key sections of the analysis routine in Appendix B.

The analysis procedure reveals several good relationships between the rainfall and flow characteristics investigated. Whilst these relationships may be used to provide an approximate guide to several runoff characteristics, their strength is not great enough to allow forecasting with a sufficient degree of certainty to warrant their inclusion in a knowledge based system.

1.3.4 Knowledge Of Model Parameter Dynamics

This section concentrates on gaining knowledge of model parameter dynamics in order to allow real-time forecast model tuning with reference to storm and catchment status. Chapter 6 outlines the advantages of modelling the rainfall-runoff process, and gives a detailed analysis of the Transfer Function (TF) model. Following from the inherent problems with the use of the hydrological utilization of the TF model, a new Physically Realisable Transfer Function (PRTF) model is described, as developed by Han, 1991. The potential for use of this model is outlined, and the adjustment techniques built in to it are explained. Finally, an overview is presented of the steps for model identification and tuning as used through section four of the thesis.

In Chapter 7 a detailed description is given of the acquisition of knowledge about the PRTF model parameter dynamics, carried out using machine induction. A kinematic wave model (KWM) is used to create flow sequences from synthetic rainfall events.

This allows control over the rainfall characteristics investigated, and the generation and analysis of a much larger number of events than would be possible using 'real' data. Rainfall input to the system is varied in extent, position over the catchment, direction of movement and intensity. A PRTF model is fitted to each rainfall-runoff event manually, and the changes in parameter magnitude with rainfall dynamics are expressed as relationships and threshold values.

The chapter also outlines a new technique of catchment status evaluation, using radar input information based on a rainfall reservoir-antecedent precipitation index (API) concept. Catchment loss rates are calculated using 'actual' storm events, and an effective rainfall threshold (ERT) is defined, where ERT is the catchment soil moisture status which leads to 'effective' rainfall generation.

The knowledge of model parameter dynamics and catchment losses and soil moisture threshold are implemented in a *Real-time Automatic Model Parameter Tuning* (RAMPART) knowledge based system in Chapter 8. The system is written in a production rule format, in VAX FORTRAN. The current status database receives inputs of forecast rainfall characteristics from a cross correlation forecasting routine for every five minute radar frame. A forward chaining inference engine is used to search through, identify and apply the relevant relationships in the knowledge base, in order to tune the model adjustment parameters. Catchment status is used in assessing the contribution of rainfall to flow with regard to knowledge of the catchment effective rainfall threshold.

The system is tested using 23 storm events and gives improvements in forecast accuracy over a static PRTF model in 14 cases. The KBS suffers from some problems, as outlined in the text. These are most likely related to the synthetic methods used to define the knowledge and inadequacies in the rainfall forecasting routine used as input to the system. However, the system is very much a first attempt at model parameter estimation using knowledge based techniques.

Improvements may lie in the refinement of the knowledge within the data base at present, or the investigation of new rainfall and catchment variables.

1.3.5 Case Studies

Chapter 9 presents an illustration of the knowledge based techniques evolved in three case studies. Storm movement is shown with the use of radar data, to demonstrate rainfall tracking over the catchment area. The synoptic charts for the period are provided to give a wider overview of each event. The radar intensity-duration-frequency system is used to provide an indication of the risk from the storms, using knowledge of catchment rainfall history. The RAMPART system is employed to set the model forecasting parameters. Comparison hydrographs are presented of actual and forecast flow, using static and adaptive physically realisable transfer function models.

1.4 Conclusions And Recommendations

Chapter 10 presents the conclusions and main points of the investigation. Recommendations are also made for the possible implementation of the work described here, and areas where the author believes further research may be carried out.

CHAPTER 2

RAPID RESPONSE FLOODING

2.1 Introduction

The 1990's have been designated as the international decade for the mitigation of natural hazards. Flooding, from all its different sources, is by far the most destructive of these hazards, surpassed in its destructiveness only by man's warfare. The work presented in this thesis is concerned with the forecasting of flooding on fast response catchments. To put this into context this chapter provides an outline of the various causes of rapid response and flash flooding. For the purposes of this investigation a break point of six hours is used to identify fast response catchments. This is similar to the duration identified by Hall (1981) to separate flash from 'normal' flooding.

2.1.1 The Scale Of The Problem

In describing the scale and severity of the flood problem internationally, it should be remembered that flooding is a natural phenomenon, and only becomes a hazard when mankind chooses to utilise the river flood plain, be it for communicational, residential or commercial purposes. The United States Disaster Assistance Agency put flooding in perspective with other major types of natural problem, as shown in figure 2.1. In England and Wales only 0.6% of the population live on river flood plains, but Haggett (1988) has estimated that up to 9500 properties are at risk from direct flooding of non tidal rivers in London, and damage to residential property alone would cost up to £17M for the 50 year flood.

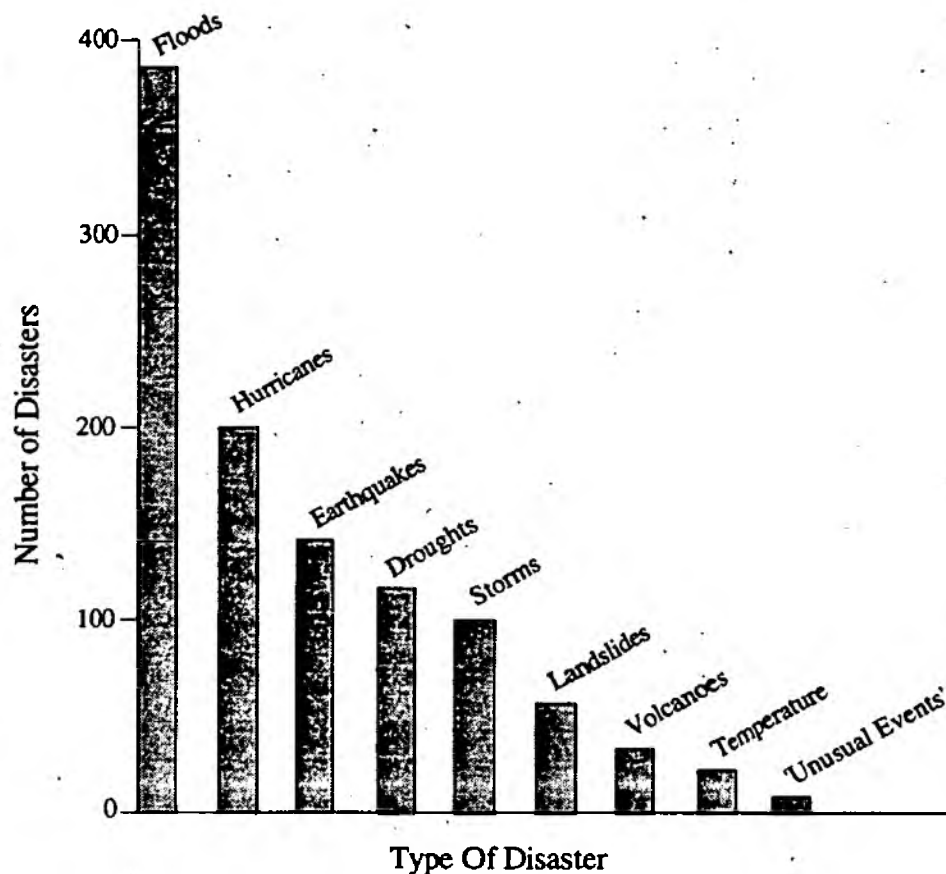


Figure 2.1 *Floods In Relation To Other Natural Disasters, World Wide.*

In other developed countries rapid response flooding is now a major problem, especially where new settlements have been created without knowledge or consideration of the inherent flood potential (Hall, 1981). In the United States of America 5-8% of the population inhabit river flood plains (Collier, 1989), and the seriousness of the problem prompted Willeke (1979) to state that "Flash floods have replaced major river floods as killers of people. Property damage from flash floods can be and has been very high because of dense, expensive development within the flood plain and because of the short time available for human response." Zevin (1986) goes further, quoting statistics as showing that 80-90% of the 200 annual flood related deaths in the USA are caused by rapid response flooding, and property damage is running at over US \$ 1 Billion per year.

Between 1971 and 1978, Mogil *et al.* (1978) noted the occurrence of over 1000 significant flash floods in the USA, going on to state: "Since 1945 more than 3000 countries have received Red Cross assistance following floods or flash floods. Although many of these did not make national headlines, they have had a devastating effect on scores of communities. But it is the catastrophic flash floods, such as Black Hills in 1972, (NOAA, 1972), (237 deaths) and the Big Thompson Canyon in 1976 (NOAA, 1976), (139 deaths), that highlight the vulnerability of the American people to these events."

Hall (1981) concludes that in the USA and Australia the annual death rate due to rapid flooding is roughly 0.0001% of the population, and countries with similar life styles, states of development, geography and climate would be expected to face a problem of similar magnitude. Developing countries, with smaller scale or non-existent flood forecasting and/or meteorological services, communications and local agencies, may well be faced with an annual death rate from rapid response floods of several times that of developed regions.

Perhaps the most well known, and catastrophic rapid flood to take place in Great Britain was the event of August 15th 1952, at Lynmouth and Lynton, Devon. In one terrible evening 34 people were killed or went missing, and 93 houses, 28 bridges and 132 vehicles were destroyed (Delderfield, 1953). The damage resulted from a sudden cloud burst (up to 125 mm/hr) after a prolonged period of heavy rain, causing rapid river level rise. More recently, on May 19th 1989, an extremely severe event near Halifax, West Yorkshire, caused 'sheets of water' to cover the hillsides, and trees and footbridges to be washed away (Acreman, 1989).

Elsewhere in Europe the devastating effect of fast flooding has been demonstrated as recently as September 22nd, 1992. A huge rainfall event caused a flood wave in the French Department de Vaucluse, resulting in damage to 63 communities along the River Ouvez. The death toll is still not known (Spring 1993), due to the high number

of people as yet unaccounted for. In the village of Vaison (population 5600) alone, however, 37 victims have been found and a further five are still missing.

2.2 Causes Of Rapid Response Flooding

2.2.1 Rainfall

In tropical and semi-tropical areas rapid flooding is often associated with intense rainfall which occurs in the monsoon season. Mountainous areas are particularly flood prone as the effect of orographic uplift may trigger intense rainfall. In non-tropical regions flash floods are frequently associated with violent, convectional storms which tend to be of short duration, often measured in minutes rather than hours. Convectional storms are also normally of small areal extent, and in the United Kingdom such extreme events are not restricted to any one accumulation period (Collier, 1989). One of the most dramatic examples of a convectional fast response flood in England resulted from the cloud bursts of June 18th, 1930 which fell on part of Stainmore Forest in the Pennines. A series of intense convection cells yielded 60 mm of rainfall in an hour at one raingauge located about a kilometre from the storm centre and resulted in a series of short-lived flood peaks which swept away bridges and field walls (Hudleston, 1933). The speed of onset, and great spatial and temporal variability of such storms makes their forecasting very difficult.

2.2.2 Dams

i) Artificial Dams

The construction and use of artificial dams is vital in the management of water resources for water supply, power generation, flood mitigation and the regulation of river flow. Retaining such enormous quantities of water creates a considerable

potential for destruction in the event of dam disasters, and, as Ward (1978) points out, when dam disasters do occur the accompanying violent flooding normally causes considerable damage and loss of life.

One of the major problems with rapid flooding resulting from dam failure is that the response time available is much shorter than with precipitation floods. For settlements close to the dam the period between failure and inundation may be measured in minutes and the "wall of water" created can cause one of the most dramatic and disastrous flash floods possible. A report by the US Army (1975) gives an inventory of Americas approximately 50,000 dams with a height greater than 7.5 metres. The report classified some 20,000 of these dams as being "so located that failure of the dam would result in loss of human life and appreciable property damage". In the United Kingdom, due to the location of population centres and the relatively small size of the country, the majority of the 2500 or so major dams would be likely to cause severe devastation in the event of failure.

The last great dam disaster in the British Isles occurred on the 11th of March 1864. The embankment of the Dale Dyke reservoir, at Bradfield near Sheffield, slipped following saturation, with the loss of 245 lives and almost 800 houses destroyed (Brooks and Glasspoole, 1928). Internationally more severe dam floods have led to even greater loss of life and property. On December 2nd 1959, the left foundation of the 66.5 m Malpasset dam near Fréjus in southern France gave way, probably due to a geological weakness, releasing 25 million m³ of water. The flood wave swept along the valley of the River Reyran, partly destroying the town of Fréjus and killing 421 people. One of the most disastrous dam floods of recent times was not due to dam wall failure, but overtopping. On October 9th 1963, at the Vaiont dam in Italy, about 115 million m³ of rock from a landslide generated a flood wave some 270 m above the still water level. The resulting 70 m wave of water swept down stream destroying

everything in its path and causing the loss of 3000 lives (Biswas and Chatterjee, 1971; Davidson and McCartney, 1975).

ii) Natural Dams

Natural damming frequently occurs on some rivers as ice breaks up in the early stages of spring melt, and piles up to cause ice-jams. Once a jam develops the water level behind it rises, often quite rapidly, until eventually the obstruction gives way (Ward, 1978). The break releases great volumes of water and debris into the downstream channel, which may lead to very rapid flooding. Hoyt and Langbein (1955) describe the flooding of the Missouri River in the Dakotas in the spring of 1952. Warm weather upstream caused ice in the tributaries to break up and move down river, jamming against the firmly frozen Missouri. Finally the ice-jam broke up, and at Bismarck, North Dakota, the discharge rose from 2120 cumecs to a peak of 14,200 cumecs in a few hours.

2.3 Flood Modifying Factors

2.3.1 Storm Variables

i) Direction

In precipitation events, the intensity and duration of rainfall are not the only factors influencing the likelihood of flash flooding. Wilson *et al.* (1979) found that the spatial distribution of rainfall has a marked effect on the behaviour of the runoff hydrograph. If a weather system producing significant rainfall moves in the direction of stormflow, the peak may be enhanced (Bedient and Springer 1979). Such conditions allow peak flows from sub-basins higher up the main basin to coincide with peak flows from lower sub-basins, so producing higher flows. This prompted Collier (1989) to say that in such situations knowledge of the distribution of rainfall in both time and space is of great importance.

ii) Location

The location of a storm event over the catchment can be of great importance in determining the nature of any subsequent flooding. When the storm takes place at the furthest upper reaches of the basin, there is the possibility of attenuation of the runoff wave as it passes along the catchment, lengthening the time to peak and reducing peak discharge. Figure 2.2 illustrates the point that the steepest flood hydrograph will be caused by the storm located closest to the basin outlet.

iii) Temporal distribution

The distribution of rainfall in time greatly influences the likelihood and type of flood occurrence. Low intensity rain, falling over a period of hours or days, may result in only a low flood peak with a long time base. The same total amount of precipitation falling in a few minutes is likely to produce very high flood peaks with a much shorter rise time, as illustrated in figure 2.3.

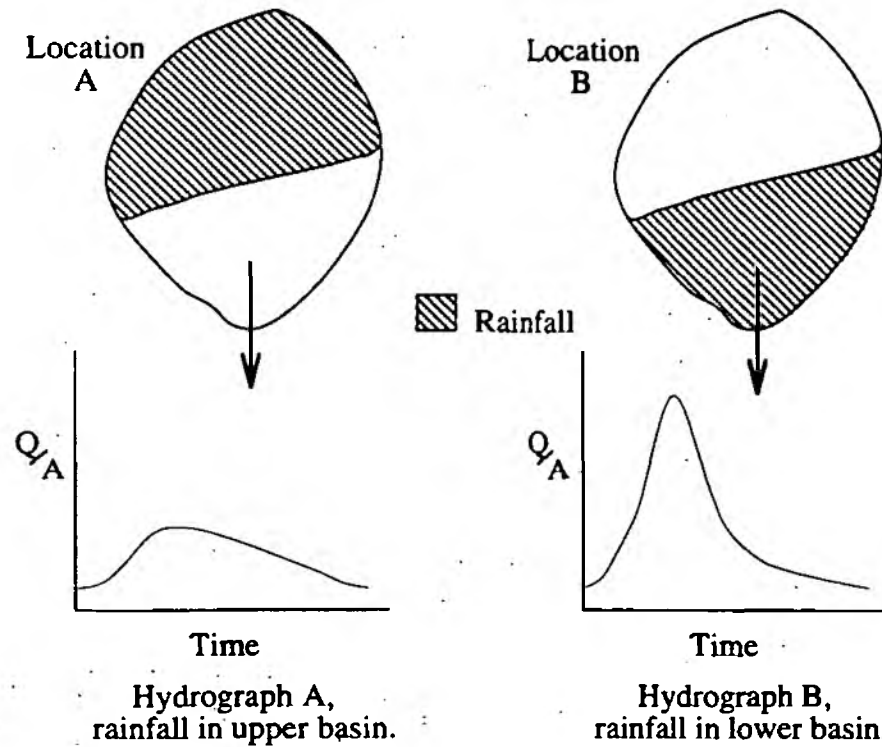


Figure 2.2 *Effect Of Rainfall Location In A Drainage Basin On Flood Hydrograph Shape (After De Wiest, 1965), where Q is Discharge and A is Area.*

2.3.2 Catchment Variables

Once an extreme rainfall event occurs the characteristics of the catchment may modify the severity of any ensuing flood. Depending upon the antecedent conditions, topography and land use, the impact of the storm may be reduced or intensified to a greater or lesser extent.

i) Antecedent moisture

One of the most important and variable of the possible influences on flash flooding is the antecedent wetness of the catchment. If precipitation is so intense that Hortonian overland flow takes place (ie. runoff due to infiltration excess, although the soil is not saturated (Horton, 1933)) then antecedent wetness will have little influence on the speed and magnitude of the flood. However this type of runoff is usually confined to areas of low infiltration capacity, bare rock, or compaction, or where very high rainfall intensities occur, particularly when these are maintained over several hours, such as the humid tropics (Ward, 1978).

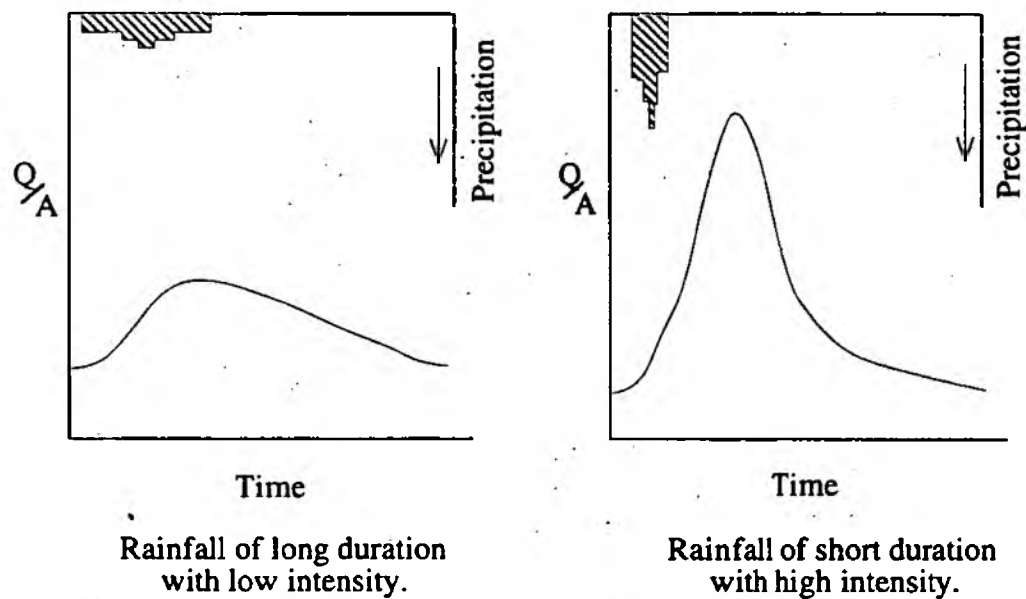


Figure 2.3 *The Effect Of Identical Rainfall Amounts, But With Different Intensities And Durations, After Ward (1978).*

Overland flow occurs more often when saturation causes the ground to act as an impermeable surface, and any precipitation to be turned at once into runoff (Hewlett, 1961). The moisture status of the catchment at the start of a rainfall event is therefore vital in determining whether rapid flooding will take place. Indeed, Istok and Boersma (1986) suggest that in climates characterised by low intensity rainfall, antecedent rainfall is more important in controlling the occurrence and amount of river runoff than is rainfall magnitude or intensity. Spatial variation of rainfall also affects the distribution of soil moisture over a river basin. In a study of small, lowland basins in south west England, Wheeler *et al.* (1982), found that basin response to rainfall varied significantly between storm events, the shape of the hydrograph being strongly influenced by the antecedent soil moisture deficit.

ii) Temperature

A further influence on the severity of flooding may be found in the antecedent temperature of the catchment. If some or all of the catchment area is frozen when heavy rainfall occurs it is more likely to act as an impermeable surface, turning precipitation directly to overland flow. This in turn will intensify the speed and volume of a flood as demonstrated in figure 2.4.

If a snow pack is present on the ground surface the situation becomes more complex. When rain falls on the snow it may be stored temporarily, or may pass straight through with melt water adding to the flood runoff generated. Investigations in Scotland showed that a blanket of snow upto 30cm thick may completely absorb a heavy rainfall event and store it for several hours before collapsing to cause a flood peak some 35% greater than would otherwise have been expected (Wolf, 1952). Thus even though the rainfall alone may not lead to flooding, when combined with melt water flash flooding may take place.

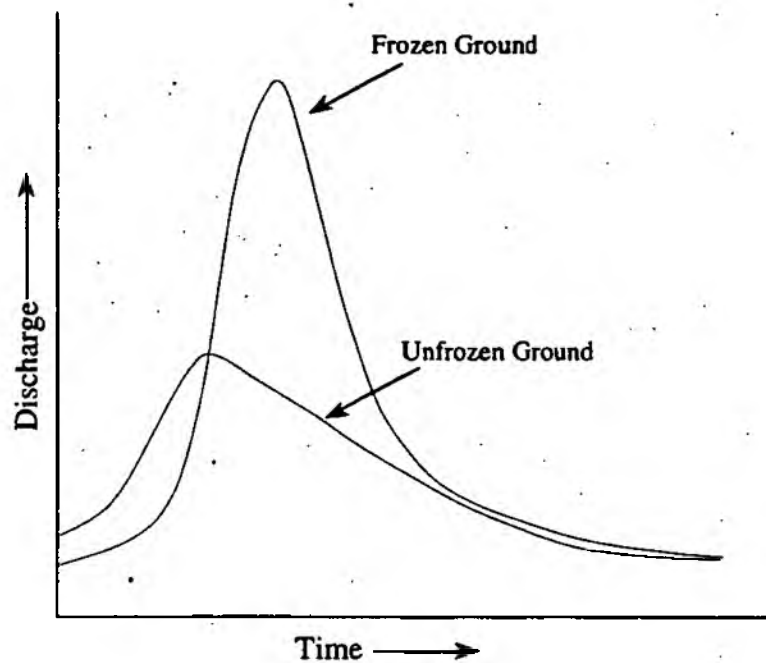


Figure 2.4 *Runoff Conditions From Frozen And Unfrozen Ground, Spring Creek Pennsylvania. (After White and Reich, 1970).*

iii) Catchment Area

The area of a catchment is of significant in two main ways. Firstly, it affects the amount of precipitation that the basin is likely to receive and thus the amount of water present in any subsequent flood event. Secondly, it affects the time of concentration, (t_c), of the basin, the time required for rain falling at the farthest point of the catchment to flow to the measuring point of the river. The smaller the catchment, all other things being equal, the lower the t_c is likely to be. The time of concentration has implications for the speed of arrival and severity of a flood wave at the outlet of the catchment.

iv) Basin Shape

The physical shape of a drainage basin may greatly influence its flood potential. Figure 2.5 shows two theoretical extremes, and the flood hydrographs associated with them. A rainfall event of similar intensity and duration falling on both catchments

would lead to a shorter, 'peakier' hydrograph at the outflow from basin "b" as the route the water takes is shorter. Also the drainage pattern of rivers and streams within a catchment influences the speed with which water arrives at the basin outlet. Drainage patterns resulting in the coalescence in the lower drainage basin of the flood flows from a number of tributaries, (dendritic), are associated with sharp high-magnitude flood peaks at the basin outlet (as in figure 2.5 (B)). Those patterns which allow the evacuation of flood flows from the downstream tributaries before the flows from upstream tributaries (trellised) result in a more muted flood response.

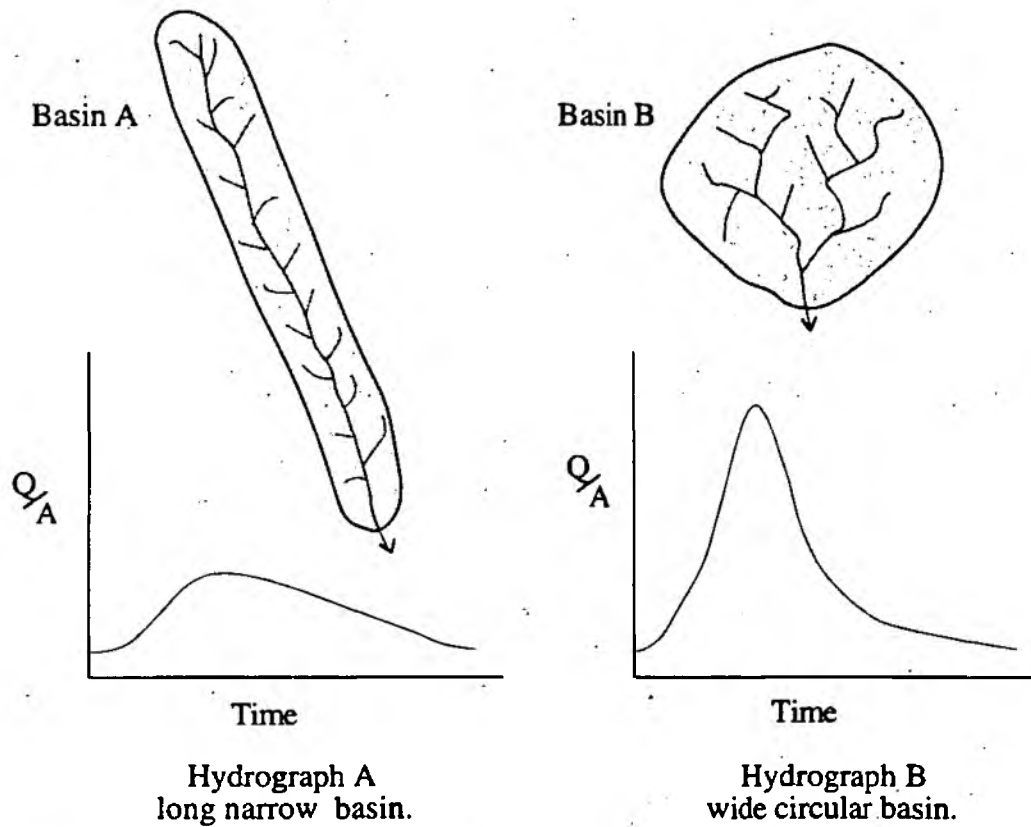


Figure 2.5 *The Effect Of Drainage Basin Shape On The Resultant Flood Hydrograph*
(After Ward, 1978).

v) Topography

Catchment topography influences not only the likelihood of rainfall, due to orographic enhancement, but also the speed at which a flash flood wave is passed along the river basin. Steep sided hills and a steep valley floor cause river flow, and overland flow, to occur at higher velocities than in areas of lower relief. The greater speed of flow also has the effect of reducing the period that runoff water is in contact with the ground, allowing less time for infiltration to occur.

vi) Orientation

Another catchment characteristic which may affect flood potential is the orientation of the drainage basin. A catchment facing into the prevailing wind is more likely to receive higher amounts of rainfall than one shielded from it. This results in the catchment having a higher antecedent moisture status for more of the time. When combined with the higher rainfall rates this leads to a greater chance of fast response flooding taking place in such areas.

2.3.3 The Influence of Mankind

As mentioned in section 2.1.2, flooding of any kind would not be a hazard if man did not occupy or utilise its pathways. In some ways, however, human activities serve as more positive agents to increase the likelihood or severity of the flash flood problem. Dam construction (see section 2.2.2) brings with it the risk of failure or overtopping. In areas without man made storage structures, the effect of land use change and development is frequently to increase the rate of runoff, and without careful planning areas prone to rapid response flooding may be created. In urban areas the flash flood potential is usually increased due to the high percentage of impervious area (see figure 2.6). Not only is the volume of runoff increased but the problem is compounded by the higher speed of runoff, and the peaks of tributary flood waves may even be combined in some instances (Hall, 1981).

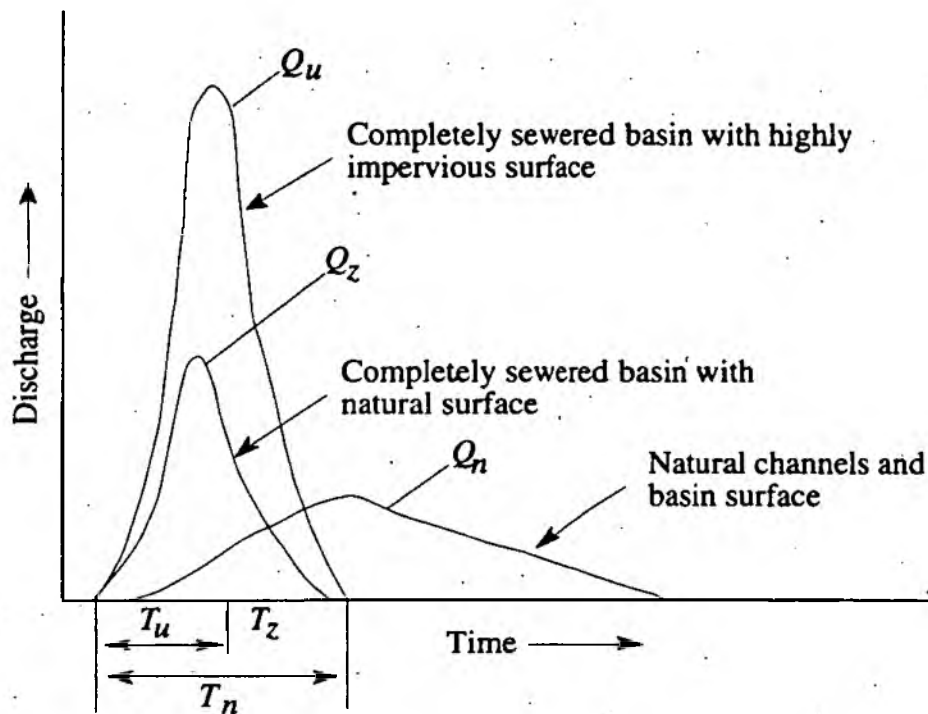


Figure 2.6 *Effect Of Urban Development On Flood Hydrographs (after Fox, 1979).*
Peak Discharges (Q) Are Higher And Occur Sooner After Runoff Starts (T).

Martens (1968) and Hollis (1975) have suggested that the effect of urbanisation is greatest on small floods, and as the size of the flood and its recurrence interval increase, so the effect of urbanisation diminishes. An explanation for this is that during a severe and prolonged storm event, a non-urbanized catchment may become so saturated and its channel network so extended that it begins to behave hydrologically as if it were an impervious catchment with a dense surface-water network (Goudie, 1986). Under these conditions, a rural catchment produces floods of a type and size similar to those of its urban counterpart.

Cities not only serve to increase the speed and volume of runoff, through their large impermeable areas, but they may actually serve to increase rainfall simply by their presence. The "heat island" effect has been investigated by several authors. Oak

(1982) quoted evidence that temperatures within an urban area can be several degrees higher than outside the city. The METROMEX project (Metropolitan Meteorological Experiment) was set up in the United States to study the effect of cities on rainfall distribution. Changnon (1981) summarises the project, and describes findings of a 30-40% increase in rainfall at La Porte, Indiana, situated down wind of the Chicago-Gary area. This increase in precipitation was explained in terms of the growth of urban development during the period 1925-1970. Whilst not all events are affected, it is suggested that in 15-20% of storms premature release of water and anomalous rainfall occur due to reduction in storm updraught buoyancy and the capacity to carry previously condensed water (Huff and Changnon, 1980).

Human modification of landuse need not be as severe as urbanisation in order to have an important effect on the runoff and flood producing potential of a given area. As long ago as the late eighteenth and early nineteenth century it was realised that torrents in the French and Austrian Alps were brought about by deforestation (Goudie, 1986). Studies in two small Australian Alps (Wallaces Creek-41 km² and Yarrango Billy River-224 km²) which were burned over, showed that rain storms, which would have been expected to give rise to flows of 60-80 m³ s⁻¹ from previous records, produced a peak of 370 m³ s⁻¹ (a five- or six-fold increase), time to peak also being significantly reduced.

2.4 Data Sources

2.4.1. Ground Stations

Rain and river gauges, in many different forms, have long been used as a primary input to flood forecasting systems. The basic requirements are the same as for conventional schemes, and although the same equipment is used it is often automated

for rapid response forecasting. Because of the short time interval (less than 6 hours) between the observed rainfall or upstream river height and the flood at the point of interest, the time delays inherent in manual observation, recording and reporting systems are usually too great for useful forecasts to be made in time (Hall, 1981).

Automatic data collection systems are usually based on digital output from the sensor. The sensing instrument may then report by telephone or radio at preset intervals, or may be interrogated by a central data collection site as and when the information is required. Raingauges are mainly the 'tipping bucket' type, which give an incremental pulse count. River height sensors may be shaft rotation or float type.

Both rain and river gauges have several problems when used in rapid flood forecasting. Apart from the problems of placement and interference, outlined in Chapter 4, a rain gauge physically covers only a very small area. Wilson *et al.* (1979) point out that even when the total depth and even temporal character of precipitation are recorded by a rain gauge network there could still be serious errors in total volume, peak and time to peak of the expected hydrograph when the spatial pattern of rainfall were not properly represented in the input data. "Such errors can be large for frontal rainfall, but were found to be even greater for convective storms." Collier (1989) concludes that "No economic network of manual observations or even automatic weather stations, can hope to observe, in real-time, precipitation distributions and their variations sufficiently reliably for operational weather forecasting." Considering storm runoff gauges, Eccles (1978) states that they are often the most accurate flood predictors, but yield the smallest warning time and require that the telephone line network be undamaged by the storm. Hall (1981) notes that in a flood situation telephone and telex lines are prone to failure.

2.4.2 Radar

Radar has several virtues when used in the estimation of precipitation. It allows the observation and measurement of rainfall, from a single site, virtually instantaneously over the region covered by the radar. A review of the advantages and limitations of radar rainfall estimation is presented in detail in Chapter 3.

2.4.3 Satellites

Satellites may be used to provide data for estimation of rainfall occurrence. Satellite imagery shows the life of the cumulus cloud and the strength of the updraught present as a function of the height or thickness of the cloud (Hall, 1981). The stronger the updraught, the higher is the input of moisture to the cloud system, leading to taller, larger clouds with generally increasing rainfall intensities. Browning (1987) states that satellite imagery can be very useful in identifying and categorising deep convective phenomena, including topographically forced patterns of convection.

Browning and Collier (1982) describe the geostationary satellite METEOSAT as providing sufficiently frequent cloud pictures for nowcasting. Cloud images are available in the visible (daytime only) and Infra Red with information also on water vapour. Put simply, the Infra Red radiance is a measure of cloud top height, and the visible brightness an indication of cloud thickness. In the hours of darkness the Infra Red imagery can be used alone to indicate areas of precipitation, but subjective analysis is needed to identify and reject of non-precipitating areas, using conceptual models of precipitation systems. During the day a computer derived combination of visible and Infra Red imagery can be used. Although only crude, this gives a more reliable indication of the probability of precipitation than either channel alone, especially when calibrated using radar data covering part of the same area (Lovejoy and Austin, 1979).

2.4.4 Satellite Deficiencies

The use of satellite imagery is again not without its problems. There may be little if any instantaneous relationship between cloud brightness and or cloud top temperatures and rainfall. Dry convective clouds without rainfall may well be as bright and or cold as highly rain productive convective systems. The sensing of precipitation using satellites suffers even more than radar from the potential problems of lateral drift due to wind at the ground surface. Precipitation may actually reach the ground at significant distances away from the position indicated by the satellite imagery, as all sensing is above the clouds.

A further problem with the use of satellite images is that, as with radar, surface rainfall intensity is not measured directly, but must be inferred by a combination of objective and subjective analyses. A further complication is the availability of information in the visible waveband only in the hours of daylight, and the subjectivity and reduction in reliability when using Infra Red and water vapour data at night.

On a purely practical level, the cost of development, construction and installation of a satellite in space can be prohibitive. This process is only really viable when the satellite is to serve several purposes once in orbit. Also, if a fault should occur when the satellite is in space, repairs to the sensors or transmission equipment are, to say the least, difficult to carry out.

2.4.5 Meteorological stations

Meteorological stations taking measurements of surface meteorological data such as air temperature, pressure and dew point temperatures (Georgeokakos, 1986) exist in certain areas. The information that these statistics reveal may be used in Hydrometeorological models. This data allows a more 'white box' approach, with the

possibility of predicting rainfall volume and impact based on the laws of physics. The main drawbacks to the use of these stations in a concerted, widespread rapid response flood forecasting system is their low number and high cost both in terms of initial construction, manning and maintenance.

2.4.6 Human monitoring

In some areas of the the USA Severe Weather Action Teams (SWAT's) have been set up. The teams consist of volunteer weather spotters trained to go out in severe weather and report on the occurrence of tornados, funnels, damaging winds, hail, heavy rainfall, severe lightning and rapid rises in creaks or rivers (Lyons and Henz, 1978). Once the SWAT observers become aware of any weather problems they report them to a central base where information is collated. In the United Kingdom water officials are also sent in to the field to take measurements and report on the extent of flooding and damage.

Schemes such as that in America provide several encouraging features. Such features combine involvement of the community in the forecasting process, training of the public to recognise potentially hazardous situations, flexibility and relatively low cost. However, there are many problems with the use of such teams. The presence of people in the field is reliant upon the good will of volunteer spotters to leave their homes on potentially hazardous nights, going into dangerous or at least unpleasant weather themselves, and leaving their families unattended. Although training may be very good, the possibility of mistakes in identification is always present. Communication of the spotters findings may be impossible if telephone lines are down due to storm conditions. Finally, the spotter can only give information on rainfall and/or river heights when they actually occur at his position, thus providing very limited lead time for forecast appraisal and dissemination.

2.5 Forecasting Techniques

2.5.1 Introduction

A brief overview is presented here of various different techniques used in rapid response flood forecasting, a more detailed examination of the use of transfer function models in forecasting is given in Chapter 6.

Hall (1981) states that in flash flood forecasting the main requirement may be the quick identification of the fact that critical danger thresholds will be surpassed, rather than the accurate definition of the magnitude and timing of the flood peak. Thus fast flood forecasting does not have to be complex, and simple models may suffice.

Techniques of flash flood forecasting can generally be seen as one of three groups :

- Those based on meteorological input only, essentially the forecasting of rainfall over an area.
- Those based on hydrological techniques which use observed rainfall and/or river height data to predict the flood height or to warn of impending river rises.
- Those which are a combination of meteorological and hydrological techniques.

The latter group is generally the most useful as it has the advantages of additional warning time based on forecast rainfall and of specific flood forecasts based on predicted and observed rainfall, usually verified against river height.

2.5.2 Meteorological techniques

Meteorological techniques are essentially those forecasting and/or advising of heavy rainfall. These techniques can be used when no hydrological model is available for an area. Rainfall may be recorded using automated raingauge or manual observers, which then report to a central collating point on interrogation or at appointed times. Radar is particularly useful as it gives areal perspective with a wide coverage and can delineate potential trouble areas, and data may be used either qualitatively or quantitatively. Haggett (1989) states that almost all Regional Water Authorities in the United Kingdom now receive radar information which can be displayed over a coastline or national grid map. Radar data presented in this form can be used by operational staff in a qualitative way to gain a general impression of weather conditions, using replay and zoom facilities.

In the United Kingdom, if meteorological conditions conducive to heavy, intense rainfall are observed or forecast, warnings of flooding are issued to the general public. Media warnings such as television and radio 'news flashes' are broadcast, and police and civil defence organisations are brought to alert. In the United States of America the Weather Service Offices (WSO's) prepare "watches" and "warnings" which are issued depending on the severity of the situation. Flash flood watches are usually valid for periods of 12 hours or less, and are given before the onset of heavy rain where possible. Warnings are issued if excessive rainfall or actual flooding is reported, and are usually for a period of less than four hours.

2.5.3 Hydrological techniques

The simplest hydrological technique is to monitor the river upstream of the point of interest and to base flood warnings on stream rises. This method, although simple, provides the public with the least amount of warning, and may be unreliable in storm

conditions due to telephone failures. The observation of rainfall rather than upstream river rises serves to increase warning times, but requires the use of some form of hydrological model to assess flood potential.

Sargent (1984) describes the Haddington flood warning scheme as using inputs from telemetered gauges to a model in two parts. Firstly, the amount of rainfall expected to appear in the river is calculated. Runoff is then distributed by time using simple delay and routing subroutines to simulate catchment response. The model operates on the contributing area theory so that all rain falling on saturated areas results in rapid runoff and the rest is delayed until after the flood peak has passed. The proportion of the catchment that is saturated thus determines the percentage of rainfall transformed into runoff. Originally soil moisture deficit was used to establish catchment wetness, but it was recognised that this is rarely available. Basin discharge, using river gauges, is now used as an indication of catchment saturation, although the effectiveness of this technique is catchment dependent (Owens, 1986; Yu, 1989).

When rainfall exceeds a certain threshold an event is deemed to have begun. River level is converted to flow and thus flood producing runoff is calculated and fed through the model along with rainfall. Warnings are issued to the police when preset levels are reached. A yellow warning indicates possible flooding, amber a minor flood and red warns of property damage.

2.5.4 Meteorological - hydrological techniques

The most effective means of forecasting fast response flooding is to combine both meteorological and hydrological forecasting techniques. Quantitative precipitation techniques can be used to extend the lead time which is the key parameter in forecasting rapid floods.

Georgeokakos (1986) outlines a generalised hydrometeorological model for flood and flash flood forecasting. The model couples storm, soil and channel states in an extended state vector to forecast flow rates at the basin outlet. A stochastic hydrological model is used which extends lead time, gives distribution of precipitation volume in the various soil zones and allows uncertainty modelling, incorporating rainfall in state vectors and the capability of updating upper soil states from only precipitation observations. Basin characteristics must be interpolated, however, due to the long distances between points where meteorological inputs are observed and where they will take place.

Meteorological data is gathered and interpolated on pressure, air temperature and dew point temperature. Topography is taken into account and the air parcel is tracked as it follows catchment relief. A three component mathematical model is then used to simulate rainfall-runoff processes. The model describes the precipitation mechanism based on simplified cloud dynamics and microphysics. A spatially lumped model is used for soil moisture and related processes. Finally, a non-linear channel routing model forecasts river flows from headwater areas.

Although a much more 'white box' approach, this type of forecasting system suffers several major drawbacks when used in real-time in a fast response flood forecasting situation. When attempting to model the atmosphere the physical constraints that govern the dynamic processes of storm formation and evolution are even now not fully understood. Increasing accuracy and reality within the model almost inevitably means increased complexity and increased data requirements. When all the data is available the mathematics needed to represent the atmosphere can become very time consuming. The great data requirements and involved mathematics used mean that this type of model take large amounts of computer time to run, reducing forecast lead time.

2.6 Warning Time

A flood warning system is only of use if the warnings it produces are timely and accurate, and consideration must be given to the time lost in the processing and dissemination of flood warnings, especially in a rapidly responding system. The type of input-storage-output (ISO) flood forecasting model in real-time use in the North West region of the National Rivers Authority, for example, affords a maximum of only four hours foresight before flooding takes place, and frequently much less for flashy catchments. Warnings are issued to the police and local authorities, but dissemination from there to the public may take at least two and a half hours (Drew, 1993). Due to time constraints as little as 10 percent of the population at risk from an event may be warned. When considering rapid response situations it is therefore vital to provide as much lead time as possible to allow action to alleviate the flood risk.

2.7 Non - Real Time Solutions

Complete prevention of flooding, regardless of speed of onset, is impossible but loss of life and damage to property can be reduced in a number of ways, ranging from temporary evacuation to the construction of costly flood protection works. As the degree of protection increases so does the cost, however, and at some point a balance has to be struck between protection and price. Evacuation plans must therefore play a vital part in the reduction of life and property loss.

Hall (1981) considers flood plain management as falling into one of three main categories:

- Non-structural measures, in which mainly regulatory methods are used. Flood plain zoning and flood forecasting are the two primary methods.

- Basin management, which is essentially the use of good conservation practices to reduce, or at least not increase, natural flood runoff.
- Structural methods, involving the construction of engineering works to control flooding.

Many of these methods are complementary and may be used within an overall plan for flood damage reduction. Practical and financial constraints usually determine the methods adopted but it should be noted that the control and prevention of river floods using physical structures is often not feasible, economic or attractive. Even when artificial smoothing and straightening is undertaken it may serve only to increase flood velocity and steepen the flood peak, resulting in greater damage if overtopping does occur, and heightening inundation due to local rainfall outside the channel (Oya and Hamyama, 1987). Accurate short term warning, however, enables precautions to be taken in the form of evacuation (people, livestock, possessions etc.), amelioration (temporary flood proofing), or control (reservoir discharge adjustment and storm tank emptying) (Reed, 1984). Flood plain zoning, ensures that those areas most prone to flooding are reserved for landuses least affected by it, and is practised by many water authorities in the United Kingdom.

2.8 Conclusion

It is clear that rapid response flooding, occurring in six hours or less, is a major problem causing loss of life and destruction of property. Many factors may lead to the formation of a flood in such a short time, and in comparison with the huge dam break floods, those from fast response rural catchments are generally much smaller. However, no matter what the cause, it is essential to extend the warning lead times in order to reduce the severity of the ensuing damage. This is the task undertaken in this thesis, using a knowledge based approach.

CHAPTER 3

WEATHER RADAR

3.1 Introduction

All of the work presented in this thesis is based on data produced by radar remote sensing of the atmosphere. An appreciation of the advantages and limitations of the data source is vital in its use, and accordingly, this chapter gives an introduction to the observation and estimation of precipitation using weather radar. Firstly, a short background is presented of the development of weather radar in the United Kingdom. A description is given detailing radar networking and its products. Radar hardware and processing procedures are outlined, together with the theories involved in the remote sensing of precipitation.

A discussion is presented setting out the major errors incurred due to radar position and hardware. Finally, variations in the rainfall reflectivity relationship, beam propagation and infilling problems are addressed.

3.2 Historical Background

Although point rainfall has been measured directly by different forms of raingauge since the fourth century B.C., radar estimation of precipitation is a relatively recent technique only made possible by the emergence of remote sensing technology. *Radio Detection And Ranging* of objects in the atmosphere first became possible in the mid 1930's with the work on VHF (Very High Frequency) and UHF (Ultra High Frequency) electromagnetic phenomena.

The military potential on the eve of war was obvious and research and development continued throughout the 1930's and 40's, during which time it was noted that the systems used were also capable of picking up 'interference' from rainstorms. On the 20th of February, 1941, a thunder storm was tracked over the south coast of England using an S-band (10 cm) radar, Ligda (1951) and Atlas (1964).

After the war, in 1946, the disused East Hill Royal Airforce station, fitted with an S-band AMES type 21 radar, was set up as a Meteorological Office radar research establishment (Best *et al.*, 1948). In the following years, much pioneering work was carried out there on echo identification and tracking, as well as short range forecasting.

During the 1950's and 60's research momentum increased pointing towards the potential of radar for the quantitative estimation of rainfall. This in turn led to the 1967 Dee Weather Radar Project (DWRP), started jointly by the Meteorological Office, Water Resources Board, The Dee and Clwyd River Authority and Plessey Radar. The project used a Plessey type 43 S-band device, sited on the Llandegla Moors, North Wales, in comparison with a dense autographic raingauge network covering an area of almost 1000 km² (Harrold *et al.*, 1947). The system came into use in 1971 and in 1973 was converted to C-band (5.6 cm) operation with a smaller 1° beam width to minimise ground impingement.

The findings of the project were published by the Central Water Planning Unit in 1977. These suggested that real time precipitation measurement of acceptable accuracy were possible within approximately 75 km of the radar, given adjustment from a sparse telemetered raingauge network. The national radar system was also standardised on the C-band wavelength following the DWRP work. This was found to provide a balance between signal strength and hardware expense. The 3 cm (X-band) device being cheaper but suffering significant attenuation when used during rain and the S-band providing superior signal power but increased areal cost.

Following the end of the DWRP in 1976 a new project was created sponsored by the Meteorological Office, North West Water Authority (NWWA), The Water Research Centre, Ministry of Agriculture Fisheries and Food (MAFF) and the Central Water Planning Unit. Started in 1977 the North West Radar Project (NWRP) had the aim of incorporating radar data into a real-time flow forecasting system (Noonan, 1985). Radar information came from a Plessey type 45 C-band device with automatic calibration from six of the interrogatable raingauges in the region.

When the project closed in 1985 it gave positive results in several important areas -

- the creation of the United Kingdom's first unmanned weather radar for the observation and estimation of rainfall in real time.
- a high degree of overall system reliability.
- development of automatic, real-time radar calibration using a small number of telemetered raingauges.
- development of quantitative radar rainfall estimates for use in hydrological forecast methods, (eg. Cluckie and Owens, 1987).

The DWRP and NWRP laid much of the ground work in the field of real-time radar use, and an operational radar network is now in everyday use in the United Kingdom (see section 3.3). Research is still continuing into real-time quantitative precipitation forecasting, however, such as the FRONTIERS (*Forecasting Rain Optimised using the New Techniques of Interactively Enhanced Radar and Satellite*) system (outlined in section 3.4.2) integrating satellite and radar data. Other projects include the automation of FRONTIERS, and a new thunderstorm forecast system called GANDOLF (*Generating Advanced Nowcasts for Development in Operational Landsurface Flood forecasting*).

3.3 United Kingdom Radar Networking

Following the work of the Dee Weather Radar Project, Bulman and Browning (1971) recommended the development of a national C-band radar network to cover the whole United Kingdom. At the same time advances in other 'enabling-technologies' such as digital signal processing, computations and communications combined to provide the climate in which a nationwide, real-time weather radar network became possible.

Developments at the DWRP site lead to the creation of a real-time radar processing system (Taylor and Browning, 1974). Further research highlighted the possibilities of processing, transmission and remote display of radar information. This in turn leading to the successful linking of three research radars and the UK's first operational remote sensing network (Taylor and Browning, 1974; Taylor, 1975).

In 1978, prompted by the positive results from the early networking experiments, the Meteorological Office began the Short -Period Weather Forecasting Pilot Project. Set to include data from 'Meteosat', Browning (1977) reports the projects aims as were follows -

- to establish and operate facilities to provide mesoscale observation of cloud and precipitation fields.
- to develop short period forecasting procedures.
- to utilise radar and satellite data for basic research.
- to consider radar data utility and extension of the facilities.

Ground based data for use in the project was sent to the Malvern network centre, in real-time, from the newly established radar sites at Cambourne, Clee Hill, Hameldon Hill and Upavon (Collier, 1980).

The Pilot Project proved successful and in 1981 a working group was established by the Meteorological Office and The National Water Council to assess the implications of a national radar network for the Water Authorities. Their findings (NWC, 1983) confirmed the advantages of a remote sensing network for flood forecasting and warning, particularly using unmanned radars such as the Hameldon Hill station. A network was proposed to allow quantitative coverage over most of England and Wales using 11 or 12 radars. Since then the network has grown and at present consists of 15 C-Band devices covering most of the British Isles (Fair and Larke, 1989). Although United Kingdom coverage is now high there are still some areas not subject to quantitative radar analysis however, (figure 3.1) notably Cumbria, Northumbria, North East Yorkshire and East Anglia.

3.4 United Kingdom Radar Products

Although still not perfect, the present day radar coverage of the United Kingdom allows the production of a variety of valuable data products as shown in Table 3.1. These may be divided into 'Single Site' data (one radar alone) and 'Network' (composite, contiguous images from several radars, giving greater coverage). Single Site data is available directly to the end user in real-time from the radar site computer, or as post event archive material from the meteorological office. Network data, at regional, national or international scales (see section 3.5 below) is disseminated again from the Meteorological Office, in near real-time, after image compositing has been carried out.

3.4.1 Data Resolution.

The meteorological data types produced by the weather radar network, from single or multiple sites, vary in their temporal, spatial and intensity resolution.

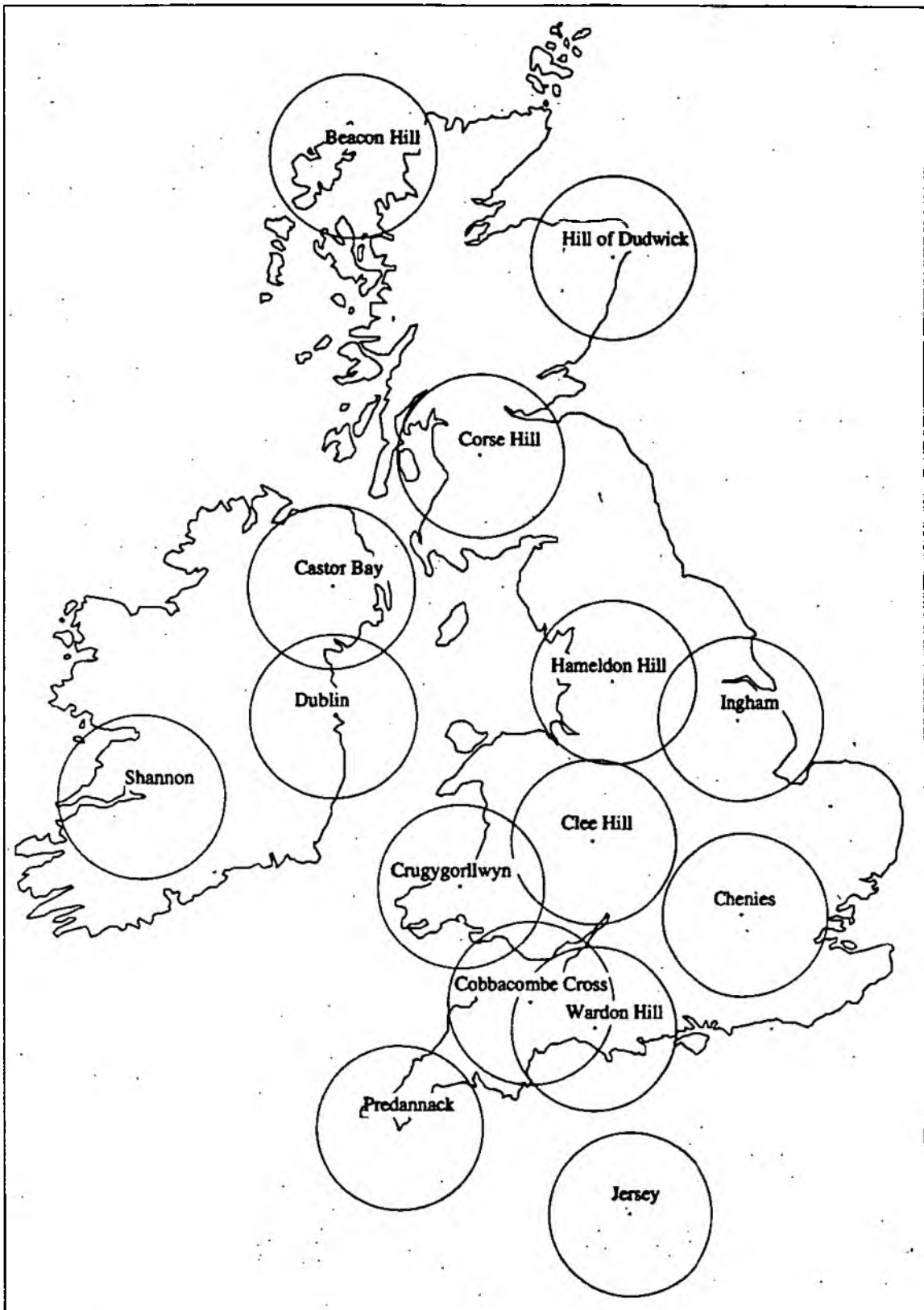


Figure 3.1. Weather radar network in the British Isles (75 km range)

i) Temporal Resolution

The five minute scanning sequence of the United Kingdom radars (as referred to in section 3.6.1) makes this the maximum temporal resolution of standard remotely sensed data. Longer time scale sampling is often used, however, in order to reduce the amount of data to be processed, and to allow time for combination with other data sources such as satellite information. For this reason many radar products are only available with reduced 15 or 30 minute resolution.

ii) Spatial Resolution.

In its initial state radar data is Polar in form and is processed at the radar site on to Cartesian coordinates, based on the National Grid (section 3.6.2). Two grid resolutions are used, 2 km squares (76 by 76) giving a measurement range of 76 km, and 5 km squares (84 by 84) giving a range of 210 km. A diagram of the two radar resolutions is given in figure 3.2.

Radar may be used quantitatively up to a range of 100 km, if uninterrupted by ground clutter, and qualitatively beyond this to the 210 km limit. The spatial resolution of a radar system is influenced by the beamwidth used, as discussed in section 3.9.3.

iii) Intensity Resolution.

Radar reflectance data is produced on a continuous analogue scale. Following quantisation of the data the levels are split into rainfall intensity classes. Intensity resolution is thus dependent upon the number of intensity classes used. In practice two resolution levels are utilized, high resolution eight bit data (208 levels) and low resolution three bit data (eight levels).

Table 3.1 United Kingdom Weather Radar Products (Collier, 1989)

Type 1 Data:	
Spatial resolution	5 km grid to 210 km range
Intensity resolution	8 intensity levels (including zero rainfall)
Temporal resolution	data collected at 5 min intervals but updated for transmission every 15 min
Other Information	date, time, radar station number, calibration information, synoptic type
Other data	Subcatchment averaged rainfall totals every 15 min, hourly and daily totals
Transmission rate, time	1200 baud (asynchronous), 35 seconds
Type 2 Data:	
Spatial resolution	2 km to 75 km range, 5 km to 210 km
Intensity resolution	208 intensity levels (eight bit data)
Temporal resolution	transmitted every 5 minutes
Transmission rate, time	1200 baud (asynchronous), 2 minutes
Other Information	date, time calibration information, synoptic type, height of bright band
Other data	subcatchment totals (updated every 15 minutes)
Comments	data can be processed by used
Type 3 Data:	
Spatial resolution	5 km to 210 km
Intensity resolution	208 intensity levels (eight bit data)
Other Information	date, time calibration information, synoptic type, height of bright band
Transmission rate, time	2400 baud (asynchronous), 27 seconds
Comments	used by the Met. Office for production of national network image
Network Data	
Spatial resolution	5 km (680 km*680 km coverage)
Intensity resolution	8 intensity levels (three-bit data)
Temporal resolution	transmitted every 5 minutes with updates at 15 minute intervals
Transmission rate, time	1200 baud (asynchronous), 2.5 minutes
Other Information	date, time, colour key for rainfall intensity, height of bright-band
Comments	suitable for display on graphics monitor
COST-73 Data	
Spatial resolution	20 km
Intensity resolution	8/1 intensity levels
Temporal resolution	60 minute
Comments	combines data from radars in 13 European countries
Frontiers 'Actuals'	
Spatial resolution	5 km (1280 km*1280 km coverage)
Intensity resolution	208/1 intensity levels
Temporal resolution	15 minute
Transmission rate	1200 baud (asynchronous)
Comments	at-site calibration removed, quality controlled in real-time, supplemented by satellite
Frontiers 'Forecast'	
Spatial resolution	5km (1280 km*1280 km coverage)
Intensity resolution	208/1 intensity levels
Temporal resolution	30 minutes
Transmission rate	1200 baud (asynchronous)
Other Information	quantitative precipitation forecasts for 1,2,...,6 hours ahead
Comments	still under evaluation not routinely disseminated

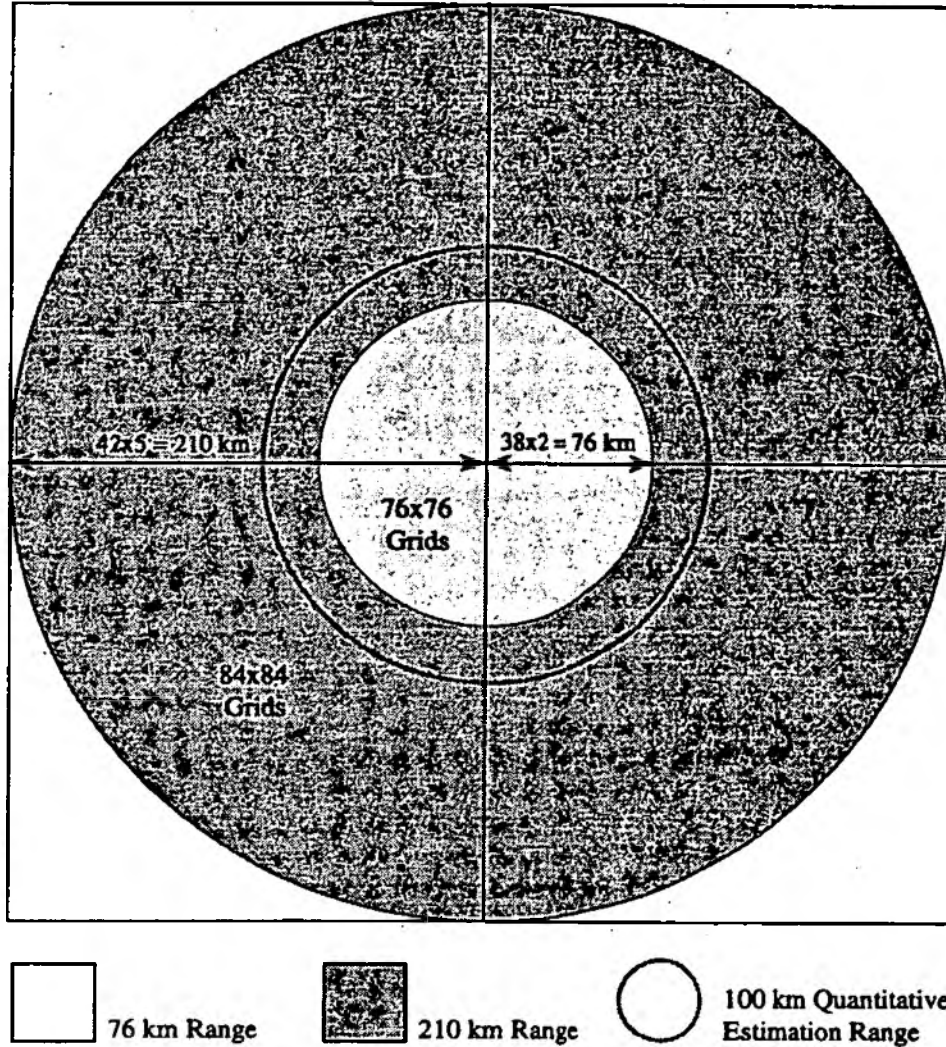


Figure 3.2 Radar Ranges of 2 km and 5 km Resolution Data

3.4.2 FRONTIERS Data.

The FRONTIERS System (*Forecasting Rain Optimised using the New Techniques of Interactively Enhanced Radar and Satellite*) was originally proposed by Browning (1979) and grew out of advancements in remote sensing both at ground level and with

satellite borne sensors. Frontiers data consists of 'Actuals', 'Forecasts' (up to six hours ahead) and hourly cumulative totals, being disseminated at 15 minute and 30 minute intervals.

All data types are formed from network information but differ from standard network images in two important respects. Firstly, Frontiers incorporates data from the Meteosat weather satellite which at present shows rain / no-rain based on cloud top temperatures. Secondly, Frontiers is quality controlled in real-time by a trained meteorological operator. Modifications are carried out to the network image interactively when the forecaster deems necessary, using menu-driven software and touch sensitive VDU screens, as outlined by Browning and Collier (1982). Decision support software is used to aid subjective decision making, and other information sources such as synoptic charts and radiosonde data are also available to the Frontiers Operator in real-time.

The applicability of Frontiers forecast data has been investigated at the University of Salford with positive results for quantitative flood forecasting (Viner and Cluckie, 1990; Viner *et al.*, 1991).

3.5 International Network Co-operation

Perhaps the most important example of international co-operation in the networking and exchange of radar data is provided by the "Co-operation in Science and Technology" (COST) programmes COST 72 and COST 73. Sponsored by the Commission of the European Community (CEC) the initiatives were a response to the need for data exchange within the growing operational weather radar network throughout Western Europe.

Newsome (1987) describes the COST 72 programme as representing a pilot project for the development of an integrated European weather network. When it started in 1979 the main concerns of the project were the measurement of precipitation and the cost-effectiveness of an integrated weather radar network, although information was to be used for other purposes such as hydrology, air traffic control and agriculture. In all, thirteen countries signed the "Memorandum of Understanding" (Collier, 1989) showing widespread interest in the plan throughout the European Community.

The COST 72 project ran for six years, and demonstrated the feasibility of real-time exchange and compositing of data from several countries (Collier *et al.*, 1988). When the programme ended in 1985 recommendations were made for further work on data quality, communications and product specification. In 1986 this was taken up by eight of the original thirteen states in signing the COST 73 agreement and over the following three years a further eight European countries joined the initiative.

The COST 73 research programme has encouraged work in five main areas -

- Radar Systems.
- Radar Site and National Network Centre Data Processing.
- Data Transmission.
- Bilateral Radar Data Exchange.
- European Network Investigations.

When the project formally ended in 1991 it was able to give positive recommendations for the continued co-operation in international radar networking. Radar data exchange still takes place between several countries within the EEC, including Great Britain, and the information received is used by the Meteorological Office in their forecasting procedures.

3.6 United Kingdom Weather Radar Hardware And Processing

3.6.1 Radar Hardware Characteristics.

The Weather Radars used in the United Kingdom are exclusively Plessey type 43-C devices, with technical characteristics shown in Table 3.2.

Table 3.2. Characteristics of the Plessey Type 43-C Radar

<i>Antenna: parabolic dish</i>	
Diameter	3.7 m
Gain	43 dB
Polarization	Vertical
Beam width	1°
Side lobes	Better than -25 dB relative to main beam
Elevation	-2° to +90°
Elevation rate	9° per second
Rotation rate	0.1-6 rpm
<i>Transmitter</i>	
Peak power	250 kW
Pulse width	2 m
Frequency	5450 and 5825 MHz (i.e. 5.6 cm wavelength)
<i>Receiver</i>	
Noise factor	8.5 dB or better
Characteristic	Logarithmic
Swept gain	1/R ² to 200 km
Frequency control	Automatic
<i>Environment</i>	
Operating temperature	external - 40°C to +55°C internal +10°C to +35°C
Radome survival	240 km/h

Normal operation of these devices is completely automatic and in use the sites are unmanned. Radar scanning takes place at four separate beam heights, between 0.5° and 4.0°, the higher elevation beams being used to fill in areas obscured to the lowest

beam by ground clutter. Each antenna rotation takes 55 seconds with a final one minute processing time after the four complete scans, giving a five minute cycle in all.

The weather radars operate in 'Plan Position Indicator' (PPI) mode allowing rainfall range and bearing to be calculated on a polar coordinate system, as discussed in section 3.7.4.

3.6.2 At Site Processing.

Radar signal theory is explored more fully in section 3.7 but the following is presented as a guide to the steps carried out by the at-site computer.

Radar reflectance data is converted to digital polar coordinates using the at site array processor, these are then passed to a DEC PDP-11/84 computer using a Radar Signal Averaging Unit (RSAU). Processing of the data then takes place to -

- average in time over 1° azimuth integration brackets.
- remove fixed 'ground clutter' echoes with a clutter map.
- correct beam occultation where a radar beam is screened by hills etc.
- convert amplitude data to rainfall intensities using a Z-R relationship.
- correct two-way beam attenuation.
- change from Polar to Cartesian coordinates, 2 km and 5 km grids based on the National Grid.
- adjust using raingauge data.
- convert data to 8-bit 'float' notation and pack for storage and transmission.

As part of the radar network the data is then transmitted to the Meteorological Office cluster of four VAX 3100 processors at Bracknell. Here it is archived and may be combined with other network data as well as Meteosat and continental radar information.

3.7 Quantitative Rainfall Estimation using Radar

3.7.1 Introduction

As electromagnetic energy passes through the atmosphere it interacts with hydrometeors, a fact which is used in active remote sensing using radar. Figure 3.3 shows the position of the radar microwave region within the electromagnetic spectrum.

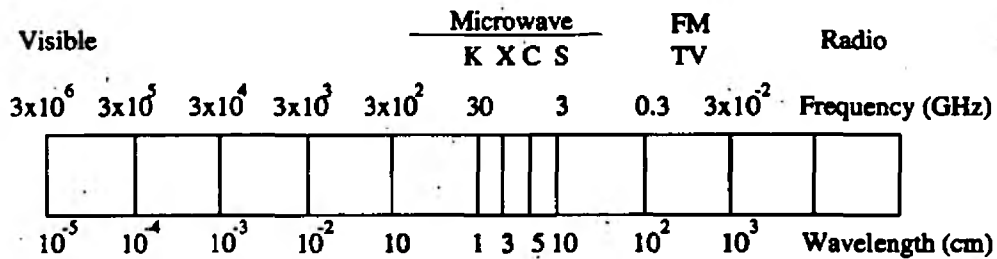


Figure 3.3 *Diagrammatic Representation of the Electromagnetic Spectrum,*

3.7.2 Measurement Techniques.

In principle there are main methods by which precipitation may be measured remotely, using differing types of radar (Collier, 1989).

i) Radar Reflection.

Measurement of the energy back scattered from precipitation particles above the ground may be related to the rainfall rate. This method is effective for quantitative assessment up to 100 km or more and at different azimuths as the radar beam rotates about a vertical axis. In practice this is the only method to have been implemented to any great extent, and will be examined in greater detail in section 3.7.3 below.

ii) Radar Attenuation.

Radiation with a wavelength of less than three centimetres suffers attenuation by rainfall, following an almost linear relationship. The integrated rainfall may thus be calculated between two points, provided that the rain is not so heavy as to remove the signal altogether. In practice, however, the difficulties of making measurements with high spatial resolution at all rates of rainfall, added to the occasional loss of the signal completely during heavy rain has led to the abandonment of this technique for operational use.

iii) Simultaneous Attenuation and Reflection at Two Wavelengths

Basically a combination of the two techniques described above, this method has been put forward in both the former USSR and the USA. At present, however, more research is necessary before it can be assessed operationally (Collier, 1989).

3.7.3 Radar Reflectivity Theory

In a reflectivity measurement system the radar acts as an echo-sounding device. An electromagnetic pulse is fired from the antenna and the range of the target is determined from the time taken for the reflected pulse to return to the radar. A simplified diagram of a typical weather radar system are shown in figure 3.4.

High power electromagnetic pulses of known power (about 100kW) and frequency are generated in a magnetron and fed via a wave guide to the transmitter antenna. The characteristics of the radiated pulse are related to antenna design, weather radars typically using a parabolic antenna to form a narrow, divergent beam, one to two degrees wide in order to sample a sufficient atmospheric volume.

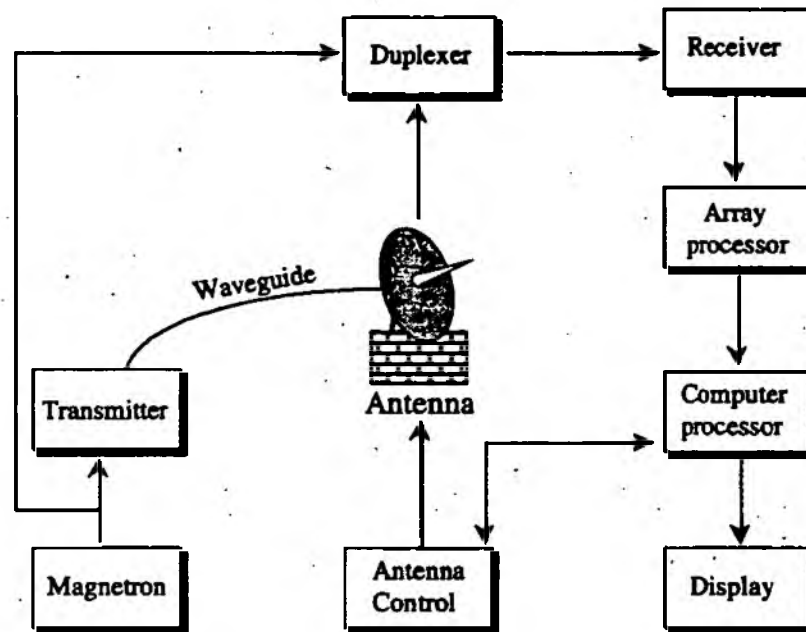


Figure 3.4 *The Weather Radar System*

Reflected energy, returning from the radar target, is detected by the antenna and routed to the receiver. In operation the radar uses a 'transmit-receive' (T/R) switch called a 'duplexer' in order to prevent damage to the receiver from high power radiation during transmission. The receiver itself is a high sensitivity device, as reflected energy may be 10^{-17} the intensity of the emitted pulse.

The power of the radar beam is not constant across its whole frontal area, with maximum intensity being concentrated along the axis perpendicular to the face of the antenna. Movement away from the centre of the beam causes a rapid fall off in power, as demonstrated in figure 3.5. In order to provide a standardised definition, beam width is taken as the angle between which beam intensity is at least 50% of maximum power.

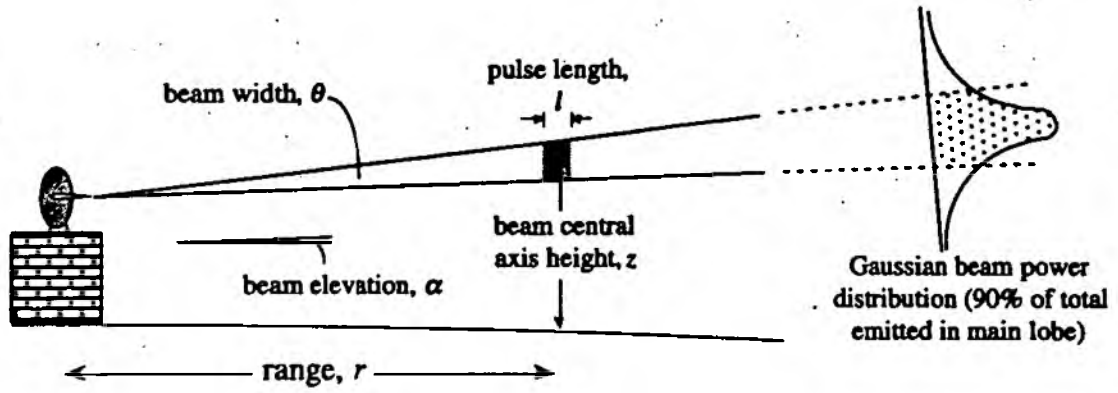


Figure 3.5 Geometry of a radar pulse volume

When the radar is operating small 'side lobe' beams are formed at either side of the main primary radar lobe, reducing in strength with increased angle from the centre axis. Figure 3.6 shows a representation of radar primary and side lobes in cross section (angles are larger than in reality, and only 1st and 2nd side lobes are shown).

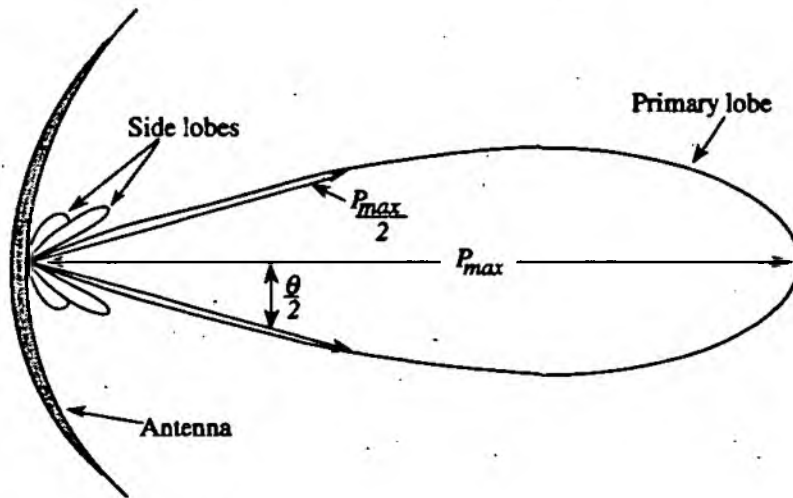


Figure 3.6 Cross-section of a radar beam from a parabolic reflector (After Clift, 1985)

3.7.4 Radar Scattering

Once the radar pulse has been 'fired', the energy reflected back depends on the number, size, shape, composition and orientation of the particles in the pulse volume of the radar beam. When the beam interacts with hydrometers, scattering of the energy does not occur isotropically (figure 3.7) and the reflection cross section (σ) is defined as the equivalent area needed for an isotropic scatter to return the actual received power to a receiver. Total reflected energy is defined as the sum of the energy back-scattered by each of the individual scattering particles.

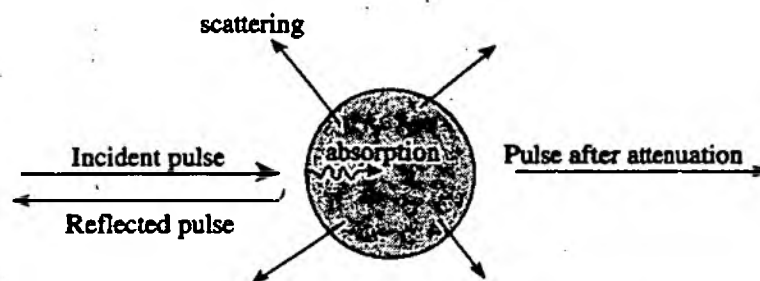


Figure 3.7 Radar pulse reflection, scatter and attenuation following interaction with a hydrometer

The complete solution for the back-scattering cross-section for spheres is given by Mie (1908) as:

$$\sigma = \frac{\pi D^2}{4\alpha^2} \left(n \sum_{i=1}^{\infty} (-1)^i (2n+1) (a_n - b_n)^2 \right) \quad (3.1)$$

where D is the drop diameter, $\alpha = \pi D/\lambda$ (called the electrical size), λ is the wavelength, and a_n and b_n are coefficients of the scattering field involving Bessel and Hankel functions which relate the scattering angle, electrical size and coupled refractive index.

When drop diameter is small compared to the wavelength (i.e. $\alpha < 0.13$), σ may be simplified and 'Rayleigh scattering' is applicable as:

$$\sigma = \frac{\lambda^2 \alpha^6}{\pi} \left| \frac{m^2 - 1}{m^2 + 2} \right|^2 \quad (3.2)$$

where m is the complex index of refraction, $n - ik$; n is the ordinary refractive index and k is an absorption coefficient. Thus equation (3.2) may be rewritten as:

$$\sigma = \frac{\pi^3}{\lambda^4} \left| \frac{m^2 - 1}{m^2 + 2} \right|^2 D^6 \quad (3.3)$$

This shows that scattering cross-section is proportional to the sixth power of the drop-size diameter.

When considering meteorological targets, the average power received is the sum of the contributions of the individual scatterers:

$$\bar{P}_r = \frac{P_t G^2 \lambda^2}{(4\pi)^3 r^4} \sum_{i=1}^n \sigma_i \quad (3.4)$$

where P_t is the transmitted power, G is the antenna gain (the amount that antenna focusing increases power) and r is the range of the target. Probert-Jones (1962) developed this equation by allowing for beam shape and other factors to give:

$$\bar{P}_r = \frac{P_t G^2 \lambda^2 \theta \phi h L}{512(2 \ln 2) \pi^2 r^2 \Delta v_{vol}} \sum \sigma_i \quad (3.5)$$

where L is the sum of all the losses, including attenuation by atmospheric gases, precipitation and the radome; θ and ϕ are the vertical and horizontal beam widths and h is the pulse length, and Δv is the pulse volume. Substitution of equation (3.3) into (3.5) gives:

$$\bar{P}_r = \frac{P_t G^2 \theta \phi h L \pi^3}{512 (2 \ln 2) r^2 \lambda^2} K^2 \frac{1}{\Delta v} \sum_{vol} D_i^6 \quad (3.6)$$

where $K = (m^2 - 1)/(m^2 + 2)$, and the radar reflectivity Z can be defined as:

$$Z = \frac{1}{\Delta v} \sum_{vol} D_i^6 \quad (3.7)$$

When a radar constant C is defined (which can be accurately determined for any radar device) to be:

$$C = \frac{P_t G^2 \theta \phi h L \pi^3}{512 (2 \ln 2) \lambda^2} \quad (3.8)$$

then (3.6) becomes:

$$\bar{P}_r = \frac{CK^2 Z}{r^2} \quad (3.9)$$

Equation (3.9) is subject to several assumptions including (after Collier, 1989):

- Rayleigh scattering theory is applicable.
- the pulse beam is completely filled with randomly scattered particles.
- the main antenna radiation pattern is, or approximates, Gaussian shape (figure 3.5).
- side lobe contribution is slight (lower than 20dB below main beam power)
- the reflectivity factor Z is uniform throughout the sampled pulse volume.
- $|K|^2$ is the same for all particles (either all water droplets or all ice particles).
- absorption of the transmitted signal by ground clutter is negligible.

The assessment of precipitation using weather radar is based on the measurement of back-scattered radiation intensity (the radar reflectivity, Z in equation (3.7)). The Z - R relationship is thus formed by empirical relation of Z to rainfall intensity:

$$Z = aR^b \quad (3.10)$$

where R is rainfall intensity and a and b are empirically derived constants. Z is usually expressed in the volume units mm^6/m^3 . The Z - R relationship is fundamental in quantitative estimation of precipitation intensity.

The values of a and b are a function of the rainfall type and radar properties and a range of values have been estimated for use in varying conditions. Battan (1973), for example, lists some sixty Z - R relationships. The most frequently used values are $a=200$ and $b=1.6$ (Marshall and Palmer, 1948). The Z - R relationship and its application is discussed further in section 3.10.1.

The problems with the transformation of radar reflectivity into rainfall rate have led some authors to attempt to side step the Z - R relationship and to use a reflectivity - discharge model instead. Trovati and Mattos (1990) produced a Z - Q translation of radar reflectivity values to basin outflow. Some success has been reported with this technique on rural catchments, although smoothing of the reflectivity signal, and parameter estimation present difficulties.

3.7.5 Radar Data Display

The method most frequently used in the display of radar data is the plan-position indicator (PPI). The display presents a view of the received signals on a polar coordinate system. In practice this provides a mapping of the target on a semi-

horizontal 'plane' and allows the quantification of areally averaged rainfall values. The PPI is 'intensity modulated', a strong echo on screen representing a high return power.

Another type of radar display in common use is the range-height indicator (RHI). This type of display is used with scanning radars which may operate through a range of beam elevations. The antenna inclination is varied through the operational range of the device producing vertical profiles of the storm for a given bearing, and is particularly useful for the study of cloud and precipitation growth. Examples of PPI and RHI are shown in figure 3.8.

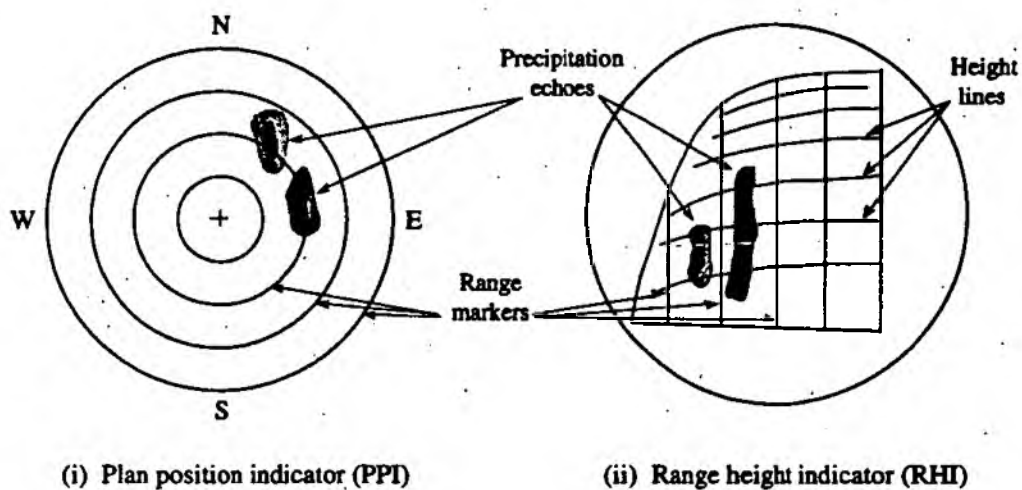


Figure 3.8 Radar display modes (after Battan, 1973)

A third display technique, the constant altitude plan position indicator (CAPPI), was developed by Marshall (1957). This method electronically synthesises the echoes taken from PPI scans at progressively greater angles into a single picture showing intensity modulated signals at a constant altitude. Display is carried out in a plan form as with the PPI display (figure 3.9).

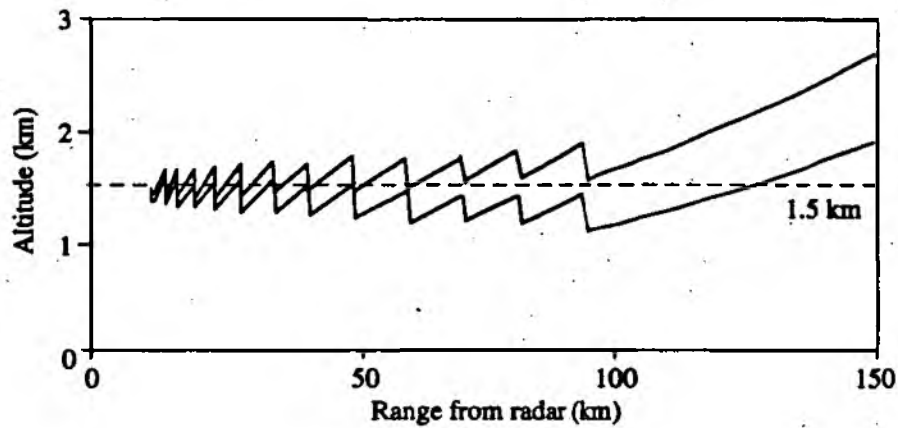


Figure 3.9 *Beam segmentation and composition for a 1.5 km Constant Altitude Plan Position Indicator (CAPPI)*

3.8 Radar Siting Problems

3.8.1 Permanent Echo

In almost all siting situations the main radiated beam and side-lobes may interact with 'ground clutter' causing strong permanent echoes. Persistent echo can be caused by beam interaction with the ground directly, or with ground based objects such as trees, towers and radio masts, and poses a significant problem. Without correction this type of reflection may give misleading results as either rainfall where none exists, or greater intensity than is taking place. Investigations into ground clutter echo show that its strength is almost independent of wavelength (Joss and Waldvogel, 1989).

Due to the seriousness of permanent echo, the choice of an obstruction free horizon is a major factor in the siting of a weather radar. Unfortunately in a real-world environment it is never possible to get away from ground clutter and to reduce the worst effects a common technique is the definition of a ground clutter map. This

method entails the creation of a digitised echo map observed under stable, dry atmospheric conditions, storing the locations of cells with higher echo than the radar noise threshold.

Once established, the ground clutter map is used to modify observations made in affected areas with interpolation from surrounding clutter-free sectors (azimuth-interpolation) and / or information from higher beam elevations (elevation-interpolation). Although technique works well it does have some limitations. Collier (1989) reports that in under conditions of orographic enhancement topographic changes can result in non-linear changes in rainfall, introducing errors into the interpolation. Also, mapping assumes consistency in clutter characteristics, which change when the atmospheric refractive index and therefore beam propagation are altered under varying meteorological conditions.

Another technique, adopted by the United Kingdom for dealing with permanent echo, is the determination of radar horizons from theodolite surveys and topographical mapping. This method, similar to the United States 'sectorized hybrid scan' (Shedd *et al.*, 1989; Hudlow *et al.*, 1989) then uses these sight horizons to determine the appropriate beam elevations for all azimuths and ranges.

3.8.2 Screening

Unfortunately, as well as causing permanent radar echo, beam interception also leads to 'occultation' or screening of the area beyond the obstruction, so that only a tiny amount of the total beam power reaches it, as shown in figure 3.10. Partial blocking takes place in areas beyond blockages produced by hills, causing echoes from precipitation observed in these regions to be weaker than they would otherwise have been, had the beam been complete.

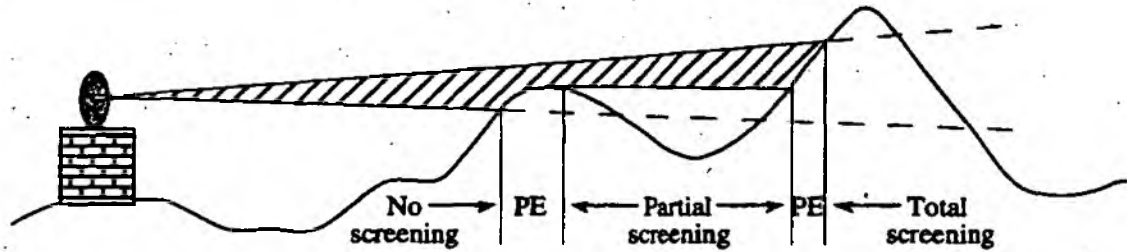


Figure 3.10 *Screening and permanent echo (PE) in a hilly region, (from Hill and Robertson, 1987)*

Compensation can be applied for occultation provided that at least 40% of the beam remains unobstructed (Harrold *et al.*, 1974). The correction factor applied in this case is a function of the beam cross sectional area percentage obstructed. Interpolated values are then used in the obstructed areas, although corrections become increasingly unreliable as range increases.

3.9 Radar Hardware Problems

3.9.1 Radar Wavelength

Radar wavelength is related to radar hardware characteristics and determines the accuracy with which precipitation may be estimated quantitatively. The hydrometeorological applications of the most commonly used wavelengths are summarised in Table 3.3.

Table 3.3. Radar system characteristics and hydrometeorological applications.

Band	Wave length	Frequency range (MHz)	Comments
L	20 cm	30 000	No hydrometeorological applications.
S	10 cm	2700 - 3000	Best suited to regions where heavy rainfall occurs and attenuation may be a problem, e.g. tropical areas. Requires a large reflector to produce a small beamwidth.
C	5.6 cm	5300 - 5700	Affords good compromise between hardware cost and precipitation estimation performance for most hydrometeorological applications in temperate regions. Qualitative range limited to about 200 km (quantitative range about half). Total cost for a working system in the region of £ 1 million (1990 prices).
X	3 cm	9300 - 10 000	In the past used mainly in polar and near polar regions where attenuation is not a major problem. Currently receiving interest for limited range applications (e.g. urban applications) in temperate regions, where range is limited to approx 35 km. Cost of a complete working system approx. £ 100 000 (1990 prices).
K	0.8 cm	37 500	Not in widespread use except in some eastern European dual wavelength systems where it is combined with a longer wavelength. Can detect the smallest cloud particles and has been used to study cloud microphysics.

3.9.2 Dynamic Range

The dynamic range of a radar receiver may be defined the range of precipitation intensities it can differentiate without distortion of their relative values. Too small a dynamic range will either lead to the non-detection of light precipitation or a reduction in the apparent intensity of heavy precipitation. The dynamic range of the system required is thus related to the region in which it is to be used. At present it is possible to create receivers with a dynamic range of 80 dB, which will accommodate mean

precipitation intensities between 0.1 mm/hr and 256 mm/hr. Accurate determination of the dynamic range needed can be problematic, however, as instrumentation is necessary to measure maximum instantaneous rainfall rates.

3.9.3 Beamwidth

Beamwidth refers to the angle between those directions in which the intensity of the beam is at least one half of the maximum, (section 3.7.2). For weather radars a beam width of 1° is used as a compromise between propagation arguments, for which a narrower beam would be preferable, and practical and economic constraints, which limit antenna diameter to around 7 m. For a circular reflector, the beam width θ (in radians), antenna diameter d and wavelength λ are related by $\theta=1.2\lambda/d$. Thus for a 10 cm wavelength system this gives a beamwidth of about 1° . Table 3.4 gives values for a range of beamwidths, beam-lobes and reflector diameters in various systems.

Table 3.4 Radar beam diameter-range and reflector-wavelength relationship

Beamwidth (degrees)	Approximate diameter of main beam lobe (m)			Reflector diameter required (m) for different wavelengths		
	50 km	100 km	150 km	10 cm	5.6 cm	3 cm
0.5	436	873	1309	13.8	7.7	4.1
1.0	873	1745	2618	7.3	3.7	2.1
2.0	1745	3490	5236	3.4	1.9	1.0

Reduction of system wavelength produces a smaller beamwidth so that only a 2 m reflector is needed to for a 1° beamwidth in a 3 cm, X-band system, making them both smaller and cheaper. Attenuation problems are increased at lower wavelengths, however, and must be considered along with beamwidth and antenna size.

A further practical consideration when selecting radar beamwidth is the spatial resolution of the system. This is important as two targets separated by less than the beamwidth cannot be resolved in space. Figure 3.11 compares observations from two systems, one with a θ beamwidth and the second with a $\theta/2$ beamwidth. In figure 3.11(i) the radar is unable to resolve individual cells, until they approach the radar and the beamwidth narrows. This wrongly gives the impression that a continuous echo has split into two cells.

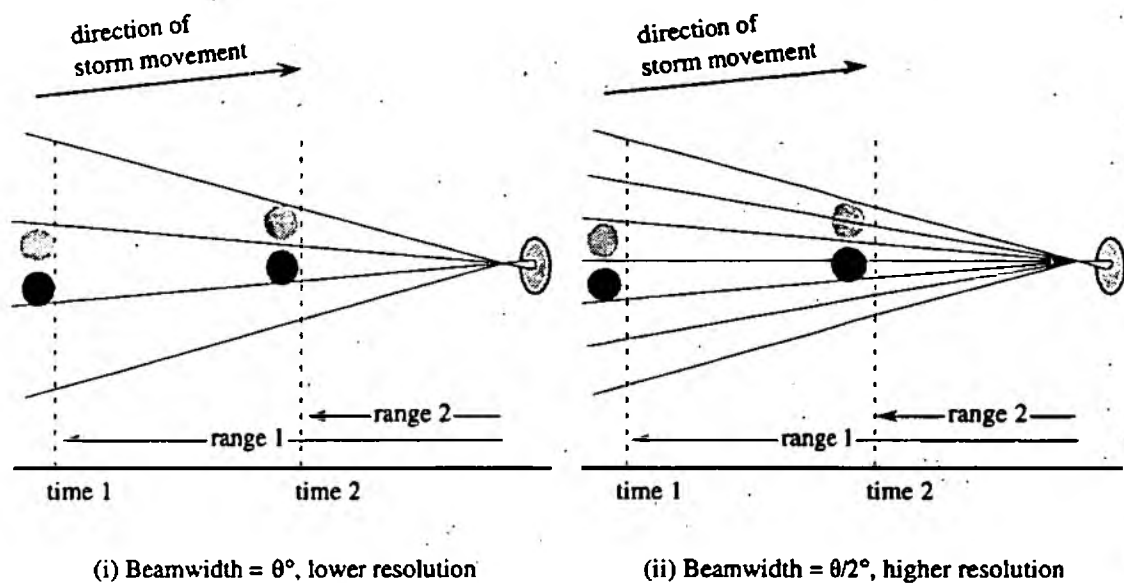


Figure 3.11 Influence of beamwidth on spatial resolution (after Tilford, 1992)

3.10 Physical Factors affecting radar

3.10.1 The Reflectance Relationship

The radar reflectance (Z - R) relationship depends on the drop size distribution of the precipitation within the radar beam volume (equation 3.10). This distribution and the speed of descent of the precipitation are affected by physical processes including

collision, coalescence, evaporation and down-draught and up-draught. Precipitation size and distribution also vary within storms, and from one rainfall type to another in both time and space. As a result of this great variation, the a and b parameters also change significantly and many studies have been carried out to assess the appropriate constants to use in the equation, Battan (1973) listing over 60 Z - R relationships.

In an attempt to simplify matters fixed values are often used for a and b , which are likely to give satisfactory results in average conditions, but less well in extreme rainfall situations. The most commonly applied is the Marshall-Palmer (1948) relationship for homogeneous rainfall and stratified events:

$$Z = 200 R^{1.6}$$

This relationship is applied in stratified rainfall in the United Kingdom, and a can be updated in real time with reference to a small telemetered raingauge network.

3.10.2 Beam Infilling

The radar reflectance relationship assumes complete filling of the radar beam by precipitation, and if this is not the case then reflected energy will be lower than the rate of precipitation and an underestimation will result. To give some idea of scale, a 1° beam width will have a 1.75 km cross section at a range of 100 km, the whole volume of which must be uniformly filled in size and number if the Z - R relation is not to be violated. In practice the risk of incomplete beam filling becomes greater with increased range, so that showers appear to increase in intensity as they approach the radar, and this is one of the major restrictions on observation range.

3.10.3 Curvature of the Earth

The refractive index of the earth's atmosphere is stratified vertically, and in 'normal' conditions this causes the radar beam path to bend close to $\frac{4}{3}$ the radius of the earth. When combined with the earth's curvature this leads to beam path divergence from the ground surface, as shown in figure 3.12, causing an area between the earth and the bottom of the beam where rainfall detection and estimation are impossible. The increase in beam height with distance, in relation to the earth's surface, also leads to the beam inevitably passing through the melting layer, causing 'bright band' problems referred to in section 3.10.6.

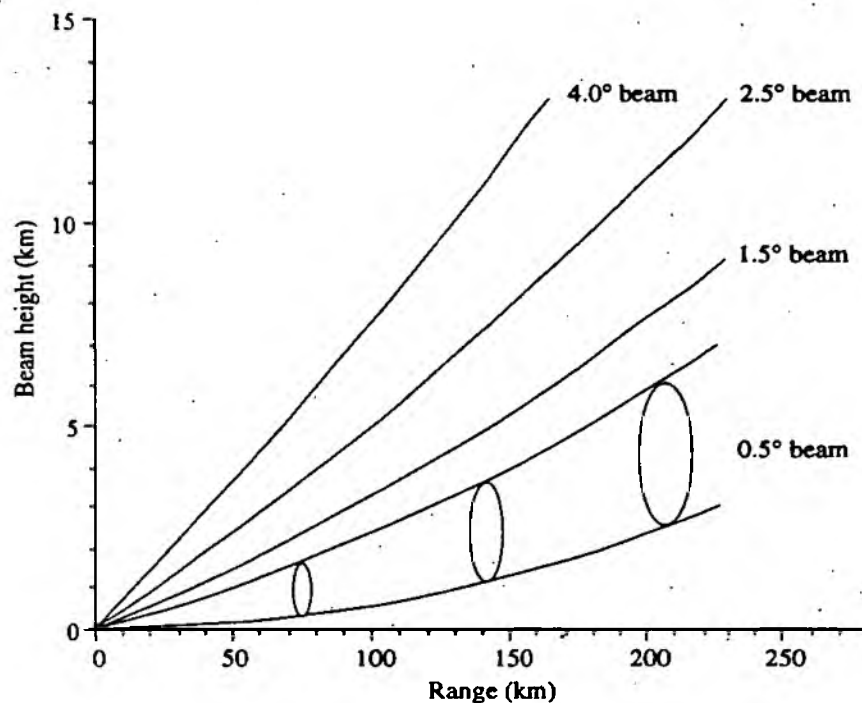


Figure 3.12 *Beam height against range for a 1° beamwidth radar, 0.5° elevation, (after Hill and Robertson, 1987)*

The loss of detection capability below the radar beam means that low level precipitation, and its enhancement, evaporation and horizontal drift are all undetectable.

3.10.4 Anomalous Beam Propagation

Anomalous propagation (or 'Anaprop') follows as a result of radar beam interaction with an 'abnormal' atmospheric refractive index structure. In certain conditions a layer of air occurs near the ground surface with a high refractive index gradient. This may be formed by temperature inversions and / or rapid increases in humidity. When radar energy intersects this layer, the beam path is refracted to such an extent that the beam comes in contact with the earth, causing inversion clutter.

When inversion clutter is observed it does not occur in all areas of the radar scan equally. Clutter may be picked up in certain regions only (most prone is rising ground facing the radar), or in narrow sectors of the radar (van Gorp,1989). A further complication is the fact that the intensity of ground echoes due to anaprop varies in both time and space, making correction very difficult. At present, although detection and correction procedures are applied, no perfect solution has been found.

3.10.5 Beam Attenuation

Attenuation of the radar beam may come from three main sources: absorption and scattering by gases liquids and solids, range and radome wetting.

i) Gasses, Liquids and Particles

Absorption by atmospheric gasses is negligible and only liquid and solid particles cause significant attenuation of radar energy. Attenuation due to precipitation is inversely related to radar wavelength, S-band (10 cm) showing very low loss except for extremely high rainfall rates and X-band (3 cm) suffering severe attenuation.

ii) Target Range from the Radar

Attenuation due to range from the radar occurs such that received power is inversely proportional to the square of the range of the target. Range attenuation can be applied in order to correct this via radar hardware or range normalisation software.

iii) Radome Wetting

The radome is the rubberized or fibreglass housing used to protect the radar antenna. The radome itself introduces an amount of constant attenuation, which is easily correctable, but also allows water droplets to collect on the exterior surface. The extent of two-way transmission loss due to radome wetting have been reported to be up to 10 dB in widespread rainfall.

3.10.6 Bright-Band

When little vertical mixing occurs within cloud layers the hydrometers become vertically stratified within the atmosphere according to temperature. The small ice particle at cloud top levels, where temperature is below freezing, produce low radar reflectivities. As these particles fall they aggregate and melt with the increasing temperature, becoming a film of water with an ice core and finally raindrops, the whole process taking only a few hundred meters (Battan, 1973). Where melting occurs there is a large increase in the reflected radar energy, the reflectivity of water being around five times that of ice, before it declines again as drop sizes decrease and fall speeds become greater.

The intersection of the melting layer by the radar beam causes bright-band reflectivity of two to five times the level of the rain below it to be produced on the radar return, figure 3.13. Bright-band thus gives an artificially high precipitation estimate, the extent of which is determined by the proportion of the beam filled by the melting layer.

Bright-band is therefore less of a problem at longer ranges, where beam volume is larger and the proportion filled likely to be smaller.

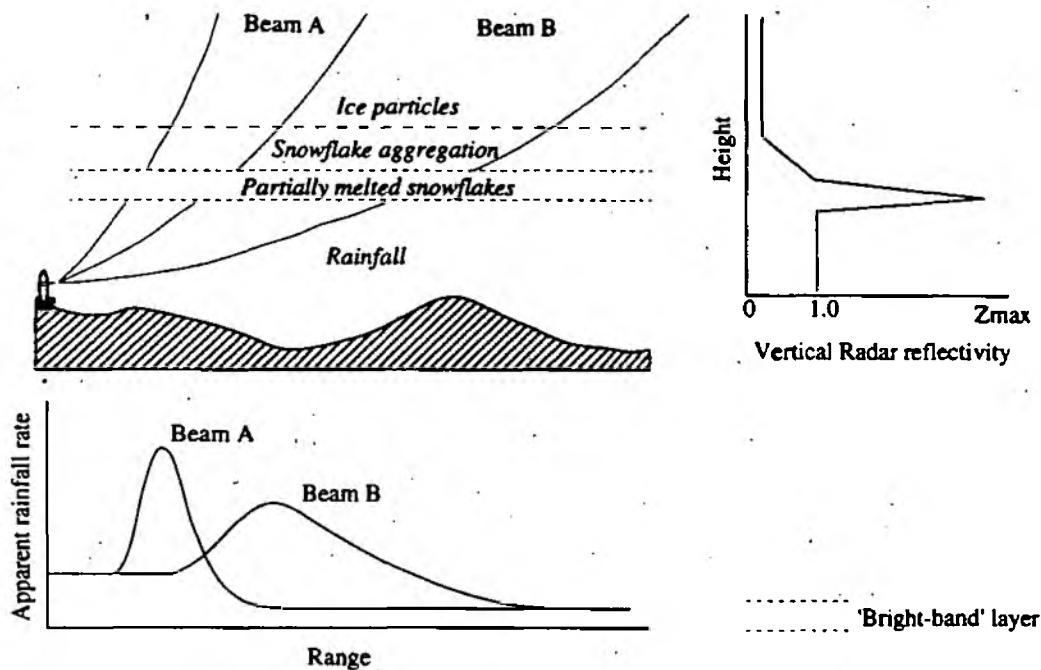


Figure 3.13 A schematic example of the effect of bright-band on a weather radar system (adapted from Smith, 1986)

In the United Kingdom no attempt is made to correct for bright-band objectively, at present, although a detection algorithm can be used (Smith, 1986).

3.11 Conclusion

All the work presented in this thesis is based on remotely sensed radar information, allowing distributed rainfall analysis, and knowledge of storm movement and change. In this chapter an introduction has been provided to a number of aspects of weather radar. The chapter covers the relatively short history, products available, hardware and theories used and problems encountered in active remote sensing by radar.

CHAPTER 4

RETURN PERIOD

4.1 Introduction

Frequency analysis aims to determine the relation between the size of an event, and the probability of that magnitude event being exceeded in the future. Thus rainfall frequency analysis entails the estimation of the rainfall which is likely to be equalled or exceeded on average once in a specified period, T years. This is the ' T ' year event, having a return period or recurrence interval of T years. The return period is a long term average of the intervals between successive exceedances, however, and the intervals may vary considerably around the average value T .

In this chapter a background is presented of some of the major developments in return period analysis. An outline is given of the problems associated with the use of rain gauge data in such analyses. Following from this a new method of distributed intensity-duration-frequency analysis is presented, using remotely sensed radar rainfall data. This enables knowledge of catchment rainfall history to be extracted and used to assess event severity in real-time, in terms of the area affected. A catchment transposition procedure is described which allows estimation of storm return period before it reaches target catchment areas. Finally, there is a discussion of the potential advantages and drawbacks of the technique.

4.2 Historical Background

Rainfall return period has long been used in a design role to assess reservoir storage capacity, barrage and spillway strength and so on. As long ago as 1888 Symons published an analysis of the intense falls reported in Great Britain during the 10 years

1879 to 1888. Symons produced a diagram with rainfall intensities in inches as the ordinate and time in minutes as abscissa. Based on Symons experience two curves were drawn on the diagram, the lower to be regarded as 'heavy falls in a short duration', and the upper defining an 'exceptional' fall. In 1908 Mill introduced a three level classification of rainfall as 'noteworthy', 'remarkable' and 'very rare', these classes later being adopted by Bilham (1935) (see section 4.2.1).

Research into rainfall frequency was extended in 1930, when the great demand for a rainfall depth-duration-return period relationship lead the Ministry of Health to form a seven person rainfall and runoff committee. The resulting report was based on seven years of rainfall data from 14 'widely distributed' stations and became adopted and used for many years. The committee's work suffered several weaknesses, however, perhaps the most serious being the wide scatter of stations on which the report was based (NERC, 1975). This necessarily led to approximate averaging of results for the country as a whole.

4.2.1 E.G. Bilham

In 1935 Bilham published an article based on data analysis from 18 rainfall stations in the British Isles over a ten years period. This work was the first to make full use of the Meteorological Office standardised rainfall intensity-duration-frequency tabulations, allowing a soundly based frequency analysis. The report grouped frequency of occurrence subjectively into 'very rare', 'remarkable' and 'noteworthy' classifications although frequencies were calculable using the formula in the equation 4.1 below.

$$n = 1.25 t (r + 0.1)^{0.282} \quad (4.1)$$

Where n is the occurrence in ten years, t is the time in hours and r is rainfall in inches.

In 1961 Holland revised and extended Bilham's work showing that his equations over estimated the probability of high intensity rainfall (above 35mm/hour). This work still suffered the fundamental problem which affected Bilham's original findings, however, as limited data availability meant results were an average for the country and rare events could only be estimated very roughly.

4.2.2 The Flood Studies Report

Return period analysis was taken a step further in 1975, with the publication of the Flood Studies Report by The Natural Environment Research Council. This weighty report covers hydrological, meteorological and flood routing studies including hydrological data and maps of the British Isles. The FSR used records from approximately 200 autographic raingauge stations, 101 of which had 20 years or more of data, in its intensity-duration-frequency analysis. The report made widescale use of regionalization to extend data records, providing a way of transferring 'experience' from nearby or similar sites, usually in the form of an average.

The Flood Studies Report Meteorological section is contained in volume 2 (FSR-II), describing the analytical techniques used and giving examples of calculation at various durations and return periods for any point or area in the British Isles. Basic maps are provided to derive five year rainfall values, ie. values reached or exceeded on average once in five years, for durations of 60 minutes and 2-days, at any given point location. The five year rainfalls of any other duration are then determined by interpolation or extrapolation from the rainfalls contained in these maps. Rainfalls of other return periods are computed using 'growth factors', given in FSR-II, from the five year value. In 1981 a revised set of growth factors were published by Folland *et al.*, although changes were of minor consequence (Clark, 1991).

Keers and Westcott (1977) note that the calculation of design rainfalls is often a tedious and time consuming task using the hand methods with tables and maps of rainfall parameters. A computerised version has been produced with the relevant mapped data from FSR-II stored as grid point values at 3.33 km intervals covering the United Kingdom.

Although adopted as the standard method for producing design rainfall and attaching return periods to past events in Great Britain, FSR-II is not without its problems. Soon after its launch, Kelway (1977) found that the methodology outlined in the FSR-II could lead to questionable results. In a comparison of frequency analyses carried out on an August 1975 storm over the Tyne catchment, he found that Bilham's formula gave him a maximum rainfall return period for the storm of 250 years, whereas the FSR-II procedure labelled it as the 1 in 2000 year event. Whilst pointing out the theoretical advantages of using generalised geographical parameters in the equation, as compared with Bilham's purely pooled data, he shows that in assessing frequency of heavy falls the Bilham technique is the safer to use. "It indicates that heavy falls are relatively more common than does the Flood Studies method", which could lead to the under design of safety structures.

The problems have not been confined to the North East, and Bootman and Willis (1977,1981) show that the FSR-II gave an underestimate of two day rainfall, on which many other assumptions and calculations are based. The differences, around Bridgewater especially, were considered important enough for the Institute of Civil Engineers to advise that local rainfall data should be used in relation to Somerset reservoir safety, rather than the FSR-II method generally chosen (ICE 1978).

More recently, in comparing the FSR-II and Bilham techniques, Clark (1991) found much larger differences in the return periods produced for rarer events than for more common storms. In explanation he states that the FSR-II was based on the station-year approach of combining records and assumed independence. This independence

was never assessed, and given the areal coverage of some large storms, this assumption seems a dangerous one. If the raingauge records were not independent then the resulting return periods calculated with the FSR-II method will be inflated leading to the problems encountered by many investigators. Clark (1991) states that it is likely that the widely spaced gauges whose records were analysed by Bilham were far enough apart to be independent, so it is not surprising that his method yields considerably lower return period than the FSR-II technique.

4.2.3 FORGE Method

Following the identification of FSR-II's serious under estimates of one day and two day rainfall frequency (Bootman and Willis, 1981) and the strong regional traits not represented in the FSR-II growth factors (Reed and Dales, 1988), Reed and Stewart (1989) developed the 'FORGE' method. FORGE (*FO*cussed *R*ainfall *G*rowth *E*stimation), like the FSR-II, uses regionalized rainfall information from 'similar sites' to extend data records in the form of an average. The sites used for combination were chosen by the use of a spatial dependency model (Reed and Dales, 1988). The modified station-year technique is intended to give emphasis to the most extreme events observed in a region, and allow rainfall growth to be 'focussed' on a particular point. For a fixed network of N gauges operating for m years the equivalent number of independent station years M_e is mN_e .

In rainfall frequency estimation the FORGE method retains the two stage approach of the FSR-II, but uses mean annual maximum rainfall (RBAR) of the appropriate duration as the standardising variable. To estimate the frequency of one day rainfall at a particular site, a value of RBAR is determined and a 'focussed' regional growth factor applied to it.

Unfortunately, the FORGE technique is not without its critics: Raingauge independence is fundamental and following the Dales and Reed (1989) methodology to assess site dependency, Clark (1991) found that only 13 of the 44 sites in South West England were 'independent'. He goes on to point out that some storms are large enough to cover most if not all of these sites so it is not yet possible to modify the station-year method to obtain truly independent raingauge sites.

In use the FORGE method can yield some results which give 'cause for concern', (Clark, 1991), as shown in table 4.1.

Table 4.1 Comparison of FSR-II and FORGE return period methods (Clark, 1991)

Date	Site	Return Period	
		FSR-II	FORGE (years)
24 Sept. 1976	St. Neot	398	240
11 July 1968	Northmoor P.S.	970	1590
12 July 1982	North Brewham	560	1000
5 Oct. 1977	Penryn Resr	266	120
28 July 1969	Launceston	335	290

Although some return periods are lower than using the FSR-II method there are some notable increases for the extreme events. Clark states that if the FSR-II results are at odds with both Bilham's and his own technique (outlined in section 4.2.4 below) "...then the results obtained using the FORGE method cannot give the user much confidence".

One final criticism of the FSR-II and FORGE methods is that they are both based on two day rainfall. This inherently masks the true rainfall intensity characteristics which occur for shorter durations.

4.2.4 Four Parameter Model

In 1991 a further method of rainfall frequency estimation was advanced by Clark, again concentrating upon the South West of England. The investigation followed in response to the problem that Bilham and FSR-II give differing results according to the rarity of the event, and the average rainfall of the site. Clark (op.cit.) carried out frequency analysis on 21 sites with greater than 15 years of data to produce a four parameter model.

The model was constructed to allow rainfall frequency to be calculated at a site without any records. The four parameters were chosen to be predictable from the average annual rainfall (AAR) for each site -

- The two year, 24 hour rainfall.
- The 24 hour - 1 hour difference in two year return period rainfall.
- The slope of the frequency curve (degrees).
- The percentage of the 24 hour - 1 hour difference in rainfall for a given storm duration.

The annual average rainfall was extracted from raingauge records, or by interpolation from the Meteorological Office 1941-1970 southern Britain maps. In comparing his results with those from the FSR-II and Bilham procedures, Clark found his work in closer agreement with Bilham. Of the 29 events analysed he states that FSR-II gave 25 return periods equal to or in excess of twice those from his method. The reason for these differences he attributes to the pooling of regional data in the Flood Studies Report 'station-year' approach.

4.3 Raingauge Problems

Aside from the statistical and analytical problems outlined in the previous section, there are several limitations suffered by all the return period assessment methods described so far. These arise from the use of raingauge data in the analyses. Raingauge records exist for quite extended periods of time, but they suffer inherent problems in instrumentation errors, site location and most significantly areal representativeness.

4.3.1 Instrumentation Errors

Raingauges measure precipitation physically, and by their very nature have to be exposed to the elements. Unfortunately this can lead to errors in the instrumentation caused by evaporation or freezing of collected rainfall, or 'splash-in' of water from around the gauge. Similarly foreign debris, such as leaves and twigs, may block the raingauge distorting measurements or impeding tipping bucket mechanisms.

4.3.2 Influence of Site Location

The location of a raingauge will strongly influence the accuracy of measurements made by the device. Precipitation rarely fall vertically and wind turbulence induced by trees and buildings near the gauge can alter the amount of rain registered. In a historical context raingauge readings will be altered by changes in their surroundings, with the growth or removal of trees or the construction of buildings. This type of change has frequently occurred with the urbanisation of the area surrounding what was originally a rural gauge. It is vital to bear in mind these effects when analysing data archives. A further problem is that the raingauge itself has been shown to produce significant changes in air flow. Neff (1977) found that gauges placed above the ground surface

caught 5 - 15% less rainfall than those at ground level, and that errors of up to 75% occurred during high wind velocities. Modern gauge designs attempt to counteract these effects. However, older gauges, with longer archives, will have turbulence problems reflected in their records, which are impossible to correct. Raingauges placement also tends to be in accessible areas, where they can be read and serviced easily, giving reduced coverage in remote regions.

4.3.3 Areal Representativeness

By far the most important problem suffered by raingauges, for return period analysis, is that of the areal representativeness of their results. The standard raingauge used in Great Britain is a circular catchment of 127 cm² (standard diameter 127mm), sited non-uniformly and at generally quite low densities. This naturally leaves extremely large areas completely unmonitored, and rainfall events may be missed entirely. Hill (1984) gives an example from June 5th, 1983, when five high intensity convective storms crossed the south coast of England (figure 4.1). In this case, none of the centres of rainfall passed over a raingauge location and thus could not have been included in even a regional return period analysis.

Point rainfall measurements necessitate some form of areal interpolation, such as Thiessen's Polygons or the isohyetal method, and the assumption that all surrounding areas are similar when carrying out the return period analysis. Spatial resolution has improved from Bilham's country-wide analysis to the smaller regional scale mapping used in the FSR-II (1975), and more recently the regional work of Stewart and Reed (1989), and Clark (1991). However, truly detailed intensity-duration-frequency investigation has not been possible in Great Britain, due to the constraints imposed by point rainfall estimates. As a consequence, rainfall return periods calculated as uniform for whole regions, will be unrepresentative for areas of local orographic enhancement, generated by hills as low as 50m (Bergeron, 1967), rainshadow or

both. A further compounding factor of most raingauge networks is that gauge density is lowest in remote and mountainous areas where the majority of water supply and flood production arises and data is needed the most.

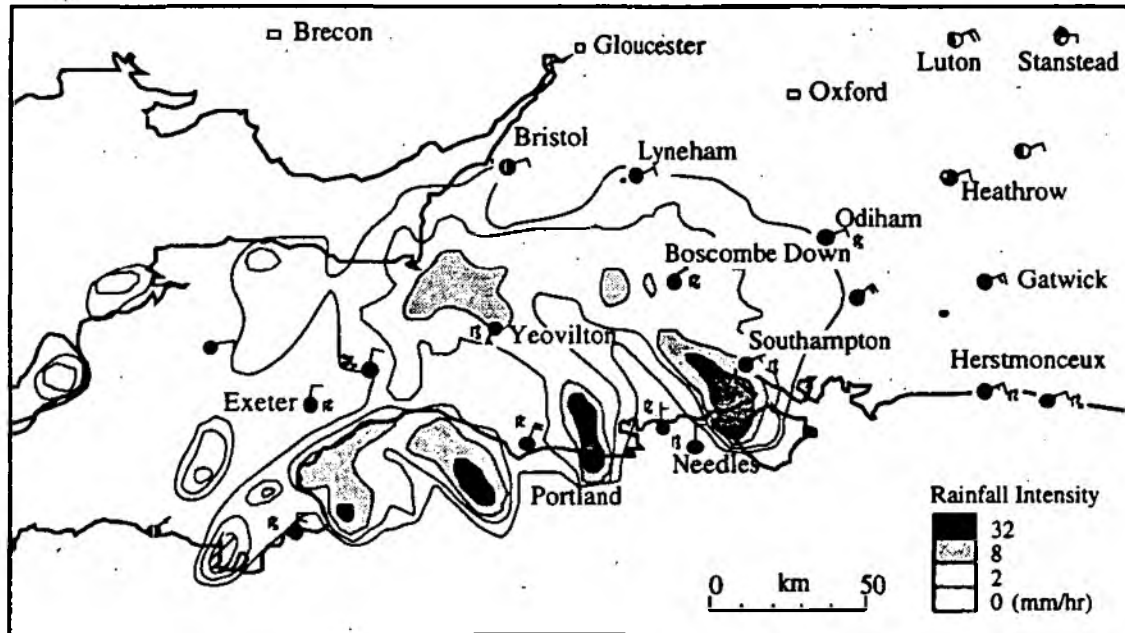


Figure 4.1 Location of Five Storm Cells Over Southern England, 5th of June, 1983 1150 GMT (after Hill, 1984)

4.4 Rainfall-Frequency Analysis Using Radar

4.4.1 Introduction

When first conceived, it was intended to use radar rainfall data from the South West of England in this investigation, to allow comparison with the work of Reed and Stewart (1989), Clark (1991) and others. Unfortunately, difficulties with data access meant that the analysis had to be moved to the North West region, served by the Hameldon Hill radar, which is used throughout the study.

From the last section it is obvious that many problems exist when calculating return periods using point rainfall estimates. Without exception, every author who has studied rainfall return period phenomena has noted the great spatial variation of rainfall intensity with time. Collinge (1961) found "marked variation in intensities from place to place for a given frequency and duration". Indeed, as long ago as 1935, Bilham lamented that "the information available up to the present is altogether insufficient to enable us to define the areas in which the [rainfall] liability is greater or less than the average". In order to counteract these problems and extend the applicability of return periods a method of rainfall frequency analysis has been developed utilising remotely sensed precipitation data. Several advantages are possible over raingauge data which should allow significant improvement in the analysis of rainfall frequency.

4.4.2 Potential Advantages of Using Radar

Firstly, and most importantly, single site radar data is available at relatively high spatial resolution (2km by 2km squares) quantitatively covering a total area 152km across. This immediately removes the need for interpolation between point rainfall measurements and, ground clutter aside, allows analysis of every individual radar pixel. Combined with the frequent (5 minute) updating and real time availability of radar data, this opens new applications for return period analysis.

In the past rainfall frequency has been used almost exclusively in the design of civil engineering projects, or in 'off-line', post-event appraisals, to attach return period to rainfall after a particularly significant storm. Radar allows rainfall fields to be tracked as they develop and move over catchment areas, and conventionally shows rainfall in six colour bands according to intensity. This is extremely useful but does not identify the severity of the event in terms of the area concerned. The use of radar derived rainfall measurements and an on-line intensity-duration-frequency database allows

event classification as it occurs in real time, or before it reaches an area using catchment transposition. Furthermore, radar also allows return period assessment to be carried out in areas where raingauge placement would be impossible, such as out at sea, to aid storm classification as the event approaches.

4.5 Statistical Distributions and Parameter Estimation

4.5.1 Representation of Extreme Hydrological Data

Chow *et al.* (1988) point out that the most extreme events in hydrology are located in the tail of the probability distribution from which they are drawn. One of the oldest and simplest methods of determining the magnitude of a given return period event from these distributions is to use plotting positions. After ranking the data, $m_{(1)}, \dots, m_{(n)}$, where $m_{(1)}$ is the largest, the assumption is made that a given data sample might reasonably have been drawn randomly from the type of distribution in question (Cunnane, 1977). The recurrence interval, T , is then calculated from one of a number of formulae, each relating to a given distribution type, such as the Gringorten equation, which relates to the Gumbel distribution (described in section 4.5.1 (iii)). Plotting position formulae only provide an approximation of a given statistical distribution, however, and no parameter estimation is carried out to provide an accurate fit to the data.

Several distributions have been applied to extreme data, some of which are outlined briefly below. For a more detailed discussion the reader is referred to the work of Kottegoda (1980). For the purposes of this investigation the Extreme Value distribution was used, with parameter estimation by Probability Weighted Moments.

i) Two-Parameter Lognormal Distribution

Whilst the normal (bell shaped) distribution is rarely appropriate for the analysis of environmental extremes, the lognormal distribution has been widely used. The probability density function of the two-parameter lognormal distribution is :

$$f(x) = \frac{1}{\sqrt{2\pi}\sigma x} \exp\left\{-\frac{1}{2}\left(\frac{\ln x - \mu}{\sigma}\right)^2\right\} \quad (4.2)$$

where μ is a location parameter, σ is a scale parameter.

The magnitude of the event with return period $T=1/p$ can be estimated from :

$$\ln X_T = \mu + \sigma Z_p \quad (4.3)$$

Where Z_p is the standard normal variate with exceedance probability p .

The lognormal distribution has the advantages over the normal distribution that it is bounded ($X > 0$) and that the log transformation tends to reduce the positive skewness commonly found in hydrological data (Chow *et al.*, 1988). However, it requires the logs of the data to be symmetrical about their mean and the use of two parameters means that the distribution does not always reproduce the observed data well.

ii) Pearson Type III Distribution

The Pearson Type III distribution, also known as the three-parameter gamma distribution, is one of a large family of probability distributions developed by Pearson (NERC, 1975). Both the exponential and gamma distributions are special cases of the Pearson Type III.

The distribution function is :

$$f(x) = \frac{(x - x_0)^{\gamma-1} \exp\left\{-\frac{(x - x_0)}{\beta}\right\}}{\beta^\gamma \Gamma(\gamma)} \quad (4.4)$$

where x_0 , β and γ control location, scale and shape respectively, x_0 constituting a lower bound. Calculating the magnitude of the event with a return period T can be difficult. The simplest approach is to use the sample mean, standard deviation and a factor K_T to estimate the T -year event :

$$x_T = \bar{x} + \sigma K_T \quad (4.5)$$

The factor K_T varies with return period (T) and sample skewness g (Kite, 1977; Linsley *et al.*, 1982). Sample skewness g can be calculated directly from the sample, or estimated from the parameter γ using :

$$g = \frac{2}{\sqrt{\gamma}} \quad (4.6)$$

Although it has been applied to extreme event analysis, the Pearson Type III distribution is difficult to apply and, because sample skewness is very uncertain, may give unreliable results, (Matalas and Wallis, 1973).

iii) Extreme Value Distribution

The distribution chosen for use in this investigation was the Extreme Value distribution described below. Extreme values selected from sets of samples of any probability distribution have been shown to be covered by one of three forms of the Extreme Value distribution, (Fisher and Tippett, 1928). The properties of the three forms were further developed by Gumbel (1941) for the EVI (or 'Gumbel' distribution), Frechet (1927) for EVII and Weibull (1939) for EVIII. Jenkinson (1955) showed EVI, EVII and EVIII to be special cases of a single distribution call the 'Generalised Extreme Value' distribution (GEV).

The probability density function for GEV is :

$$f(x) = \exp\left[-\left(1 - k \frac{x-u}{\alpha}\right)^{1/k}\right] \quad (4.7)$$

where u is the location parameter, α is the scale parameter and k is the shape parameter. The shape parameter (k) determines which Extreme Value distribution is represented.

For $k=0$ use Extreme Value I (Gumbel). Here the GEV distribution simplifies to the EVI distribution, having two parameters, the probability distribution being :

$$f(x) = \exp\left[-\exp\left(-\frac{x-u}{\alpha}\right)\right] \quad -\infty \leq x \leq \infty \quad (4.8)$$

where u is the location parameter and α the scale parameter.

The magnitude of an event x_T with return period T is estimated from :

$$x_T = u + \alpha y_T \quad (4.9)$$

where y_T , the 'Gumbel reduced variate' is calculated from :

$$y_T = -\ln\left[\ln\left(\frac{T}{T-1}\right)\right] \quad (4.10)$$

When $k < 0$ an EVII distribution follows for which the equation applies for :

$$(u + \alpha/k) \leq x < \infty \quad (4.11)$$

Here x is bounded from below by $u + \alpha/k$.

When $k > 0$ an EVIII distribution is indicated for which the equation applies for :

$$-\infty < x \leq (u + \alpha/k) \quad (4.12)$$

Here x is bounded from above by $u + \alpha/k$.

The magnitude of an event with return period T years can be determined by :

$$x_T = u + \alpha \left(\frac{1 - \exp(-ky_T)}{k} \right) \quad (4.13)$$

where y_T is the 'Gumbel reduced variate' as shown in equation 4.10.

The EVI, or Gumbel distribution, has been widely used in frequency analysis of extreme hydrological data. This is partly due to its ease of application, and partly because of the theoretical arguments developed by Gumbel to support it. The GEV family of distributions is a flexible one, which has been found to fit both rainfall and flood extremes in a variety of environments (Chow *et al.*, 1988).

4.5.2 Parameter Estimation

i) Method Of Moments

The parameters of a probability distribution can be expressed in terms of moments of the distribution. If these can be estimated from a data sample then it is possible to estimate the distribution parameters. However, estimates of higher moments, such as skewness, may be uncertain when made from small samples. Also, the method has been shown to give unreliable estimates for distributions with three or more parameters (Kite, 1977).

ii) Method Of Maximum Likelihood

The probability of obtaining a particular sample from a probability distribution with specified parameters can be defined from the 'likelihood' function :

$$L = \prod_{i=1}^N f(x_i|\theta) \quad (4.14)$$

where the probability density function, $f(x_i|\theta)$, is the probability of an event of magnitude x_i occurring given a distribution parameter θ , and N is the sample size.

The parameters producing the value of the likelihood function are assumed to be those which 'most likely' generated the observed sample. These are thus Maximum Likelihood estimates of the distribution parameters. The ML procedure is based on large sample theory, and when used with large samples this technique gives the 'best' estimates of all methods. However, for sample sizes of less than 50 or so other methods may give parameter estimates that are statistically more efficient (NERC, 1975).

iii) Probability Weighted Moments

The method of parameter estimation chosen for use here was that of Probability Weighted Moments. This method, a generalisation of the usual moments of a probability distribution, was introduced to hydrology by Greenwood *et al.* (1979). The general form for a PWM is :

$$M_{r,s,t} = \int x^r F(x)^s (1 - F(x))^t f(x) dx \quad (4.15)$$

where $f(x)$ is the probability density function, and $F(x)$ is the cumulative distribution function. If s and t are zero, this reduces to the conventional moments expression, PWM being analogous to conventional moments, but defined either by :

$$M_{1,0,t} = \int x(1 - F(x))^t f(x) dx \quad (4.16)$$

or

$$M_{1,s,0} = \int xF(x)^s f(x)dx \quad (4.17)$$

The choice is related to the particular probability distribution being used. Parameter estimation procedures tend to be easier to apply than Maximum Likelihood methods, involving little or no iteration, and being more robust than conventional techniques (Hosking, 1986). Uncertainties in sample estimates of high conventional moments arise mainly due to the observed values being raised to a high power (eg. three for skewness). The moments derived are thus sensitive to quite small data volume changes especially when these are unusually large or small. Probability Weighted Moments are all linear functions of the sample data and so are much less sensitive to data idiosyncrasies. PWM estimation has also been found to be more efficient than Maximum Likelihood procedures for the small sample sizes usually available in hydrology (Hosking *et al.*, 1985). This was thought to be especially useful for the short record available for radar data.

4.6 Distributed Intensity-Duration-Frequency Analysis

4.6.1 Rainfall Data

The radar chosen for use in the investigation was the Hameldon Hill device which covers the North West region of England. This has the longest weather radar data record, having run virtually continuously since its launch in 1978. Although it was originally hoped to use all the significant events from this archive, the size of the original data record and time constraints forced the use of a synthetic database. This was formed for one catchment, for 20 years duration, as outlined below. The catchment chosen for the analysis was Blackford Bridge, details of which can be found in Chapter 5.

In creating an artificial radar data archive, analysis was first carried out on five years of event raingauge data for Blackford Bridge, to find a realistic number of rainfall events per year. Interrogation of the National Rivers Authorities RAINARK system showed that rainfall of greater than 15 minutes duration occurred on average 34 times per year. This gave a total of 680 such events over a 20 year period. A synthetic data archive of 684 storms was then formed using 19 clearly delineated frontal events, all observed within the quantitative range of the radar.

Each storm event was passed over the Hameldon Hill radar area 36 times, the Blackford catchment being transposed to 36 different positions as shown in Figure 4.2. Each replay of the storm, with the catchment in a new position, created a 'different' rainfall event. This effectively created the theoretical number of storms necessary, and although it is not claimed to be truly representative of 20 years of radar data, it did provide a data archive to carry out the distributed Intensity-Duration-Frequency analysis and apply the technique.

4.7 Analysis of the Rainfall Archive

4.7.1 Data Extraction

The first step in the analysis procedure was to find the rainfall intensity figures for set durations at each of the 2km by 2km radar pixels covering the Blackford Bridge subcatchment.

$$\hat{\alpha} = \frac{\hat{k}(2M_1 - M_0)}{\Gamma(1 + \hat{k})(1 - 2^{-\hat{k}})} \quad (4.21)$$

$$\hat{u} = M_0 + \hat{\alpha}[\Gamma(1 + \hat{k}) - 1] / \hat{k} \quad (4.22)$$

Note that $\Gamma(x)$ is the Gamma Function and is defined by Abramowitz and Stegun (1972) as :

$$\Gamma(x) = \int_0^{\infty} \exp^{-y} y^x dy \quad \text{and} \quad \Gamma(1 + x) = x! \quad (4.23)$$

Effectively the information within each pixel / duration / intensity rank distribution has now been reduced to the three parameters k , α and u . The distribution estimation parameters were also assessed for the catchment averaged rainfall. These variables were stored for each radar pixel and duration in a separate 'Parameter' array matrix for use in real-time return period assessment (sections 4.8 and 4.9) and post-event appraisal (section 4.10).

4.8 Real-Time Use

4.8.1 Real-Time Return Period Assessment

Having carried out the intensity-duration-frequency analysis on the artificial radar data record an actual storm event was replayed over the Hameldon Hill radar area. For every 5 minute image the rainfall was extracted from the radar array corresponding to the Blackford Bridge area and its intensity and duration recorded for each individual radar pixel. In this way, rainfall duration was assessed for each 2km by 2km square from the start of precipitation on that pixel.

With the arrival of each new radar image the appropriate k , α and u values were obtained from the 'Parameter' array for the relevant radar area and rainfall duration. The rainfall magnitude x_T was then assigned a return period (T) from the relevant distribution. If $k = 0$ then the GEV simplified to the EVI (Gumbel classification), such that :

$$T = \frac{-v}{1-v} \quad (4.24)$$

where v is given by :

$$v = \exp\left[\exp\left(-\frac{x_T - \hat{u}}{\hat{\alpha}}\right)\right] \quad (4.25)$$

When the k value for a pixel intensity-duration data set differed significantly from zero, a GEV distribution was applied. Here the return period (T) of the x_T event was derived from :

$$T = \frac{1}{1 - \exp[-\exp(-\eta)]} \quad (4.26)$$

where η is calculated from :

$$\eta = \frac{-\ln\left[1 - \hat{k}\left(\frac{x_T - \hat{u}}{\hat{\alpha}}\right)\right]}{\hat{k}} \quad (4.27)$$

This procedure was quick to perform in simulated real-time, due to the relative simplicity of the calculations. Once identified, the return period for each 2km by 2km pixel was displayed using UNIRAS graphics. Figures 4.4 and 4.5 show examples from the display produced in the real-time simulation as storm rainfall fell over the catchment.

Figure 4.4 *Blackford Bridge : Storm Return Period Analysis*

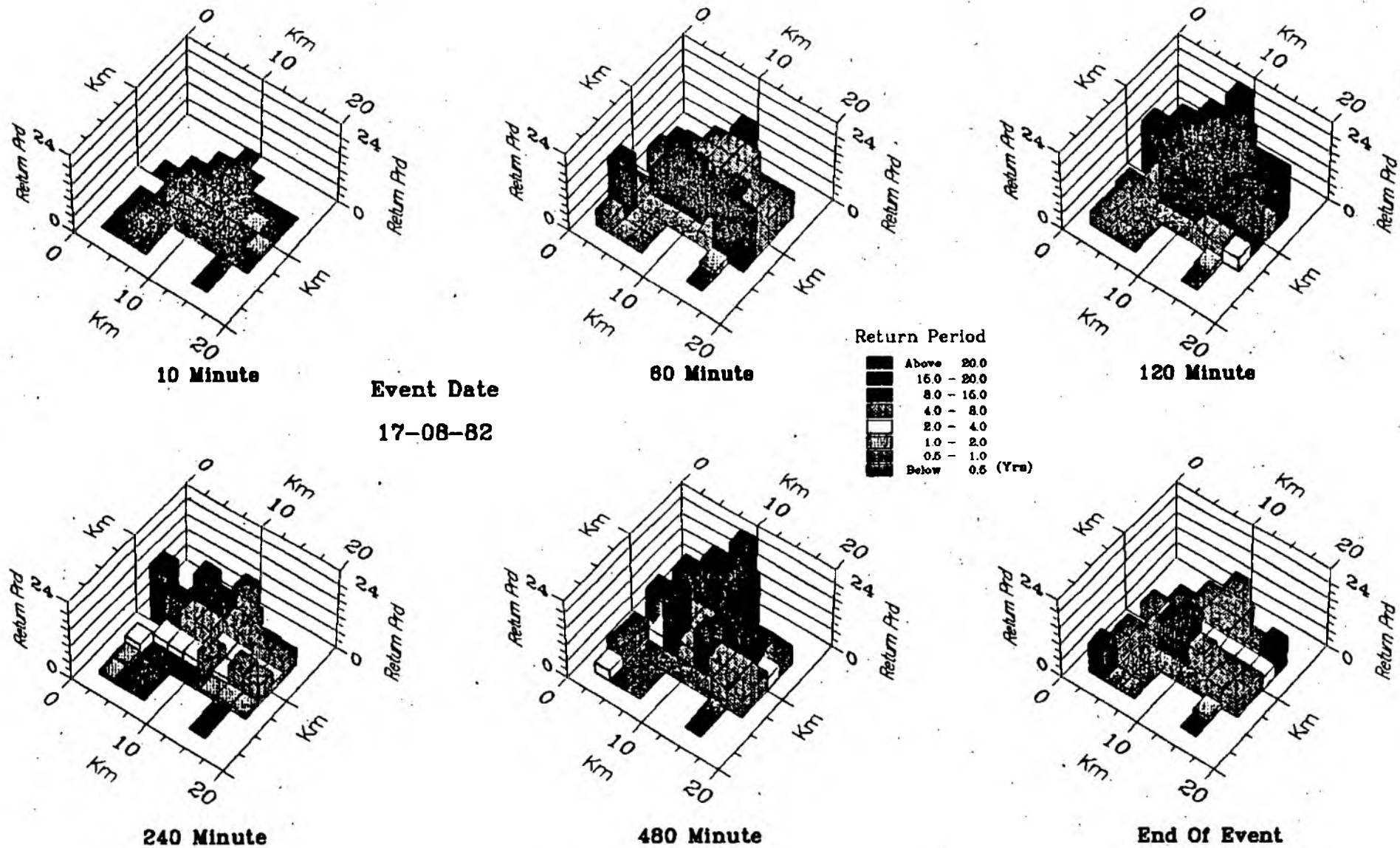
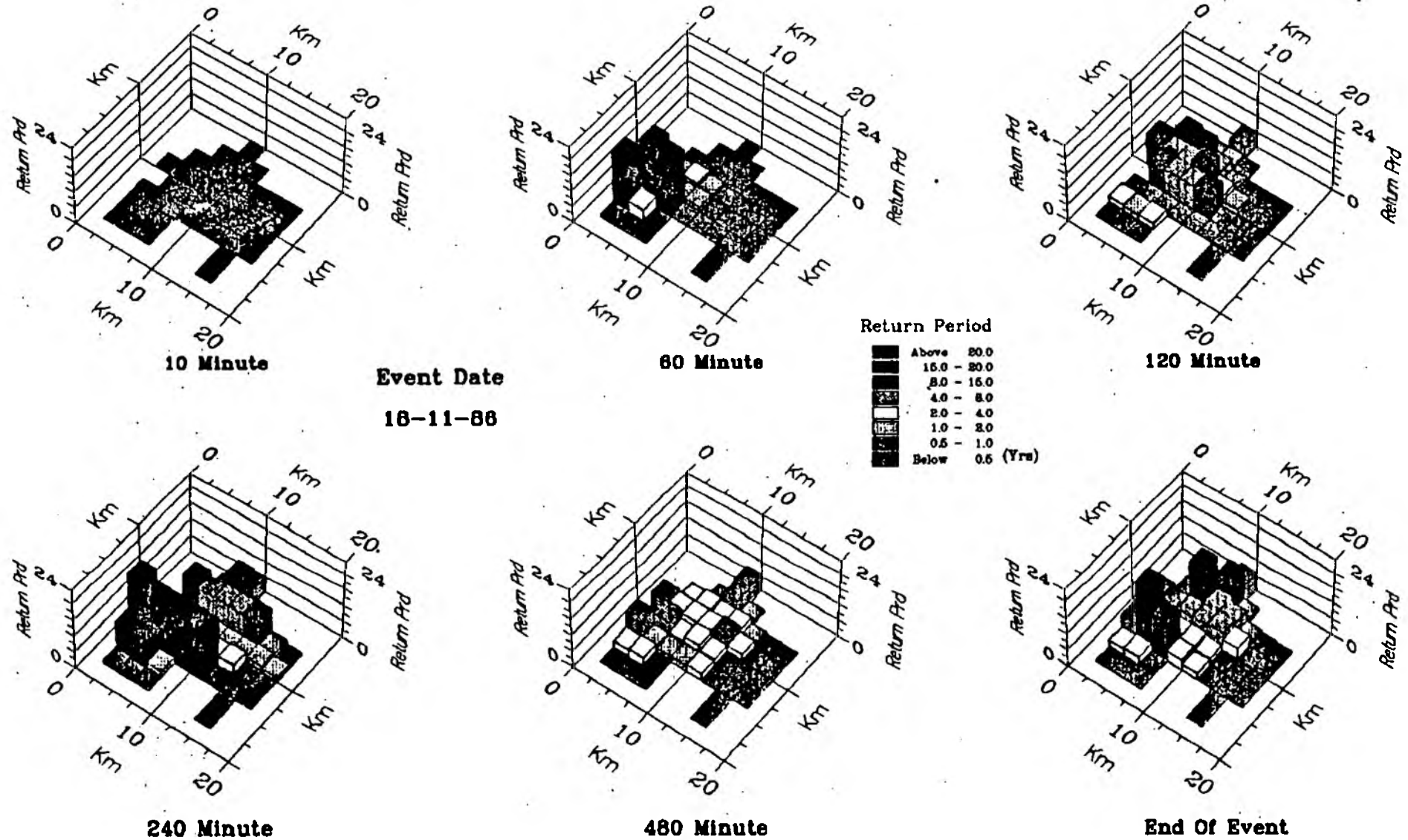


Figure 4.5 Blackford Bridge : Storm Return Period Analysis



These figures demonstrate how the return period of the rainfall at each catchment pixel varies with time, using knowledge of catchment history to label its severity. The return period plots reflect the occurrence interval of the rainfall up to the last radar image. It should be noted that the 'true' return period is that generated at the end of the event, when the full precipitation and duration are known.

4.8.2 Database Updating

Any incoming event, as well as being classified for recurrence interval, should also be added to the database distribution. Unfortunately this is not possible as the storm takes place. Firstly, the maximum rainfall values for each duration cannot be identified until the end of the event. Also, adding to the database, ranking of the data and parameter estimation would be time consuming to perform in real-time. To deal with this problem, a short routine was written to store the rainfall intensity and duration values for each radar pixel as the storm takes place. The analysis subroutine, described in section 4.7.1 was then called and the resulting rainfall values included in the database matrix.

The event was considered to have ended when no rainfall had occurred over the catchment for a period of n hours (a value of $n = 2$ being used for this investigation). The analysis subroutine was then called and the database matrix updated and re-ranked, including the new rainfall values. Probability Weighted Moments were fitted to the new distributions and the resulting α and u estimates stored with k in the 'Parameter' array. Even though it is dealing with large amounts of information, the system update procedure takes only a few seconds and is then ready for an incoming event again. In an operational setting, it would be possible to keep two database matrices, one updating whilst the other is ready for use. This would reduce any possibility of the system being unavailable when an event arrives.

4.9 Catchment Transposition

A technique was evolved to effectively transpose the catchment from its actual position, into the path of the incoming storm, if it was perceived to be moving towards the 'target' catchment area. In order to assess the likely return period of the event, before it hits the catchment, the operator enters the start and stop times of previous radar frames to be replayed. Thus, if the time now is 16:45 then a start time of 16:00 and stop time of 16:35 may be used giving the event 35 minutes to pass over the catchment. Coordinates are then entered by the user to position the top left hand coordinate of the catchment in front of the storm, so that it will pass over it in the 35 minute period. These coordinates are used to change the position in the radar data array from which radar intensity values are read. In a 'Windows' based system the catchment could be 'grabbed' and moved manually to the desired position using a mouse, although this approach was not adopted here.

With the catchment position transposed, the seven radar frames from 16:00 to 16:35 are then replayed and rainfall intensities extracted to give a forecast return period for the event in terms of the catchment of interest. An example of this procedure is given in figure 4.7. This procedure may be carried out as many times as required when new radar data becomes available, so that the event risk may be identified as becoming more or less severe as the storm approaches. An alternative to catchment transposition is the cross correlation forecasting system outlined in Chapter 8, using linear extrapolation to move the storm event over the stationary catchment.

4.10 Off-Line Use

As well as providing real-time applicability the technique developed and outlined above still allows the more 'traditional' use of return periods. Here it can be used to

attach a recurrence interval to a past event or define the rainfall expected of a given return period and duration.

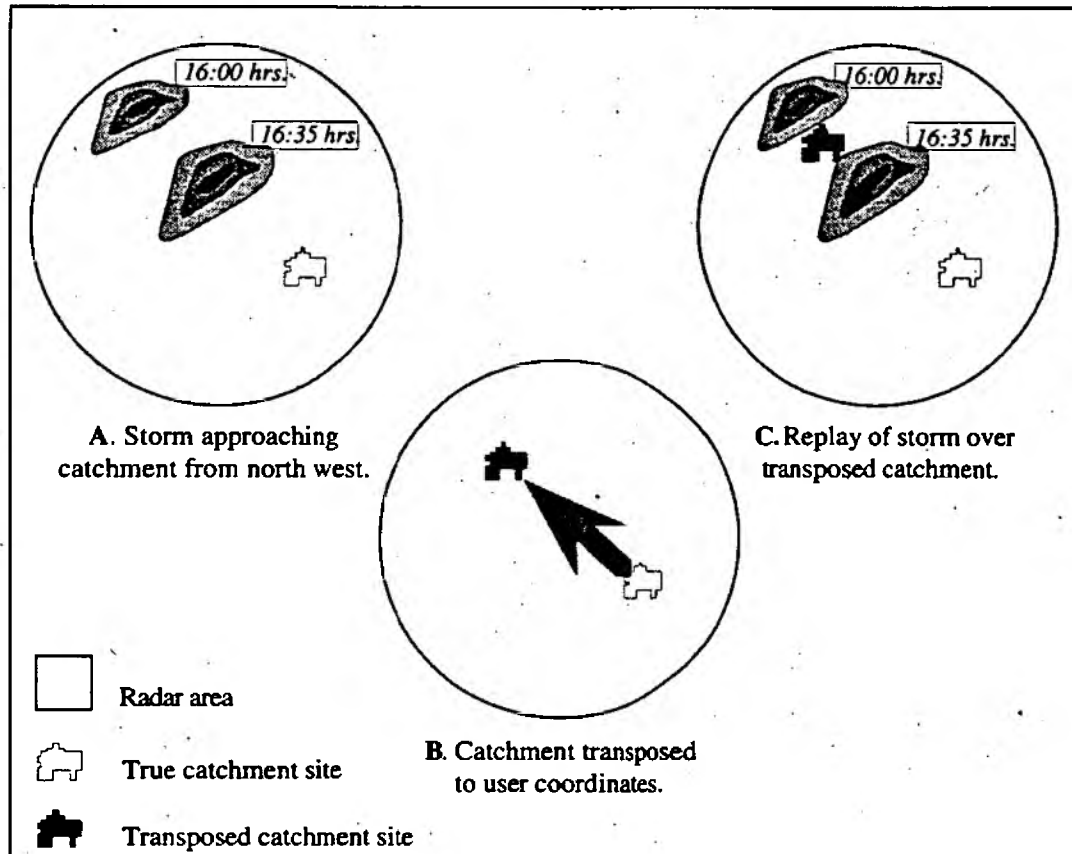


Figure 4.7 Catchment transposition to allow return period forecasting

4.10.1 Post-Event Appraisal

When assessing the return period of an archive event of severity x_T , the distribution estimation parameters k , α and u are used for the area and duration of interest, be it distributed pixels or catchment wide. The Gumbel equation is then used as in equations 4.24 and 4.25 when $k = 0$. The GEV distribution is applied if k differs significantly from zero, using equation 4.26 and 4.27.

4.10.2 Design Use

Perhaps the most frequent application of the return period principle has been in defining the rainfall magnitude expected from an event of given recurrence interval. The distributed intensity-duration-frequency analysis proposed in this chapter lends itself well to this use of the analysis. The results obtained should also be more accurate, given the availability of a sufficiently long radar record.

An enormous advantage of radar is the wide spatial coverage it brings to rainfall-frequency analysis. In so doing, it significantly reduces the number of 'ungauged catchments' for which no knowledge exists of the rainfall characteristics. With a GEV I distribution fitted to the pixel or catchment data, the rainfall x_T of a given return period (T) may be found by :

$$x_T = u + \alpha y_T$$

For a GEV II or III distribution, the T year rainfall is determined by :

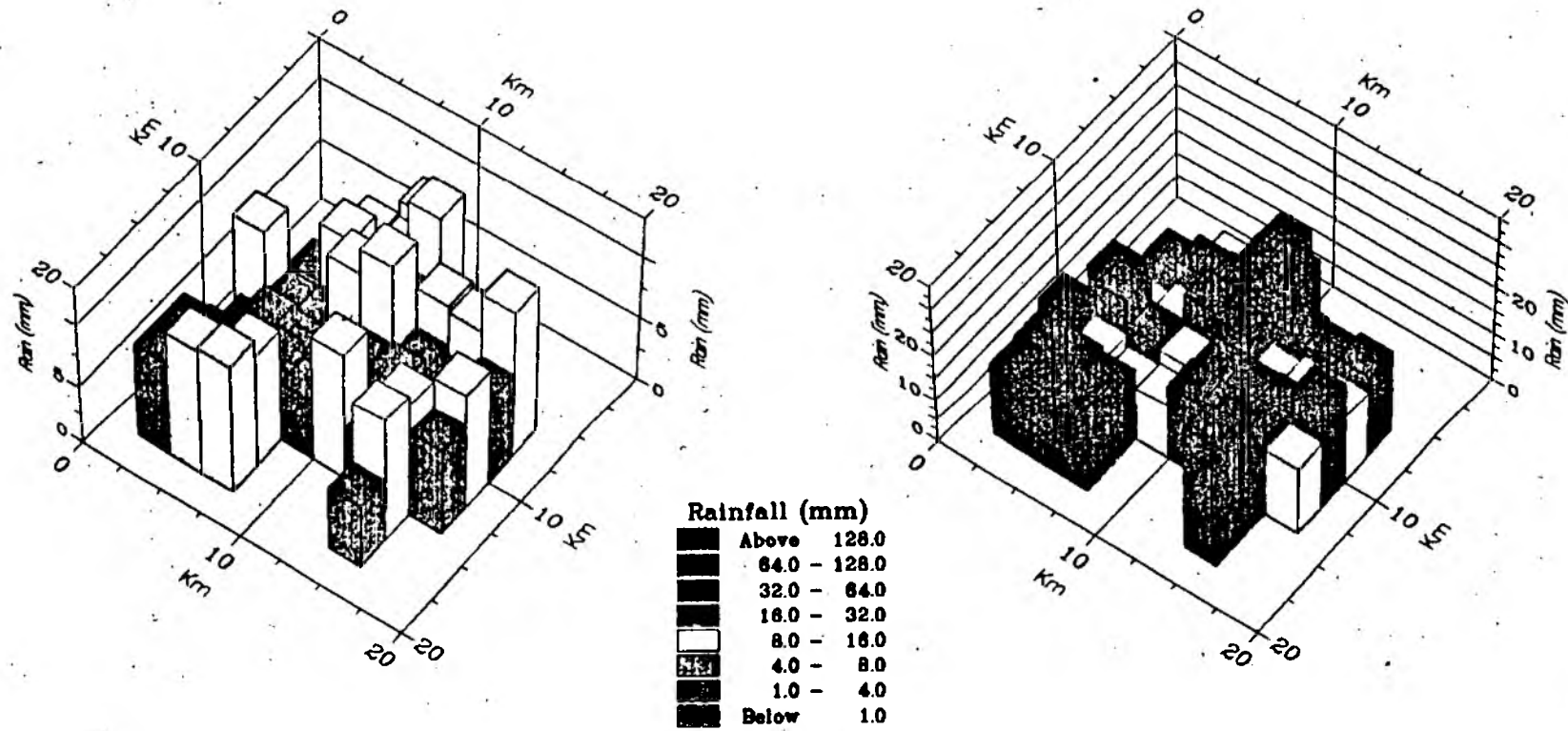
$$x_T = u + \alpha \left(\frac{1 - \exp(-ky_T)}{k} \right)$$

where y_T , the 'Gumbel reduced variate' is calculated from :

$$y_T = -\ln \left[\ln \left(\frac{T}{T-1} \right) \right]$$

This procedure is easily automatable, using the distribution estimate parameters α and u , discussed in section 4.7.3. The user need only enter the area and return period of interest to assess a magnitude for the desired event. Figure 4.8 Shows the distributed rainfall over the Blackford Bridge area for the (a) 20 minute, 1 in 10 year event, and (b) 2 hour 1 in 20 year event, from the synthetic data-base.

Figure 4.8 *Blackford Bridge : Rainfall Return Period Examples*



a) 20 Minute Rainfall, 10 Year Return Period

b) 120 Minute Rainfall, 20 Year Return Period

4.11 Discussion

The techniques outlined above for attaching risk to storm events in terms of rainfall return period have some drawbacks. Firstly, the radar rainfall record is limited to a present maximum of 14 years, not all of which is held in archive form. Hershfield (1961) found that a 50 year record should be used to ensure a stable data set. However, from his work a 10 year record may still be applicable with a 5% increase in mean and a 30% increase in standard deviation. The data record is set to increase in the future, however, as all signs point to the continued and more extensive use of radar technology. A further problem is the definition of the start and finish of a rainfall event. This is essential for return period assessment, and may be difficult during long and fragmented rainfall. Also, remotely sensed data inherently suffers from those problems detailed in chapter 3 sections 3.8, 3.9 and 3.10. Finally, rainfall of a given return period does not necessarily lead to flooding of the same rarity, Kidd and Packman (1980) stating that the one in ten year flood may result from anywhere between the one year and 40 year rainfall. Procedures have been evolved to relate rainfall return period to flow return period, however, NERC (1975).

Against these problems, however, there are a number of potential advantages to this technique and its use of radar derived rainfall measurements. One significant plus point is the reduction in analysis scale possible with radar. Intensity-duration-frequency analysis can be carried out on a 2km by 2km square grid. This allows the capture of local orographic effects and answers for the first time the problems identified by Bilham, over 55 years ago. Alternatively data may be 'lumped' on a catchment wide basis if a less distributed study is needed. The broad areal quantitative coverage offered by radar also drastically reduces the number of 'ungauged' catchments in the United Kingdom (a map of radar coverage is shown in figure 3.1, chapter 3). This again removes generalisations about areas under investigation, and the need to apply regional, or averaged parameters. The existing

methods of collection, processing and dissemination of radar information, using computer networks, allow the automation of the IDF analysis on a pixel or catchment-wide basis and could easily be added to present-day systems.

The constantly updating nature of radar means that rainfall return period assessment can be carried out in real time on the precipitation occurring up to the last five minute image. This could also be used to complement post-event appraisal carried out on heavy rainfall.

Remotely sensed data is routinely displayed as rainfall intensities occurring at each radar pixel. However, this gives no indication as to the severity of the event in terms of the area under the precipitation, a 25 mm fall in five minutes being quite common in parts of the world but extremely rare in England, for example. Potyondy (1987) states that "Linking forecasts to frequency concepts holds promise for better understanding potential flooding problems and the likelihood of their exceedance". The technique described here allows transformation of precipitation 'data' into comprehensible 'information', using knowledge of the catchment rainfall history.

The methodology outlined in this chapter has been developed to show event risk in terms of return period at the catchment of interest, and has been described as "a very good way of classifying an event before it happens" (Pearse, 1992). The technique provides a useful descriptive tool and offers an effective means of summarising the vast quantities of information contained within a sequence of radar data. It also provides a basis for the effective comparison of different storm events.

The use of recorded radar images and catchment transposition in return period forecasting has its pros and cons. Although catchment positioning is user defined, the procedure assumes that storm movement is fairly uniform in direction and velocity and as such it has less applicability to convective events. However, work is under

way at the Meteorological Office on the GANDOLF (*Generating Advanced Nowcasts for Development in Operational Landsurface Flood forecasting*) project to forecast thunderstorm activity, which may yield success in this field. In frontal situations, on the other hand, the ability to artificially pass the storm over the catchment area allows changes in risk to be assessed as it approaches. This also gives the opportunity to carry out analysis where rain gauge placement is impossible, such as out at sea. Designating the approaching precipitation in this way may aid the duty hydrologist in the decision to monitor river levels, disseminating warnings and so on, in a potential flood situation. This is especially important in rapid response areas where lead time is at a premium.

4.12 Conclusion

Storm return periods have long been used in a design role to assess the rainfall expected from an event of given recurrence interval. Intensity-duration-frequency analyses have mainly been carried out with point rainfall estimation from raingauges, using regionalization to extend record length. The relationships gained have then been assigned to large regions of 'uniform' rainfall. The problems at each stage of this type of analysis - raingauge representativeness, regionalization and widespread areal application of the results has lead to the development of the IDF procedure described in this chapter.

Here, remotely sensed precipitation data was used to calculate intensity-duration-frequency relationships for each of the 2km by 2km radar pixels, giving wide areal coverage and detailed resolution. An Extreme Value Distribution was fitted to the data using Probability Weighted Moments, for each radar square at rainfall durations from 5 minutes to 12 hours. The use of radar information, with its real-time updating, allows a new application for return periods. Using this technique rainfall severity, or 'risk', may be assessed as an event takes place, using knowledge of the catchments

rainfall history. A simple transposition and replay procedure was developed to allow catchment placement in front of the event and determination of recurrence interval before the storm reaches the catchment.

The distributed IDF technique is rapid to apply and would slot readily into the existing radar data processing system. In this way, automatic and constant updating of the event database would provide return period information for every 4km^2 within the radar range. Perhaps the greatest drawback to the technique is the relatively short record of radar data available. However, in many instances the low areal coverage raingauges leaves many areas completely unsampled, necessitating the use of averaging techniques, simply because no data is available. In this case, the short record of wide coverage radar data is better than no data at all.

CHAPTER 5

RAINFALL ANALYSIS

5.1 Introduction

At its most basic river flood production may be thought of as a simple input - output system. In an upland rural drainage system input comes from precipitation, principally in the form of rainfall in the area under study. Once precipitation occurs its effects are modified by the form and state of the catchment before output takes place as runoff. In this chapter, analysis is concentrated on the input to the system as experienced by the catchment in the form of the rainfall hyetograph.

As outlined in section 1.2 attempts were made at knowledge engineering to establish information about how an experienced duty officer carries out flood forecasting during a flood event. Unfortunately the knowledge gained was too vague and lacking in firm 'rules' to be used in a knowledge based environment. With this in mind, analysis was undertaken to determine which individual rainfall characteristics are of most importance in flood production on an single area basis and which are bear little or no relevance. It was hoped that once established, this 'expertise' may be put to use in forecasting the likelihood and severity of any future rapid response event by examination of storm characteristics upwind of the catchment 'target' area, using knowledge based techniques. Whilst it is realised that the status of the catchment, be it dry, saturated or snowbound for example, will greatly modify the type of flood which takes place, flooding will not occur without the initial precipitation input.

For the analysis of the nature and form of flood producing storm events, Blackford Bridge, a subcatchment of the Irwell, was chosen (see figure 5.1). This subcatchment, lying on the river Roch, has been a Meteorological Office defined radar

area since 1986 and is well within the coverage of the weather radar at Hameldon Hill. The catchment itself covers 186 km² and has a rapid time of concentration, peaking at 4.5 hours (Davidson, 1980). The subcatchment is predominantly elevated moorland with approximately 8% urban coverage (Owens, 1986).

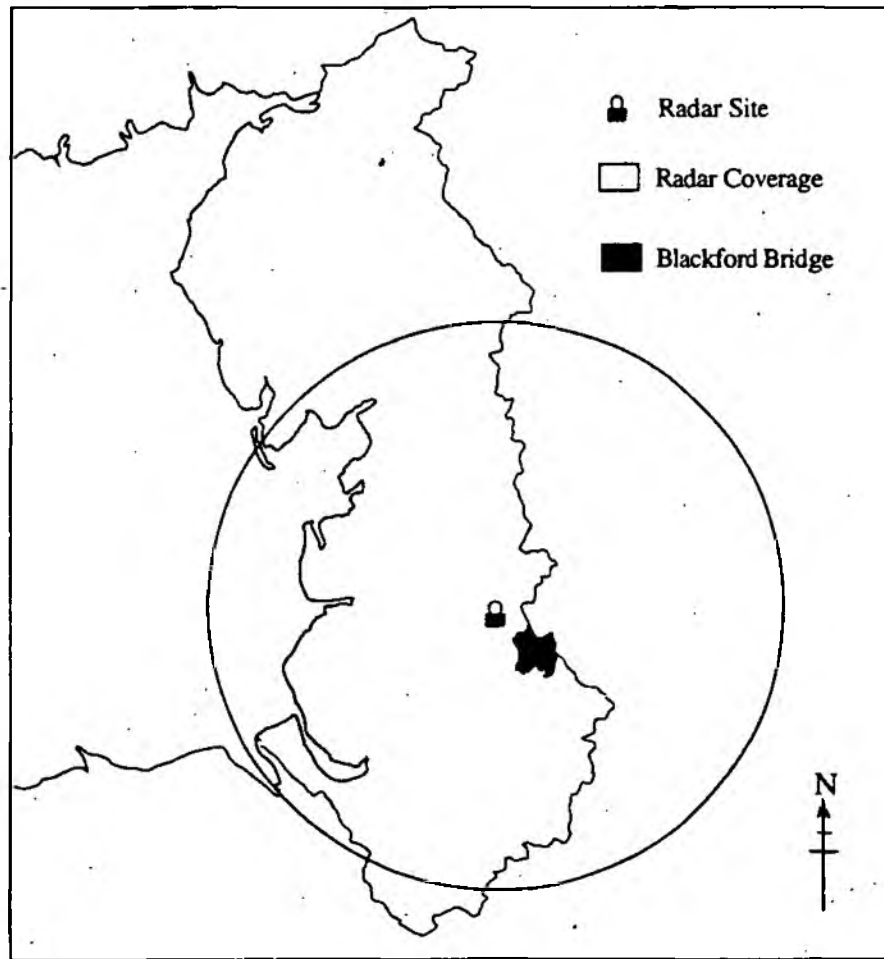


Figure 5.1 *The North West Region, Showing Hameldon Hill Radar with 75km Quantitative Range and The Blackford Bridge Subcatchment*

5.2 Rainfall - Runoff Data

5.2.1 Data Sources

Rainfall data for the Blackford Bridge area is available from the Hameldon Hill weather radar station 21Km to the north. The radar produces quantitative subcatchment rainfall totals at 15 minute intervals processed and calibrated at-site. Flow data for the catchment comes from the non-standard broad crested, crescent shaped weir at Blackford Bridge and is available also at 15 minute intervals.

Figure 5.2 shows the location of the Blackford Bridge area in relation to the National Grid. The figure also marks the position of the flow measuring weir and raingauge within the catchment.

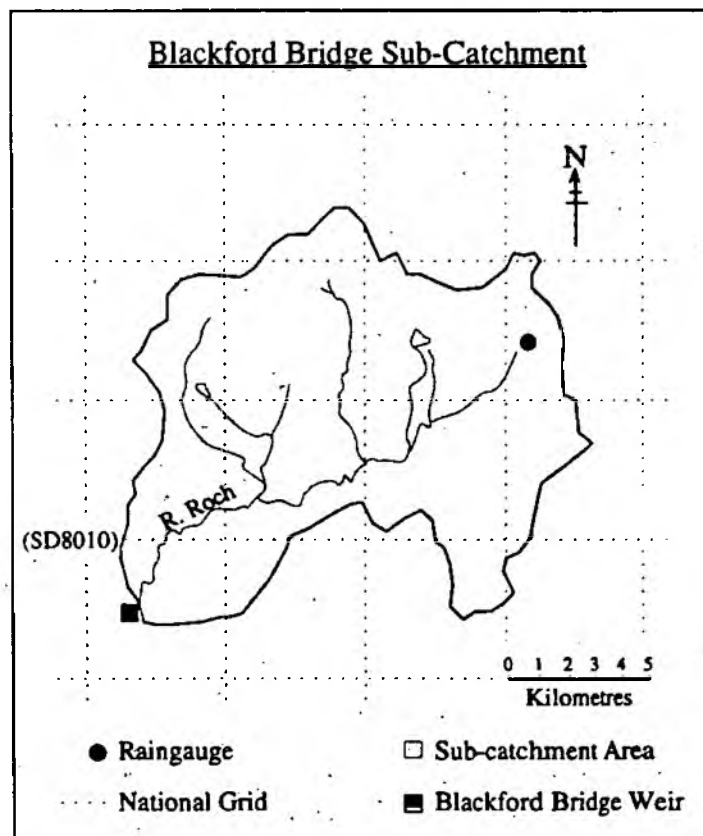


Figure 5.2 *The Blackford Bridge Subcatchment*

5.2.2 Event Selection

Rainfall-runoff events were chosen subjectively, each one being clearly delineated from previous precipitation or flow sequences. Long and complex rainfall sequences were avoided in order to simplify the identification of any input - output relationships. A full list of all storm events used, together with their rainfall and runoff characteristics is shown in table 5.1.

5.2.3 Data Pre-Processing

i) Radar Information

Initial processing of the radar data was carried out manually to identify and remove any errors in the event record, such as missing frames, anomalous propagation or bright-band (discussed in Chapter 3). In order to analyse and display the data, software was developed by the author in VAX FORTRAN to read Meteorological office magnetic tapes on which radar data is disseminated post event. Each radar frame consists of a header, containing information about the date, time, radar site and resolution of the data. This is followed by the rainfall information, in the form of rainfall volume over the defined subcatchment.

Once read from the magnetic tape each event was saved as a rainfall file to the hard disk of a MicroVax II. Data visualisation was carried out using the UNIRAS FORTRAN Graphics Libraries. The UNIRAS system allows FORTRAN code to be combined with calls to a library of subroutines. These subroutines create graphics for output to workstations and plotters, etc. This system was used to create a radar replay program, whereby the radar frames could be displayed one by one, to track storm movement and identify any problems such as bright-band. Figure 5.3 shows six frames from a typical rainfall radar sequence. This form of processing led to the rejection of several events which contained potential data errors.

Figure 5.3 Radar Rainfall Movement



Time 9:28



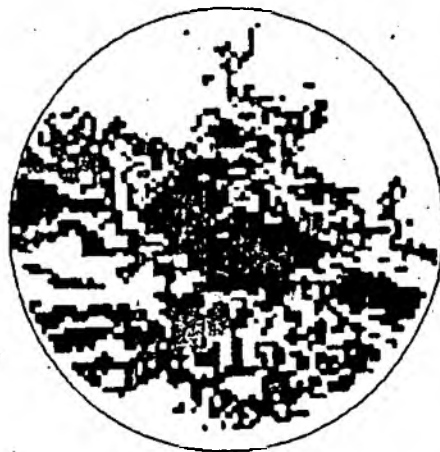
Time 9:32



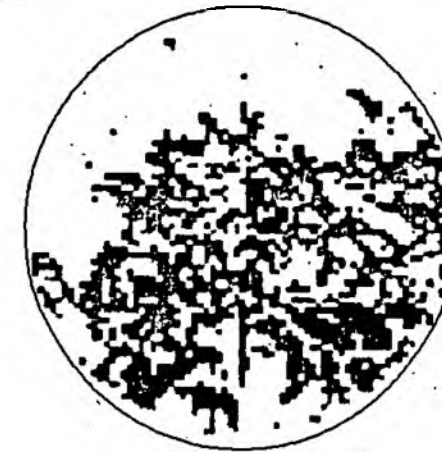
Time 9:37



Time 9:52



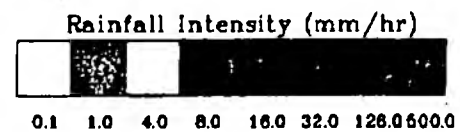
Time 10:12



Time 10:32

Hameldon Hill Radar

Date : 02 / 11 / 84



The use of the radar display program made it possible to identify the start and finish of rainfall events. This was used to ensure that only clearly delineated storms were used in the analysis to aid identification of relationships in the rainfall-runoff process.

ii) Runoff Information

Runoff data was obtained in the form of river stage or height. Processing of the information consisted of conversion from stage to flow, using the National Rivers Authority stage-discharge parameters in a rating equation, as shown below :

$$Q = a(H+b)^c \quad (5.1)$$

where: Q is discharge (cumecs)

H is stage height (metres)

a, b, c are station constants.

For Blackford Bridge : $a = 44.558$, $b = 0.173$, $c = 2.408$

In order to assess the amount of flow due to the rainfall event alone (i.e. net runoff) the baseflow of the river, prior to hydrograph rise, was removed. 'Base flow' was taken as the initial flow occurring immediately before hydrograph rise took place. Separation was carried out by drawing a horizontal line, parallel to the time axis, to intersect with the hydrograph recession limb (see figure 5.4). As all the events used were quite large this simple method of separation was seen as adequate, since errors caused by inaccurate base flow calculation become less significant with the higher flows occurring in flood situations (Owens, 1986). The combined rainfall hyetographs and runoff hydrographs for each event used in this analysis are shown in Appendix A.

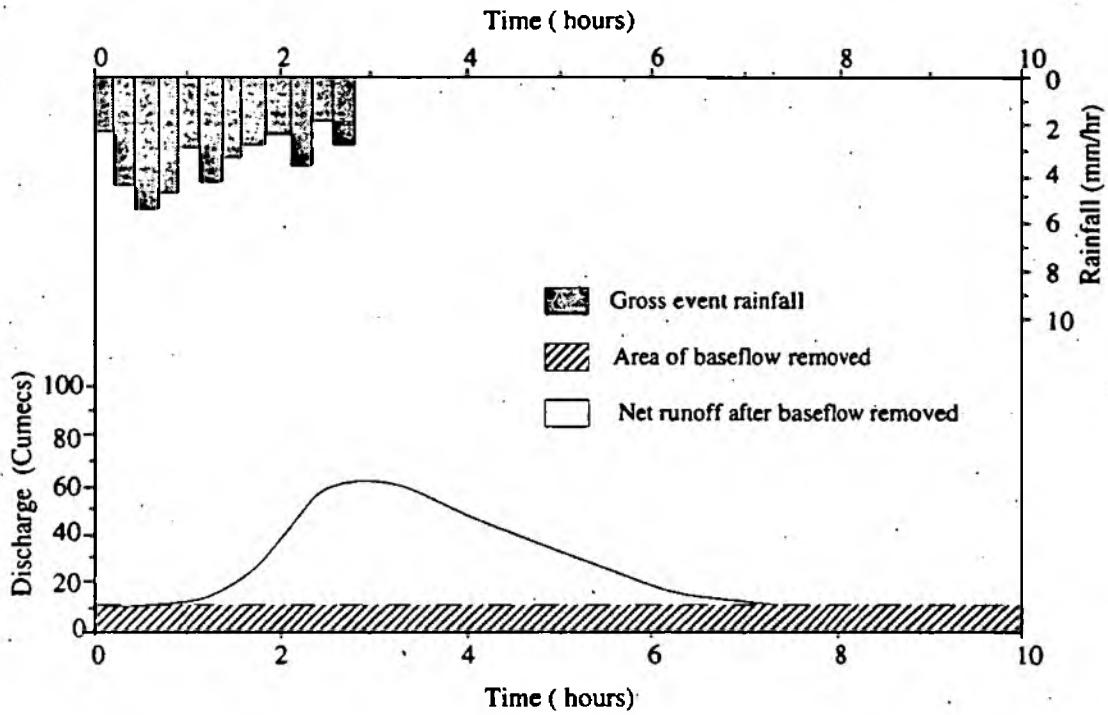


Figure 5.4 *Diagrammatic Representation of the Method of Base Flow Removal from Net Runoff Volume.*

5.3 Rainfall Analysis

Although using remotely sensed rainfall information, this investigation was aimed away from the analysis of atmospheric storm pattern characteristics addressed by other authors (eg. Austin and Bellon, 1982; Shepherd, 1987). Instead, research was focused on the rainfall hyetograph characteristics experienced by the catchment, in order to gain knowledge of any links between these and the form of the runoff hydrograph. The methods of rainfall input and runoff output analysis are outlined below. The resulting information about rainfall - runoff characteristics is shown in table 5.1, parts one and two.

Table 5.1 Storm Event Characteristics (part 1)

Date Of Event	15min Peak Intensity	30min Peak Intensity	45min Peak Intensity	60min Peak Intensity	90min Peak Intensity	Ave Rain Intensity	Rain Volume /1000000	Rain Duration	Centre Of Gravity
	(mm/hr)	(mm/hr)	(mm/hr)	(mm/hr)	(mm/hr)	(mm/hr)	(m ³)	(hours)	
020382	2.3	1.8	1.5	1.1	1.0	0.576	3.962	7.75	0.665
250682	4.0	1.4	1.1	0.7	0.6	0.234	4.241	11.25	0.399
170882	2.6	2.4	1.6	1.2	1.1	0.567	6.324	11.50	0.627
181282	3.1	2.8	1.6	0.8	0.7	0.523	6.026	11.00	0.703
140183	9.7	6.0	5.3	1.5	1.2	1.020	5.822	6.25	0.735
310183	2.8	2.0	1.2	0.8	0.6	0.235	5.506	13.75	0.327
070683	10.0	6.5	0.2	0.1	0.1	2.160	4.073	2.75	0.564
050284	5.8	4.0	1.0	0.9	0.5	0.443	8.054	13.00	0.455
160384	2.6	2.5	1.7	1.6	1.6	0.334	5.189	9.75	0.765
171084	2.4	1.5	1.3	1.0	0.4	0.249	3.627	12.25	0.407
021184	8.0	3.8	1.9	1.8	1.4	0.309	19.604	32.00	0.547
290185	1.9	1.7	1.0	0.8	0.7	0.361	3.757	10.00	0.639
261085	2.3	1.5	1.0	1.0	0.5	0.254	3.943	10.00	0.672
121285	1.7	1.3	1.2	0.8	0.3	0.353	2.623	6.75	0.371
090186	1.7	1.0	0.7	0.7	0.4	0.310	3.274	8.00	0.520
250886	3.2	1.9	1.6	1.6	1.3	0.447	14.378	24.50	0.265
260886	3.2	1.9	1.6	1.6	1.3	0.404	14.117	24.25	0.324
251086	1.9	1.8	1.3	1.2	1.2	0.143	5.115	15.50	0.209
301086	0.8	0.7	0.1	0.1	0.0	0.062	0.484	2.00	0.229
181186	2.6	1.8	1.4	1.4	1.2	0.922	6.938	9.25	0.765
141286	2.1	1.5	1.5	1.5	0.8	0.822	4.259	6.75	0.558
291286	3.4	1.8	1.5	1.5	1.3	0.414	17.000	31.25	0.266
030187	1.4	1.4	1.0	0.8	0.7	0.463	3.534	8.00	0.604

Table 5.1 Storm Event Characteristics (part 2)

Date Of Event	Hyetograph Variance	Hyetograph Skew	Rain Volume / Centre Gravity	Impulse Time (hours)	Peak Flow (cumecs)	Time To Peak (hours)	Flow Volume /1000000 (m3)	Base Flow (cumecs)	% Runoff (%)
020382	1.772	-0.652	5.958	2.00	18.747	3.5	0.573	2.781	14.457
250682	0.221	0.796	10.602	5.53	36.357	8.00	1.673	3.484	39.447
170882	2.018	-0.124	10.086	4.00	42.861	7.25	1.548	3.087	24.472
181282	3.628	-0.688	8.572	3.00	80.588	6.75	2.544	5.677	42.210
140183	0.509	-2.110	7.921	3.00	52.442	4.00	1.610	6.004	27.648
310183	0.126	1.241	16.837	5.00	107.217	8.50	4.869	6.797	88.430
070683	0.156	0.659	7.222	3.00	35.131	3.25	0.553	2.474	13.580
050284	0.175	0.793	17.696	6.00	81.654	5.75	2.897	13.552	35.976
160384	0.601	-0.239	6.784	3.00	85.372	4.00	2.448	6.137	47.168
171084	2.352	0.258	8.909	4.00	21.579	8.50	0.946	2.997	26.078
021184	6.412	0.776	35.840	4.00	96.604	14.5	5.049	4.587	25.757
290185	2.779	0.072	5.880	3.11	44.451	9.00	1.775	8.973	47.249
261085	1.398	-1.316	5.868	4.11	44.773	5.25	1.379	9.970	34.975
121285	2.081	0.818	7.069	3.00	49.198	4.50	1.833	5.904	69.883
090186	1.930	-0.044	6.295	4.00	59.805	6.25	2.600	3.155	79.431
250886	0.075	1.969	54.256	5.00	69.118	12.75	3.199	1.448	22.250
260886	2.662	1.325	43.572	3.51	69.118	13.00	3.138	1.391	22.227
251086	0.058	-0.407	24.474	5.25	40.083	6.50	1.076	7.345	21.034
301086	0.601	0.956	0.627	3.11	15.967	1.75	0.128	7.233	26.368
181186	1.531	-0.345	9.069	3.00	121.353	6.00	3.603	4.474	56.808
141286	2.493	-0.258	7.633	4.00	54.351	5.75	1.277	7.196	29.989
291286	9.080	1.126	63.911	5.00	132.429	17.75	9.593	6.549	56.430
030187	1.156	-0.485	5.851	3.00	57.786	5.75	1.766	8.036	49.974

5.3.1 Rainfall Intensity

Analysis was carried out to assess the importance of rainfall intensities persisting for different durations in the production of storm runoff. A computer program was written in VAX FORTRAN to calculate, for each storm hyetograph, the maximum rainfall intensity sustained for periods of 15, 30, 45, 60 and 90 minutes.

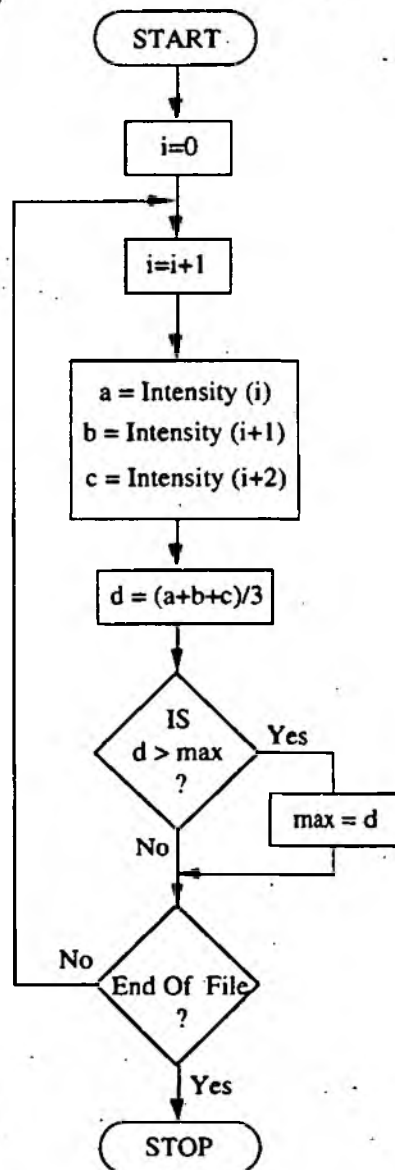


Figure 5.5 Finding Highest Average Rainfall Intensity For a 45 Minute Period

The routine written to perform this analysis used a loop to search through the 15 minute data to find the highest average intensity for each of the given durations. Figure 5.5 shows a flow diagram to assess the greatest average intensity maintained for a 45 minute period within the rainfall record.

Starting at the beginning of the hyetograph record the rainfall intensity for the three 15 minute time periods was examined. The average intensity for that 45 minute period was calculated and stored. Following this the three 15 minute steps starting from the second rainfall block were examined. The average intensity for the 45 minute duration was found, and compared with that from the previous period. The highest of these was kept and the cycle continued until the end of the rainfall record was reached. In calculating the 30 minute intensities only two time period rainfall blocks were examined at a time. For the 60 minute analysis four consecutive rainfall values were assessed and so on.

Analysis was carried out for greater time intervals than the standard 15 minute data in an attempt to reduce the effects of any extremely high rainfall intensities persisting for very short durations.

5.3.2 Storm Duration

For the purposes of this study storm duration was defined as being the time in hours from start to finish of all rainfall contributing to one flow hydrograph event. Although this was the length of a single coherent storm event it occasionally included short periods of no rainfall. The accuracy of storm duration was, of necessity, to within 15 minutes, as this was the temporal resolution of the data used. In practice storm duration was relatively easy to assess as all rainfall - runoff sequences were well

separated from previous and following events. This was established using the radar viewing program outlined in section 5.2.3.

5.3.3 Gross Rainfall Volume

The total (gross) volume of rainfall which caused each of the flow hydrograph peaks was derived from the lumped subcatchment radar totals remotely sensed from Hameldon Hill radar. The volume was calculated by transferring the rainfall totals (mm) to cubic metres of precipitation over the catchment as a whole. This was carried out by multiplying the rainfall values by the 10^6 * catchment area (to change from kilometres to metres), and dividing by 10^3 to change from millimetres to metres. In short :

$$\text{Total Rainfall Volume (m}^3\text{)} = \text{Hyetograph Volume} * 10^3 * 186$$

5.4 Rainfall Hyetograph Characteristics

Statistical analysis has in the main only been used to describe and fit probability distributions to hydrological data such as rainfall depths, intensities, peak annual discharge and flood flows etc. When rainfall is input to a system it is the amount and distribution of that input through time (ie. the rainfall hyetograph) to which the catchment responds. In this chapter, work has been carried out using statistical techniques to establish information about the form of rainfall hyetographs and their relation to catchment runoff.

5.4.1 Standardised Duration

In order to allow comparison of hyetographs from storms of differing duration, the rainfall distributions were standardised for time. This procedure was carried out within a simple FORTRAN routine written to perform the analysis. Firstly, the radar rainfall data was read into an array, and the length of the event found by searching through the record one step at a time. The length of the event in 15 minute blocks was then used as the standardising variable, such that :

$$\text{Standardised Time Step} = \text{Time Step Number} / \text{Event Length (Steps)}$$

For the fourth 15 minute step, therefore, of a five hour event, this becomes :

$$\text{Standardised fourth step} = 4 / 20 = 0.2$$

The mid way point in any rainfall event thus becomes 0.5, and full duration becomes 1.0, as shown in figure 5.6.

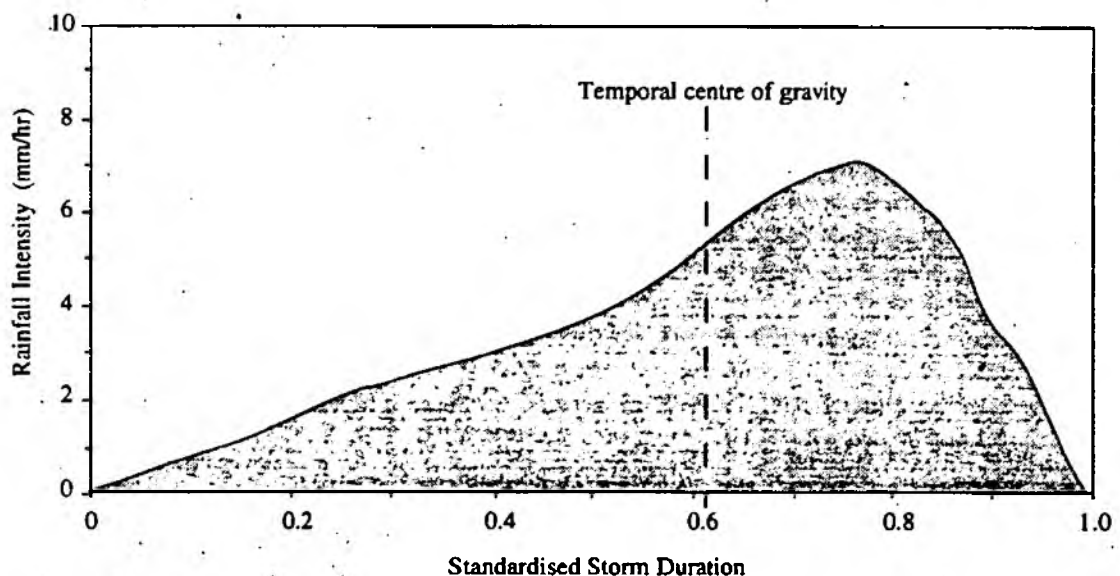


Figure 5.6 First Moment of the Hyetograph Data - Temporal Centre of Gravity.

5.4.2 Moments Of The Rainfall Distribution

With the duration of each event standardised, the characteristics of the rainfall distribution throughout the event were examined by finding the moments of the data. This technique involves assigning a hypothetical 'mass' equal to the frequency of occurrence and of the data, and conceptually rotating the system of masses about the origin ($x=0$) (Chow *et al.*, 1988).

The first moment of the data (M1) is given by :

$$\frac{\sum r_i t_i}{\sum r_i} \quad (5.2)$$

where r_i is rainfall at increment i and t_i is time at increment i .

This is equivalent to the centroid of a body, and in the present context it is analogous to the temporal centre of gravity of the hyetograph. When viewed in this way, the centre of gravity describes when the mid point of rainfall occurred in the standardised duration of the storm record, as shown in figure 5.6. The event centre of gravity was investigated to assess the importance of rainfall volume occurring early or late in the hyetograph in changing the runoff hydrograph shape.

The second moment of the data (M2) relates to the variance of the distribution about the mean, given by :

$$\frac{\sum r_i (t_i - t_c)^2}{\sum r_i} \quad (5.3)$$

where t_c is storm centre of gravity.

In the context of rainfall distribution input, the variance gives information about how precipitation is spread temporally about the centre of gravity, as demonstrated in figure 5.7.

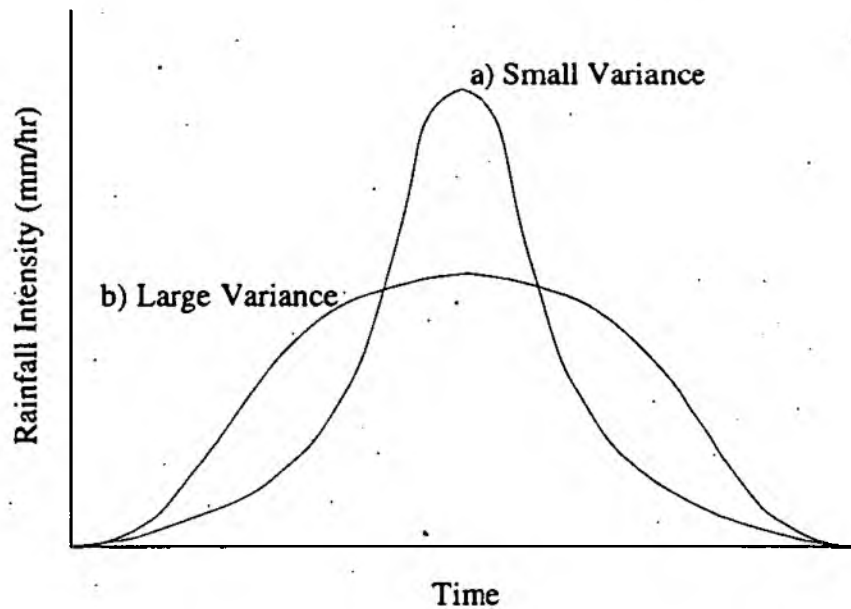


Figure 5.7 *Second Moment of the Data - Variance about the centre of gravity*

The final moment of the data chosen for use in this investigation was the distribution skew. For a distribution symmetrical about its mid point, the value for skew will be zero. A non-symmetrical distribution will produce values greater or less than zero, related to the direction and extent of the skew, as shown in figure 5.8.

The third moment (M3) is given by :

$$\frac{\sum r_i (t_i - t_c)^3}{\sum r_i} \quad (5.4)$$

This provides a measure of hyetograph type, describing whether the bulk of the rainfall occurred at the beginning or end of the event. This was then related to

catchment runoff characteristics to assess the importance of storm skew in influencing the outflow hydrograph.

5.4.3 Impulse Response Time To Peak

When using a transfer function for hydrological forecasting, model calibration is carried out using past events, and an averaged, 'best fit' model is formed, as explained in more detail in Chapter 6. However, the resulting model will only perform most accurately when it is used in situations similar to those used for calibration. Thus, a model calibrated with low intensity storms will perform less well with more severe events. In an attempt to reduce forecast errors, Viner (1992) evolved a series of three 'grouped' static TF models, calibrated under varying rainfall conditions, to be used instead of the catchment average model, see figure 5.9.

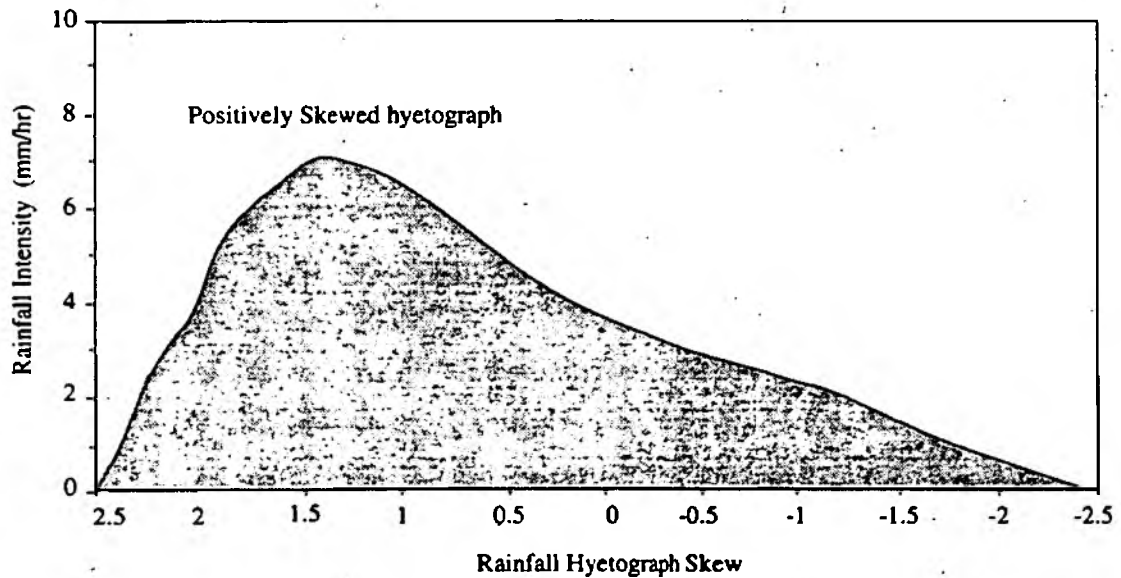


Figure 5.8 *Third Moment of the Hyetograph Data - Temporal Skew*

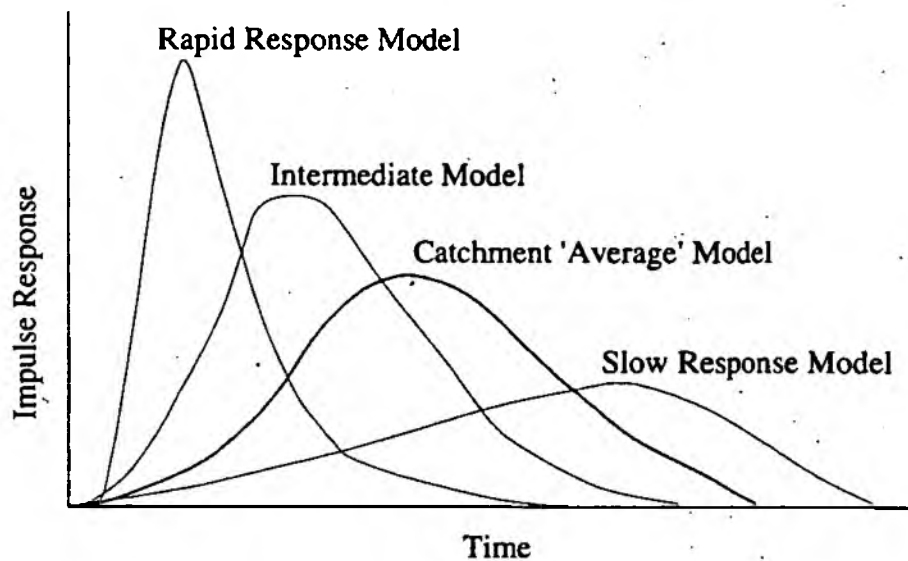


Figure 5.9 *Grouped Impulse Responses Compared with Catchment 'Average' Response Model (After Viner, 1992)*

Viner (op.cit.) found that the use of grouped models in most cases lead to greater flow forecast accuracy, and a reduction in the associated RMS errors. No attempt was made to relate the model impulse responses to physical rainfall characteristics, however. In the present study, catchment hyetograph characteristics were used in attempt to assess the viability of transfer function model 'tuning'.

A transfer function model was evolved manually to relate gross rainfall to net runoff for each individual storm event. This procedure was carried out using the calibration program 'MATH' developed at the Water Resources Research Group (WRRG, 1992). The TF model, discussed in more detail in Chapter 6, is structurally simple, parametrically efficient and robust to data loss or error, using feedback from recently observed rainfall/flow to make maximum use of data (Yu, 1989).

The MATH calibration program read rainfall and river stage values as data files. An equal order search (discussed in section 6.3.2) was then carried out by hand, MATH providing the magnitude of the model parameters and comparison forecast and actual

hydrograph using the parameters chosen. In calibrating the model for each event a compromise approach was adopted between absolute forecasting accuracy and model complexity. The most effective model order proved to be (2,3), i.e. two flow and three rainfall parameters, which was used for each model calibration. Once calibrated the unit impulse response of the model (analogous to a unit hydrograph) was plotted and the impulse time to peak of each event calculated. If a relationship could be established between rainfall hyetograph and model impulse response time-to-peak then forecast rainfall could be used to select the 'correct' TF model for the event whilst the storm is upwind of the catchment.

A full list of all relationships established between rainfall hyetograph and flow hydrograph characteristics can be seen in table 5.2.

5.5 Runoff Analysis

5.5.1 Flow Characteristics

River flow characteristics were examined for each event in order to establish links with rainfall hyetograph inputs.

i) Peak Flow

Peak flow was calculated as the maximum river discharge in cumecs after removal of base or initial flow, as discussed in section 5.2.3. The figure for peak flow was obtained using a program loop to search through the flow record, remove base flow (the value just before the start of hydrograph rise) and find the highest discharge value. This was regarded as maximum river discharge due to the event.

ii) Runoff Volume

The runoff volume due to the event was established by calculating the volume of flow resulting from the rainfall input once base flow was removed. Firstly, each 15 minute runoff value was changed from cumecs (cubic metres per second) to cubic metres of flow. These figures were then summed to give the volume of rapid runoff from the event.

iii) Percentage Runoff

Once the gross rainfall contributing to the hydrograph peak was established it was combined with net flow to calculate event percentage runoff, given by :

$$\text{Event Percentage Runoff} = (\text{Runoff Volume} / \text{Rainfall Volume}) * 100$$

iv) Hydrograph Time-to-Peak

Hydrograph time-to-peak was defined as the duration, in hours, from the start of hydrograph rise until peak discharge occurred. This value was calculated manually with reference to the catchment outflow hydrographs. When peak discharge was maintained for an extended period, the time-to-peak was taken as the duration to the point where maximum runoff was first achieved.

5.6 Graphical Analysis

Once the rainfall characteristics had been extracted from the storm data, graphical analysis was carried out to assess their relative importance in storm runoff production. Analysis was carried out using Cricket Graph software. The rainfall and flow characteristics were entered into the package and graphical testing used to identify any relationships between the two sets of data. In exploring the strength of the link between the explanatory and response variables, a maximum of two parameters were fitted, and often only the strongest was used. When fitting the data, inclusion of a

Table 5.2 Rainfall - Runoff R^2 Regression Coefficients

Rainfall \ Runoff	Peak Flow	Runoff Volume	Percentage Runoff	Time to Peak	Impulse Time
15min Peak Intensity	0.013	0.009	0.116	0.004	0.001
30min Peak Intensity	0.006	0.000	0.122	0.013	0.008
45min Peak Intensity	0.023	0.012	0.019	0.006	0.016
60min Peak Intensity	0.236	0.205	0.018	0.296	0.013
90min Peak Intensity	0.248	0.201	0.026	0.245	0.002
Average Intensity	0.001	0.025	0.082	0.065	0.112
Rainfall Volume	0.391	0.564	0.021	0.755	0.105
Moment 1 C Gravity	0.022	0.149	0.011	0.347	0.466
Moment 2 Variance	0.218	0.500	0.010	0.484	0.000
Moment 3 Skew	0.092	0.218	0.031	0.200	0.539
Rainfall Duration	0.323	0.586	0.003	0.888	0.210
Volume/ Centre of Gravity	0.281	0.560	0.008	0.778	0.223

large enough number of parameters may make the model fit as closely as desired, but can lead to a loss of robustness, greatly increased complexity and unrealistic results. For example, a 'perfect' fit may be obtained to n data points with a polynomial of degree $n-1$. In this investigation simplicity and parsimony were seen as most desirable, a 'substantially' correct model giving better predictions than one that includes unnecessary extra parameters, (McCullagh and Nelder, 1983).

The strength of fit between the data and the modelling curve was expressed as a coefficient of determination, R^2 :

$$R^2 = \frac{SS_R}{S_{YY}} = \frac{\sum_{j=1}^n (\hat{y}_j - \bar{y})^2}{\sum_{j=1}^n (y_j - \bar{y})^2} \quad (5.6)$$

The value of R^2 lies between zero and one such that $0 < R^2 \leq 1$. This value provides information about the proportion of variability in the data explained by the model (Montgomery, 1984). There are no hard and fast rules for the interpretation of R^2 values which indicates a significant relationship. When evaluated, relationships from this analysis were considered to be of significance if they produced R^2 values of 0.55 or greater. Following this procedure it was possible to determine several good causal relationships as well as some lower significance 'trends'. Values lower than this were regarded as possible 'trends', but not as being significant.

5.6.1 Linear Relationships

i) Rainfall Duration - Time To Peak

The strongest links between rainfall input and the resulting runoff peak appeared to exist in relation to simple hyetograph duration and volume. The rainfall duration - time to peak analysis yielded a relation of :

$$\begin{array}{l} \text{Time To Peak} = 1.6128 + 0.45619 \text{ Rainfall Duration} \quad R^2 = 0.888 \quad (5.1) \\ \text{(Hours)} \qquad \qquad \qquad \qquad \qquad \qquad \text{(Hours)} \end{array}$$

The relationship showed that time to peak of hydrograph flow increased with longer rainfall durations (see figure 5.10) with quite low scatter about the regression line.

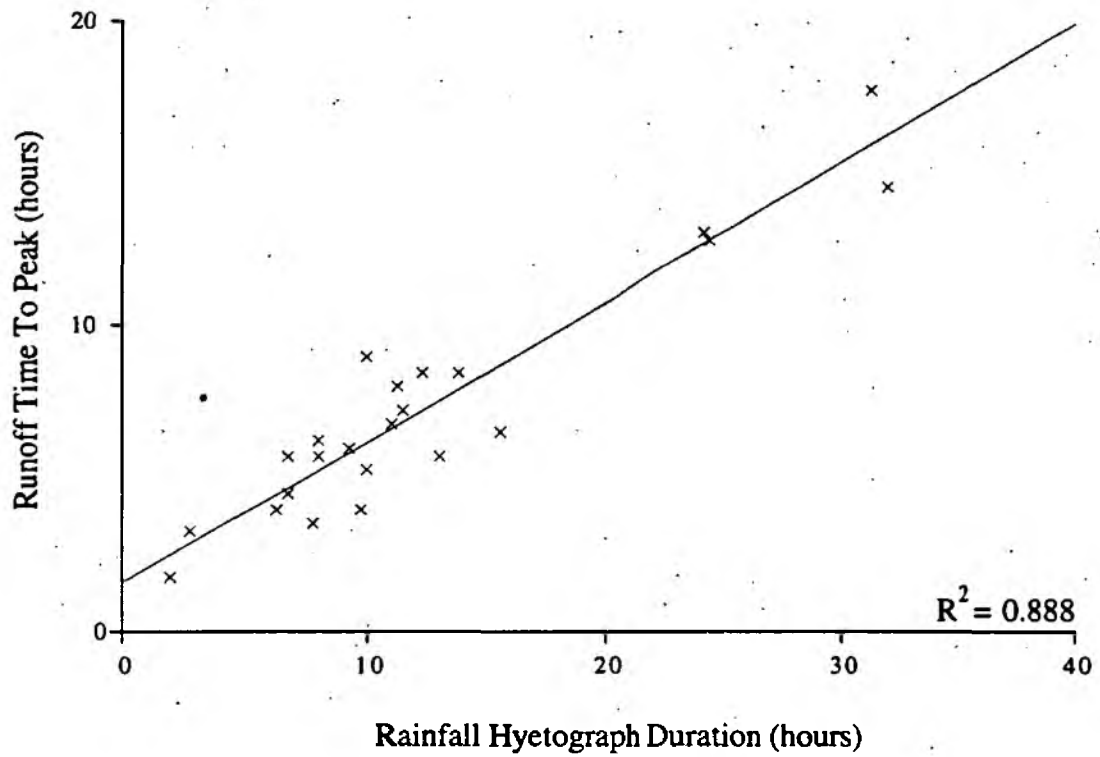


Figure 5.10 Effect of Hyetograph Duration on Runoff Time to Peak

ii) Gross Rainfall Volume - Time To Peak

Runoff time to peak also demonstrated a positive relationship with increasing rainfall volume (as shown in figure 5.11). Although slightly weaker, the relation was still thought to be relevant described by the equation :

$$\text{Time To Peak (Hours)} = 2.7263 + 0.69506 \text{ Gross Rain Volume (Metres}^3\text{)} \quad R^2 = 0.755 \quad (5.2)$$

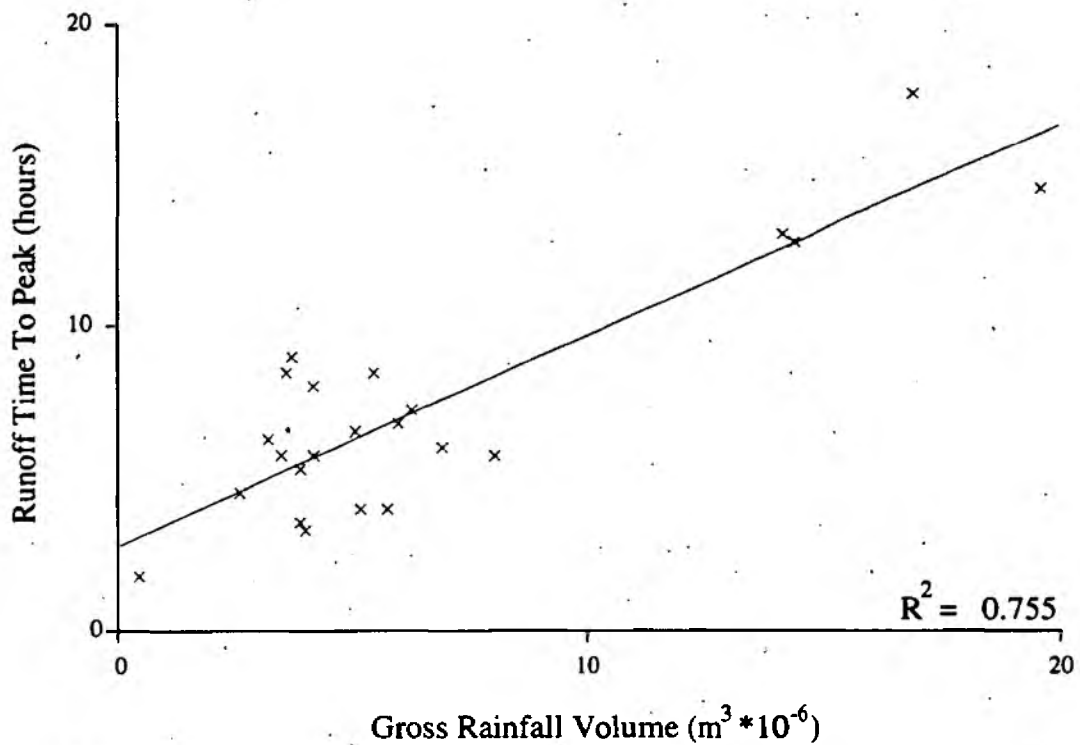


Figure 5.11 *Effect of Gross Rainfall Volume on Runoff Time to Peak*

iii) Rainfall Volume / Centre Of Gravity - Time To Peak

When a connection was found between hyetograph centre of gravity and time to peak (see section 5.5.2 (v)) gross rainfall volume was divided by centre of gravity to provide a combined hyetograph factor. This, when plotted against time to runoff peak, gave an improved R^2 of 0.778, as can be seen in figure 5.12, given by the equation :

$$\text{Time To Peak} = 2.7263 + 0.6951 \text{ Rain Volume/Centre Of Gravity } R^2 = 0.778 \quad (5.3)$$

(Hours)

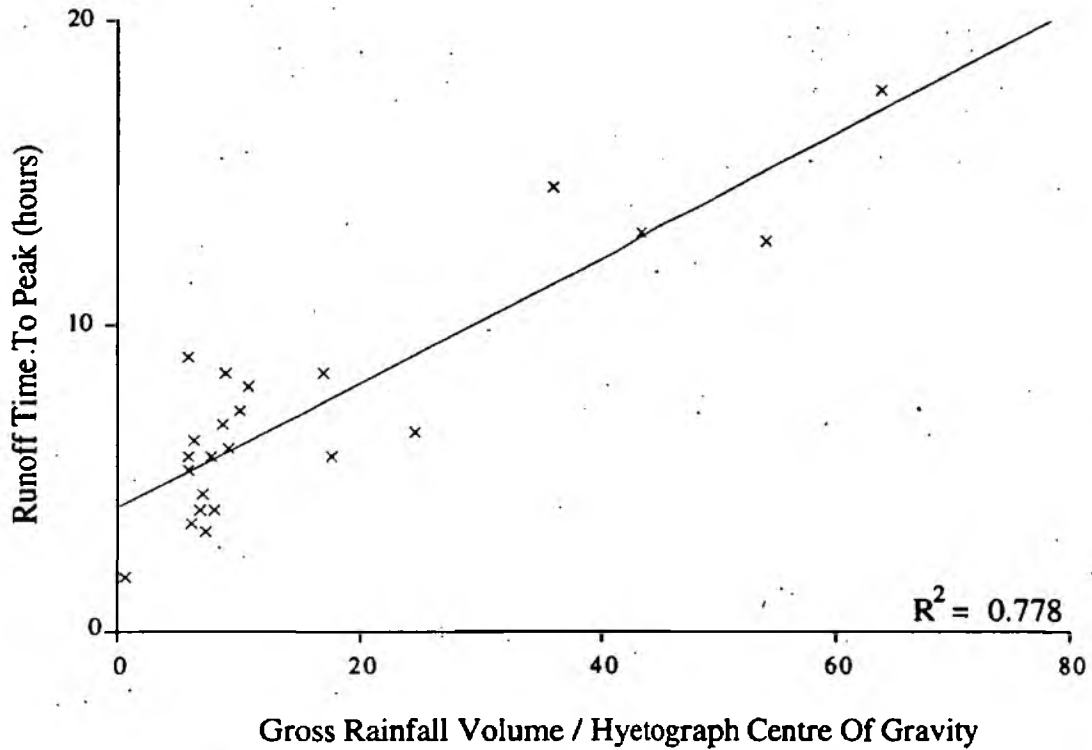


Figure 5.12 Effect of Gross Rainfall Volume / Hyetograph Centre of Gravity on Runoff Time to Peak

Unfortunately this combination factor lead to a worsening of relationships when plotted against all other flow characteristics.

iv) Gross Rainfall Volume - Net Flow Volume

As may have been expected the volume of net storm runoff showed a positive relationship with increasing rainfall volume (see figure 5.13). The equation fitted to the relationship took the form :

$$\text{Net Flow Volume (Metres}^3\text{)} = 0.39830 + 0.30896 \text{ Gross Rain Volume (Metres}^3\text{)} \quad R^2 = 0.564 \quad (5.4)$$

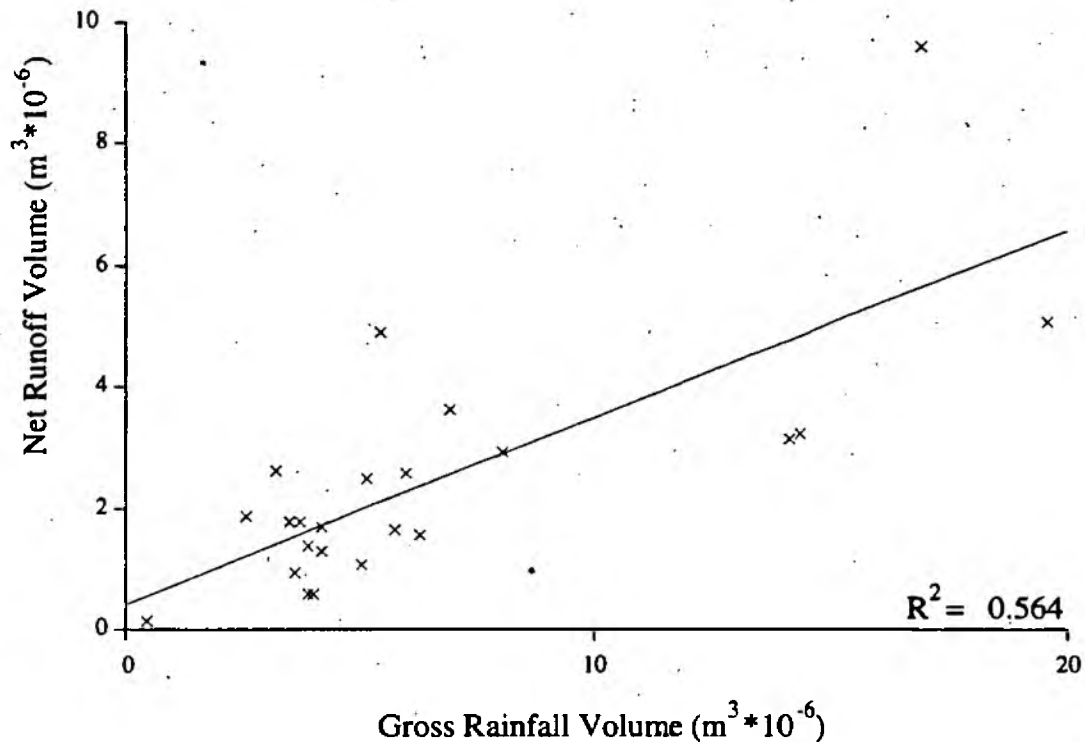


Figure 5.13 *Effect of Gross Rainfall Volume on Net Runoff Volume*

5.6.2 Graphical Trends

Although weaker, several graphical 'trends' were found to exist between some of the rainfall and flow characteristics examined.

i) Hyetograph Skew - Impulse Response

The third moment of the of the rainfall hyetograph (skew) demonstrated a good trend with time to peak of the storm TF model impulse response. The relation, shown in figure 5.14, took the form :

$$\text{Impulse Response (Hours)} = 3.6691 - 0.84053 \text{ Hyetograph Skew} \quad R^2 = 0.539 \quad (5.5)$$

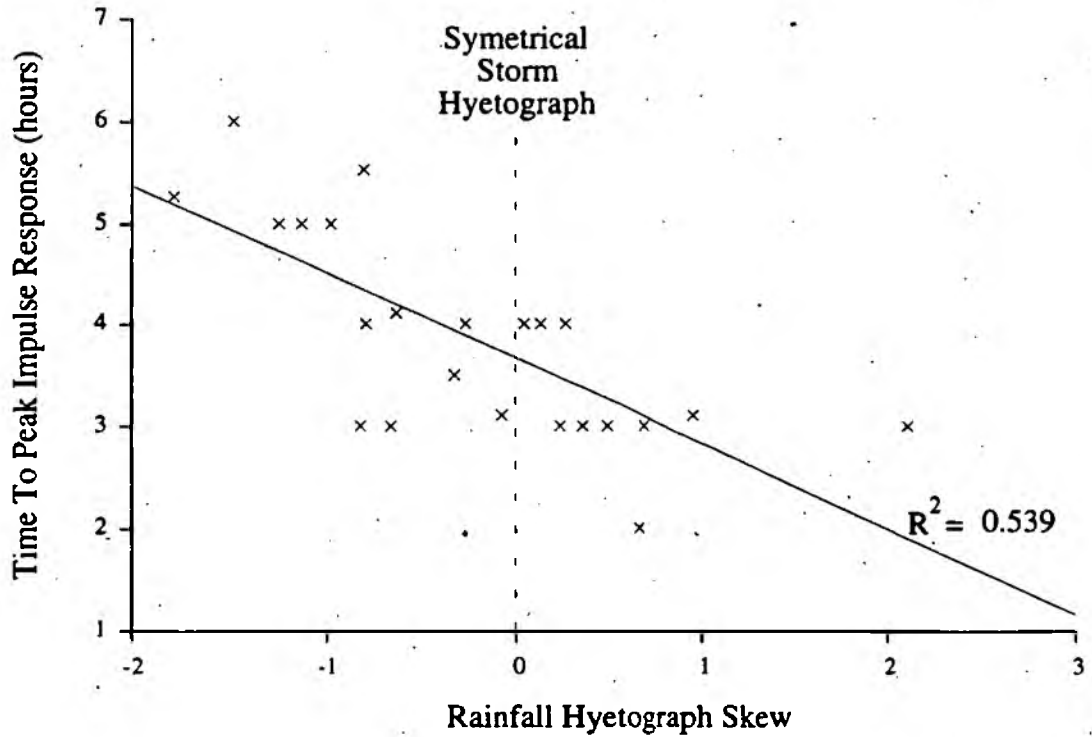


Figure 5.14 Effect of Rainfall Hyetograph Skew on Event Transfer Function Model Impulse Response

The relationship indicated that positively skewed hyetographs tended to result in shorter time to peak of the transfer function model impulse response.

ii) Variance - Time To Peak

The second moment of the data (temporal spread about the mean) showed a good trend with time to peak of the runoff hydrograph (see figure 5.15). As the magnitude of variance increased flow time to peak was delayed, giving the relationship :

$$\text{Time To Peak} = 4.9079 + 1.2637 \text{ Variance} \quad R^2 = 0.484 \quad (5.6)$$

(Hours)

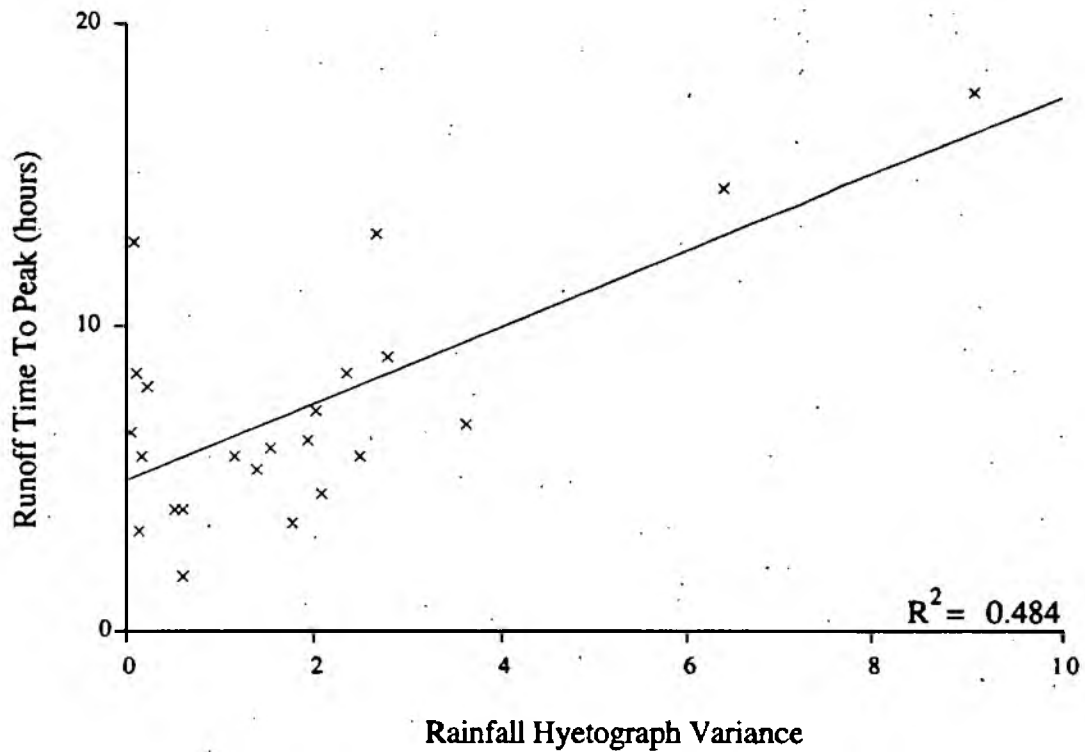


Figure 5.15 *Effect of Rainfall Hyetograph Variance on Runoff Time to Peak*

iii) Hyetograph Centre Of Gravity - Impulse Response

The first moment of the hyetograph (storm temporal centre of gravity) gave a trend with TF model impulse response time. The relationship (as shown in figure 5.16) tended to produce longer impulse models when the centre of gravity of the data was sited near the end of the event, the correlation equation being :

$$\text{Impulse Response} = 1.9959 + 3.9399 \text{ Centre Of Gravity} \quad R^2 = 0.466 \quad (5.7)$$

(Hours)

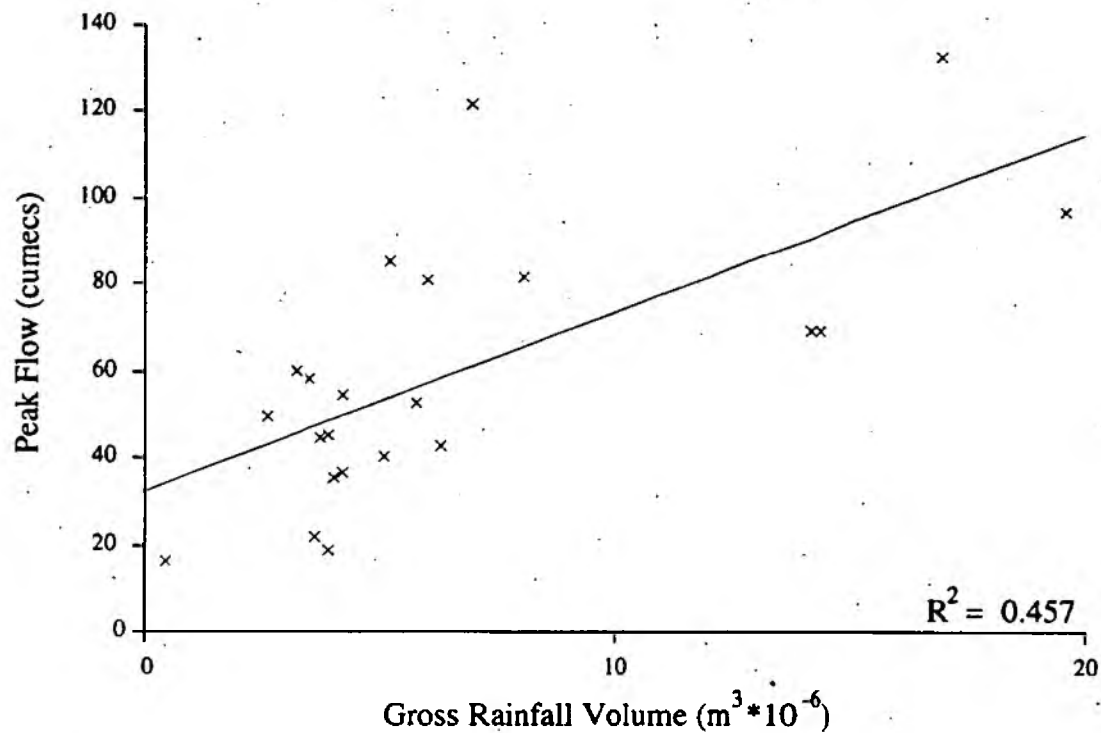


Figure 5.17 *Effect of Gross Rainfall Volume on Peak Flow*

v) Hyetograph Centre Of Gravity - Time To Peak

The first moment of the storm rainfall hyetograph, analogous to the temporal centre of gravity of the event as experienced by the catchment, followed a trend with time to peak of the flow hydrograph. The relationship, shown in figure 5.18, displays a reduction in time to peak with the 'lower' centre of gravity values occurring when the bulk of the storm hits the catchment first. The relation took the form :

$$\text{Time-Peak (Hours)} = 1.2212 + 12.930 \text{ Storm Centre of Gravity} \quad R^2 = 0.347 \quad (5.9)$$

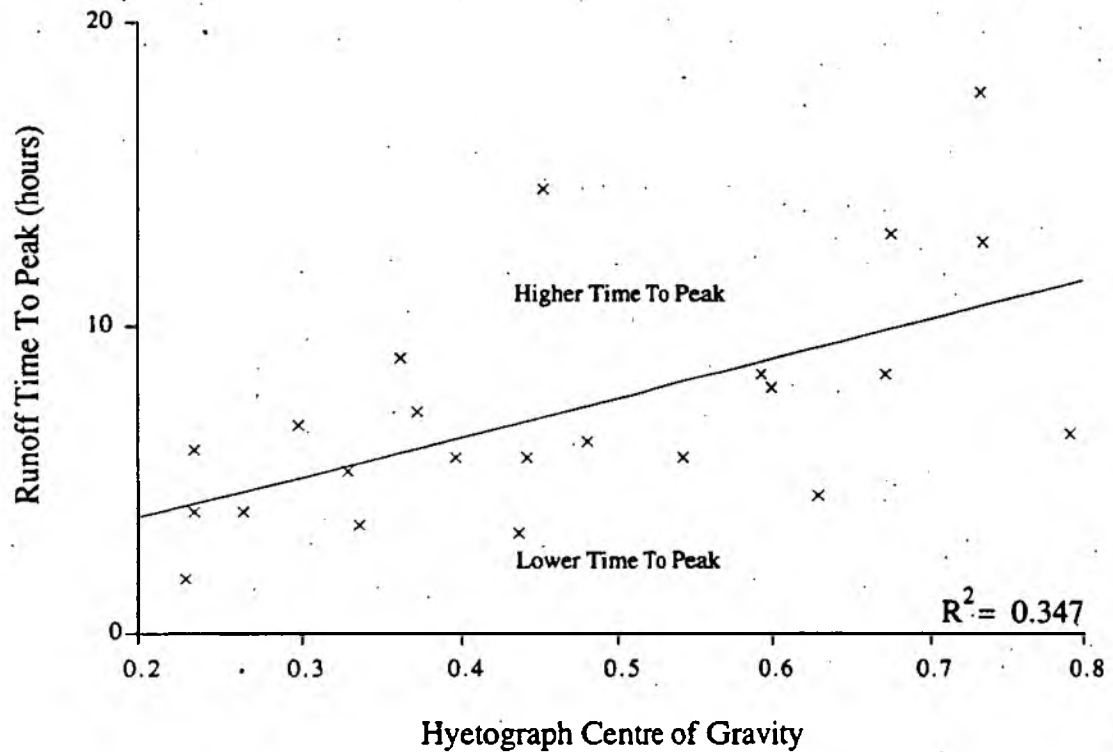


Figure 5.18 *Effect of Hyetograph Centre of Gravity on Runoff Time to Peak*

5.6.3 Anomalies

During the course of the investigation some of the relations obtained could not be explained in hydrological terms as causal links and were thought to be due to either coincidence or one variable acting as a surrogate for another.

Rainfall duration showed a positive relation to flow volume with an R^2 of 0.586. The increase in duration was seen as a surrogate for increasing volume of rainfall, with which it correlated with an R^2 of 0.889. Also, variance, the second moment of the hyetograph data, gave a correlation of $R^2=0.500$ with flow volume. This again was seen as a non-causal, accidental link.

5.7 Discussion

When attempting to forecast the potential severity and time of occurrence of a rapid response event it is important to know the maximum height that the flood waters will reach, when this will take place and the volume of water within the flood peak. This knowledge enables an element of 'risk' to be applied to the incoming storm in the context of an individual catchment, and action to be taken on the ground to reduce the potential impact of the event.

Of the above criteria perhaps the most important is the extent of peak flow, which relates to the level of overtopping likely to occur, the amount of evacuation to advise to the public down stream, and at its most basic whether a flood is survivable within a given area. Using rainfall hyetograph characteristics alone it was found impossible to forecast the peak runoff from an event with any great certainty. Rainfall volume gave the highest correlation with peak flow ($R^2 = 0.457$) but there was considerable scatter about the regression line.

The relationships between rainfall characteristics and time at which peak flow occurs proved to be more significant. Time to peak of the flow hydrograph correlated well with storm duration ($R^2 = 0.888$). Knowledge was also gained about rainfall volume which demonstrated a good correlation ($R^2 = 0.755$) with time to peak, and was increased to an R^2 of 0.778 if hyetograph centre of gravity was taken into account. The second moment of the hyetograph data (variance) also brought knowledge of a potentially useful trend an with R^2 value of 0.484 when correlated with time to peak of flow.

The third important flow factor, that of net runoff volume, was found to correlate with duration of rainfall, giving a value of 0.586, although taking account of the position of

hyetograph centre of gravity reduced the correlation. Gross rainfall volume also demonstrated a relation with net flow volume showing an $R^2 = 0.564$.

Knowledge was gained in this investigation about the nature of the relationship between storm hyetograph characteristics at the Blackford Bridge site and the transfer function model impulse response produced for each event. Rainfall skew showed a trend with TF model impulse response giving an R^2 value of 0.539, positive skew decreasing model impulse time. The first moment of the hyetograph gave a trend with model impulse response where $R^2 = 0.466$, higher centre of gravity values generally producing models with longer impulse times. Although far from perfect, these relationships point to the possibility of using a 'tuned' transfer function in flow forecasting, rather than the catchment averaged model generally applied of necessity. Once hyetograph shape is assessed from the rainfall data then models with the most appropriate impulse response may be identified and used to forecast runoff from the event. It was decided not to pursue the application of static models here, due to its inherent lack of flexibility. Instead, work was concentrated on the adaptive, physically realisable transfer function model outlined in Chapters 6 and 7, with its increased sensitivity and flexibility.

Rainfall peak intensities within the hyetograph, although showing loose trends at longer sustained durations, did not demonstrate significant relationships with any of the flow characteristics examined. This is perhaps surprising given that the Flood Studies Report (1976) describes the Blackford Bridge area as having low rainfall acceptance potential, and in general a high intensity storm generates faster response than a low intensity one.

5.8 Conclusions

In this chapter research has been concentrated on storm rainfall characteristics as experienced by the catchment and their influence on the event runoff hydrograph. Examination of rainfall hyetograph characteristics in isolation does reveal some useful links between the storm hyetograph of the drainage area, and the ensuing flood runoff. All of the storm characteristics used in this analysis may be found by using weather radar to observe a rainfall event up wind of the target catchment area. Storm velocity and areal extent can be used to estimate rainfall duration expected over the catchment. This, combined with radar rainfall intensities, allows forecasting of the volume of precipitation and hyetograph form likely to be experienced by the catchment area. Centre of gravity and skew can then be calculated from the forecast rainfall hyetograph.

In carrying out this analysis it was hoped that knowledge would be gained in the form of 'rules' for inclusion in a knowledge based system. The relations found to exist between rainfall and flow were encouraging, and in a forecasting context could be used to give a rough indication of several runoff characteristics. However, it was not found possible to forecast flow characteristics with a sufficient degree of certainty. Many of the relationships established showed considerable scatter about the regression line. Much of this 'noise' may have been related to the influence of other factors, related to changing vegetation cover, land use, season or soil moisture status. In order to examine the effect of catchment status and allow the analysis of a much greater number of events, a synthetic data set was developed in gathering rules and relationships, presented in Chapter 7. The use of artificial data also allowed the organised inclusion of a number of other influencing variables such as rainfall position, direction and movement.

CHAPTER 6

RAINFALL - RUNOFF MODELLING

6.1 Introduction

The hydrological system is extremely complex, and one which is vital to human life. Modelling of the system allows simplification, and is carried out for many functions including water quality, supply and hydrological engineering. It is in the field of flood warning that modelling plays one of its most important roles, however, forecasting one of the most destructive of all natural hazards. The flood warning system as a whole contains many elements, as represented in figure 6.1, concerned with data collection and warning dissemination, but it is the hydrologist and the models he uses which lie at its heart.

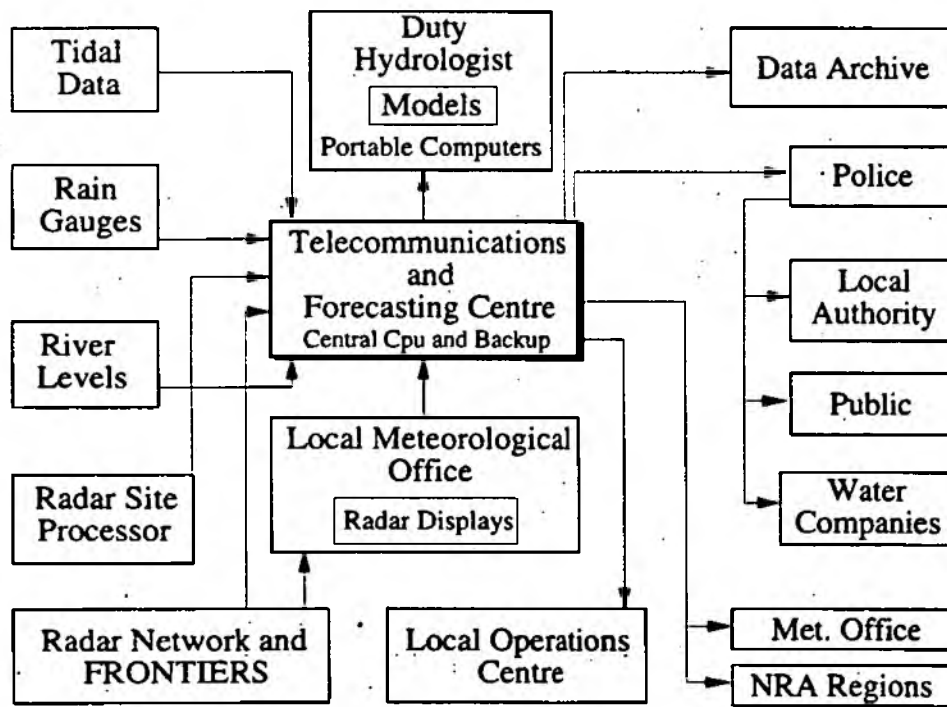


Figure 6.1 Representation of a typical Flood Warning System (after Noonan, 1987)

This chapter outlines the mathematical principles behind the physically realisable rainfall runoff model used in Chapters 7, 8 and 9 of this thesis. In order to place the model in context, a detailed explanation is presented of transfer function models and their hydrological utilisation. This is followed by a description of the problems encountered in using TF models in a flow forecasting situation. The advantages of the *Physically Realisable Transfer Function* model (PRTF), as developed by Han (1991) are then outlined, together with an illustration of the theory of model adjustment.

6.1.1 Rainfall Runoff Representation

Various approaches have been used to represent the rainfall-runoff process, ranging from detailed physically based techniques, to simplified phenomenological or 'black box' models, in which the physical mechanisms are left unexamined. In real time forecasting situations it is the black box approach which has been applied most successfully, partly due to the complexity of the physical phenomena, and partly due to the scarcity of data required for physical simulation. It is not proposed to provide here a comprehensive review of all the many types of rainfall-runoff models which have been evolved, for which the reader is referred to the works of Reed (1984) and O'Connell and Clark (1986). Instead, this chapter will concentrate in some detail on the transfer function model, and its derivative, the PRTF model.

Of all the phenomenological models, perhaps the most well known is the Unit Hydrograph, pioneered by Sherman (1932). This deterministic method, although widely documented and implemented (NERC, 1975), has been criticised for its inefficient parametrisation and lack of suitability for real time forecasting (Moore and O'Connell, 1978; Moore, 1980).

6.2 Transfer Function Models Structure

In answer to the problems found in the Unit Hydrograph method, transfer function models have been developed to simulate the rainfall-runoff process (Box and Jenkins, 1970). Essentially the transfer function approach recasts Unit Hydrograph methods in a stochastic framework, whereby it is efficiently parametrised and naturally suited to real-time use (Reed, 1984). Transfer function models give a forecast based on recently observed rainfall and flows, the number of parameters making up the model's 'memory'. It has been reported that model identification requires more statistical expertise than does a Unit Hydrograph, but a method of model calibration, using gross rainfall as input, has been developed by Owens (1986).

6.2.1 The Systems Approach

If the hydrological process is viewed as a system, then for a known input time series $u(t)$ and output time series $y(t)$, it may be described by a system function, as shown in figure 6.2.

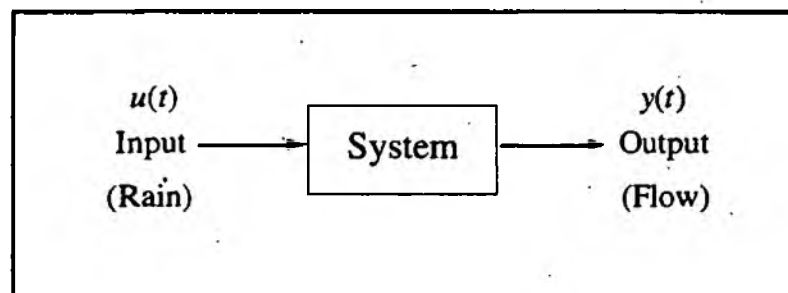


Figure 6.2 *Representation of a Single Variable Dynamic System*

In general any system is made up of three elements :

- i) Input
- ii) Output
- iii) Translation Operator linking (i) and (ii)

The rainfall-runoff process is a continuous system in which both input and output are continuously variable. In practice the unbroken data are transformed into discrete data variables due to sampling by radar, raingauges and flow measuring stations. If the two sequences of discrete variables are defined as $\{U_t\}$ and $\{Y_t\}$, and the translation operator S , then the system may be characterised by the transformation equation :

$$Y_t = S(U_t, t) \quad (6.1)$$

The transformation operator S may be referred to as the transfer function of the system, transferring the single variable sequence $\{U_t\}$ into the the sequence $\{Y_t\}$. The transfer function therefore defines the system output $\{Y_t\}$ at any point in time, t . A transfer function linking one input to one output is usually termed a 'univariate system TF model', as it is defined at a single point, or aggregated over space.

The rainfall runoff process is a class of nonlinear, nonstationary system; the transfer function being a function of the magnitude of the input, and varying with time. During minor storm events much of the rainfall may be absorbed by the soil, or intercepted by vegetation. In this case, water will take longer to reach the basin outlet, and a large proportion may be lost to evaporation or evapotranspiration. Large and severe storms, on the other hand, may cause early soil saturation, and runoff is likely to reach the main drainage channel much more quickly than for small events. Thus TF parameters vary for differing input magnitudes and time steps. In practice, restrictions are usually placed upon the magnitude of the input sequence and time period used, and a linear, stationary model is applied to describe the system, being easy to initialise and typically robust.

6.3 Simulation and Forecasting Using TF Models

Simulation of the rainfall run-off process may be carried out using the transfer function formula shown in equation 6.2 :

$$y_t = a_1 y_{t-1} + a_2 y_{t-2} + \dots + a_p y_{t-p} + b_0 u_t + b_1 u_{t-1} + b_2 u_{t-2} + \dots + b_q u_{t-q} \quad (6.2)$$

where a_i, b_i are model flow and rainfall parameters respectively, y_t is river flow at time t and u_t is rainfall at time t .

In a forecasting situation, with forecast lead time 1 the transfer function model may be written as :

$$Y_{t+1} = a_1 y_t + a_2 y_{t-1} + \dots + a_p y_{t-p} + b_0 U_{t+1} + b_1 u_t + b_2 u_{t-1} + \dots + b_q u_{t-q} \quad (6.3)$$

where Y_{t+1} is predicted flow at lead time 1, U_{t+1} is predicted rainfall rate at lead time 1 and y_i and u_i are measured flow and rainfall rate respectively.

In a real catchment system a time lag of some magnitude almost always exists between rainfall and resultant flow, and the term U_{t+1} may be neglected in most cases.

An alternative method of describing a linear system is by means of the 'frequency response function' (Chatfield, 1984). This is a Fourier transform of the impulse response function, defined by :

$$H(\omega) = \sum_k h_k e^{-i\omega k} \quad (6.4)$$

The weighting function h_k provides a description of the system response in the time domain. The discrete function $\{h_k\}$ is called the impulse response function (sometimes known as the unit sample response function).

6.3.1 Steady State Gain

In the Unit Hydrograph model the volume of input must implicitly be in balance with the output. The TF model, by contrast, uses total rainfall, and its steady state gain (SSG) may be defined as the ratio of steady output to a constant input of unit magnitude. The steady state gain is directly analogous to runoff percentage and indicates the fraction of the rainfall volume input which appears as river runoff output. System gain is defined as :

$$SSG = (b_0 + b_1 + b_2 + \dots + b_q) / (1 - a_1 - a_2 - \dots - a_p) \quad (6.5)$$

6.3.2 Transfer Function Model Calibration

Calibration of the transfer function model is vital in order to identify optimal model structure, and best describe the rainfall-runoff process with as few parameters as possible. It is also used to establish the model parameter values and optimum model interval.

i) Model Structure

A crucial part of model calibration is the determination of the optimal model structure for the data, combining forecast accuracy with parametric economy (parsimony). An equal order model search, where $p=q=1$, $p=q=2$, $p=q=3$ etc. is carried out until further increase in model order no longer produces a significant improvement in model accuracy. A reduction in model order is then often possible, as the number of flow parameters can frequently be reduced without any detrimental effect on the model, such that $p < q$.

ii) Parameter Estimation

Once a model order is determined, the parameters of the TF model may be estimated. After a study of parameter estimation procedures, Harpin (1982) concluded that the recursive least squares (RLS) method provides good parameter estimates. Although a biased estimator, RLS does not produce significantly worse results than more complex procedures such as the instrumental variable-approximation maximum likelihood method (Cluckie and Ede, 1985).

iii) Optimal Model Interval

The optimum model interval is largely governed by catchment characteristics. If the model interval is too small in relation to catchment response, then unnecessarily large amounts of data will be required. If it is too large then the essential information will be missed. A model interval of one hour has been successfully applied as a good starting point (Owens, 1986).

6.4 Transfer Function Model Adjustment

One of the main problems in the real-time operation of a hydrological model, is that the simulated runoff is generally derived using runoff observations made at the time of forecast. To gain maximum benefit from the real-time runoff measurements used in the forecasting procedure, some form of model updating is preferable before the forecast is made. Several methods have been developed for model forecast updating including error prediction, state updating and parameter updating, discussed in more detail below.

6.4.1 Error Prediction

In any real-time forecasting situation a discrepancy will exist between the model forecast and the observed river flow. Error prediction attempts to anticipate the size of

this error and take this into account when providing the forecast. This procedure is relatively easy to implement and generally works well when errors have the same trend in the near future as in the past. However, the benefit is often least in the vicinity of the hydrograph peak, where the error displays lowest temporal persistence. Also, this form of updating has limited effectiveness in the case of timing errors, as distinct from volume or shape errors. These are illustrated in section 6.8.

6.4.2 State Updating

The state updating technique works on the premise that the model will perform well in the future if it is right at time 'now'. An observable quantity, such as catchment runoff acts as a 'state variable' and observed values are used to update the model state directly as soon as they become available. The formulation of the TF model makes this method very easy to apply, but improvements to the forecast are not necessarily consistent, and frequent or perpetual re-initialization is required.

6.4.3 Parameter Updating

In this approach, a small number of the most sensitive model parameters are updated in order to minimise forecast error. The Kalman Filtering technique has been widely used in the updating process, for example Moriyama and Hirano (1991), having the capacity to deal with a non-stationary system. The most applicable form is the vector Kalman Filter, when the process can be described as an auto-regressive moving average (ARMA) type. Here, a simple random walk is used, the parameters being allowed to vary in accordance with probabilistic laws.

The main drawback to the Kalman Filter is that it requires explicit knowledge of the environment in the form of correlation functions, state-space models or probability

density functions. In many situations such functions are unknown, and / or time varying, and an adaptive filter may be used to realise an optimal estimator. Cluckie and Harpin (1982) investigated several adaptive schemes and found it difficult to apply them to flood forecasting models. A new, simple approach was proposed by Cluckie and Smith (1980) and further developed by Cluckie and Owens (1986), in terms of updating model gain, outlined in section 6.4.4.

6.4.4 Model Gain Updating

The difficulty in defining effective rainfall, especially in a real-time situation, led Owens (1986) to develop a transfer function model using total rainfall. This method aims at updating the percentage runoff represented by the model. A multiplying variable, 'delta' (Δ), is introduced to adjust the gain of the model and act as a real-time correction factor. Only the rainfall parameters of the model are scaled, as shown in equation 6.6 :

$$Y_{t+1} = a_1 y_t + a_2 y_{t-1} + \dots + a_p y_{t-p} + \Delta (b_0 U_{t+1} + b_1 u_t + b_2 u_{t-1} + \dots + b_q u_{t-q}) \quad (6.6)$$

where :

$$\Delta_t = \mu \Delta_{t-1} + (1 - \mu) \frac{y_t (a_1 y_{t-1} + a_2 y_{t-2} + \dots + a_p y_{t-p})}{b_1 u_{t-1} + b_2 u_{t-2} + \dots + b_q u_{t-q}} \quad (6.7)$$

$0 \leq \mu \leq 1$ is a smoothing factor.

The use of delta affects only the impulse response function (described in section 6.7), and does not influence model stability (Cluckie and Ede, 1985). As delta is concerned with the proportion of rainfall contributing to flow, it may be related to

antecedent catchment conditions. However, owing to the difficulties involved in estimating initial conditions a default value of $\delta = 1.0$ is often applied.

In some situations the use of δ to update percentage runoff has been found to produce detrimental effects. This relates to the fact that δ modifies the moving average (b-parameter) part of the model. In some cases the MA parameters may be small, equal to zero or become negative, which prohibits the application of δ . The problems encountered in the use of δ lead to the development of a physically realisable transfer function model, as outlined in section 6.8.3 (i).

It is fair to say there are no hard and fast rules to dictate which adjustment approach should be used in maximising forecast accuracy. Since this thesis concentrates on the use of transfer functions, parameter updating is applied to correct forecast deviation. A further discussion is presented in section 6.8, concerned with parameter updating in detail.

6.5 The Z-Transform

The Z-transform is a powerful analysis methodology for linear, time invariant, discrete systems, a diagrammatic representation of which is shown in figure 6.3. Consider the discrete time sequence $u(t)$, where $t = 0, 1, 2, \dots$. Most physical systems are based upon a causal sequence, thus the right-sided Z-transforms will be emphasised, i.e. sequences for which the time index t is defined for only positive values. The Z-transform of this sequence is defined as :

$$U(z) = Z[u(t)] = \sum_{t=0}^{\infty} u(t)z^{-t} \quad (6.8)$$

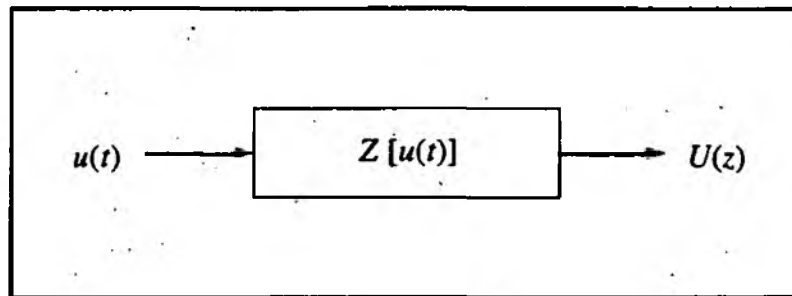


Figure 6.3 Representation of the Z-Transform Process

The Z-transform process is an operator on the input signal, mapping the input sequence $u(t)$ onto a complex function $U(z)$, the magnitude of which must be finite. The 'region of convergence' (ROC) may be defined as the set of all z in the complex z -plane for which the magnitude of $U(z)$ is finite. If z is represented in a polar form then :

$$|U(z)| = \left| \sum_{t=0}^{\infty} u(t)z^{-t} \right| \leq \sum_{t=0}^{\infty} |u(t)|r^{-t} < \infty \quad (6.9)$$

In order that the sums of equation 6.9 be finite, the condition that $|u(t)| \leq MR^t$ must be satisfied for $t \geq 0$, the series converging outside a circle of radius R . On substituting these bounds into equation 6.9 :

$$\sum_{t=0}^{\infty} |u(t)z^{-t}| \leq M \left[\sum_{t=0}^{\infty} R^t r^{-t} \right] \quad (6.10)$$

The sum in equation 6.10 is now finite only when $R/r < 1$, and thus equation 6.8 converges absolutely for all z in the region of convergence $R < |z|$ as shown in figure 6.4.

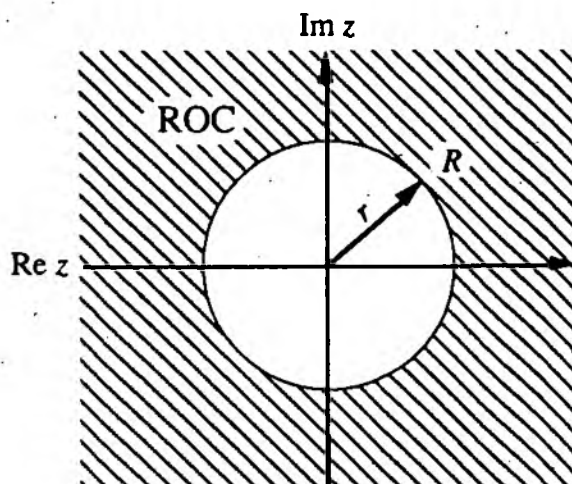


Figure 6.4 The Region of Convergence $|z| > R$ (after Defatta et al., 1988)

For causal sequences then, the region of convergence lies outside a circle passing through the pole farthest from the origin in the z -plane. Since the Z -Transform does not converge at a pole, no poles $U(z)$ can occur within the ROC. If the sequence is stable then all poles lie within the unit circle and the ROC includes the unit circle.

6.5.1 Time Delay

The time delay property of the Z -Transform is very important in the interpretation of transfer function models. For causal sequences, the delay theorem may be expressed as :

$$Z[u(t-k)] = z^{-k}U(z) + z^{-k} \sum_{m=-k}^{-1} u(m)z^{-m} \quad k \geq 0 \quad (6.11)$$

where k is an arbitrary delay factor.

The time delay is of use when considering a system with non-zero initial conditions.

For zero initial conditions, when $u(t) = 0$, $t < 0$ then :

$$Z[u(t-k)] = z^{-k}U(z) \quad (6.12)$$

This may be used to transform difference equations to the z-domain when initial conditions are zero.

From the definition of the unit impulse function :

$$Z[\delta(t)] \quad \text{ROC : } |z| \geq 0$$

As $Z[\delta(t)]$ is independent of z , the region of convergence is the whole z-plane. Since $Z[\delta(t)] = 1$, that is $U(z) = 1$, then the impulse response of a discrete system may be obtained by finding the inverse Z-Transform of the system transfer function.

The technique most generally applied to recover the original sequence from its Z-Transform, is complex integration. Here the method of residues is used to evaluate the complex inversion integral, to derive the unit impulse response of a transfer function model.

The Z-Transform inversion integral can be derived using Cauchy integral theorem from complex variable theory, and from :

$$U(z) = Z[u(t)] = \sum u(t)z^{-t} \quad (6.13)$$

Multiplication by Z^{m-1} and integration around a closed contour in the Z-plane, it follows that :

$$\oint_C U(z)z^{m-1} dz = \oint_C \sum_{n=0}^{\infty} u(t)z^{m-t-1} dz \quad (6.14)$$

From the Cauchy integral theorem, if the integration path is within the region of convergence, and the ROC includes the unit circle, then the series $u(t)$ is absolutely convergent. Interchange of the summation and integration is then valid, giving :

$$\oint_C U(z)z^{m-1} dz = \sum_{n=0}^{\infty} \oint_C u(t)z^{m-t-1} dz \quad (6.15)$$

According to Cauchy integral theorem, if the path of integration encloses the origin, then the integral on the right is zero, except where $m = t$, in which case the integral reduces to $2\pi j$. The final Z-Transform inversion integral is thus :

$$u(t) = Z^{-1}[U(z)] = \frac{1}{2\pi j} \oint_C U(z)z^{t-1} dz \quad (6.16)$$

This represents a contour, C , within which $U(z)$ is analytic, ie. let the poles of the system, p_i , be within the closed contour C . For rational Z-Transforms, the contour integral given by equation 6.16 may be evaluated using the Cauchy residue theorem.

Firstly, $U_0(z)$ is defined as a rational function with the denominator expanded in a product of pole factors :

$$U_0(z) = U(z)z^{t-1} = \frac{N(z)}{\prod_{i=1}^N (z - p_i)^{m_i}} \quad (6.17)$$

where N is a positive integer representing the total number of poles, and m_i is the pole order.

Then, from the residue theorem, it can be found that for poles within the contour of integration :

$$u(t) = \sum_{i=1}^n \text{Res}[U_0(z)] \quad t \geq 0 \quad (6.18)$$

where for simple poles ($m = 1$), the residue of $U_0(z)$ is given by :

$$\text{Res}[U_0(z)] = \lim_{z \rightarrow p_i} [(z - p_i)U_0(z)] = (z - p_i)U_0(z) |_{z=p_i} \quad (6.19)$$

For the poles of $U_0(z)$ outside the contour of integration, the sum of the residues of $U_0(z)$ is given by :

$$u(t) = -\sum_{i=1}^N \text{Res}[U_0(z)] \quad t < 0 \quad (6.20)$$

It should be noted that the terms in the inverse Z-Transform are determined by the poles of the transform function, with zeros only affecting the magnitude of the terms.

6.6 Z-Transform Analysis of the TF Model

In a general form, the transfer function model may be derived as :

$$Y(t) = \sum_{i=1}^N a_i Y(t-i) + \sum_{j=0}^M b_j U(t-j) \quad (6.21)$$

which can be rearranged to give :

$$Y(t) - \sum_{i=1}^N a_i T(t-i) = \sum_{j=0}^M b_j U(t-j) \quad (6.22)$$

Applying the Z-Transform to both sides, this may be written as :

$$Z[Y(t) - a_1 Y(t-1) + a_2 Y(t-2) + \dots + a_N Y(t-N)] = Z[b_0 U(t) + b_1 U(t-1) + b_2 U(t-2) + \dots + b_M U(t-M)] \quad (6.23)$$

Thus equation 6.23 may be expressed as :

$$A(z) Y(z) = B(z) U(z) \quad (6.24)$$

where $A(z) = 1 - a_1 z^{-1} - a_2 z^{-2} - \dots - a_N z^{-N}$

and $B(z) = b_0 + b_1 z^{-1} + b_2 z^{-2} + \dots + b_M z^{-M}$

Let:

$$H(z) = \frac{Y(z)}{U(z)} = \frac{\sum_{i=0}^M b_i z^{-i}}{1 - \sum_{i=1}^N a_i z^{-i}} \quad (6.25)$$

$$Y(z) = H(z) U(z) \quad (6.26)$$

Thus $H(z)$ is the transfer function of rainfall and runoff, such that :

$$\text{Flow}(z) = H(z) \text{Rain}(z)$$

The excitation of $y(t)$ by a unit impulse sequence, produces the unit impulse response, $h(t)$, of the system, analogous to the unit hydrograph. Since $H(z)$ takes the form of a rational function with real coefficients (ratio of polynomials), $h(t)$ is of infinite duration. Figure 6.5 shows a typical impulse response shape for a stable and physically realisable transfer function model. This is one with no fluctuation or negative component in the impulse response. The difficulties in obtaining this are addressed in the next section.

6.7 Problems with the Hydrological Use of Transfer Functions

The response of a transfer function model is uniquely characterised by its impulse response function. Given a unit input, applied instantaneously at time τ (a 'unit impulse'), the system response at time t later is described by the unit impulse response function $u(t - \tau)$, where $t - \tau$ is the time lag since the impulse was applied. When the transfer function model is used in simulating the rainfall-runoff process the impulse response it produces must be 'physically realisable'. Three main problems can arise with the transfer function model, causing physically unrealisable responses. These are instability, fluctuation and negative response.

A basic single pole model may be defined as :

$$H(z) = \frac{(-\beta)}{(z^{-1} - \beta)} = \frac{z}{\left(z - \frac{1}{\beta}\right)} \quad (6.27)$$

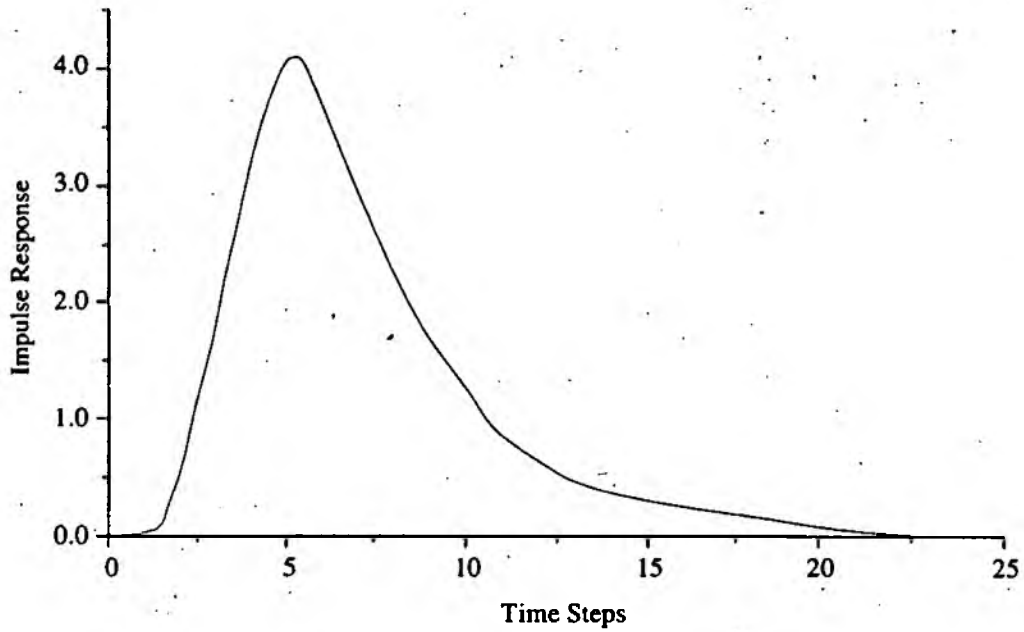


Figure 6.5 *Typical stable and physically realisable TF model impulse response*

6.7.1 Impulse Response Instability

Instability of the impulse response may occur if the model poles fall outside the unit circle, ie. when β falls inside the unit circle, causing the problems shown in figure 6.6.

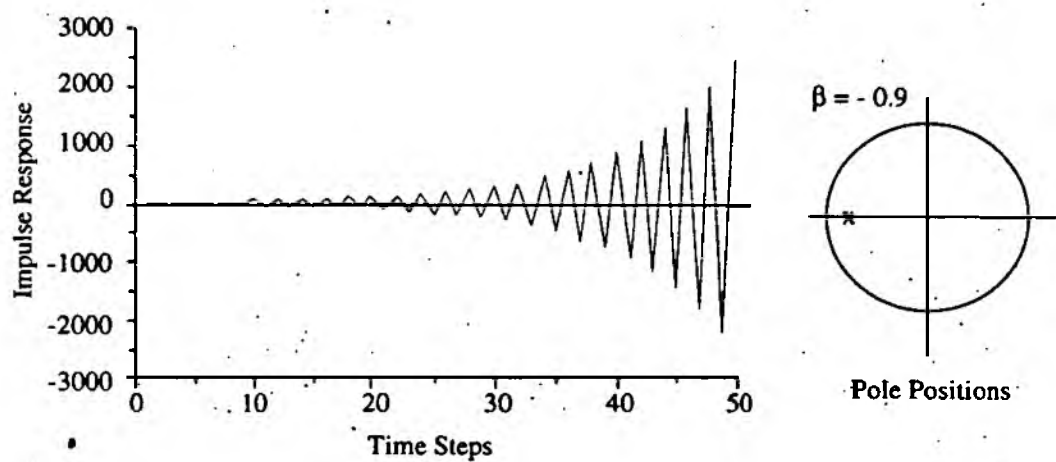


Figure 6.6 *Unstable TF Model Response*

Stability may therefore be evaluated by examination of the TF model poles. It should be noted that the poles of $B(z)$ are located at the origin in the z -plane, and so $B(z)$ are always stable.

6.7.2 Impulse Response Fluctuation

Impulse response fluctuation, or oscillation, arises when $h(t)$ is alternately greater or less than zero, see figure 6.7.

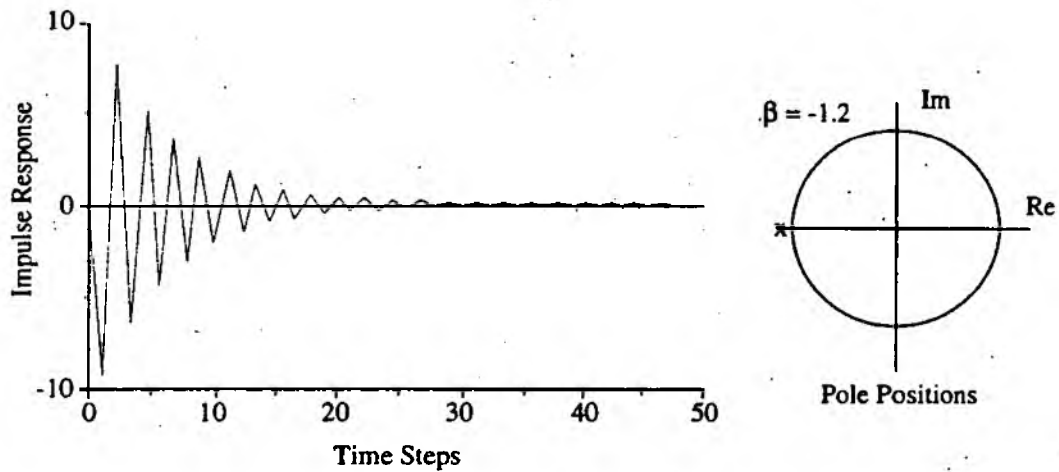


Figure 6.7 *Stable but Oscillatory TF Model Response*

The reason for a stable but fluctuating response may be found in using the inverse Z-Transform :

$$H_0(z) = H(z)z^{t-1} = \frac{z^t}{z - \frac{1}{\beta}} \quad (6.28)$$

$$h(t) = \operatorname{Res}_{z=\frac{1}{\beta}}[H_0(z)] = \left(\frac{1}{\beta}\right)^t, \quad t = 1, 2, 3, \dots \quad (6.29)$$

Thus when $\beta < -1$ (or $1/\beta < 0$) then :

$$h(t) > 0 \text{ when } t = 2i, \quad i = 1, 2, 3, \dots$$

$$h(t) < 0 \text{ when } t = 2i-1, \quad i = 1, 2, 3, \dots$$

6.7.3 Negative Impulse Response

The negative response is a special type of fluctuation (see section 6.7.2), usually found in the tail of the response, as illustrated by figure 6.8.

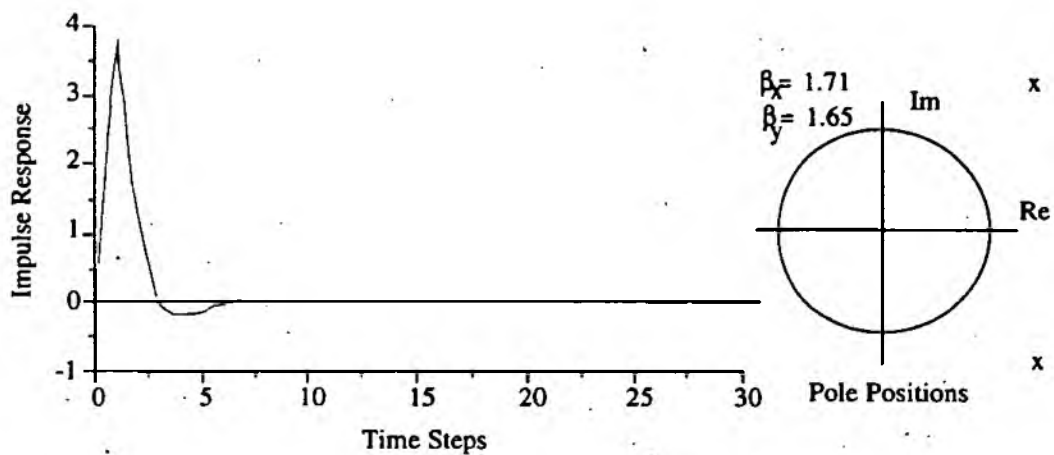


Figure 6.8 Negative TF Model Response

Even though this response is very close to the physically realisable one, it is still not usable for hydrological applications.

6.8 The Physically Realisable Transfer Function (PRTF)

In order to counter act the problems of instability, fluctuation and negative response, Han (1991) developed the Physically Realisable Transfer Function model. PRTF has features in common with the standard TF model, but a major difference is the constraints placed upon the model poles. The locations of a transfer function's poles can influence its stability and dramatically affect its impulse response. An important feature of the Physically Realisable Transfer Function model is that its impulse response shape may be adjusted by directly altering the pole's position and order.

6.8.1 Identification of a PRTF model

Least squares estimation has been used successfully to estimate linear system model structure and parameters, but has been found to be unsuitable for direct application to transfer function models, yielding unstable and fluctuating impulse response functions which are physically unrealisable. To overcome these problems a recursive least squares algorithm may be used in a modified, two-step form, paying attention to pole location and order (WRRG 23, 1992).

6.8.2 Adjustability of PRTF Responses

The impulse response of a TF model is crucial to the accuracy of the forecast model. The runoff process is non-linear and time variant, and to provide accurate forecasts the model should reflect current rainfall and catchment characteristics. Catchment hydrograph response variation may be divided into three main types, as illustrated in figures 6.9 to 6.11.

Figure 6.9 shows differing response time to peak, depending on rainfall and catchment conditions. For example, rapid response may result from an extremely heavy rainfall event or precipitation falling on a saturated catchment. Figure 6.10 gives an illustration of how catchment response may vary with respect to volume. A high level of catchment wetness may result in increased river flow production, and conversely a dry catchment may give a reduced output response.

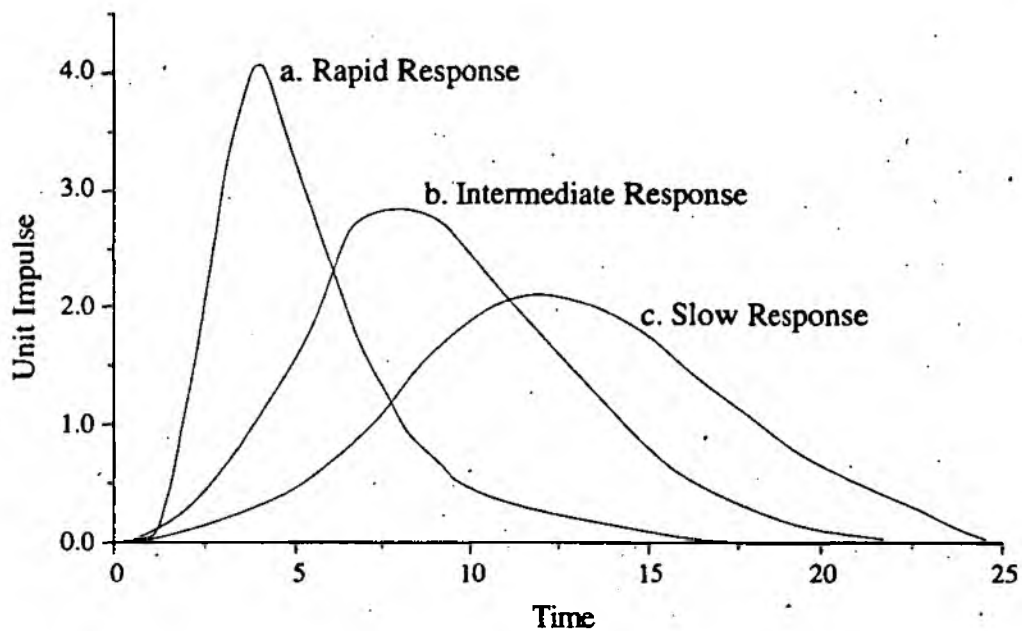


Figure 6.9 *Varying Impulse Response Shape*

In figure 6.11 an example is given of the variation in timing of catchment response. Perhaps the most obvious cause of outflow timing differences is the position of rainfall within the catchment. Precipitation falling on the upper part of a catchment will lead to a retarded response compared to a similar event occurring in the lower reaches.

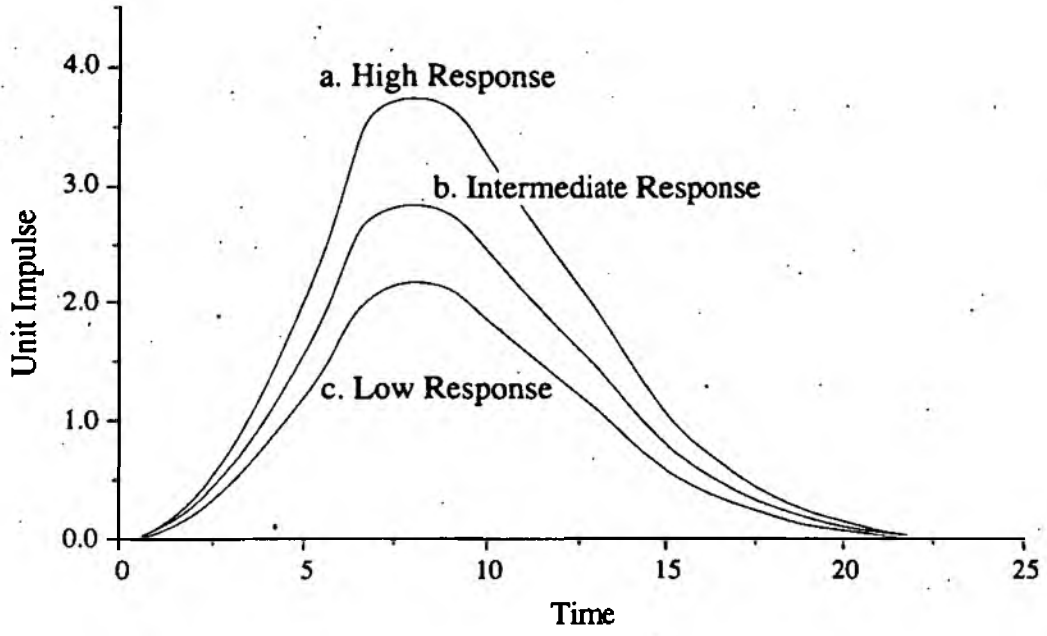


Figure 6.10 Varying Impulse Response Volume

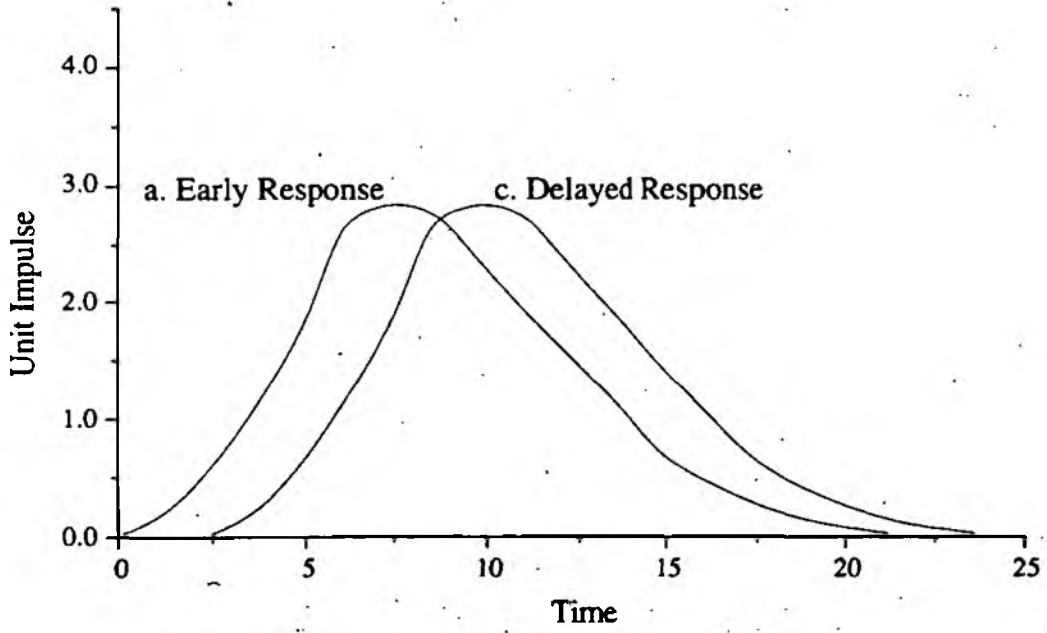


Figure 6.11 Varied Impulse Response Timing

The three types of catchment response variation outlined may occur separately or in combination, depending on the conditions at the time of the event. A major problem with the use of static model form is that it can only simulate one type of catchment response. This means it will only forecast well when the operational event is similar to those used for calibration. When the static model used is unsuitable for the conditions errors are produced related to the type of model inadequacy, as shown in figure 6.12 to 6.14.

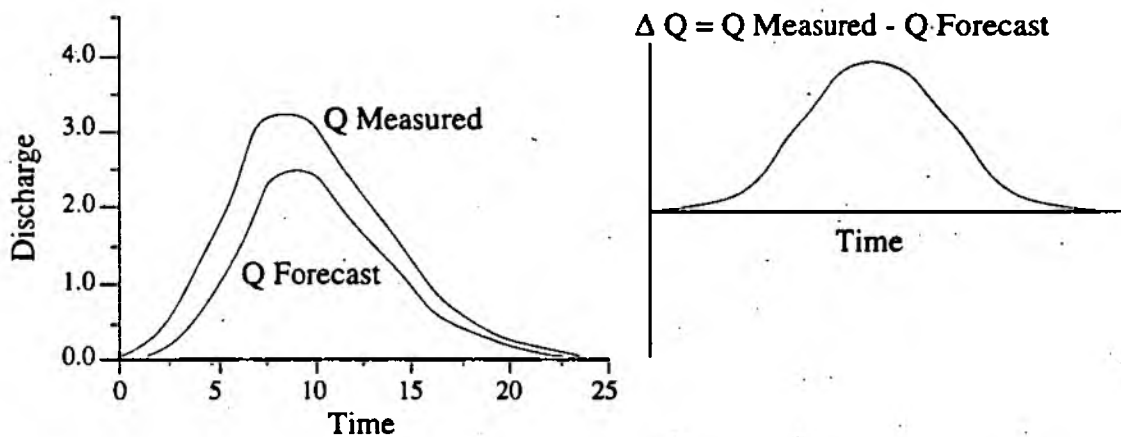


Figure 6.12 *Incorrect Impulse Response Volume Error*

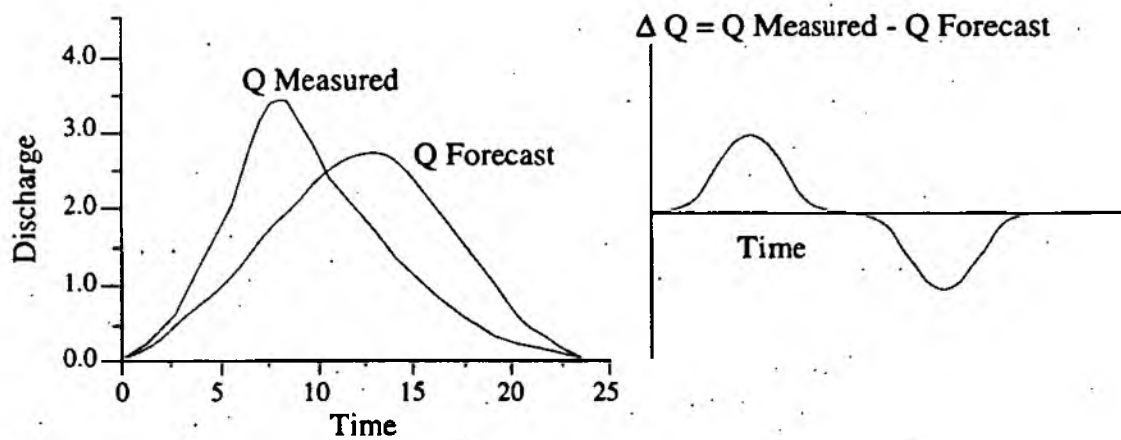


Fig. 6.13 *Incorrect Impulse Response Shape Error*

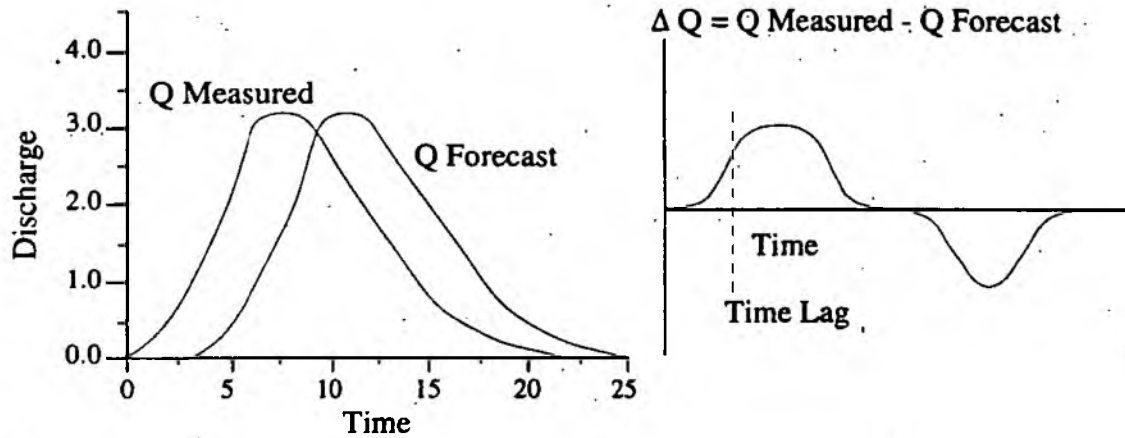


Fig. 6.14 *Incorrect Impulse Response Timing Error*

In order to address these problems, and improve forecast performance three adjustment factors were developed by Han (1991), and incorporated into the PRTF model. These parameters are used to adjust response shape, volume and timing, discussed further in section 6.8.3 below.

6.8.3 PRTF Impulse Response Adjustment

Parameter updating is one of several methods of model forecast updating, others being outlined in section 6.4. The most commonly used technique is to apply real time filter theories to estimate new parameters from recent observations. However, although many methods, including Kalman Filters, have been investigated, it has proved difficult to apply them in a real-time flood forecasting situation (Cluckie and Harpin, 1982).

The PRTF procedure allows the derivation of an adaptive transfer function model which can be easily and robustly updated. The Impulse response $(H(z))$ of an adaptive TF may be written as :

$$H(z) = F(\alpha, \gamma, \tau, z) \quad (6.27)$$

where α is a volumetric factor, examined in section 6.8.3 (i)

γ is a shape factor, examined in section 6.8.3 (ii)

and τ is a timing factor, examined in section 6.8.3 (iii)

Each factor influences only one aspect of the PRTF model, and by adjustment of all three it is possible to greatly improve accuracy over the standard transfer function model. Detailed mathematics are not included here, and the reader is referred to WRRG 23 (1992) if these are required.

i) Volumetric Factor, α

Impulse response volume is altered by the use of a constant factor $(1+\alpha)$, as illustrated in figure 6.15. The α factor represents the percentage of volume change introduced into the model, and is analogous to percentage runoff, and the delta variable outlined in section 6.4.4.

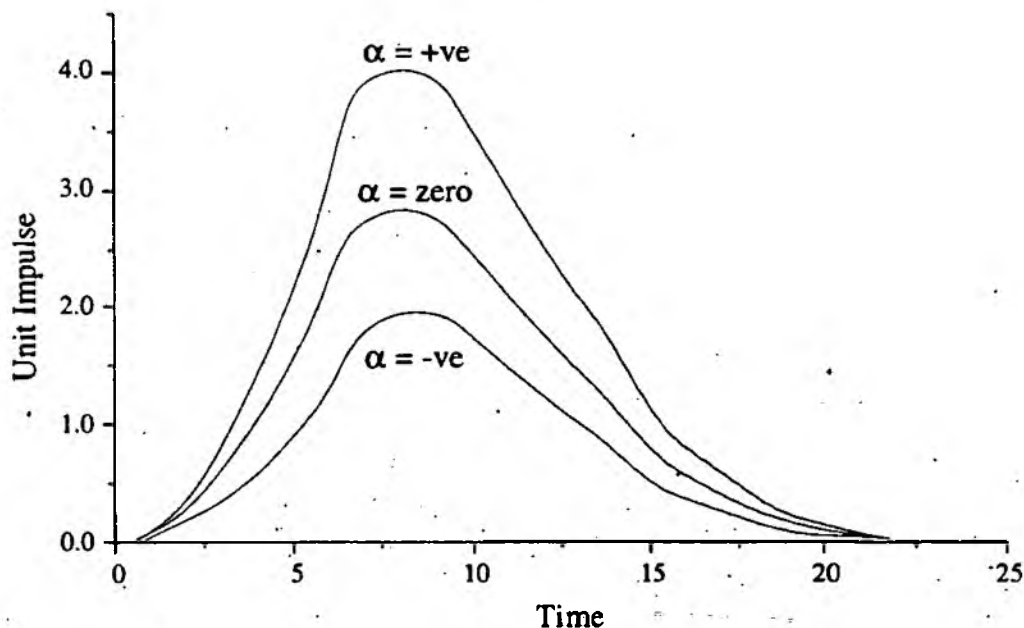


Figure 6.15 Effect of The Volumetric Adjustment Factor (Alpha)

The volumetric factor adjusts impulse response volume only. No distortion is caused to the shape or timing of the response.

ii) Shape Factor, γ

The adjustment factor, γ , is used to control the shape of the impulse response. The unit of γ is the time step of the model, and may be a real number as distinct from an integer. Figure 6.16 shows the effect of γ on impulse response shape.

When implemented, the γ parameter does not influence the volume or starting time of the model.

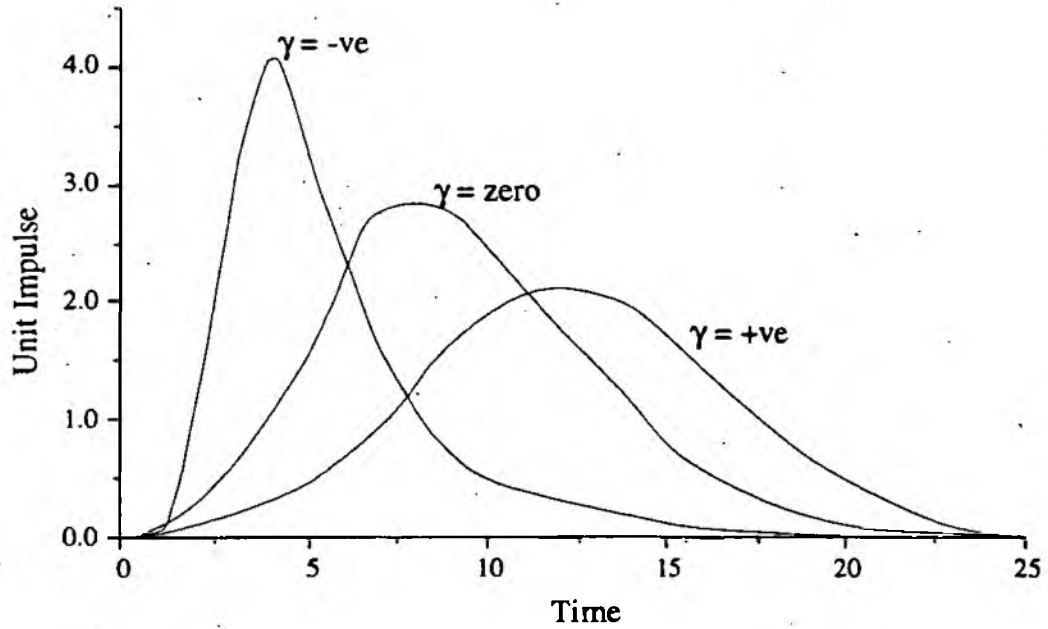


Figure 6.16 *Effect of The Shape Adjustment Factor (Gamma)*

iii) Timing Factor, τ

The timing of the response from a PRTF model may be adjusted by use of a time shift operator applied to the rainfall terms of the equation.

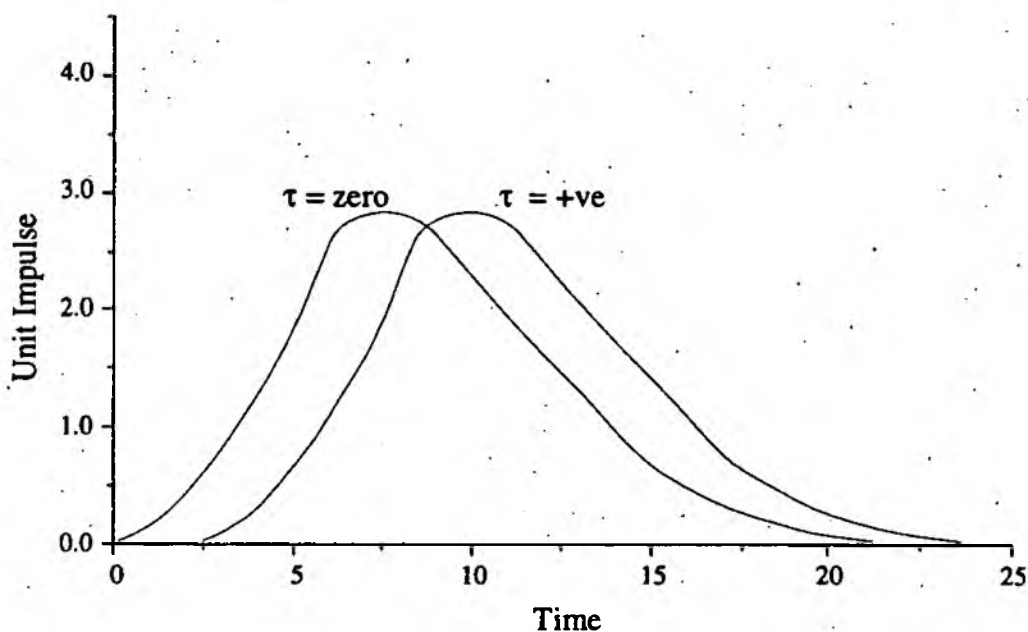


Figure 6.17 Effect of The Timing Adjustment Factor (τ)

The use of the timing factor, τ , effectively alters the impulse response timing of the PRTF model. As shown in figure 6.17, no change is made to the volume or shape of the response.

6.9 The MATH System

Following the development of the PRTF technique a model parameter estimation program called MATH (*Model Application Tool for Hydrology*) has been evolved at the Water Resources Research Group at the University of Salford to optimise standard TF and PRTF models. The program is described here to illustrate the steps followed in defining the models used in this thesis. A more detailed outline is available in Water Resources Research Group internal report 23, 1992. The MATH system developed from the standard transfer function calibration program, TFCal (Tilford, 1990) to provide a degree of automation in model development.

6.10 Conclusion

As noted in this chapter, the rainfall-runoff process is non linear and time variant. An outline has been presented of the utilisation of transfer function models in representing the rainfall runoff process, and the problems they produce. The physically realisable transfer function model has been outlined, and its advantages described. The ease of adjustment and robustness of the PRTF allows the use of the model in a non-static form, as compared with the linear, stationary transfer function generally used in forecasting.

The successful adjustment of the models α , γ and τ parameters in real-time depends on the knowledge of the factors which influence their behaviour. In Chapter 7, work is presented to relate and quantify the PRTF parameters with relation to the physical processes of a rainfall event. These relations are then incorporated into a knowledge based forecasting system in Chapter 8.

CHAPTER 7

KNOWLEDGE ACQUISITION

7.1 Introduction

It may be an over-statement to say that once knowledge is available is it a simple matter to build a knowledge based system (KBS). However, it is undoubtedly true that without knowledge in one form or another, the construction of such a system is extremely difficult. Conventional methods of knowledge engineering, as used in Chapter 1, did not yield rule-base or heuristic (rule-of-thumb) information of sufficient detail to use in a KBS. Similarly, although the investigation detailed in Chapter 5 produced useful information about rainfall runoff trends, the relationships themselves were too weak to be used in a flow forecasting situation.

This chapter presents work carried out to examine the dynamics of the PRTF parameters described in section 6.8 with a view to applying and tuning the model in real-time. Much work has been carried out in the meteorological community into storm pattern recognition (eg. Brice and Fennerma, 1970; Duda and Blackmer, 1972) and applying expert systems techniques in forecasting weather patterns (eg. Conway, 1989). The work described here was aimed at investigating the rainfall input as experienced by the catchment in order to define relationships and thresholds in PRTF for use in a simple knowledge based system. A method of defining catchment status in terms of antecedent precipitation index is also developed, based on rainfall input from radar information. This is used in a catchment reservoir representation in order to assess loss rate and the threshold of 'effective' rainfall generation within the drainage area.

7.2 Variables Investigated

Several authors have looked into the factors which influence river flow production. Shanholtz *et al.* (1981), in investigating the effect of rainfall, land use, soil and cover conditions, concluded that rainfall was the most sensitive variable affecting the run-off hydrograph. Hamlin (1983) also named rainfall as one of the most variable of the hydrological processes. In view of this it was decided initially to examine rainfall characteristics in isolation from catchment status and its modifying influence, using the Kinematic Wave model in creating synthetic rainfall runoff events.

The small areal extent of most rapid response catchments lessens the usefulness of routinely available catchment status information such as MORECS (*Meteorological Office Rainfall and Evaporation Calculation System*) which covers only large areas (40 x 40 km). In an operational system, data assimilation and processing must take place quickly, and the sheer number of catchments involved at a regional scale makes complex lysimeter calculations out of the question.

Difficulties with estimating catchment status accurately have been discussed by Owens (1986), who concluded that although relations have been found elsewhere (eg. Sargent, 1984), river base flow could not be used as an indicator of catchment wetness in the Blackford Bridge area. Langdon (1984) was similarly unable to discover a well-defined relation between baseflow and average percentage runoff. All these problems highlight the need for a simple and accurate indicator of catchment moisture status, which is easy to calculate and available for use in real-time. In response to this, a procedure was evolved using Antecedent Precipitation Index (API) principles combined with a reservoir, or tank, representation of the catchment. The dynamics of the tank-API system were investigated by analysis of actual rainfall events, to gain knowledge of the system and its applicability in a flow forecasting context.

7.3 The Use of Synthetic Data

The analysis carried out in Chapter 5 revealed several links between rainfall hyetograph and rainfall hydrograph characteristics. However, 'noise' in the data signals, and the influence of catchment conditions distorted and reduced the strength of the relationships, most proving too imprecise to be applied to a forecasting situation. In searching for the knowledge to enable 'tuning' of a PRTF model, synthetic data creation was applied to define 'machine induced rules' using the Kinematic Wave Model (KWM) outlined in section 7.4. Slatter (1987) states that it is reasonable to use machine induced rules in order to improve on an 'experts' performance, which may be inconsistent or unreliable. Indeed, Michalski and Chilauski (1980) showed the potential of this form of knowledge gathering for some simple tasks such as crop disease diagnosis.

The use of a synthetic database brings many advantages besides potentially improved performance. Firstly, it enables rapid production of large numbers of rainfall runoff events which would normally take years to acquire and process, if they were available at all. The use of the KWM also allows control over the type of events produced. This enables one variable, such as storm intensity or location, to be altered whilst all others are held constant, greatly aiding the identification of causal links. Finally, although simplified representations of reality, the simulated rainfall, catchment and flow characteristics are based on those in the area of interest. Thus, any relationships found should be at least qualitatively correct.

7.4 The Kinematic Wave Model

The Kinematic Wave Model is a simplified version of the Saint-Venant equations, used in modelling unsteady flow in open channels and is the simplest distributed model.

For a Kinematic wave, the motion is described principally by the Continuity equation, which is given by :

$$\frac{\partial A}{\partial t} + \frac{\partial Q}{\partial x} = q \quad (7.1)$$

where momentum is :

$$\frac{\partial V}{\partial t} + V \frac{\partial V}{\partial x} + \frac{g}{A} \frac{\partial (yA)}{\partial x} + \frac{Vq}{A} = g(S - S_f) \quad (7.2)$$

where V is flow speed, x is the distance along the channel, Q is the channel flow, A the cross sectional area, t the time, q the distributed flow along the side of the channel, g the acceleration due to gravity, S is the gravity slope and S_f is the friction slope.

In the KWM, local acceleration, corrective acceleration and pressure terms are all ignored, the friction force S_f and gravity force S being assumed to cancel each other.

From this the KWM is defined by the momentum being :

$$S = S_f \quad (7.3)$$

Thus equation 7.3 may be otherwise expressed as :

$$A = \alpha Q^\beta \quad (7.4)$$

where α and β are coefficients.

7.4.1 Application to the Rainfall-Runoff Process

The Kinematic Wave method has been applied as a model of the rainfall-runoff process in describing flow over plains (Chow *et al.*, 1988). Here, lateral flow is defined as being equal to the difference between rainfall and infiltration rates, and channel flow is taken as being flow per unit length of plain. The outflow hydrograph may be simulated from rainfall of a given duration, by analytical solution of the characteristic equations.

The KWM, when used in the rainfall-runoff process, offers the advantage over unit hydrograph methods in that it is a solution of the physical equations governing surface flow. The solution is only for one-dimensional flow, however, whereas the actual watershed flow is in reality two-dimensional, following land surface contours. As a result of this, the Kinematic wave parameters, such as Manning's roughness coefficient (n), must be adjusted to produce a realistic outflow hydrograph. Detailed information for the application of KWM's to the rainfall-runoff process is presented by Eagleson (1970), Overton and Meadows (1976) and Stephenson and Meadows (1986).

7.4.2 Finite Difference Approximations

The Saint-Venant equations for distributed routing are only amenable to analytical solution in a few special simple cases. They are partial differential equations that must be solved in general by the use of numerical methods. Solution may be carried out using Finite Difference (FD) and Finite Element (FE) methods.

The Finite Element method uses piece-wise continuous polynomials to interpolated between points or nodes. Although the points play a part in finite element theory,

emphasis is directed more towards the interpolation functions. The FE method has advantages when solving highly spatially dependent problems, but is less efficient when used in time dominated situations. The finite difference methods, employed here in solving the partial difference equations are discrete techniques wherein the domain of interest is represented by a set of nodal points. Information between these points is commonly obtained using Taylor Series expansions (Chow *et al.*, 1988). The FD method provides only approximations of complex spatial boundaries but is excellent for solving essentially time dependent problems.

A fundamental concept in this form of approximation theory is that the domain of solution of the given partial differential equation is first sub-divided by a net with a finite number of mesh points. The derivative at each point is replaced by a finite difference approximation. This discretization procedure may be visualised as the replacement of the solution of the partial differential equation with a polynomial, and the differentiation of this polynomial.

Equation 7.1 may be expressed in finite difference form as :

$$\frac{Q_{i+1}^{j+1} - Q_{i+1}^j}{\Delta x} + \frac{A_{i+1}^{j+1} - A_{i+1}^j}{\Delta t} = \frac{q_{i+1}^{j+1} + q_{i+1}^j}{2} \quad (7.5)$$

and the equation of momentum (7.3) may be rewritten as :

$$\begin{aligned} A_{i+1}^{j+1} &= \alpha(Q_{i+1}^{j+1})^\beta \\ A_{i+1}^j &= \alpha(Q_{i+1}^j)^\beta \end{aligned} \quad (7.6)$$

Substitution of (7.6) into (7.5) and rearrangement produces :

$$\frac{\Delta t}{\Delta x} Q_{i+1}^{j+1} + \alpha(Q_{i+1}^{j+1})^\beta = \frac{\Delta t}{\Delta x} Q_i^{j+1} + \alpha(Q_i^{j+1})^\beta + \Delta t \left(\frac{q_{i+1}^{j+1} + q_{i+1}^j}{2} \right) \quad (7.7)$$

In equation (7.7) the unknown discharge has been arranged to the left-hand side and all the known quantities are on the right. The non-linear nature of the equation requires the use of a numerical solution scheme such as Newton's Method. Figure 7.1 shows the grid used for numerical solution by finite differences.

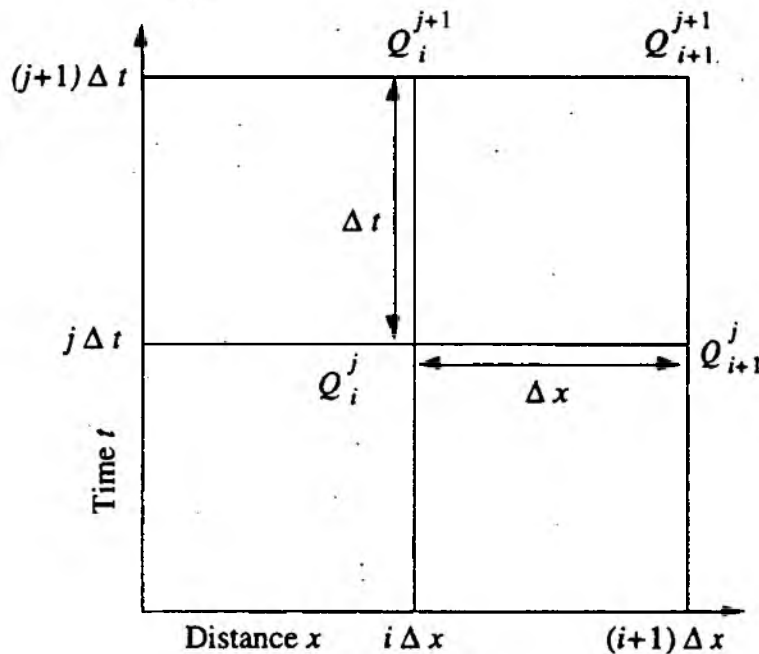


Figure 7.1 Finite Difference Box for Numerical Solution by Finite Differences (After Chow et al., 1988)

At each finite difference grid point the known right-hand side can be written as :

$$C = \frac{\Delta t}{\Delta x} Q_i^{j+1} + \alpha(Q_i^{j+1})^\beta + \Delta t \left(\frac{q_{i+1}^{j+1} + q_{i+1}^j}{2} \right) \quad (7.8)$$

The residual error from this may be defined as :

$$f(Q_{i+1}^{j+1}) = \frac{\Delta t}{\Delta x} Q_{i+1}^{j+1} + \alpha(Q_{i+1}^{j+1})^\beta - C \quad (7.9)$$

and the first derivative error by :

$$f'(Q_{i+1}^{j+1}) = \frac{\Delta t}{\Delta x} + \alpha\beta(Q_{i+1}^{j+1})^{\beta-1} \quad (7.10)$$

Applying Newton's Method with iterations $k=1, k=2, \dots$ (Chow *et al.*, 1988) :

$$(Q_{i+1}^{j+1})_{k+1} = (Q_{i+1}^{j+1})_k - \frac{f(Q_{i+1}^{j+1})_k}{f'(Q_{i+1}^{j+1})_k} \quad (7.11)$$

The convergence criterion for the iterative process is :

$$|f(Q_{i+1}^{j+1})_{k+1}| \leq \epsilon \quad (7.12)$$

where ϵ is an error criterion.

From this the KWM may be solved and used to simulate the rainfall-runoff process to obtain the relationships outlined below.

7.5 Synthetic Database Creation

In order to form a synthetic database to gain knowledge of the rainfall-PRTF parameter links, an artificial catchment was defined. To retain simplicity no attempt was made to artificially recreate the Blackford Bridge catchment and all its drainage network.

Instead, a simulated catchment was evolved as illustrated by Figure 7.2, using actual values for roughness, slope and so on.

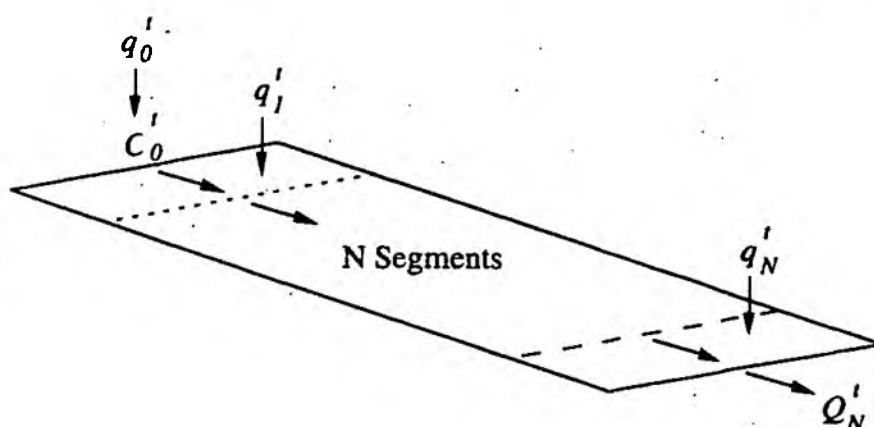


Figure 7.2 Kinematic Wave Model Simulation Catchment

The simulation catchment was defined as being 5km long to enable investigation of the effect of storm movement over the basin area. Lateral storm movement was not addressed, and a value of 0.5km was used for catchment width. A bedslope value of 10% was assigned to the model as begin typical of a fast response catchment. In keeping with the natural stream formation of the area, a Manning's roughness coefficient (n) of 0.035 was used (NERC, 1975).

The boundary and initial values may be defined as :

$$Q_i^j|_{j=0} = Q_0 \quad (i)$$

$$Q_i^j|_{i=0} = 0 \quad (\text{Start of Catchment Flow}) \quad (7.13)$$

Manning's equation for channel width B , where $P \approx B$ and $S_D = S_f$, may be written as :

$$Q = \frac{S_0^{1/2} A^{5/3}}{nP^{2/3}} \quad (7.14)$$

Solving for A , this may be rewritten :

$$A = \left(\frac{nP^{2/3}}{\sqrt{S_0}} \right)^{0.6} Q^{0.6} \quad (7.15)$$

Thus, $\beta=0.6$ and :

$$\alpha = \left(\frac{nP^{2/3}}{\sqrt{S_0}} \right)^{0.6} \quad (7.16)$$

7.5.1 PRTF Model Identification

Once the simulation catchment was defined in the Kinematic Wave program, a PRTF model was identified for it. In order to do this a random sequence of rainfall was generated to simulate precipitation over the whole catchment area. This rainfall data was then routed through the KWM to produce an outflow response.

Model identification was carried out to find the optimum PRTF model for the catchment, as outlined in Chapter 6. The identification procedure produced a model with a (3,3) structure and impulse time-to-peak of 12 minutes. Figure 7.3 shows the impulse response function produced.

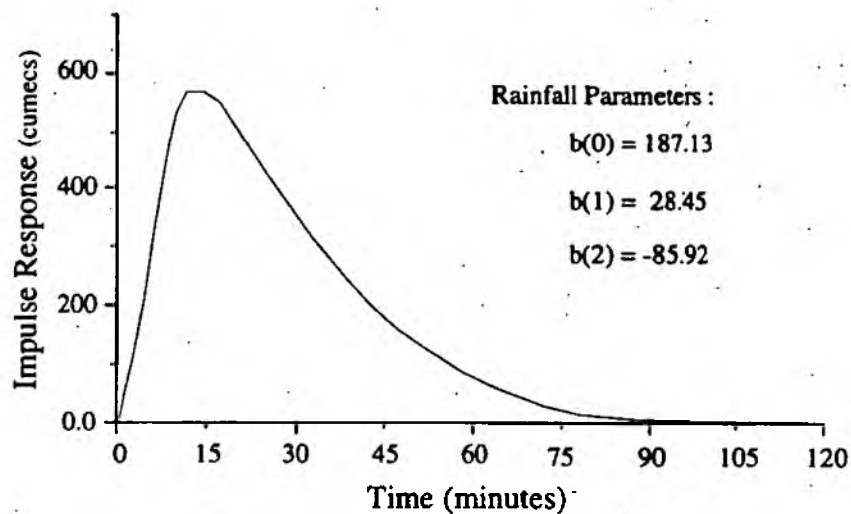


Figure 7.3 *Kinematic Wave Model Impulse Response Function*

7.6 Rainfall Characteristics Investigated

One of the greatest advantages of using synthetically produced rainfall and flow data in the search for machine induced rules is that it allows the variation in one factor to be examined whilst all others are held constant. In order to identify the nature of the influence of individual rainfall characteristics on flow formation, several rainfall variables were selected as outlined in section 7.7 to 7.9 below. The driving factors divided into two types, storm dynamic variables such as storm movement relative to the catchment and the rainfall characteristic, intensity. The rainfall variables investigated were those identified as important by a domain 'expert', Ray Rushton. As such they reflect his underlying conceptualisation of the problem, and are structured around human knowledge (Slatter, 1987).

In concentrating on storm and rainfall characteristics, as opposed to hyetograph characteristics, a simple bell shaped rainfall input was used to perturb the Kinematic Wave Model, as shown in Figure 7.4.

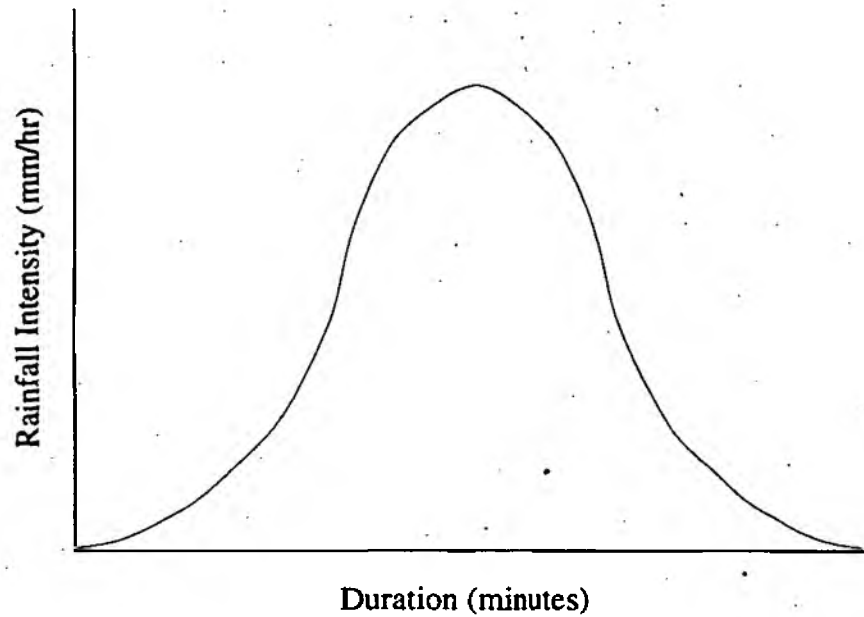


Figure 7.4 *Bell Shaped Rainfall Input to KWM*

No rainfall loss was included in the KWM chosen for this investigation, and runoff volume is addressed in section 7.11. The γ and τ values obtained for each rainfall dynamic and intensity investigation are shown in Appendix B, with the RMSE values produced by the optimised and standard PRTF simulations when compared to actual flow.

7.7 Catchment Wide Rainfall

An assessment was made of the effect of rainfall occurring at the same intensity over the whole catchment at once, such as may take place during a large frontal event. Figure 7.5 shows the effect of average rainfall intensity for a single duration on the impulse response of the synthetic catchment, three intensity levels being represented.

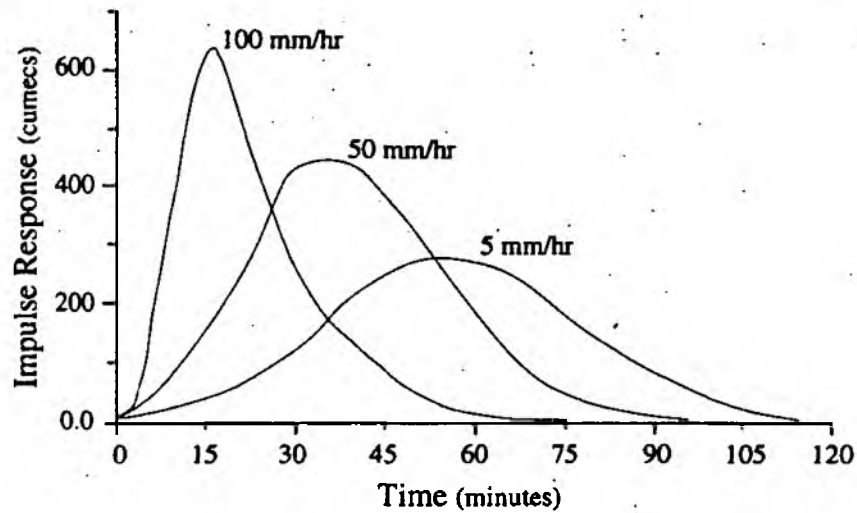


Figure 7.5 Effect of Varying Rainfall Intensity on Model Impulse Response, With Catchment Wide Rainfall

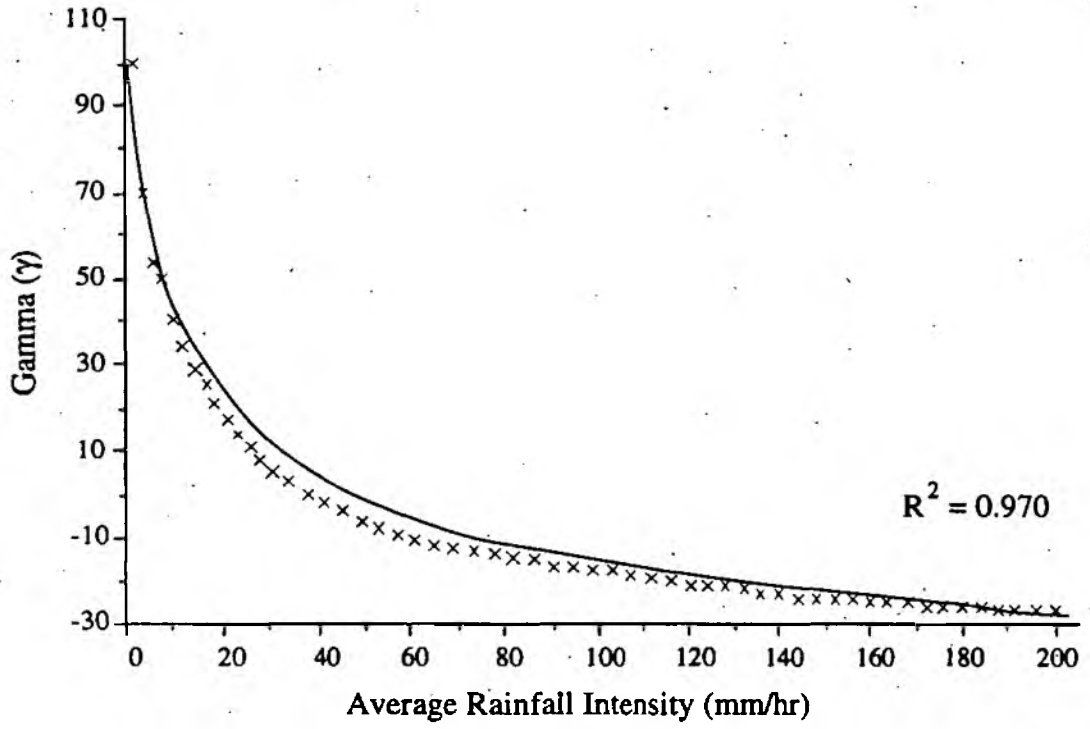
An optimised PRTF model was then fitted to each of the rainfall-runoff sequences by hand, using the MATH system outlined in Chapter 6. As rainfall intensity increased over the whole catchment, so impulse response changed (as illustrated in Figure 7.5 above). In order to model this the PRTF shape parameter (γ) has to be decreased in magnitude, as shown in Figure 7.6.

As rainfall intensities increased, peakier responses were produced, and the value of Gamma (γ) had to be reduced to represent this in the impulse response. The relationship for catchment-wide rainfall was summarised as :

$$y = 93.272 + -55.471 * \text{LOG}(x) \quad R^2=0.970$$

were x is rainfall intensity and y is gamma.

The timing parameter (τ) did not change regardless of rainfall intensity, as can be seen in Figure 7.5, no delay being present before the start of hydrograph rise.



• Figure 7.6 Average Rainfall Intensity - Gamma (γ), Catchment-Wide Rainfall

7.8 Static Rainfall Location

The position of rainfall within a catchment can greatly effect the runoff response provoked, producing rapid, high or attenuated flow. The influence of rainfall location was examined by splitting the catchment into three sections longitudinally. Figure 7.7 shows the areas defined as upper, middle and lower reaches.

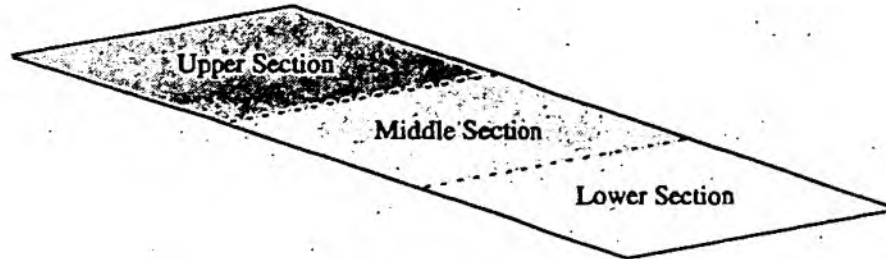


Figure 7.7 Three Static Rainfall Positions Over Synthetic Catchment

The simulations of precipitation concentrated in one of the three sections represents rainfall being stationary or moving laterally across the catchment, but contained within one of the sub-areas. Movement up or down the catchment (with respect to river flow direction) is address in section 7.9.

A bell shaped rainfall event was used as input to the model for each of the catchment reaches. The fitting of a PRTF model to each response showed that rainfall in the lower catchment results in a fast, steeply peaked response as shown in Figure 7.8 (a). In the middle reach the attenuating influence increases time-to-peak response, introducing a time delay and causes a smoother impulse response (Figure 7.8 (b)). With the storm centred over the upper reach, attenuation is greater, leading to an increased delay before response rise, and a lower peak IR as demonstrated in Figure 7.8 (c).

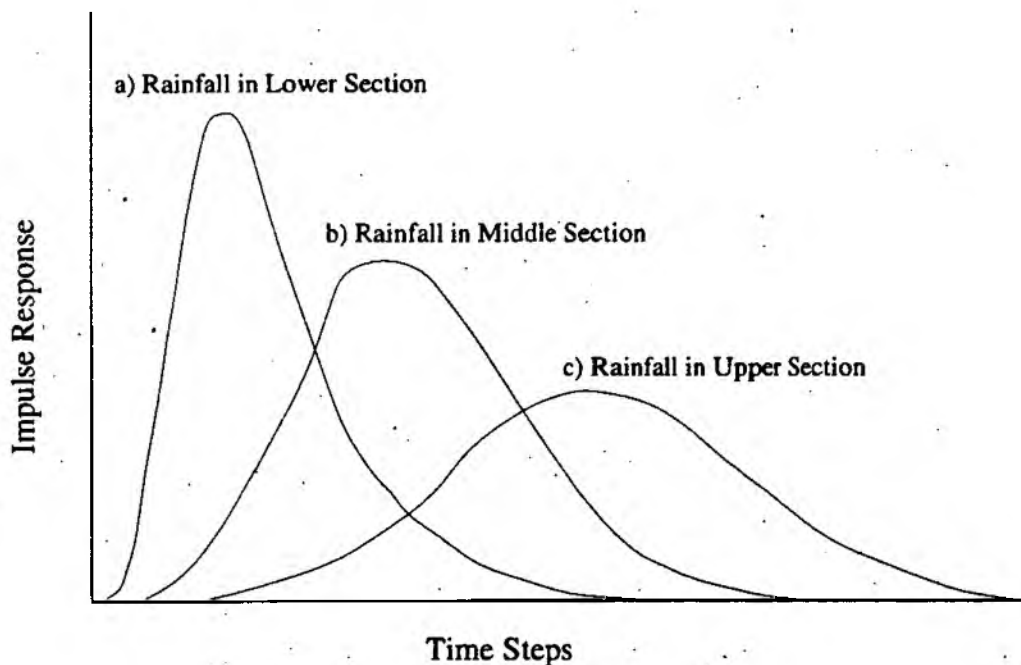


Figure 7.8 *Impulse Responses From the Three Catchment Sections*

In order to represent the changes in catchment runoff response, both the shape and timing parameters must be adjusted. This may be subdivided into two processes, firstly, impulse response transposition by time τ to align the start of response rise, as shown in Figure 7.9.

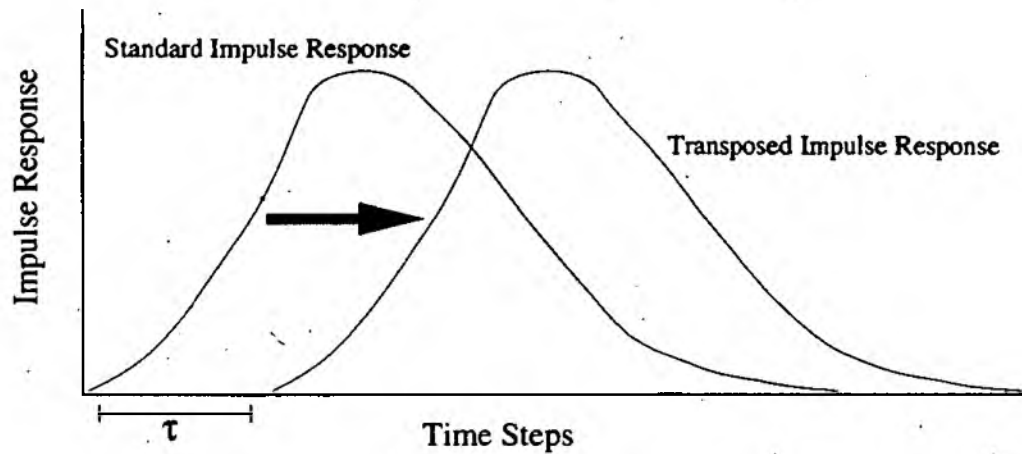


Figure 7.9 Impulse Response Transposition by Time τ

The second phase is the tuning of γ to reform the response shape, represented in Figure 7.10.

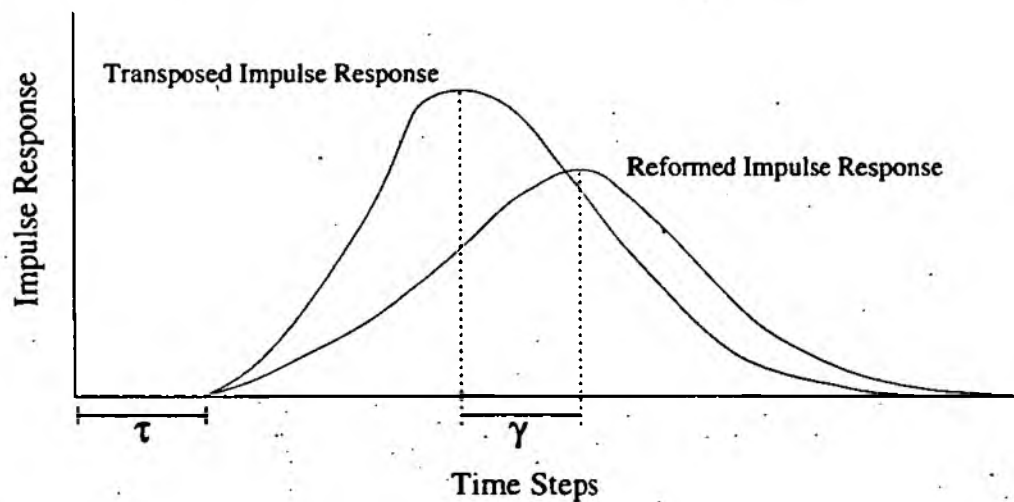


Figure 7.10 Impulse Response Reformation by Shape Parameter (γ)

7.8.1 Influence of Rainfall Intensity

In order to assess the effect of precipitation intensity on the hydrograph produced by rainfall at each of the three locations, storms were generated from 1 to 200 mm/hr average intensity. These were routed through the kinematic wave model for each catchment rainfall position, and a PRTF model fitted to each event. The model parameters were optimised manually, using the MATH parameter tuning program.

The general form of the relationships found was similar for each of the three rainfall positions. However, the relationships themselves varied considerably. With rainfall situated on the lower part of the catchment there was no need to introduce a time delay in to the model, and for all rainfall intensities the value of the timing parameter (τ) was zero. The effect of increasing rainfall intensity on the shape adjustment parameter (γ) is shown in figure 7.11.

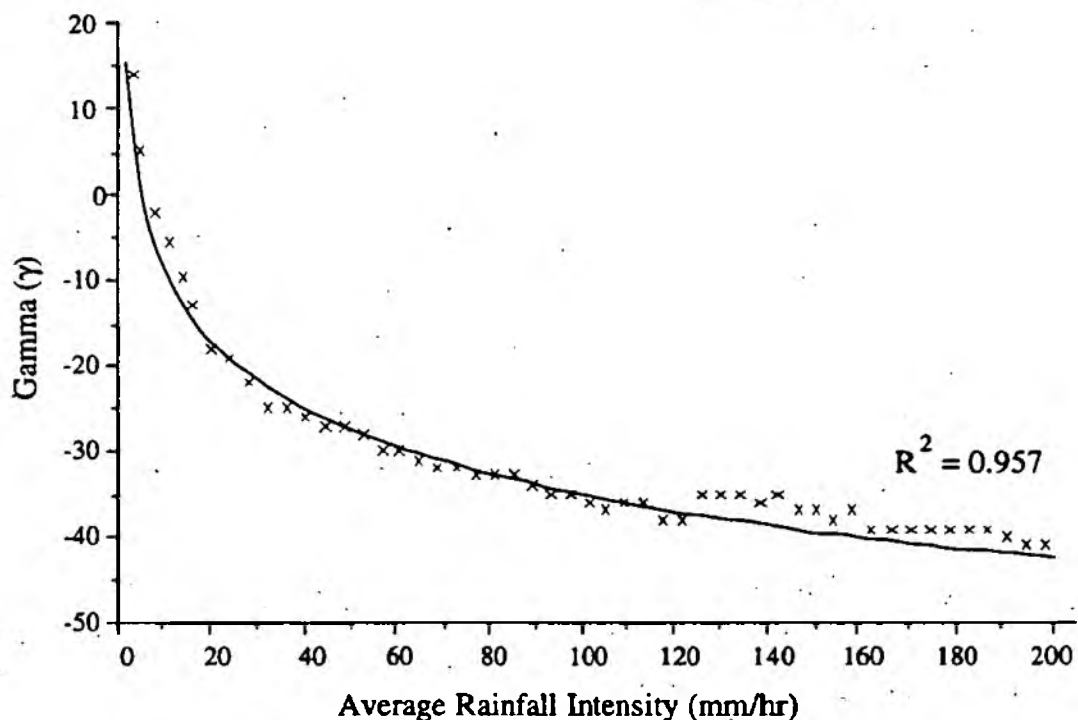


Figure 7.11 Rainfall Intensity - Gamma Relationship, Lower Reach

Higher rainfall intensities lead to peakier hydrographs, and a need to reduce the value of γ to represent this in the impulse response. To summarise the lower reach - rainfall intensity information, a relation was fitted to the data points :

$$y = 19.141 + -26.696 * \text{LOG}(x) \quad R^2 = 0.957$$

where x is rainfall intensity and y is gamma.

When the same set of storms were used as input to the middle section of the catchment a response time delay was found to be necessary at all intensities, as shown in figure 7.12. No relationship was fitted to this graph as τ takes only integer values. Instead the changes in tau to model increasing in rainfall intensity were noted as thresholds.

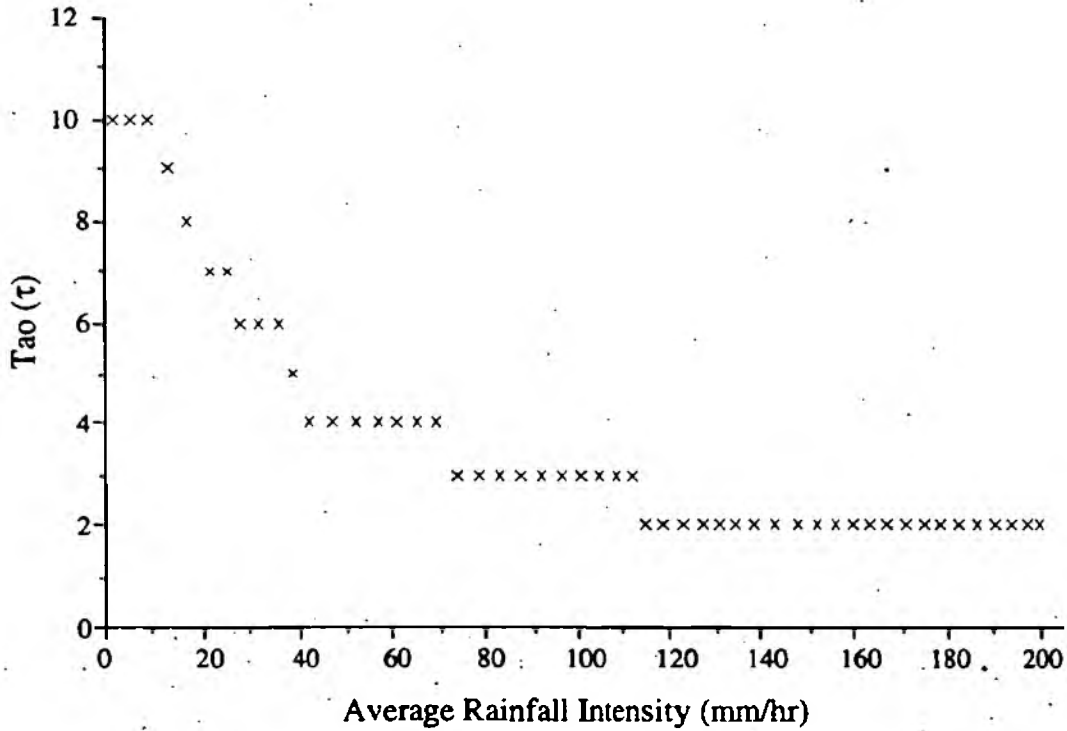


Figure 7.12 Rainfall Intensity - Tao Relationship, Middle Reach

As with the lower catchment, higher rainfall intensity caused greater 'peakedness' of the response. To account for this γ was decreased as rainfall became more severe, demonstrated by figure 7.13.

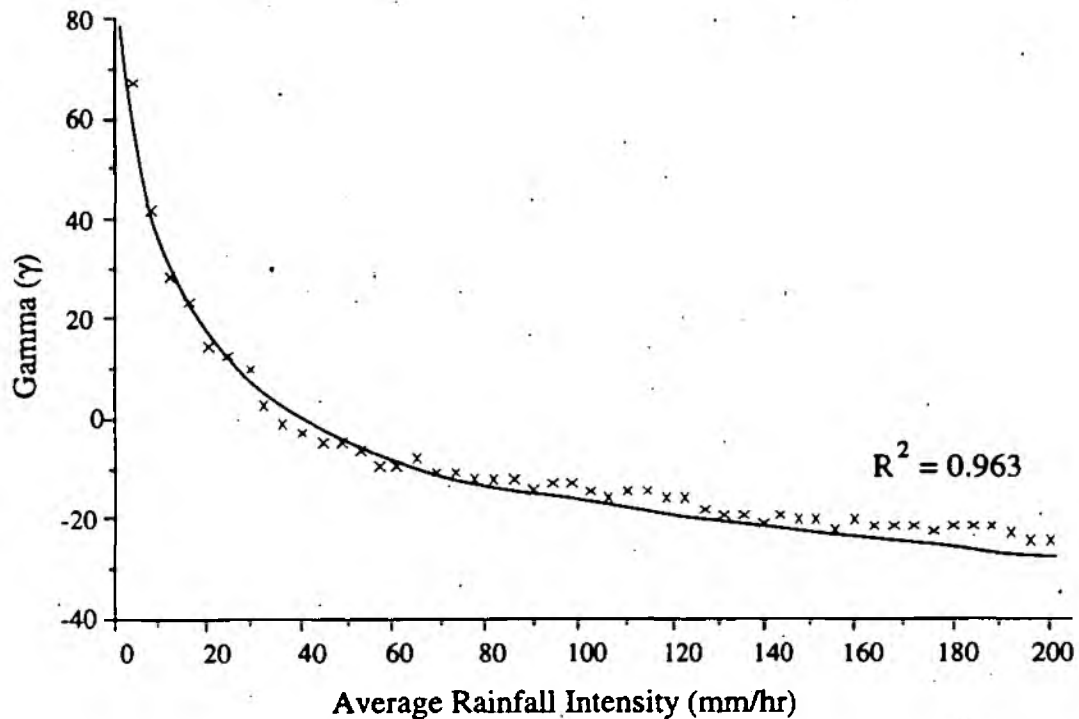


Figure 7.13 *Rainfall Intensity - Gamma Relationship, Middle Reach*

Although values of γ reduced with higher rainfall intensity, equivalent intensity events required it to be greater in the middle reach than the lower. This may be explained by the additional 'smoothing' effect of the catchment. A relationship was fitted to the graph shown in figure 7.13, giving the equation :

$$y = 82.691 + -51.426 * \text{LOG}(x) \quad R^2 = 0.963$$

where x is rainfall intensity and y is gamma.

With rainfall situated on the upper catchment area the time delay required to replicate outflow response was higher than for the middle section, as shown in figure 7.14.

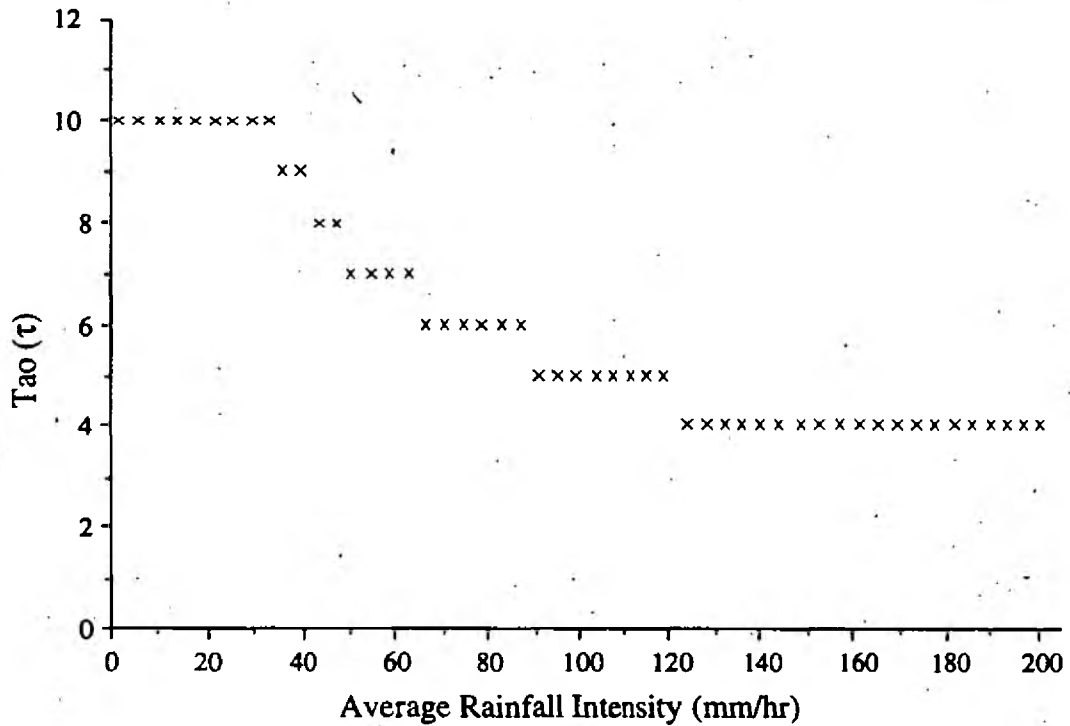


Figure 7.14 *Rainfall Intensity - Tau Relationship, Upper Reach*

This again reflects the time delay imposed by moisture movement down the catchment to the outflow point. As with the middle section no relationship was fitted to the intensity-tau graph, but the intensities leading to a change in τ were noted as threshold values.

Figure 7.15 shows the intensity-gamma relationship to model rainfall on the upper catchment. As seen in the middle and lower sections, increasing rainfall severity lead to reduced γ values to produce the correct impulse response. The 'smoothing' effect of the catchment lead to less peaked responses, and necessitated higher values of γ overall when compared to the relationships for the other catchment sections.

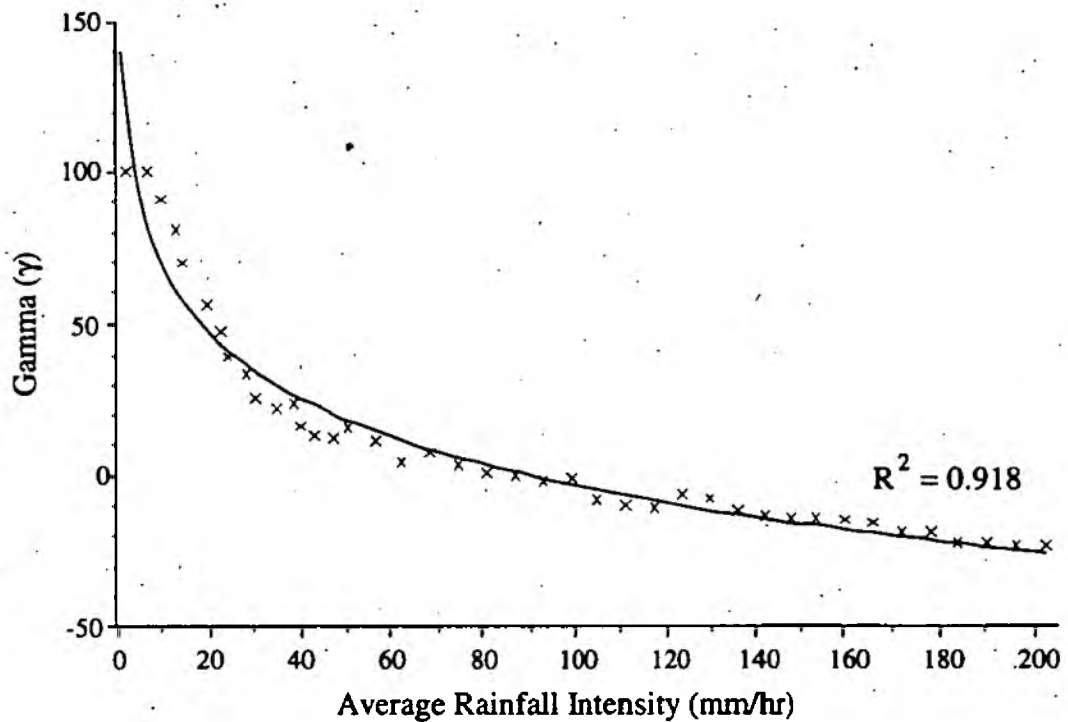


Figure 7.15 *Rainfall Intensity - Gamma Relationship, Upper Reach*

The information about rainfall on the upper part of the catchment was summarised by a logarithmic relationship, in the form :

$$y = 140.67 - 72.176 * \text{LOG}(x) \quad R^2 = 0.918$$

where x is rainfall intensity and y is gamma.

7.9 Rainfall Movement

The effect of storm movement along the catchment, with or away from the direction of main stream flow, was again investigated using the KWM. In the analysis, identical rainfall events were generated so as to replicate storm movement up or down the drainage area, as demonstrated in figure 7.16.

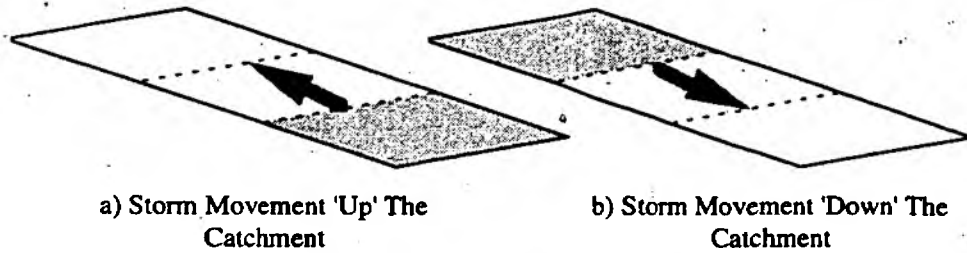


Figure 7.16 Synthetic Storm Movement In Relation To The Catchment

Figure 7.17 shows the model impulse response with storm movement commencing at the basin outfall and moving 'up' the catchment (away from the direction of flow). Here, the response produced is relatively rapid, due to the close initial proximity of the storm to the catchment outlet. However, the response peak is lower than for the catchment's standard model impulse response, as moisture is evacuated from the catchment by the river whilst precipitation continues further up the basin. This in turn leads to a longer recession limb as river flow is bolstered for longer due to continued rainfall higher in the catchment.

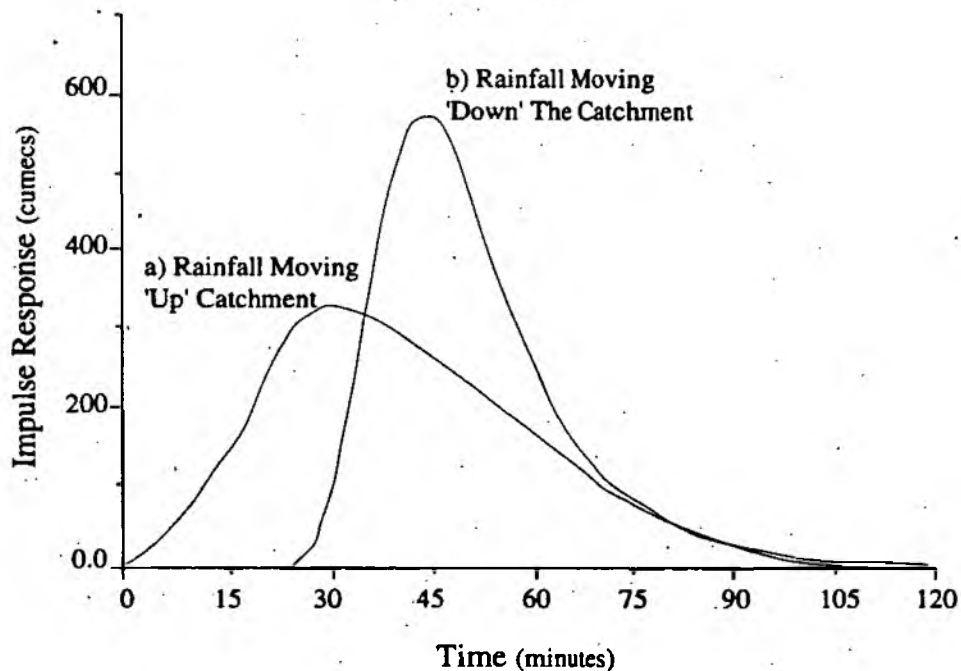


Figure 7.17 Impulse Responses Due To Direction Of Rainfall Movement

With event movement in the direction of stream flow ('down' the catchment) the event response was delayed, as would be expected when rainfall commences at the 'top' of the drainage area. However, the impulse response itself proved to be 'peakier' and of shorter duration than the standard catchment response. This was thought to be due to the additive effect of flow from higher up the catchment combining with storm rainfall moving down the river basin.

The effect of changing rainfall intensity was again examined using synthetic storms from 1 to 200 mm/hr. Each event was routed through the KWM, rainfall moving with and against the direction of main stream flow. A PRTF model was then optimised manually for each individual event.

As with stationary precipitation (section 7.8) the general form of the shape and timing parameter changes was found to be similar as rainfall intensity increased, but the detailed relationships varied significantly.

With rainfall movement from the basin outflow 'up' the catchment, the shape (γ) values needed to represent catchment response decreased with storm severity, as shown in figure 7.18.

Gamma values were generally lower for events moving against the direction of river flow, giving the relationship :

$$y = 178.97 + -87.373 * \text{LOG}(x) \qquad R^2 = 0.956$$

where x is rainfall intensity and y is gamma.

With the storm commencing at the outflow of the catchment, rainfall input was converted into flow with no timing delay, and τ was found to be consistently zero.

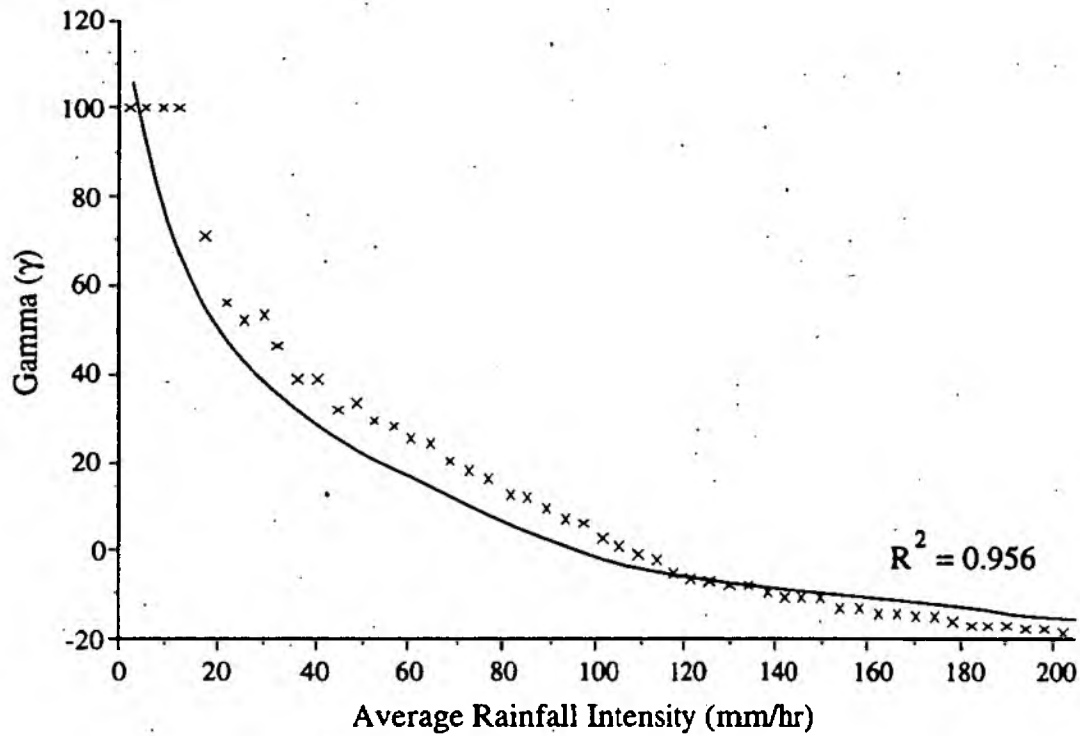


Figure 7.18 Rainfall Intensity - Gamma Relationship, Moving 'Up' Catchment

Rainfall movement with the stream direction required reduction in γ values to model catchment response, reflecting the 'peakier' impulse responses produced. Figure 7.19 demonstrates that increased rainfall intensity necessitated lower values of γ as runoff time-to-peak was reduced. The form of the intensity- γ relationship is given by :

$$y = 184.76 - 99.903 \cdot \text{LOG}(x) \quad R^2 = 0.943$$

where x is rainfall intensity and y is gamma.

With rainfall entering the catchment farthest from the outflow, a time delay was always apparent before runoff hydrograph rise. Increasing storm intensity caused a decrease in the time delay, as shown by the optimised τ values in figure 7.20. As before the values of τ were noted at rainfall intensity thresholds and no relationship was fitted.

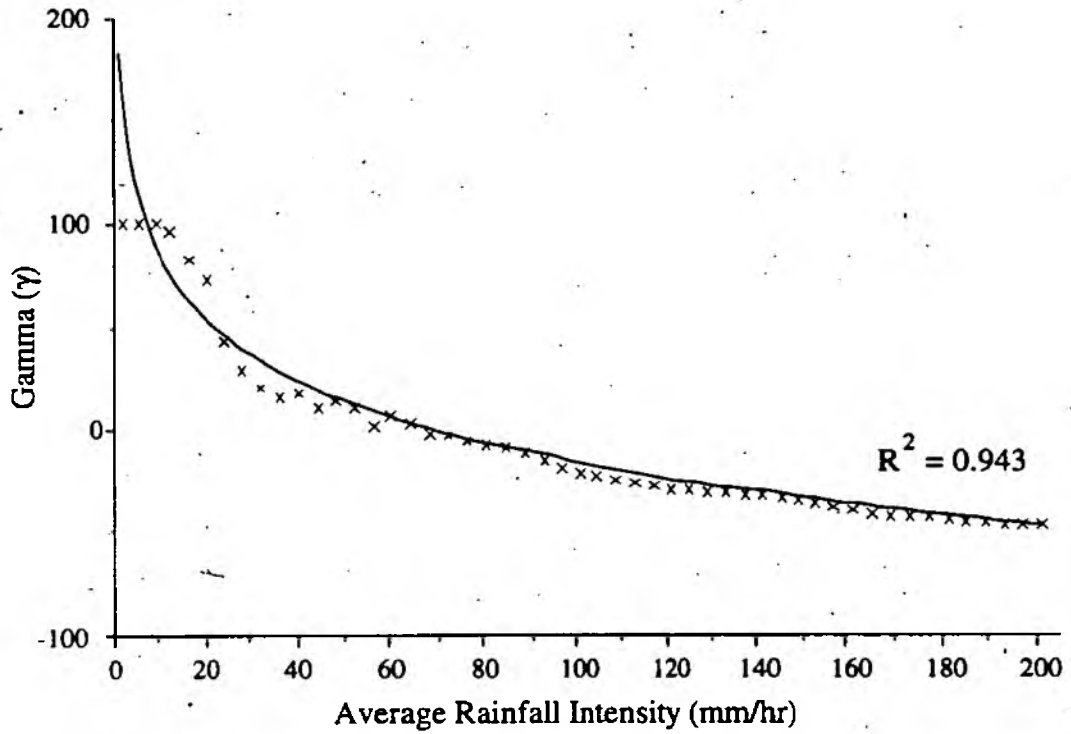


Figure 7.19 Rainfall Intensity - Gamma Relationship, 'Down' Catchment

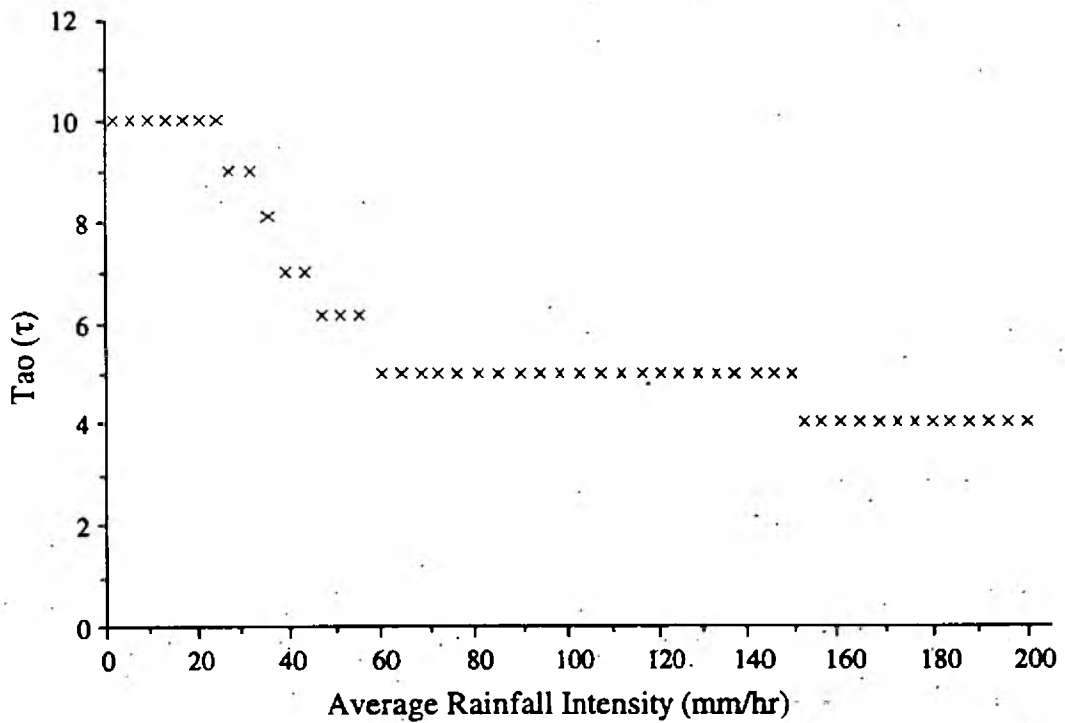


Figure 7.20 Rainfall Intensity - Tao Relationship, 'Down' Catchment

7.10 Testing the Knowledge

Having established the relationships and thresholds linking rainfall position, movement, areal extent and intensity to runoff hydrograph shape and timing, the knowledge was tested to find whether it could be used to provide improved flow simulations on the artificial catchment. The assessment was carried out by generating random intensity rainfall events, routed through the kinematic wave model, moving or stationary over the synthetic catchment. The attitude (ie. concentration position or direction of movement) of the storm was set within the program and the average rainfall intensity being defined for each storm. These rainfall characteristics were then used to set the PRTF shape and timing parameters from the relationships established in sections 7.8 and 7.9. Since runoff volume was not addressed using the KWM the volumetric factor α was tuned by hand after the shape and timing ones, in order to provide the lowest RMS error.

7.10.1 Testing Procedure

Testing was carried out with events at five average intensity levels, 10 mm/hr, 25 mm/hr, 40 mm/hr, 70 mm/hr and 120 mm/hr. The five random events were routed through the KWM, producing outflow hydrographs from the three concentrated storm positions, and similarly event movements with and against the direction of flow. A further five random events were created covering the whole catchment area.

The PRTF model parameters were tuned manually with reference to the event's position, direction, intensity etc., and the input rainfall sequence routed through the model. The modelled hydrographs were then compared with the flow hydrograph produced by the KWM. Root mean squared errors (RMSE) values were used to provide a measure of accuracy between the estimated and 'actual' runoff sequences,

given by :

$$RMSE = \sqrt{\left\{ \frac{1}{N} \sum_{i=1}^N (E_i - R_i)^2 \right\}} \quad (7.17)$$

Where E_i is the estimated variable (in this case modelled flow), R_i is the reference variable (in this case the KWM output hydrograph) and N is the total number of values.

A static PRTF model, optimised for the catchment using catchment-wide medium intensity rainfall, was used for comparison to assess the effectiveness of parameter tuning. The PRTF model used in static form is analogous to the standard non-adaptive TF model routinely used in flow forecasting (as outlined in Chapter 6). RMSE values were again used as comparison between actual and forecast flow, as shown in equation 7.17.

In each of the 30 evaluation events, the tuned PRTF model produced at least comparable simulations compared with the static model. The RMSE values obtained for each simulation for the static and tuned models are shown in Table 7.1.

The most significant improvements over the static model came when rainfall was particularly intense, took place away from the catchment outlet or moved in the direction of river flow. These were the situations when the model impulse response required greatest adjustment, either in shape or timing, to represent the catchment response. Figure 7.21 shows an example of stationary, medium intensity rainfall (average 40 mm/hr) on the upper part of the catchment.

Table 7.1 RMSE Values From Tuned And Static PRTF Models

Intensity Rain Level Dynamic	10 mm/hr	25 mm/hr	40 mm/hr	70 mm/hr	120 mm/hr
Upper Catchment	15.48	12.33	11.63	16.21	14.91
	29.66	28.82	23.44	27.03	31.33
Middle Catchment	11.26	9.44	9.78	10.09	12.61
	24.34	19.64	18.99	23.44	25.03
Lower Catchment	4.88	5.93	6.05	5.39	5.11
	14.23	12.67	8.73	9.98	10.40
'Up' Catchment	6.93	4.31	6.17	7.88	8.82
	11.51	10.19	7.31	9.42	9.62
'Down' Catchment	7.02	9.30	8.59	11.22	9.48
	24.77	20.40	19.02	19.33	21.80
Catchment Wide	5.11	3.01	2.05	4.72	5.44
	4.71	2.44	1.53	3.68	6.21

Upper Value = Tuned PRTF

Lower Value = Static PRTF

In this simulation, the standard non-adaptive PRTF model for the catchment responds too quickly, the τ value of 9 delayed the tuned hydrograph, giving a more accurate starting point for the rising limb. Figure 7.22 depicts the hydrograph produced by a high intensity random event moving with the direction of main stream flow.

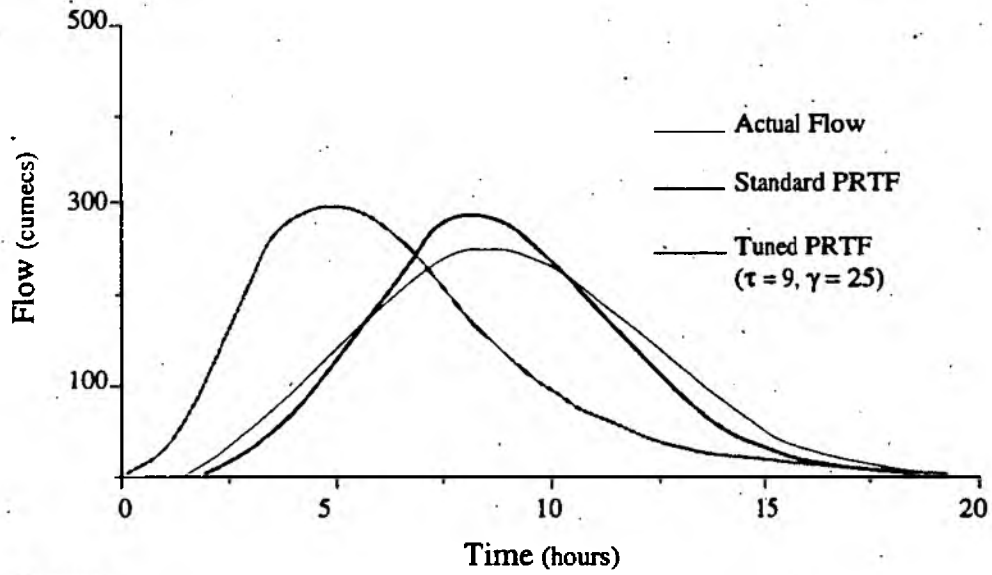


Figure 7.21 Stationary, Medium Intensity Rainfall, Upper Catchment Reach

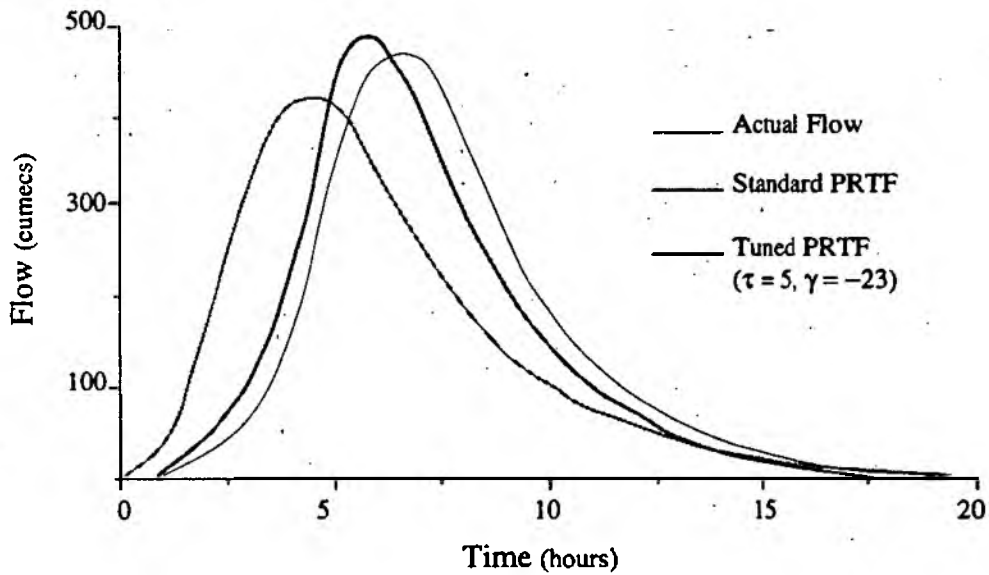


Figure 7.22 High Intensity Event Moving With flow

The increased peakedness of the catchment response is not well reproduced by the static model. The tuned PRTF simulation, however, produced a more accurate

representation of maximum flow and its time of occurrence, by decreasing γ to form a 'peakier' hydrograph.

From this testing procedure, it is clear that knowledge of the influence of rainfall position, movement and intensity may be applied in setting the shape and timing parameters of a physically realisable transfer function model. The flow simulations achieved using this form of parameter tuning were generally better than those achieved with a static transfer function model, especially when rainfall input varied significantly from that used for calibration. Information of rainfall direction and coverage in combination with data relating to rainfall intensity may thus be used to tune model parameters and better represent the runoff hydrograph.

7.11 Knowledge of Rainfall Runoff Percentage

In assessing rainfall runoff percentage from the catchment, analysis was carried out using the actual event data. Although this meant fewer events were available, it provided a feel for what actually took place in the drainage area. A synthetic analysis was considered but the type of rainfall loss at work in the catchment would have had to have been defined using a loss-rate mechanism, such as those shown in Figure 7.23. Although similar in some ways, each loss-rate method will result in a different contribution of rainfall to flow. The use of actual event data allowed the thresholds at work to be identified, instead of imposed by the model chosen.

7.11.1 Rainfall Losses

The volume of runoff from any given precipitation event will vary depending upon the antecedent soil moisture status and vegetation conditions of the catchment. Gray (1970) expressed this as a continuity equation :

$$\text{Precipitation} = \text{Depression Storage} + \text{Evapotranspiration} + \text{Infiltration} + \text{Interception} + \text{Surface Runoff}$$

The precipitation input to a PRTF model is gross (total) rainfall. In order to establish the net or 'effective' rainfall (which becomes surface runoff in the continuity equation) a method is required to estimate percentage runoff from the event. Several techniques have been developed to define net rainfall based around various mechanisms, the most popular being the loss rate methods and Horton's decay curve (Figure 7.23).

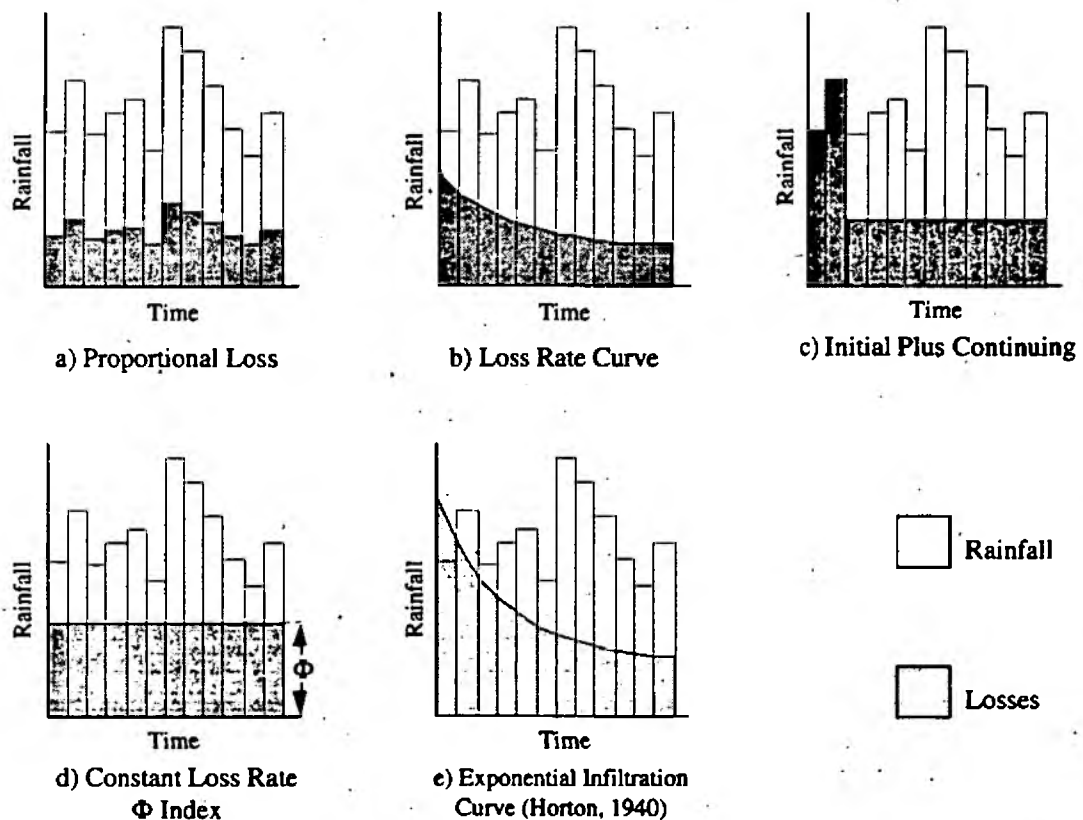


Figure 7.23 Rainfall Loss Methods, After NERC (1975) and Shaw (1983)

7.11.2 Problems with Rainfall Scaling

The PRTF model was defined by Han (1991) as using a single percentage runoff factor (α) to adjust rainfall input volume, as described in section 6.8. However, the use of a scaling variable, such as alpha, on all rainfall values does not adequately represent the true catchment processes which take place. In a real drainage basin, rapid runoff will occur due to infiltration excess (identified by Horton, 1933), when rainfall intensity is greater than infiltration rate, or saturation excess (after Hewlett, 1967) when the infiltration capacity of the ground is exceeded. The latter is the most common in the UK and the one which dominates on the Blackford Bridge subcatchment (Palmer, 1992). Both processes represent a threshold rather than scaling approach, effective rainfall being produced when a certain limit is exceeded.

To account for this Han (1991) put forward the concept of a rainfall separation reservoir, or 'tank'. This represents varying catchment wetness, and introduces the threshold element as outlined in section 7.11.3.

7.11.3 Rainfall Separation Reservoir

The idea of catchment representation in tank or reservoir form is not a new one, for example Chow (1951) and Nash (1957) used cascades of equal linear reservoirs to transform effective rainfall into runoff. Han (1991) proposed a rainfall separation tank of the type shown in Figure 7.24 .

Here, tank height (H) represents the catchment absorption capacity, tank level (C) represents current moisture status, and losses (L) represents evapotranspiration, interception, basin outflow etc.

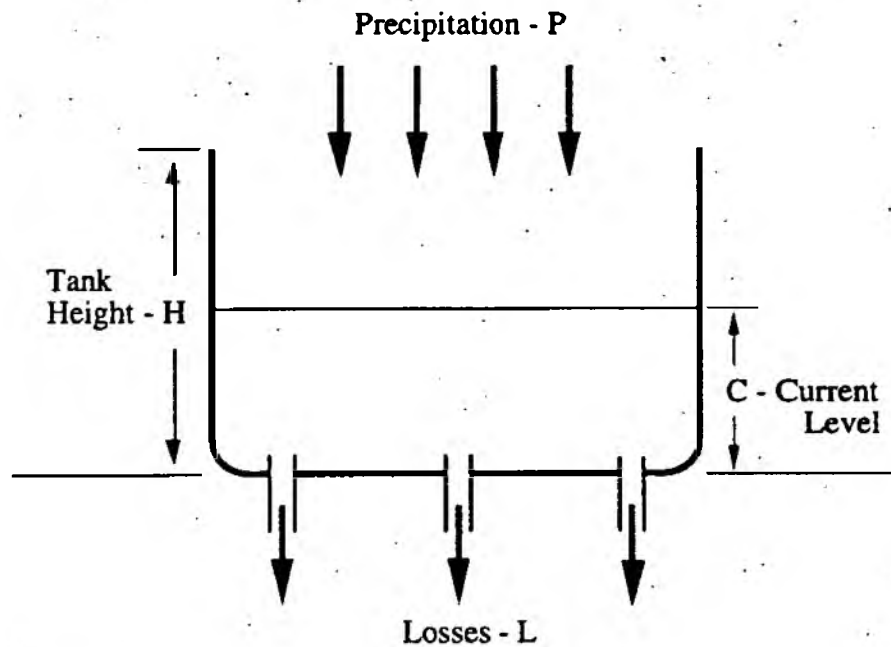


Figure 7.24 RST, No Effective Rainfall Produced (After Han, 1991)

When rainfall occurs, precipitation will be added to the tank. If rainfall rate is greater than loss rate then the tank level (C) will rise, such that :

$$C_{(t)} = C_{(t-1)} + P_{(t)} - L \quad (7.18)$$

If rainfall continues at a higher level than losses, then eventually the level of tank moisture (C) will become equal to tank height (H). From this point effective rainfall (E) is produced (Figure 7.25) where :

$$E_{(t)} = C_{(t-1)} + P_{(t)} - L - H$$

where $P_{(t)} - L > H$

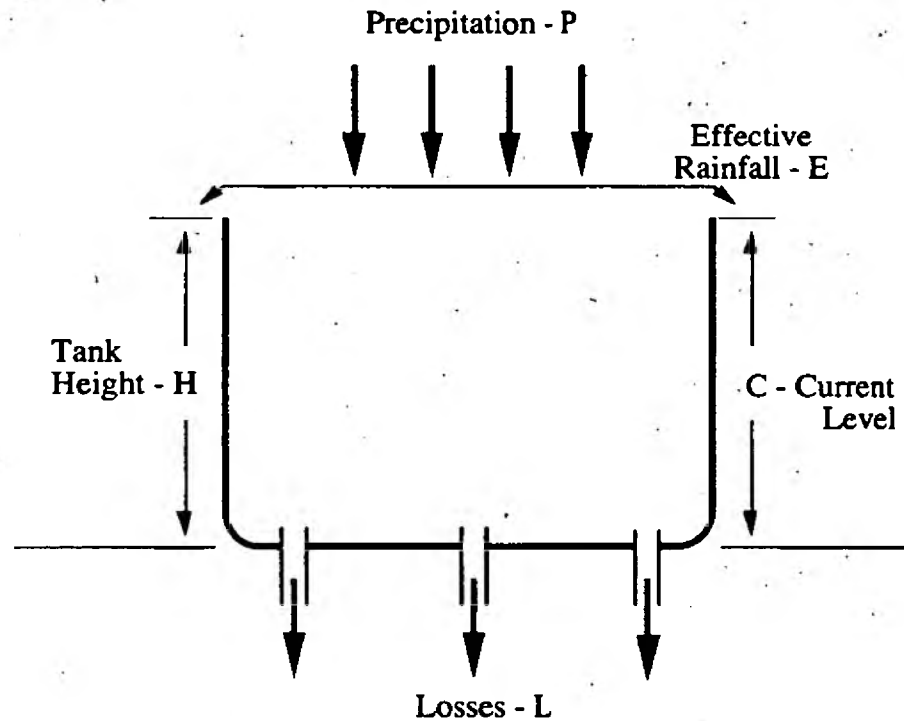


Figure 7.25 RST, With Effective Rainfall Production (After Han, 1991)

Here, the tank acts as a 'switch', effective rainfall only being produced when all catchment storage is used up. In this way, the reservoir can simulate the changes in catchment soil moisture status due to changing rainfall intensity, by rise or fall of the current tank level (C).

Thus far, no attempt has been made to calibrate the rainfall tank with reference to real catchment conditions, examine the dynamics of the system or apply it in any forecasting situation. In order to make the technique usable in a real time forecasting context, a method of antecedent precipitation index (API) calculation was evolved to use radar data. This was combined with the rainfall reservoir to assess catchment conditions as precipitation occurs.

7.12 Antecedent Precipitation Index

The method chosen to represent catchment status in this study was Antecedent Precipitation Index (API). Although providing only an index of the rainfall at the site of interest, as opposed to the direct measurements by some other methods, API brings several advantages. Direct estimation of the soil moisture status of a catchment area may be carried out in several ways. Lysimeters provide relatively high accuracy estimation of soil status, using a large block of undisturbed soil surrounded by a water-tight container which is weighed from below. These devices are complex, expensive to install and provide information for the sampling point only, making them inappropriate for this study. Soil Moisture Deficit (SMD) information was also seen as an unsuitable measure of catchment status during winter events, which do not generally have a deficit of soil moisture. In this investigation, the areal coverage and real-time availability of radar rainfall information were seen as ideal for assessing overall catchment status. A simple average-loss method was used to represent evapotranspiration and drainage losses from the soil as outlined below.

7.12.1 Calculation of Antecedent Precipitation Index

Antecedent precipitation index provides a measure of the catchment soil moisture status at a given time. Calculation is based on the premise that soil moisture is depleted at a rate proportional to the amount in storage in the soil, such that :

$$API_t = k \cdot API_{t-1} \quad (7.19)$$

where API_t is the index t days after the first value (API_0). The constant value k is dependent on the potential loss of moisture from the soil, varying seasonally between 0.85 and 0.98 (Shaw, 1983).

When rainfall takes place, this is added to the index so that calculation for the eight day would be :

$$API_8 = k \cdot API_7 + R_7 \quad (7.20)$$

where R_7 is rainfall on the seventh day.

Shaw (1983) states that an arbitrary value of 20 mm may be selected for API_0 , the transient effect of this initial value being lost after about 20 t periods.

The index has been used to provide an indication of event runoff, and Linsey *et al.* (1958) provide a detailed description of daily API based on a graphical coaxial relationship. Traditionally API has been calculated and updated only on a daily basis, limiting its effectiveness. However, the frequent updating and wide areal coverage of radar data, as outlined in Chapter 3, makes the technique applicable in real time using remotely sensed precipitation input. In the present study the rainfall separation tank was combined with API to assess catchment soil moisture status and provide a threshold above which effective rainfall would take place in a real time system.

7.12.2 Radar Based API

Radar data is available at a maximum 2km by 2km resolution, but since distributed modelling of soil moisture movement was not carried out, API was calculated only at a catchment average scale. In order to relate the tank parameters to catchment API, the threshold height (H) and losses (L) were defined empirically from the 10 events shown in table 7.2.

Several methods exist for identifying catchment losses to evapotranspiration. Perhaps the best known is Penman's (1948) equation :

$$H = E_0 + Q$$

where H is available heat, E_0 is energy for evaporation and Q is energy for heating the air.

The values of E_0 and Q can be defined from aerodynamic equations, based on humidity, temperature, saturated vapour pressure and so on. These measurements are not available in real-time, and are only carried out routinely at meteorological stations, and so have low areal coverage.

Direct measurement of eddy-flux evaporation is possible using devices such as the Institute of Hydrology's 'HYDRA' (Shaw, 1992). This battery powered device uses vertical windspeed sensing and infrared hydrometers to measure effective evaporation from the ground surface. Although its output is potentially available in real time, its low spatial representativeness and relatively high cost make less suited to widescale application in a flood forecasting system.

In this study, the single, simple loss factor used in API calculation was seen as preferable. This is necessarily less accurate over short time periods and at a single point than devices such as the HYDRA. However, its speed of application in catchment status calculation was thought to be more than compensation, given that the correct magnitude of loss could be established.

The API loss factor varies seasonally between 0.85 and 0.98 for daily calculation. These figures equate to loss factors between 0.9971 and 0.9966 respectively for five minute data. In order to allow testing to be carried out with those events shown in

Appendix A, analysis was undertaken using 10 different storm events which became available during the course of the investigation. All were frontal, with varying durations of radar record. Due to the relatively limited number of events available, the effect of seasonality was not addressed in this analysis, and moisture loss was assumed to occur at the same rate during rainfall as between events. A PRTF model was optimised for each individual event with regard to response shape and timing, as outlined in section 6.9, the volumetric parameter (α) being set to zero. The length of the radar rainfall record for each storm was identified manually from the Meteorological Office magnetic tapes, and varied between two and eleven days. An arbitrary API value of 20 mm was set at the start of each of the radar record periods.

An incrementing step-wise algorithm was constructed in VAX FORTRAN to find the optimum values of loss (L) and effective rainfall threshold (ERT) for each event. Initial values were set for loss (0.9950) and ERT (10 mm). Starting with the initial value of ERT a program loop increased the loss parameter by 0.0001, running through the radar record before the storm to calculate the API at the time of the event. A simulation hydrograph was then produced based on these loss rate and threshold values, such that rainfall contributed to flow only if catchment API was greater than ERT.

When this process was complete, the runoff simulation hydrograph, was compared with the actual storm hydrograph and an RMSE value calculated showing the difference between two. After this the loop updated the loss value by 0.0001 and carried out the procedure again with the same ERT value. When the loss parameter reached 0.9999 it was reset to 0.9950 and the effective rainfall threshold increased by 0.05 mm. The procedure continued to a maximum rainfall threshold value of 50 mm. A schematic diagram of the algorithm process is presented in Figure 7.26.

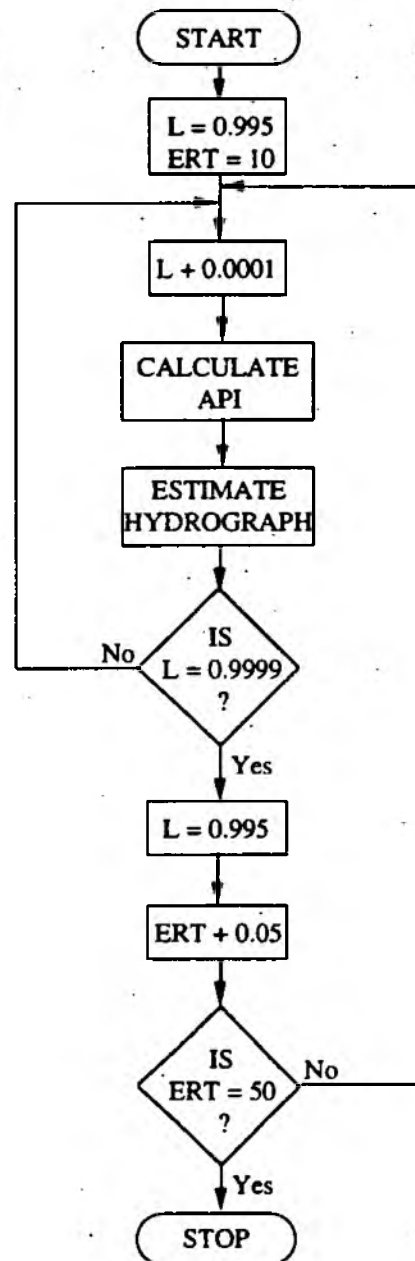


Figure 7.26 Schematic Diagram Of Loss And ERT Calculation

Table 7.2 shows the loss and threshold values giving the lowest RMSE figures, along with the length of radar record before the event simulated.

Table 7.2 Optimum Loss and Threshold Values For Storm Events

Date Of Event	Best Loss Value	Best ERT Value (mm)	Best Simulation RMSE	Length Of Radar Record (days)
110184	0.9967	31.80	3.45	4
191285	0.9970	31.60	8.19	3
031186	0.9969	28.15	6.77	2
141087	0.9966	28.65	5.02	7
020188	0.9967	29.45	9.38	3
040788	0.9969	28.05	7.35	6
110888	0.9971	30.35	10.21	4
020988	0.9967	28.70	2.31	5
191988	0.9968	31.15	6.89	3
140289	0.9969	29.95	4.08	5

Variation in the loss and effective rainfall threshold figures may be due to the relatively short radar rainfall record available for some of the events. In these cases the initial value selected for API would be more influential, having less opportunity to stabilise to the correct level with time. Other possible influences could be the amount and type of vegetation cover in the catchment, which affects interception and evapotranspiration between events.

On the basis of this work the average values of 0.9968 and 29.79mm were chosen to represent antecedent precipitation losses and the effective rainfall production threshold (analogous to the conceptual height of rainfall separation tank).

7.13 Conclusion

This chapter contains a description of the work carried out, using synthetic and real data, to gain knowledge of the dynamics of PRTF parameters. Estimation of catchment status was also undertaken, to allow model tuning in real-time with reference to storm and catchment characteristics.

In investigating event rainfall dynamics and their effect on model shape and timing, a synthetic rainfall database of over 700 events was used. This allowed greater control over the storm characteristics under investigation, and the generation of a larger number of storms than would normally be available. Event routing through the KWM revealed links between rainfall characteristics such as position and intensity, and the γ and τ values required to represent the changes to the flow hydrograph.

The original PRTF volume scaling factor, alpha, was rejected in favour of a more threshold based reservoir approach. In assessing the loss rate, and conceptual 'height' of this rainfall separation tank, 10 actual rainfall - runoff events were analysed. Modelling the catchment loss would necessitate the inclusion of some form of loss in the KWM. To avoid assumptions about the type of loss rate mechanism operating within the catchment, the actual radar rainfall and catchment runoff record was used. The relatively low number of rainfall-runoff events available meant that only one loss rate was identified, rather than a seasonally variable value. The reservoir framework of the effective rainfall threshold and API approach creates a system which is analogous to the initial plus continuing mechanism. Here, however, the exact loss rate and rainfall contribution threshold are known from the analysis. Antecedent precipitation index is calculated for the catchment from the radar rainfall information, and the appropriate loss rate. In Chapter 8, these relationships are built into a simple knowledge based system, for real-time model parameter tuning.

CHAPTER 8

KNOWLEDGE BASED FORECASTING

8.1 Introduction

A knowledge-based system (KBS) has been defined as one containing domain knowledge, which is able to perform tasks requiring intelligence if done by human beings (Beynon-Davies, 1991). This type of artificial intelligence system has been developed since about 1975, well known examples being the medical base MYCIN (Shortliffe, 1976) and the geological PROSPECTOR (Duda *et al.*, 1979). In more recent years knowledge based representation has found its way into the water resources community, and a review is presented of some of the hydrological knowledge based system applications which have been developed. The field of knowledge-based and 'expert' systems research is a huge area in its own right, and contribution to the esoteric forms of cognitive architecture and information retrieval is beyond the scope of this thesis. Rather, the intention here is to apply knowledge of the influence of rainfall characteristics and catchment status in a relatively simple real-time model tuning system, to better forecast the rapid response flow hydrograph.

8.2 Knowledge Representation Software

8.2.1 Languages

Perhaps the most significant difference between knowledge based systems and conventional computer programs is that the latter typically consist of algorithmic procedures, written in a 'conventional' language. This type of system comprises the data being held separately from the program which manipulates it, and does not

encode information in a way designed to capture its meaning. The knowledge based approach, by contrast, attempts to make explicit the inherent relationships within the data. This involves the use of modular 'chunks' of knowledge in the form of rules and facts, relating data to other entities in a given domain (Beynon-Davies, 1991).

The knowledge base and expert system languages, such as LISP and Prolog, offer certain advantages over conventional languages. LISP, for example, allows network structures to be defined in great complexity, and is extremely useful in handling series' of lists (Naylor, 1985). However, all languages are a compromise of what can be done in machine code, and specialist languages have their drawbacks in other areas. Mathematical calculation, for example, can become very complex in LISP. The simple FORTRAN statement $A=2+2$ in LISP becomes (SETQ X ADD(22)), simply because it was not designed to carry out mathematics.

Essentially, the difference between conventional algorithm programming and the knowledge based approach is a conceptual one of coding technique, the language aiding the tasks that may be required to be performed in the given environment. The system being built in this investigation is, of necessity, a relatively simple one, having to perform quickly to set model parameters in real-time. This, combined with the existence of the necessary control structures (IF-THEN statements) and its much wider usage within the hydrological community led to the use of FORTRAN for coding of the knowledge based system.

8.2.2 Shells

An alternative to the 'scratch' encoding of a knowledge based system is the use of ready made 'shells', such as Leonardo and Prometheus. These contain a predetermined structure into which data and relationships are fitted. The use of a shell

was not seen as appropriate for this investigation for several reasons. Firstly, the availability of 'real-time' shells is very limited. Also, some of the data formats and relationships established in this work may not be applicable to the pre-defined structure, many shells accepting only production rules, and not relationships summarised in any other way. Finally, given the relatively small number of rules, the greater control in building the system as a whole was seen as preferable to the 'convenience' of a shell environment.

8.3 Expert Systems In Water Resources

Simonovic (1991) states that there is an honest belief that some of the principles of artificial intelligence may help in the application of existing hydrological concepts and act as an inspiration for development and new discoveries. Since their introduction to water resources in the early 1980's, knowledge based and expert systems have begun to find their way into to the fields of hydrological design, planning and operation, discussed in more detail in section 8.3.1. Within water resources, Simonovic and Savic (1989) provide the definition that "A water resources expert system is a computer application that assists in solving complicated water resources problems by incorporating engineering knowledge, principles of systems analysis and experience, to provide aid in making engineering judgments and including intuition in the solution procedure."

The hydrological disciplines of processes, measurements, analyses and design (Chow *et al.*, 1988) have been categorised by Alim (1987) in terms of the problems they suffer. These have been defined as :

- Inherent Imprecision
- Paucity and Incompleteness of Data

- Fuzzy Decision Process
- Heavy Reliance on Expert Views

Through combination with computer graphics, systems analysis techniques (simulation and optimization), hydrological expertise and databases, expert systems technology may act as a mediator and translator between experts and other affected parties. In this way the computer application becomes a "vehicle for communication, learning and experimentation" (Fedra and Russel, 1986).

In considering the possible applications of knowledge based systems , Jenkins and Jowitt (1987) refer to the three most prominent problem-solving assets of an expert as archived data, theoretical knowledge and operational expertise (heuristics). In a hydrological context problem solving is achieved through combined use of these three knowledge sources.

i) Data Collection and Analysis

This is a structural aspect of hydrological problem solving. Problems exist in the spatial and temporal representivity of the data, its accuracy, what information may be excluded, and the method of analysis and statistical significance if the analysis results. In answer to these problems, an expert may often rely on past experience to judge representativeness, using statistical techniques to determine data significance, accuracy and reliability.

Use of knowledge based systems in dealing with data problems may be made in constructing a knowledge base which guides the user in the collection of data, tests to be performed and the interpretation of results. Here, a relatively low amount of judgment is required, and the experts procedures may be encoded and used with little or no input from the expert. In those cases where greater experience is required, the KBS may be used to provide suggestions, but the final decision calls for an expert's judgment.

ii) Theoretical Knowledge

In relation to hydrology, theoretical knowledge may include scientific aspects of the physical system, its components and the processes at work within it. Information may also be held about factors affecting the data and analytical or procedural techniques. In this context the expert uses his knowledge to match the appropriate analysis to the particular problem. Here he applies cognizance of connections between the available data, theoretical knowledge and operational experience. In a knowledge based environment an expert system may be used to capture the logic behind the analysis or model process.

iii) Operational Experience

Operational experience, or heuristics, divides an expert from a novice in a given domain. The hydrologist builds his expertise through time and experience. The knowledge is learned by experience and comparison, generating new information. This generally involves the integration of new facts, addition and / or deletion of heuristics and adjustment of reasoning procedures. In carrying out this process, the hydrologist must take note of the range of successes and failures, and the similarities and differences between them.

An experienced hydrologist may demonstrate expertise in problem clarification, suggestion of the type of procedures to use, judging the reliability of facts and identifying whether a solution is reasonable (Duda and Shortliffe, 1983). This demonstrates the theoretical and experience forms of expertise within hydrology. It is the need to maintain expertise within an organisation which has led to much of the expert systems development to have taken place in recent years. Strzepek *et al.* (1988) provide one such example, describing the 'expert crisis' facing the Bureau of Reclamation in the USA, following the introduction of an early retirement scheme, going on to discuss the use of expert systems to retain expertise within the Bureau. It is this type of knowledge which should be reflected in a hydrological KBS.

8.3.1 Hydrological Expert Systems Applications

The first water resources application of artificial intelligence was the HYDRO system, an expansion of the mineral exploration PROSPECTOR, developed by the Stanford Research Institute (Gashing *et al.*, 1981). HYDRO was developed as a domain independent reasoning mechanism, used to determine parameter values in describing physical watershed characteristics. In more recent years, the use of knowledge based techniques has been applied to many areas of water resources and hydrology in particular. Examples are given below of some of the types of system developed, under the general headings of water quality, supply management and flow and runoff modelling.

i) Water Quality

Knowledge based techniques have been used for many applications in the field of water quality. In the area of water treatment plant operation, Collins *et al.* (1991a) developed a tutoring expert system to enable new operators to learn about plant control. The system explains the possible reasons for common problems, and gives feed back to the user on the parameters selected, it allows visualisation of the results on the actual treatment process, and provides tuition in chemical dosage control. In a less operational role, Males *et al.* (1992) report the development of a KBS for dealing with customer enquiries. Here, the system allows non-technical administrative staff to give answers concerning water quality which would otherwise require lab personnel.

In the area of 'real-time' expert systems, Dandy and Simpson (1991) discuss the use of the CRYSTAL shell in the development of an operator assistant system. Two implementations are described, advising on the action to be taken following an alarm, and providing decision support for changes to chemical concentrations used. In an alternative direction work has been carried out on the integration of expert systems

with other software systems. Collins *et al.* (1991b) discuss the benefits of coupling an expert system with a database in aiding operators of small water treatment plants in fault diagnosis, including a tutorial element and statistical analysis to make the system more site specific.

ii) Water Supply Management

In dealing with water supply, knowledge based systems have been developed to aid in areas such as drought management and reservoir operation. Walker *et al.* (1991) have developed a decision support system for use in drought management, and Clarkson and Hartigan (1989) describe an expert system for use in storage evaluation within a pumped storage water supply system, to guide reservoir operation decisions. The system also uses historical drought conditions for comparison with current status to provide the user with a perspective on the current situation.

The real-time operation of reservoir systems has also been addressed by Floris *et al.* (1989), in an attempt to retain expert knowledge and experience. The system developed utilizes weather databases and real-time field data (levels and flows) together with mathematical models to apply the relevant expertise. The system provides decision support for operation, and theory and expertise for training new operators.

iii) Flow and Runoff Modelling

The creation of a knowledge based snow-melt runoff forecasting system has been addressed by Engman (1988). Engman (*op cit.*) discusses development of the EXSRM for a well established snow-melt model. In operation the system assists unfamiliar users in model set-up and running. Once results are obtained, the system provides support for their interpretation, and in modifying the model parameters and inputs to improve model simulations.

Knowledge based systems have also been applied to calibrate the storm water management model (SWMM), developed to simulate all aspects of the hydrological cycle. The SWMM is made up of several blocks, including runoff, transport and mixing. Baffault and Dellur (1989) outline the development of an expert system for use in calibration of the hydrological parameters within the runoff block.

The aims of the expert system are the selection of computational options to provide reasonable initial parameter values, the evaluation of simulation results by comparison of simulated and observed hydrographs, and to modify parameters to provide a better fit between simulated and observed hydrographs. The system works on a production rule basis in reducing the differences between simulation and actual flow.

All of the systems discussed above have been developed either for use 'off-line' or in a consultation role in real-time. The system developed here follows a more 'embedded' approach, basing its decisions on real-time remotely sensed data and taking appropriate action autonomously, as outlined below.

8.4 Knowledge And Expertise

In answer to the knowledge engineering problems outlined in Chapter 1, synthetic rainfall-runoff data was used in Chapter 7 to infer knowledge of the dynamics of the PRTF model parameters in relation to rainfall characteristics. Information was also established about the conditions of soil moisture status which led to the creation of 'effective' rainfall. It is this knowledge which was encoded in the real-time knowledge based system detailed in this chapter.

8.4.1 KBS Architecture

In the field of information processing, parallels may be drawn between the architecture of human cognitive systems, and knowledge based systems (Slatter, 1987) :

Human	Knowledge Based
Long Term Memory	Knowledge Base
Working Memory	Current Status Database
Mental Operations	Inference Engine

Slatter (op. cit.) goes on to state that in the machine environment the knowledge base is a static store of permanent knowledge represented in some explicit form, such as production rules or 'frames' (see section 8.5). The current status database is a dynamic store for holding temporary data and partial solutions. Finally, the inference engine acts as a processing element, using the expertise in the database to make inferences based on the updatable temporary information.

8.5 The Knowledge Base

Knowledge gained about a system may be represented in one of several different ways, depending on which is the most appropriate. As Beynon-Davies (1991) points out, however, it is the rules and facts which are most important. One form of knowledge representation is the semantic network, information being expressed as a series of 'nodes', representing concepts and 'links' to incorporate the relationships between them. An alternative method is the use of stereotyped situations known as 'frames'. Here, each frame has information attached to it in terms of 'slots' and 'fillers' to include attributes and knowledge for its use.

The form of knowledge representation used in the present study was the 'rule based' approach. This is a well-established, simple and popular method, Simons (1983) stating that the term 'expert system' is sometimes formally defined as using rule based techniques. The rule based approach involves the representation of an item of information in the form :

IF this condition is true, THEN this action is appropriate

These relationships are commonly referred to as production rules, as they produce an outcome or conclusion (Frenzel, 1987).

Psychological research dating back to Newell and Simon (1972) has shown that empirical associations and procedural knowledge may be represented in human problem solving in a rule-like form. This makes the production rule approach an ideal one for representing the knowledge gained in the present investigation. As well as having psychological support, the rule based approach also has important knowledge engineering virtues such as modularity, and ease of linkage representation and conceptualisation.

The production rules used within the knowledge base were those derived from the investigation in Chapter 7. Information was represented in the form of IF-THEN rules, based on rainfall areal extent, position and direction, and catchment status.

Once the extent and type of rainfall was established, a further set of production rules, based on rainfall intensity relationships, was developed to tune the individual PRTF parameters. The relationships obtained for the shape variable (γ) were maintained in their graphically summarised forms. The thresholds defined for setting the timing factor were encoded as production rules, as tau changes in discrete steps. Finally, the effective rainfall threshold (ERT) value, for defining rainfall contribution to flow, was converted to a production rule and included in the knowledge base.

All the rules constructed in the knowledge base were written in VAX FORTRAN. Each block was written as a subroutine in to order focus inference, and allow the easy inclusion of further relationships at a later date. Examples of the code are given in Appendix C.

8.6 Current Status Database

The current status, or dynamic, database carries information relevant to the current problem (Frenzel, 1987), consisting of data, goals and intermediated results. In this system the dynamic database was written as a subroutine fed from the rainfall forecasting program outlined in section 8.8. The database consisted of six variables giving information about rainfall direction, extent and intensity, as well as catchment status :

DIRN - A variable indicating rainfall direction in degrees, used to identify whether storm movement coincides with main stream flow orientation. Examined in more detail in section 8.10.1

PCTCOVA - Percentage of the total catchment rainfall volume forecast to fall on the upper reach of the catchment.

PCTCOVB - Percentage of the total catchment rainfall volume forecast to fall on the middle reach of the catchment.

PCTCOVC - Percentage of the total catchment rainfall volume forecast to fall on the lower reach of the catchment.

RFINT - Average precipitation intensity forecast to occur over the catchment pixels receiving rainfall.

FAPI - Forecast catchment average antecedent precipitation index used to establish the generation of effective rainfall.

The number of variables assessed and stored in the dynamic memory was deliberately kept small in order to minimise the amount of processing time required. In addition, all variables were obtainable directly or indirectly from radar rainfall measurements. This increased speed of assessment, and data availability and thus allowed the application of the system in real-time.

8.7 Inference Engine

The system inference engine, or rule interpreter, uses the held within the dynamic memory to make inferences based on the production rules. There are two type of inference or reasoning mechanism, 'backwards chaining' and 'forward chaining'.

8.7.1 Backward Chaining

Also known as goal directed reasoning, this method of inference begins with the output or 'goal', and works backwards to find if the conditions which will make it true are satisfied (Frenzel, 1987). The disadvantage to the use of backward chaining is the heavy cognitive load imposed in managing goal and sub-goals, and storing and retrieving partially complete equations and relations. Larkin *et al.* (1980) provide a good analogy for these problems in finding the velocity, v , of an object. In order to determine v the backward chaining system would first have to find an acceleration, a . If this is also undefined, then an equation must be found with a as the resultant. This process continues, working further and further back, until a full set of equations is found from which a solution can be derived.

Backward reasoning has been found to be the method of investigation most used by 'novices' within a particular field (Anderson, 1985). By contrast, a domain 'expert' tends to reason forwards as outlined below.

8.7.2 Forward Chaining

This method of reasoning uses a data directed approach, building up from the available information about a problem in order to deduce a conclusion (Beynon-Davies, 1991). This technique was the one chosen for use in the present investigation, as it is well suited to situations where the number of conclusions is great relative to the number of initial input states (Slatter, 1987). Here, the initial conditions of rainfall and catchment status are few, whereas the number of potential model parameter settings is very large.

The forward chaining inference procedure was written as a simple condition driven cycle. As the dynamic memory became updated a program loop compared the new input data with the condition (IF) part of the production rules. When a condition was satisfied it passed to the relevant subroutine, comparing the data with the conditions there, and forward chaining through the production rules until it arrived at the appropriate parameter values. The settings were then returned for use in tuning the PRTF model. For ease of reference, the knowledge based system established was named the *Real-time Automatic Model Parameter Tuning (RAMPART)* system.

8.8 Rainfall Forecast Input

Although the great majority of knowledge based and expert systems operate from manual input, asking the user questions and acting upon his replies, this is quite impractical in a real-time forecasting situation. Of necessity in a real-time system is the constant monitoring of changes to the system input, in this case rainfall. In order to automate the data gathering procedure, information about rainfall coverage, movement and intensity was gained from the Cross Correlation Forecast routine (CCF), developed by Water Resources Research Group at the University of Salford.

The CCF procedure was originally developed for use in the Weather Radar Information Processing (WRIP) system for real-time flood forecasting in the Wessex region of the National Rivers Authority. The forecasting technique is based on simple pattern recognition to establish storm extent, and then linear extrapolation to generate advection forecasts. A storm radar pattern represents a 'concrete' pattern item, as opposed to an 'abstract' one like a solution or an argument. In forecasting storm movement, the CCF procedure receives the storm pattern from weather radar information in the form of a two dimensional digital array. Pattern recognition is then carried out based on the membership-roster concept, using template matching. Here, sets of patterns belonging to the same pattern class are stored in a recognition system. The arrival of an unknown pattern stimulates the system to compare it with those stored, defining it as a class member if it matches on of them.

The CCF procedure was carried out on single site Hameldon Hill radar data. This provides a 76x76, 2km grid, the forecasting area being shown in Figure 8.1.

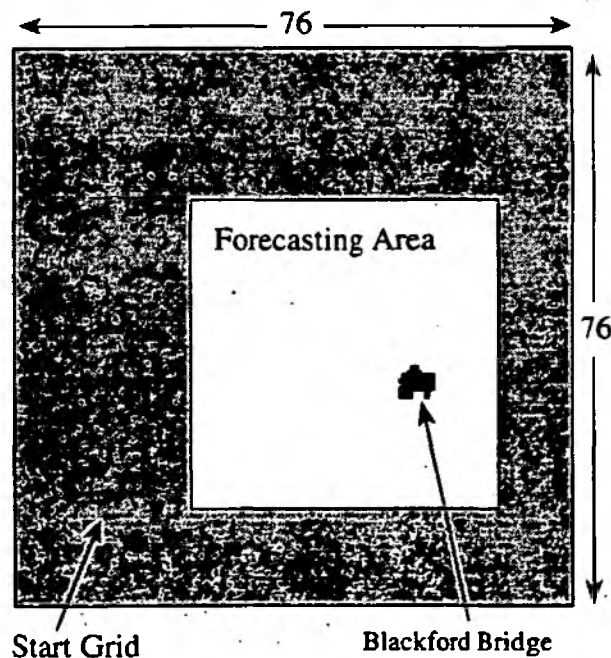


Figure 8.1 Cross Correlation Forecasting Area, And Blackford Bridge Subcatchment

The name of the CCF procedure comes from its method of assessing the speed, direction and volumetric change of a rainfall event. This is achieved by carrying out a cross correlation between two radar data fields on successive 5 minute time frames, as shown in Figure 8.2.

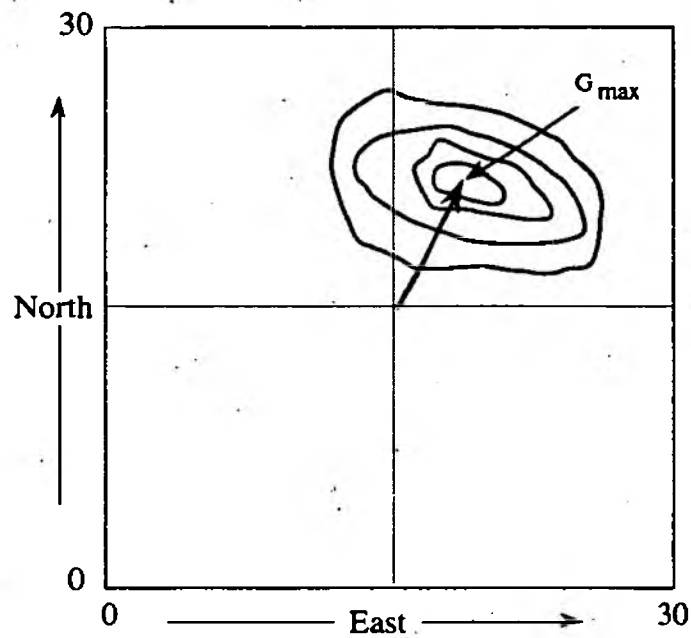


Figure 8.2 Cross Correlation Surface Of North West Region

In calculating the cross correlation coefficient, let x, y represent the two radar frames respectively. Thus the radar data are denoted by $(x_{1,1}, y_{1,1}), (x_{1,2}, y_{1,2}), (x_{1,3}, y_{1,3}) \dots (x_{i,j}, y_{i,j})$. The correlation coefficient may then be written as :

$$r = \frac{\sum (x_{i,j} - \bar{x})(y_{i,j} - \bar{y})}{\sqrt{[\sum (x_{i,j} - \bar{x})^2 \sum (y_{i,j} - \bar{y})^2]}} \quad (8.1)$$

where :

$$\bar{x} = \sum_i \sum_j x_{i,j} / (N - 1)$$

$$\bar{y} = \sum_i \sum_j y_{i,j} / (N - 1)$$

The point G_{\max} is then estimated by polynomial approximation. Once the G_{\max} point is found, the four sites around it are used in calculating the maximum point location, P_{\max} , as shown in Figure 8.3.

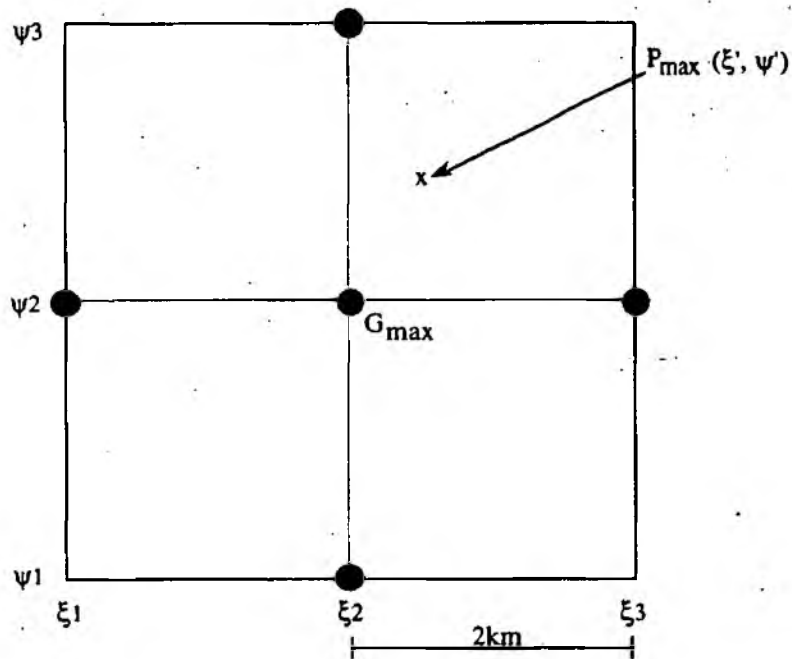
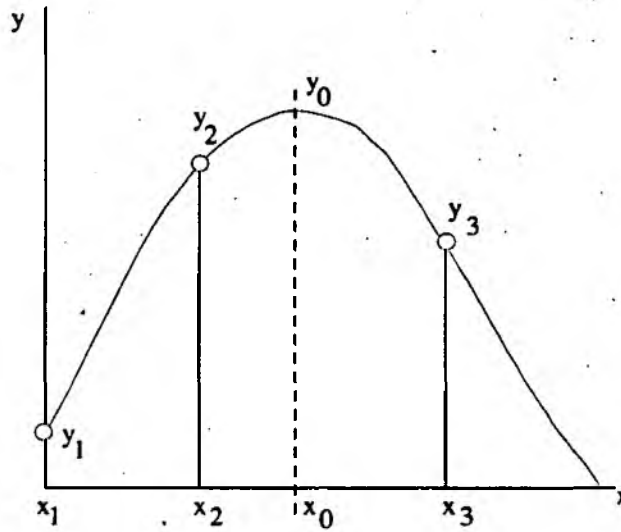


Figure 8.3 'Maximum Point' Grids

A parabolic curve is then used to fit three point data in each direction as represented in Figure 8.4, where the curve function is described as :

$$y - y_0 = a(x - x_0)^2 \tag{8.2}$$

where x_0 is the point of maximum correlation in that direction.

Figure 8.4 Parabolic Curve Fitting For P_{max}

The three parameters are established from three data points (x_1, y_1) , (x_2, y_2) , (x_3, y_3) given by :

$$y_1 - y_0 = a(x_1 - x_0)^2 \quad (8.3)$$

$$y_2 - y_0 = a(x_2 - x_0)^2 \quad (8.4)$$

$$y_3 - y_0 = a(x_3 - x_0)^2 \quad (8.5)$$

Several conditions, based on knowledge of the radar grid, are substituted into these equations in order to simplify the derivation. The spacing between all three data points is the same, and equal to 2km. The point location may be described, therefore, as an integer multiplied by the 2km distance.

$$x_1 = (j - 1) * 2$$

$$x_2 = j * 2$$

$$x_3 = (j + 1) * 2$$

where $j = 0, 1, 2, \dots$

From this the final form of the maximum point location equation is given by :

$$x_0 = 2 \left[j - \frac{1}{2 \left(1 - 2 \frac{y_1 - y_2}{y_1 - y_3} \right)} \right] \quad y_1 \neq y_3 \quad (8.6)$$

or

$$x_0 = x_2 - \frac{2}{2 \left(1 - 2 \frac{y_1 - y_2}{y_1 - y_3} \right)} \quad y_1 \neq y_3 \quad (8.7)$$

and

$$x_0 = x_2 \quad y_1 = y_3$$

Once P_{\max} is established, the speed, direction and volumetric change of the radar image may be calculated, such that :

$$\text{Speed (km/hr)} = S = \text{Sqrt}(\text{Sqr } S_x + \text{Sqr } S_y) * 4 \quad (8.8)$$

$$\text{Direction (Degrees)} = D^\circ = \text{ATAN} (S_y / S_x) \quad (8.9)$$

$$\text{Volume Change (\%)} = V = (\text{New Volume} - \text{Old Volume}) / \text{Old Volume} \quad (8.10)$$

where S_x and S_y are the coordinates of P_{\max} .

Having found the speed, direction and volume changes, short term advection forecasts are then made, based on these parameters. Thus the storm is moved with speed S and direction D , with a volume increase or decrease V , starting with the last five minute radar image, as shown in Figure 8.5.

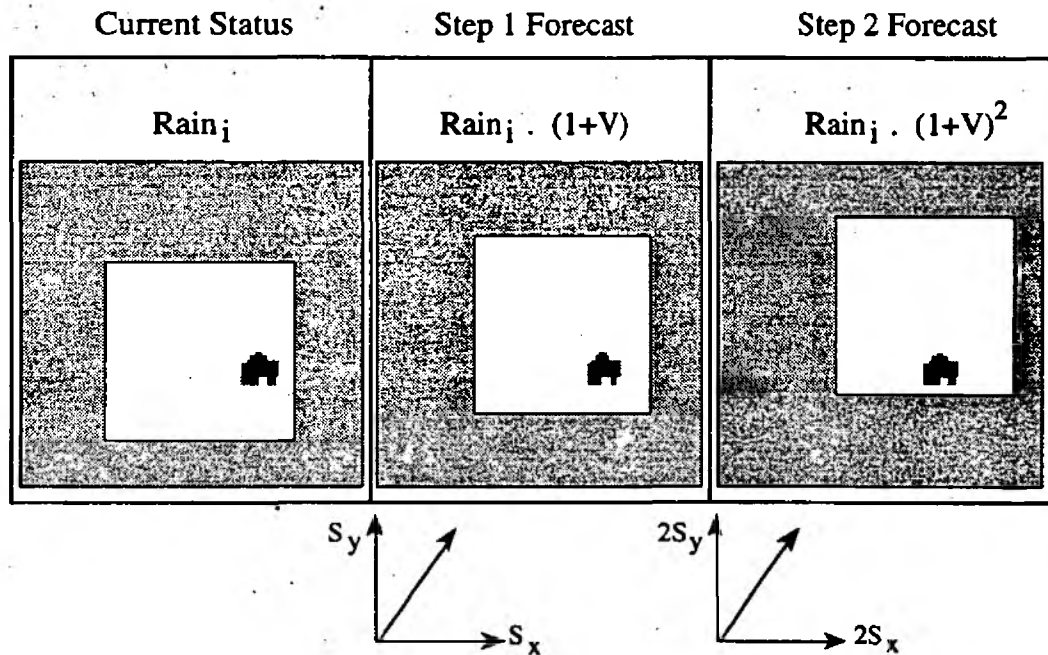


Figure 8.5 Storm Forecasting Procedure

The CCF system has been shown to produce reliable short term forecast, giving greatest accuracy up to two hours ahead (WRIP, 1992). Since it is a linear extrapolation procedure, and takes no account of storm type, it is most accurate in forecasting frontal situations, being less effective with convective events. In this investigation the CCF procedure was applied to a limit of two hours ahead, the resulting forecasts being used to assess storm intensity, movement and coverage, and API at the Blackford catchment, as outlined in section 8.9.

8.9 Rainfall Characteristics And Catchment Status

The CCF system produced storm movement forecasts to two hours ahead, in the form of 24 five minute radar images. In order to calculate the information required by the knowledge base in tuning the model parameters, a short routine was written, again in VAX FORTRAN, to extend the output of the CCF. This estimated the percentage

coverage of the upper, middle and lower catchment, and the actual antecedent and forecast precipitation index, as outlined below.

8.9.1 Catchment Division

In order to estimate the areal extent of the storm, the catchment was divided into three equal areas, based on the 2 km radar grid. Division was made as near perpendicular to the direction of main stream flow as possible, in order to define upper, middle and lower sections, based on distance from the basin outlet, as shown in Figure 8.6.

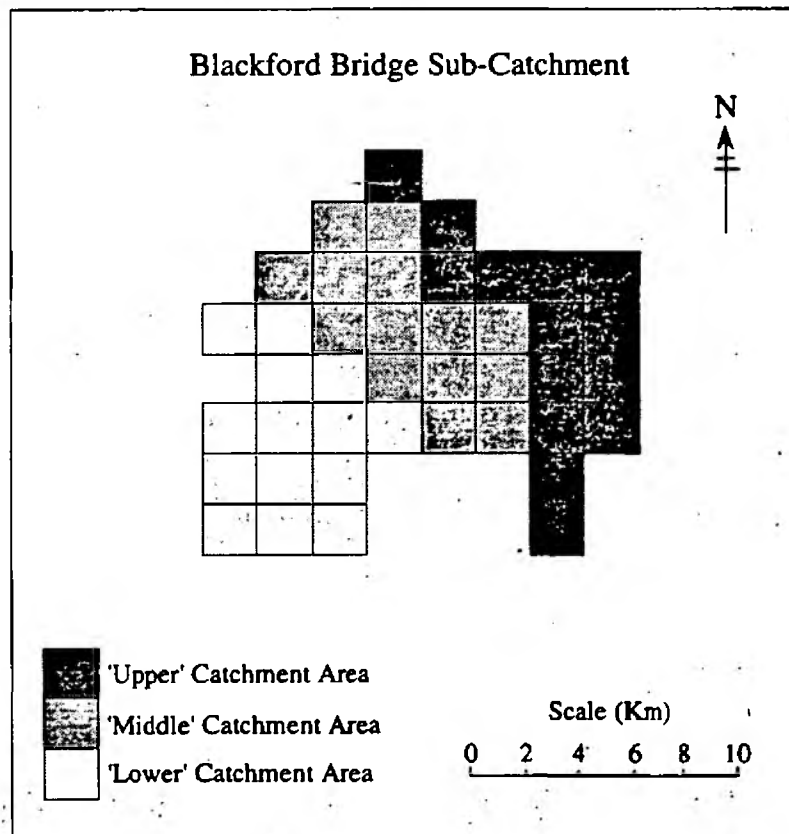


Figure 8.6 Catchment Division; Upper, Middle And Lower in Terms Of 2Km Radar Grid

8.9.2 Rainfall Areal Percentage Cover

The precipitation volume forecast to fall on the catchment as a whole was calculated from the images created by the CCF routine, converting rainfall intensity (mm/hr) at each pixel into mm of precipitation depth. The same procedure was then carried out for each of the three defined sub-areas, shown in Figure 8.6. The forecast volume figures were then converted to percentage cover for each of the three sections, such that :

$$\text{PCTCOVA} = \text{Upper Catchment Volume} / \text{Total Catchment Volume} * 100$$

$$\text{PCTCOVB} = \text{Middle Catchment Volume} / \text{Total Catchment Volume} * 100$$

$$\text{PCTCOVC} = \text{Lower Catchment Volume} / \text{Total Catchment Volume} * 100$$

These figures were then used as input to the dynamic, or working, memory. The information was used to determine the areal extent of the storm, and thus the appropriate PRTF forecasting parameter values when rainfall movement did not follow stream flow orientation, as examined in section 8.10.1.

8.9.3 Average Rainfall Intensity

The average rainfall intensity was calculated from the CCF routine two hour ahead forecasts. Each catchment radar element covered by precipitation was used, those receiving no rainfall being ignored. The average rainfall intensity was then determined as :

$$\text{RFINT} = \text{Sum of Pixel Rainfall} / n$$

where n is the number of catchment radar pixels covered by rainfall input in the two hour ahead forecast.

8.9.4 Forecast and Actual API

In order to give information on catchment status, the actual API was calculated for the basin as a whole, with rainfall from the last five minute radar frame, using the loss value (k) found in Chapter 7 :

$$API_{\text{now}} = k \cdot API_{\text{last}} + \text{Rainfall}_{\text{last}} \quad (8.11)$$

Forecast information about soil moisture status was projected by a forecast precipitation index using the CCF rainfall information. Calculation was carried out as above, but using the rainfall values at each five minute step. The starting value for each two hour ahead precipitation index forecast calculation was the level up to the last real radar image.

8.10 Knowledge Base Operation

With rainfall movement forecasts provided by the cross correlation forecast procedure, storm coverage and intensity and catchment soil status estimated, this information was used as input to the knowledge based system. Figure 8.7 illustrates the decisions and actions taken by the production system.

A 'demon' was set to wait for each new radar rainfall update. When triggered the demon carried out the analysis as follows. Firstly, storm direction was estimated to assess whether it coincided with the direction of catchment drainage. If this was the case, the stream flow oriented subroutines were called depending on whether storm movement was with or against of drainage. Following this, the appropriate shape and timing parameters were located for the average rainfall intensity forecast to occur over the catchment.

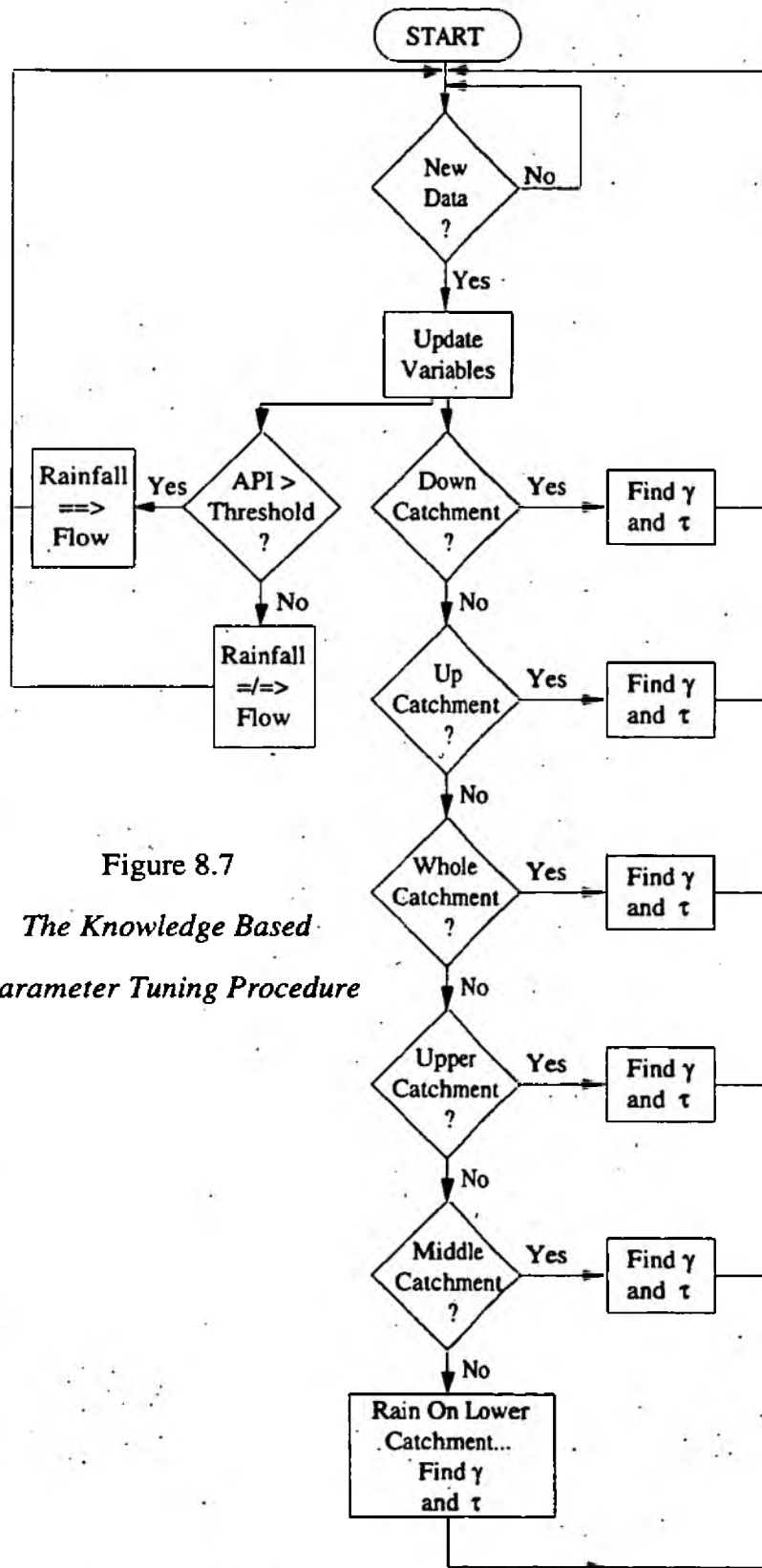


Figure 8.7
*The Knowledge Based
 Parameter Tuning Procedure*

When storm direction did not coincide with catchment drainage direction, then it was considered that its path would take it horizontally across the catchment. A decision was then made as to whether the rainfall would cover the whole catchment, or only one section. If the entire drainage area was forecast to receive rainfall, then the relevant γ and τ settings were chosen, based on storm rainfall intensity. For events when the catchment would be 'clipped' by a storm, and rainfall would be concentrated only in one area, the effected section (upper, middle or lower) was located. The gamma and tau values were then assessed with reference to rainfall severity.

Finally, information on catchment moisture status was used to assess whether rainfall would contribute to rapid runoff. The individual process stages are discussed and examined in more detail below.

8.10.1 Storm Direction

The direction of main stream drainage in the Blackford Bridge catchment is primarily Northeast to Southwest (Figure 8.8), roughly 42° to 223° .

Information on overall storm movement was generated by the CCF routine in degrees as outlined in section 8.8. This information was passed as a variable 'DIRN' to the dynamic memory. To define movement with similar orientation to catchment drainage, an arbitrary value of 30° either side of main drainage direction was chosen, as shown in Figure 8.9.

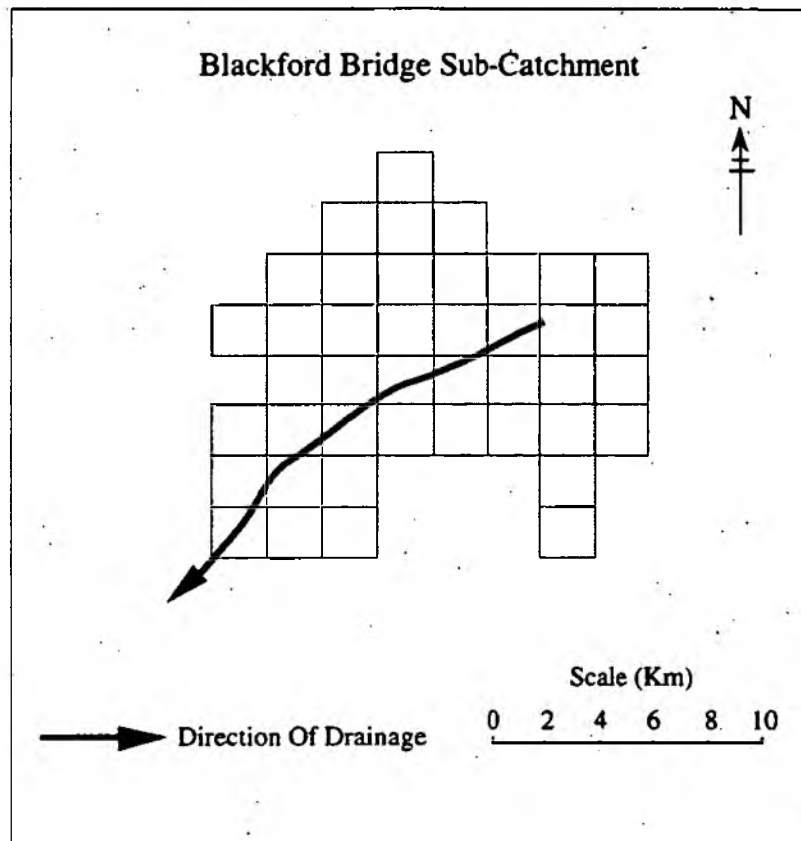


Figure 8.8 *Direction Of Mainstream Drainage, Blackford Bridge Subcatchment*

This provided a 60° acceptance angle to classify storm movement as drainage oriented. In practice, the decision as to whether a storm was aligned with main flow direction was made by the production rules :

```

IF  $193 \leq \text{DIRN} \leq 253$  THEN CALL DOWNCAT
ELSE IF  $12 \leq \text{DIRN} \leq 72$  THEN CALL UPCAT
ELSE CALL ACROSSCAT
END IF

```

The inference engine was then passed to the relevant storm subroutine.

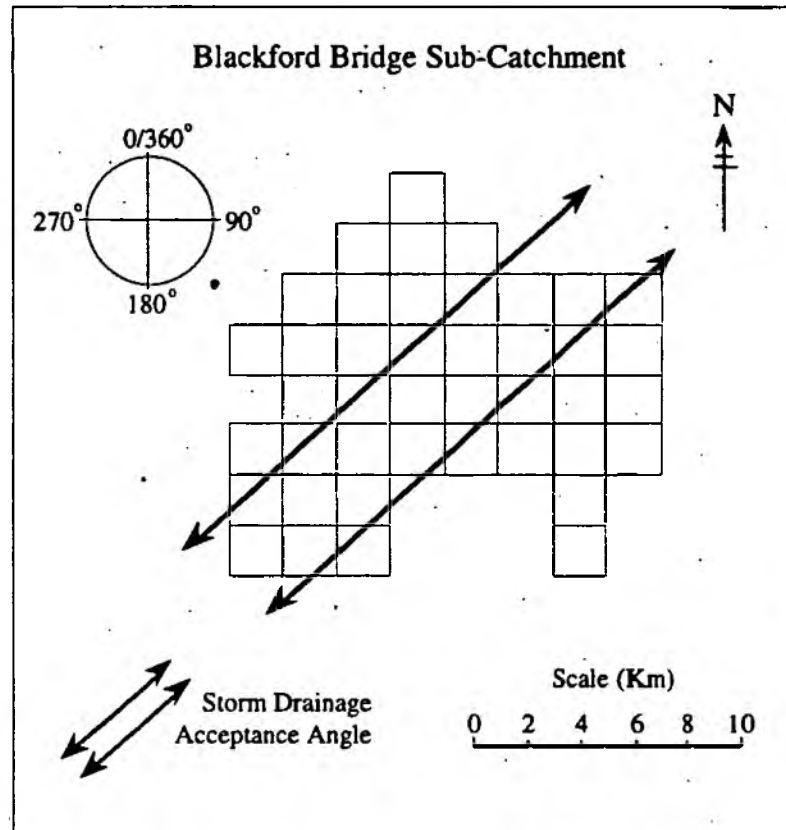


Figure 8.9 Storm Movement Acceptance Angle
With Regard To Catchment Drainage

8.10.2 Storm Movement With Flow

If the direction of overall storm movement was with the direction of catchment drainage flow, then the storm was assumed to enter the catchment farthest from the outflow point. The rainfall intensity was then used to determine the appropriate shape and timing parameters.

The shape value (γ) was set with reference to the summarising equation :

$$\gamma = 184.76 - 99.903 * \text{LOG} (\text{Rainfall Intensity}) \quad (8.12)$$

The timing parameter (τ) was set using the rainfall threshold rule values :

```

IF RFINT < 24 THEN  $\tau$  = 10
IF 24 ≤ RFINT < 36 THEN  $\tau$  = 9
IF 36 ≤ RFINT < 40 THEN  $\tau$  = 8
IF 40 ≤ RFINT < 48 THEN  $\tau$  = 7
IF 48 ≤ RFINT < 60 THEN  $\tau$  = 6
IF 60 ≤ RFINT < 152 THEN  $\tau$  = 5
IF RFINT ≥ 152 THEN  $\tau$  = 4

```

The parameter values were then returned and API examined, to test effective rainfall generation, as outlined in section 8.9.9.

8.9.3 Storm Movement Against Flow

With the rainfall moving up-stream, away from the direction of flow, the event was taken as entering the drainage basin at the outflow point. Once movement in this direction was established, the average rainfall intensity value was again used to define the PRTF model shape parameter as :

$$\gamma = 178.97 + -87.373 * \text{LOG}(x) \quad (8.13)$$

where x is average rainfall intensity (mm/hr).

The timing factor (τ) was found to be zero for all rainfall intensities when storm movement travelled from the outlet up along the catchment.

8.10.4 Storm Movement Across the Catchment

When storm movement was outside the drainage orientation acceptance angle, the system assess the extent and positioning of rainfall coverage. This was achieved by comparison of the percentage of precipitation volume on each catchment section, which was stored in the dynamic memory. Rainfall was assumed to be concentrated in one section when greater than 65% of the forecast precipitation volume occurred in that section :

```

IF PCTCOVA > 65 THEN CALL UPPERSECTION
IF PCTCOVB > 65 THEN CALL MIDDLESECTION
IF PCTCOVC > 65 THEN CALL LOWERSECTION
ELSE CALL CATCHMENT WIDE

```

The value of 65% rainfall concentration was chosen arbitrarily, but ensured that the majority of precipitation was sited over one sub-area. Once the coverage of the event was established, the relevant program subroutine was called passing the forecast average rainfall intensity.

8.10.5 Catchment Wide Rainfall

If the rainfall was established as moving across the basin, and covering more than one section, then the PRTF shape parameter was set for catchment wide rainfall. The gamma value was tuned using the relationship found in Chapter 7 such that :

$$\gamma = 93.272 + -55.471 * \text{LOG}(x) \quad (8.14)$$

where x is average rainfall intensity (mm/hr).

When rainfall coverage was forecast to be catchment wide the time adjustment factor τ was set to zero.

8.10.6 Rainfall Concentration on the Upper Reach

When more than 65% of the forecast rainfall volume took place on the upper reach of the catchment the storm was assumed to be concentrated there. The model value of γ was set using rainfall intensity according to the relationship :

$$\gamma = 140.67 - 72.176 * \text{LOG}(x) \quad (8.15)$$

Forecast average rainfall intensity was also used to define the value of τ such that :

IF RFINT < 36 THEN $\tau = 10$

IF $36 \leq$ RFINT < 44 THEN $\tau = 9$.

IF $44 \leq$ RFINT < 50 THEN $\tau = 8$

IF $50 \leq$ RFINT < 68 THEN $\tau = 7$

IF $68 \leq$ RFINT < 92 THEN $\tau = 6$

IF $92 \leq$ RFINT < 122 THEN $\tau = 5$

IF RFINT \geq 122 THEN $\tau = 4$

8.10.7 Rainfall Concentration on the Middle Reach

As with rainfall concentration on the upper catchment section, the PRTF γ value was set according to the relevant summarising equation, where :

$$\gamma = 82.691 + -51.426 * \text{LOG}(x) \quad (8.16)$$

The τ value was determined using the average rainfall intensity according to the production rules :

```

IF RFINT < 12 THEN  $\tau$  = 10
IF 12  $\leq$  RFINT < 16 THEN  $\tau$  = 9
IF 16  $\leq$  RFINT < 20 THEN  $\tau$  = 8
IF 20  $\leq$  RFINT < 28 THEN  $\tau$  = 7
IF 28  $\leq$  RFINT < 40 THEN  $\tau$  = 6
IF 40  $\leq$  RFINT < 44 THEN  $\tau$  = 5
IF 44  $\leq$  RFINT < 72 THEN  $\tau$  = 4
IF 72  $\leq$  RFINT < 112 THEN  $\tau$  = 3
IF RFINT  $\geq$  112 THEN  $\tau$  = 2

```

8.10.8 Rainfall Concentrated on the Lower Reach

When storm movement led to rainfall concentration on the lower catchment section only no runoff time delay was introduced and so tau was set to zero.

As with the upper and middle sections the magnitude of the shape adjustment factor was defined with reference to the summarising equation relating it to average rainfall intensity :

$$\gamma = 19.141 + -26.696 * \text{LOG}(x) \quad (8.17)$$

Once established, the tau and gamma values were returned for use in the flow forecast PRTF model.

8.10.9 Catchment Moisture Status

Information on the forecast catchment average precipitation was passed from the extended CCF procedure to dynamic memory for every five minute radar update.

This index value was based on the 'actual' basin index, up to the last radar image, plus forecast rainfall from the CCF routine. In accordance with the rainfall separation tank concept (section 7.11), effective rainfall was considered to be produced when the precipitation index value (analogous to current moisture level) exceeded the threshold value of 29.79 mm (equivalent to the tank height).

In practical terms :

IF FAPI > ERT THEN Rainfall Contributes to Flow

where FAPI is the forecast catchment antecedent precipitation index, and ERT is the effective rainfall threshold.

Once the appropriate rules had been applied, the gamma, tau and rainfall contribution factors were returned to the PRTF model. The forecast rainfall input, taken from CCF, was then routed through the model to provide the two hour ahead forecast flow hydrograph. Section 8.12 shows the results of model testing using the 23 rainfall events shown in Appendix A.

8.11 Decision Justification

A key element of a knowledge based system is that it should not merely provide answers in isolation, without any indication of the 'decision making process' which led to them. Michie (1980) took this further, recommending a conceptualisation of the knowledge and inferencing techniques used, in the form of a 'Human Window', to aid user understanding of the system. This type of 'humanising' is considered vital to systems employed in high risk applications (Welbank, 1983), an example of which is flood forecasting. Accordingly, an explanation was attached to every rule, so that when a decision was taken it explained the inference made. In practice, this was

achieved by the inclusion of an explanatory statement in each rule. Thus, when the conditional (IF) part of a rule was satisfied, the appropriate action (THEN) was taken, and a statement typed to the screen stating why the rule had been triggered. For example, with the storm moving down the catchment, in the direction of flow :

```
IF 12 ≤ DIRN ≤ 72 THEN
  TYPE*, 'Rainfall is moving against the direction of flow'
  CALL UPCAT
END IF
```

8.12 System Testing

In order to test the model parameter tuning system, and the relations established in a realistic framework, a simulated real-time structure was defined. Rainfall input to the system came from radar rainfall data, processed by the cross correlation forecasting (CCF) routine outlined in section 8.8. From the rainfall forecasts this produced, the direction, catchment percentage coverage, rainfall intensity and API were calculated and fed to the RAMPART system. With each update of the dynamic memory a new set of PRTF parameters were determined, as outlined in section 8.10. The forecast rainfall contribution to the flow was defined with reference to the forecast catchment status, using the loss rate effective rainfall threshold from section 7.12.

8.12.1 Rainfall - Runoff Events

In testing the system, those rainfall-runoff events shown in Appendix A, and analysed in Chapter 5, were used. These storms were analysed using the loss rate (L) and effective rainfall threshold (ERT) for the catchment, as defined in Chapter 7. Due to

the relatively narrow range of 'optimum' L and ERT values for the individual events, the use of average magnitudes for these variables was seen as appropriate. A further three 'new' storms are analysed in Chapter 9 as case studies.

8.12.2 Methodology

The first step in the analysis was the identification of a PRTF model for the Blackford Bridge subcatchment. This was achieved using the MATH system, a (2,3) configuration providing the best balance between forecast accuracy and parsimony. Figure 8.10 shows the impulse response of the PRTF model defined.

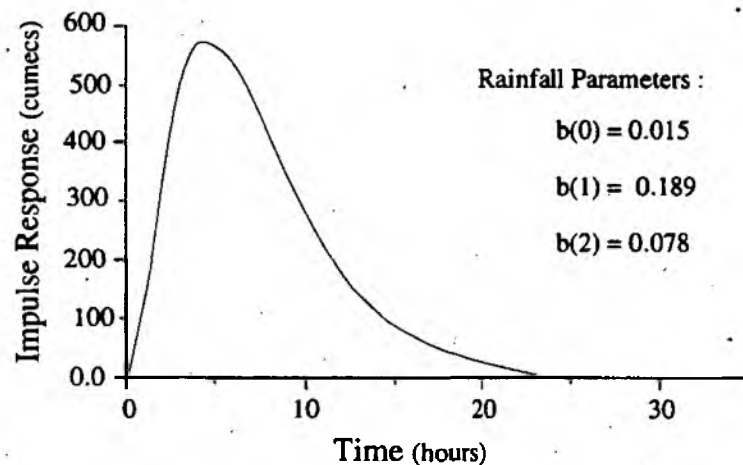


Figure 8.10 *PRTF Model Impulse Response, Blackford Bridge*

With the model defined, each of the 23 storms was set to have an initial catchment API value of 20mm. In order to simulate real-time use, the whole radar-rainfall record for each event was replayed, rainfall input and the standard loss rate being used to define catchment status. At each five minute time step the two hour ahead rainfall forecast, from the CCF routine, was analysed to determine the rainfall characteristics required as input to the RAMPART system. Once established, these triggered the update

demon, and the inference engine chained through the production rules to find the most appropriate values of γ and τ . With the shape and timing parameters defined, rainfall contribution to flow was assessed by the catchment moisture section, comparing forecast API to the threshold effective rainfall threshold.

The run time of RAMPART is very fast, taking less than a second to complete on a VAX 3100 Workstation. Once the parameters and contribution to flow were defined the values were used by the PRTF model in generating the next five minute, two hour ahead forecast, such that :

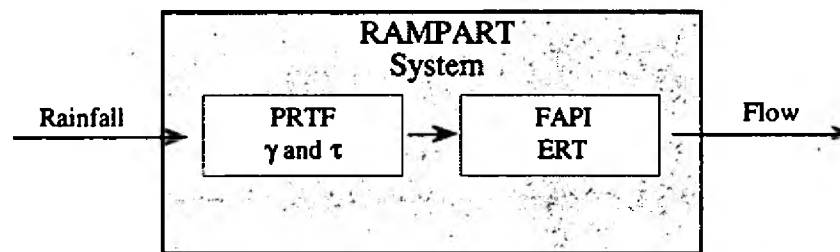


Figure 8.11 RAMPART System, Defining Shape, Timing And Rainfall Contribution

In this way, the forecast hydrographs were produced for each of the storm events, using forecast rainfall input and tuned shape, timing and rainfall contributing factors.

To enable comparison with the tuned models, the rainfall events were re-run, using a static PRTF model to produce forecast flow. Here, event percentage runoff was defined using 'delta' as a rainfall scaling factor, as outline in section 6.4.4. The delta value was determined manually for each event to give the best fit to the actual flow hydrograph. All other factors were kept the same, rainfall input again coming from the CCF program as before. An 'optimum' simulation of each event was also carried out, again using the forecast rainfall to establish the 'best' flow forecast possible with the input data. Here the event model parameters were tuned manually, using the

MATH program, to provide the lowest errors for the simulation hydrograph. The forecasts produced by the RAMPART system are shown in Appendix A, to provide a visual comparison with the observed runoff event.

To provide an objective assessment of rainfall model tuning performance, the forecast and simulation flow hydrographs were compared with the true catchment outflow. An RMSE value was calculated for each event, as shown in table 8.1. In all, 14 of the 23 rainfall-runoff events used in the investigation were forecast more accurately using parameter tuning. In several of the events the tuned model gave results which were very close to the optimised simulation. In each of the 9 cases where the static model out-performed the the tuned model, the difference was within a factor of two.

Some of the forecasts show underestimation of the rising limb, such as the 18/11/86 event, (Appendix A). This may be due to the definition and use of only one rainfall tank loss factor (L). Where forecasts are too low the loss term is set too high, such that precipitation input is used in attaining the ERT, whereas it is effective rainfall in the actually catchment.

The RMSE provides a good measure of flow accuracy over the hydrograph as a whole. As mentioned in section 6.9.2, however, it is the precision with which the magnitude and timing of peak runoff is modelled which is most important in a flood warning context. In this sense a 'bad' forecast may be defined as one which forecasts runoff peak at the right time, but too low, underestimating the severity of the flood, or gives correct magnitude but with a time lag, providing a reduced sense of urgency about the event. The 'worst' forecast case would be the one where both volumetric and timing errors are evident, giving a false sense of security about the scale and immediacy of the action required.

In order to address these points a more detailed investigation was performed on the magnitude and timing of the flow peak.

Table 8.1 RMSE Values From Static, Tuned And Optimum PRTF Models

Date Of Event	Static PRTF Error	Tuned PRTF Error	Optimized PRTF Error
020382	14.06	4.21	3.03
250682	9.34	2.62	2.11
170882	13.27	3.8	2.43
181282	11.35	9.50	9.13
140183	15.43	4.19	3.82
310183	28.33	21.02	9.80
070683	17.96	11.41	4.74
050284	13.91	7.28	4.06
160384	7.62	16.85	5.13
171084	7.89	1.94	1.50
021184	19.68	8.22	6.35
290185	3.59	9.27	2.18
261085	6.42	7.43	2.43
121285	7.38	12.32	4.55
090186	9.68	14.21	5.52
250886	26.40	9.57	7.83
260886	26.27	8.44	7.74
251086	5.78	4.54	1.60
301086	2.61	3.39	1.34
181186	16.33	30.62	9.51
141286	8.99	6.64	3.28
291286	26.59	29.35	7.83
030187	8.25	9.83	5.22

i) Peak Volume

To provide an indication of the error between the actual and forecast flood event magnitudes the difference in river discharge (in cumecs) was analysed at peak flow. This gives a representation of the physical error in flood severity forecast. The relevant stage heights were related to NRA warning levels, and are shown in table 8.2.

ii) Peak Timing

In order to assess the accuracy of flood forecast timing, a percentage term was defined

relating the forecast timing inaccuracy to the time to peak of the event, such that percentage timing error was defined as :

$$\text{Timing Percentage Error} = (\text{Timing Inaccuracy} / \text{Event Time To Peak}) * 100$$

This technique reflects the importance of increased forecast timing accuracy the shorter the lead time available.

Table 8.2 RAMPART Timing, Volume and NRA Warning Errors

Date Of Event	Percent Timing Error	Flow Error (Cumecs)	Stage Error (Metres)	Forecast NRA Warning	Actual NRA Warning
020382	+27.86	+1.07	+0.04	No	No
250682	+0.13	+0.91	+0.03	Yes	Yes
170882	+31.28	+0.66	+0.01	Yes	Yes
181282	+16.94	+1.78	+0.09	Yes	Yes
140183	+22.30	+1.20	+0.05	Yes	Yes
310183	+23.79	+1.82	+0.09	Yes	Yes
070683	+9.84	+0.84	+0.02	Yes	Yes
050284	+24.47	-1.07	-0.04	Yes	Yes
160384	+18.95	+0.96	+0.03	Yes	Yes
171084	+12.11	+0.66	+0.01	No	No
021184	+8.63	0.00	0.00	Yes	Yes
290185	+18.45	-1.20	-0.05	Yes	Yes
261085	+28.31	+1.47	+0.07	Yes	Yes
121285	+42.30	0.00	0.00	Yes	Yes
090186	+32.48	+0.66	+0.01	Yes	Yes
250886	+7.61	+1.33	+0.06	Yes	Yes
260886	-2.40	-1.47	+0.07	Yes	Yes
251086	+14.81	+0.66	+0.01	Yes	Yes
301086	+43.19	+0.84	+0.02	No	No
181186	+23.35	-1.63	-0.08	Yes	Yes
141286	+11.72	-1.33	-0.06	Yes	Yes
291286	+8.58	-0.66	-0.01	Yes	Yes
030187	+9.27	+0.66	+0.01	Yes	Yes

The analysis of runoff peak timing and magnitude in detail shows that the RAMPART system performs well in forecasting the severity of the flow peak, being consistently

less than 0.1 metres in error (1.95 cumecs), and often better. This meant that the runoff level was accurately forecast in relation to the NRA flood warning for each event. The most significant problem occurred in the timing of the forecast of peak discharge. Here errors of up to 43% of the time to peak were evident in the forecasts produced by the system.

8.13 Distributed Rainfall-Runoff Models

8.13.1 Introduction

The spatial distribution of rainfall is important in its influence on the runoff hydrograph from a storm event, addressed in the RAMPART system by model parameter tuning, and being more widely and better understood with the increasing use of radar for precipitation measurement. In an attempt to take into account the influence of detailed rainfall spatial distribution, both semi-distributed and fully distributed models have been developed. This section provides a brief introduction to such models, and describes work carried out on the Blackford Bridge area, followed by a comparison of with the RAMPART system forecasts.

8.13.2 Distributed and Semi-Distributed Models

The distributed modelling approach includes consideration of storm and catchment characteristics in forecasting the flow hydrograph from a rainfall event. The rainfall-runoff process over a basin may be generally simulated by three hydrological components :

- Abstraction loss (interception, surface depression, infiltration etc.)
- Rainfall-runoff transformation of net rainfall
- River flow transportation

The main principle of the semi-distributed model is its consideration of rainfall at a subcatchment scale. In this way a rainfall-runoff model is used for each sub-catchment area to transform precipitation to river flow. Single input single output (SISO) models have been used in this way, but owing to the high heterogeneity of rainfall spatially, and the differences in response of tributaries within a large basin it may be advantageous to fit different models for each sub-catchment. The use of multiple input single output (MISO) models provides a means of addressing this problem when the catchment is primarily influenced by spatial rainfall distribution and drainage basin sub-catchments have different responses. However multicollinearity (ie. high cross correlation between inputs) is a major problem in MISO systems (Harpin, 1982), resulting in one input being incorrectly labelled as having made a greater contribution to the output than it did, whilst the impact of another may be reduced.

It is not intended here to provide a comprehensive list or explanation of the many distributed and semi-distributed models which have been developed. For this, the reader is referred to the work of Bevan (1985, 1989, and 1991), Wood *et al.* (1988), and Loague and Freeze (1985).

8.13.3 Distributed Modelling Of Blackford Bridge

Yu (1989) adopted a distributed approach to modelling the Blackford Bridge catchment, using a grid based representation. In order to describe the surface and subsurface characteristics of the catchment and their heterogeneity, the input data relating to the physical conditions of the basin were prepared with reference to a grid based mesh, including :

i) Basin Size And Shape

The catchment was first simplified by dividing the actual basin into a grid based mesh, as shown in figure 8.12.

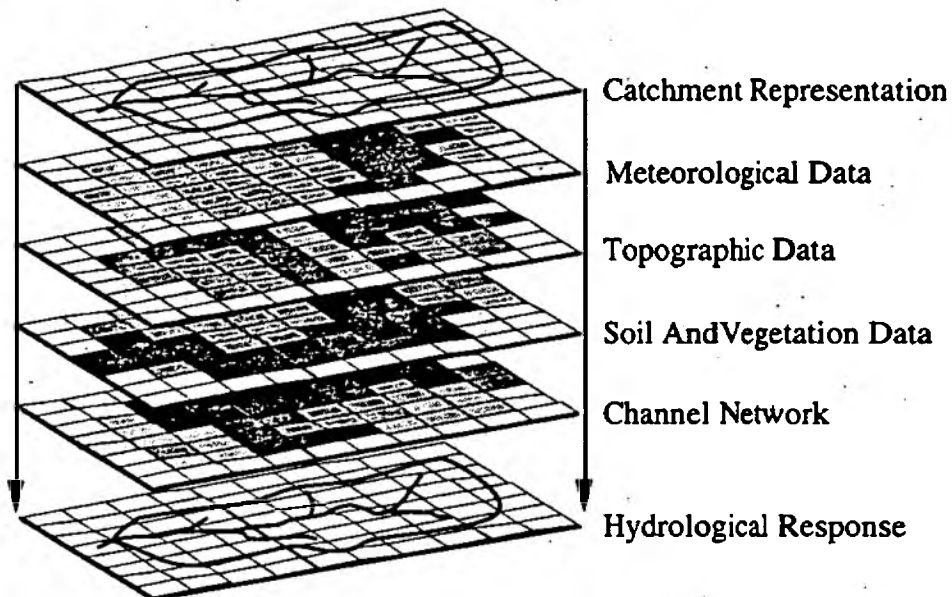


Figure 8.12 Grid Based Model Input Characteristics (After Yu, 1989)

Each grid was given an area percentage to define the amount of each square belonging to the study area.

ii) Meteorological Data

The only meteorological input considered was rainfall intensity at each grid square, losses due to evaporation being neglected. The rainfall at each grid was calculated as the percentage area multiplied by the rainfall intensity at that grid.

iii) Soil Type

A soil map of the catchment area was used to identify the infiltration loss parameters for rainfall occurring at each grid square. Excess rainfall was obtained in terms of the interaction between rainfall intensity and the relevant infiltration capacity curve.

iv) Topography

When excess rainfall lead to overland flow the ground surface topography was used to move water to the neighbouring grids. The topographic representation was simplified to an average flow direction, slope and length, within each 2km by 2km square. Direction of flow was determined subjectively from a contour map. Surface slope also came from a contour map, being taken as the average of four central point surface slopes within one grid square. Overland flow length was defined as the length that overland flow was delivered to the next neighbour grid or the river.

v) Vegetation Type

Vegetation cover was used in the assessment of Manning's N, defining surface roughness, which in turn influences the storage coefficient. A higher surface roughness leads to lower flow velocities and longer residence times, allowing a greater chance of infiltration.

vi) Channel Configuration

A description of the river network was included in the Yu model, as its form directly influences storm runoff hydrograph. The procedure used consisted of channel order identification and code number labelling from lower to higher order streams, and down stream to upstream.

The rainfall data used for input to the model was 2 km by 2 km radar data, a basic 4km² grid mesh being used in simulating surface and subsurface characteristics. The processes of runoff transformation were realised as an integrated effect of rainfall passing through different layers of catchment characteristics.

8.13.4 Comparison With The RAMPART System

In testing the grid based distributed model (GBDM), Yu (1989) applied five of the same events as used in the present investigation. Figures 8.13 to 8.17 show the comparison hydrographs between the observed event runoff and the GBDM and RAMPART forecasts. Table 8.3 shows the timing, volume and NRA warning errors.

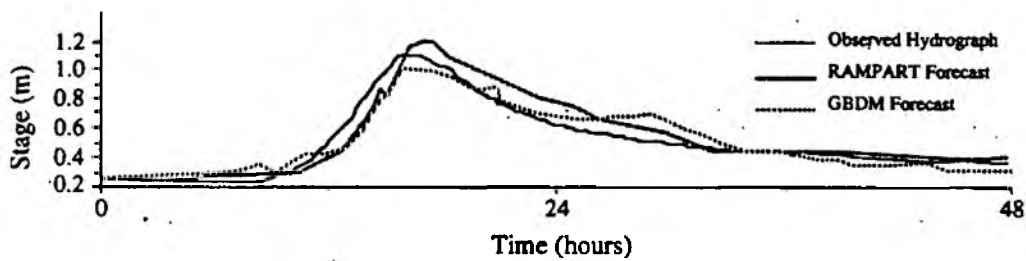


Figure 8.13 Event Of 18th December, 1982, Observed And Forecast Hydrographs

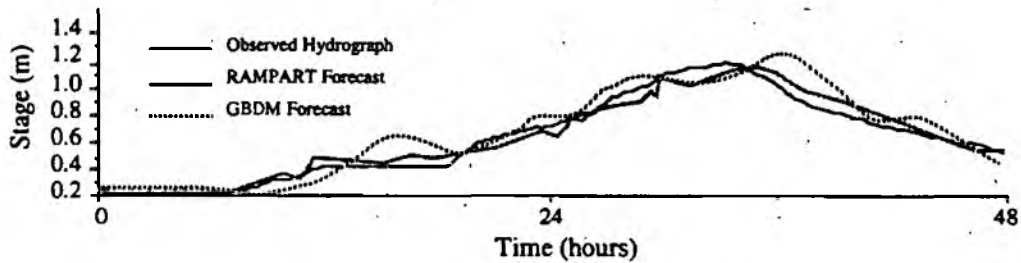


Figure 8.14 Event Of 2nd November, 1984, Observed And Forecast Hydrographs

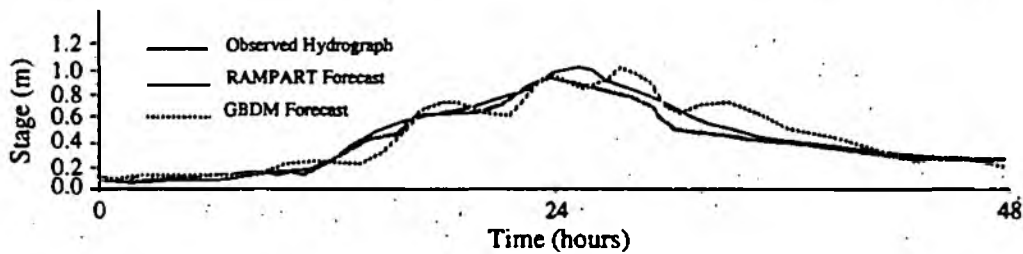


Figure 8.15 Event Of 26th August, 1986, Observed And Forecast Hydrographs

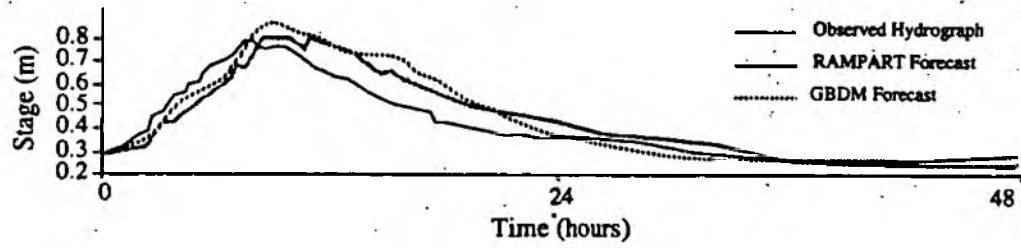


Figure 8.16 Event Of 25th October, 1986, Observed And Forecast Hydrographs

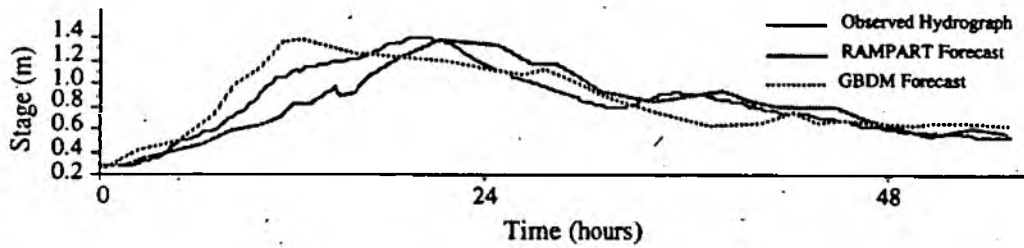


Figure 8.17 Event Of 29th December, 1986, Observed And Forecast Hydrographs

Table 8.3 GBDM Timing, Volume and NRA Warning Errors

Date Of Event	Percent Timing Error	Flow Error (Cumecs)	Stage Error (Metres)	Forecast NRA Warning	Actual NRA Warning
181282	+8.31	-1.07	-0.04	Yes	Yes
021184	+12.83	+1.78	+0.09	Yes	Yes
260886	+11.97	+0.84	+0.02	Yes	Yes
251086	+22.35	+1.82	+0.09	Yes	Yes
291286	+37.62	+0.95	+0.03	Yes	Yes

Comparison of the forecasts made using the GBDM and RAMPART systems shows both able to represent river flow magnitude quite accurately. The RAMPART system provides better forecasts in three of the five events, although all are within 1.95 cumecs of the observed peak runoff. Examination of event peak timing forecast using

the two systems shows that RAMPART produces the lowest errors for four of the five storms, the grid based distributed model being better on the event of December 18th 1982. The error range (as a percentage of time to peak) for the RAMPART system is -2.0 to +16.95. The GBDM is considerable less accurate producing forecasts between -8.31 and +37.62 in error. Visual assessment of the forecast hydrographs shows that the GBDM suffers problems with fluctuation of both the rising and recession limbs, being more severe than that affecting the RAMPART forecasts.

Visual analysis of the GBDM forecasts reveals problems with hydrograph oscillation or fluctuation, especially in the rising limb. This may be due to the high sensitivity the distributed system shows to errors in rainfall input. Net rainfall in the GBDM is estimated by considering the physical catchment conditions, but no technique is used to update the rainfall data. Precipitation errors are thus passed to the ground surface without any corrections. In this way, Yu (1989), states that rainfall positive errors will cause more overland flow and the GBDM state updating is unable to update this error. In the events of 25/10/86 and 28/12/86 the RAMPART system proved unsuccessful in representing the hydrograph rising limb. A possible reason for this is the identification of rainfall in the upper section of the catchment, causing a delaying and reshaping of the forecast. The observed flow for the event was higher, due to action of heavier rainfall in the middle section, causing a higher and more immediate response than forecast by the RAMPART system.

It is difficult, and possibly misleading, to draw conclusions from such a small sample of events, but it suggests that the greatly increased complexity of model structure and associated data needs of the grid based approach do not serve to improve forecasts. Added to this is the increased model running time needed to process the greater quantities of distributed data, which may be a severe disadvantage in a real time flood warning system. These problems led to the conclusion that, for the present at least, a lumped modelling system, following a knowledge based approach, is more efficient

and accurate in a flood forecasting context. A similar conclusion was also reached by Yu in 1989, who states "...it seems that GBDM does not have significant benefit over lumped models. From the point of view of model input and rainfall error influence, the lumped models have the advantage over GBDM."

8.14 Discussion

The RAMPART system presented in this chapter is a first attempt at using knowledge based techniques in flow forecasting. Instead of error prediction or state updating, the system applies knowledge of the interaction of rainfall and catchment as they influence model parameters. The knowledge is applied as the event takes place, parameter estimation being carried out with reference to forecast rainfall and catchment status at each 5 minute radar step.

The forecasts obtained using the RAMPART optimised PRTF model gave encouraging results. In almost two thirds of the cases examined parameter tuning resulted in a reduction in hydrograph errors when compared with a static PRTF. Detailed examination of the RAMPART forecasts revealed that where problems did occur they were mostly related to the timing parameter. This may be due to differences between the synthetic catchment used to infer the τ settings, and the Blackford Bridge area where they were applied. In each case the shape adjustment factor, γ , performed well, emulating the actual hydrograph form better than the static model.

A further problem in some runoff sequences was hydrograph fluctuation, related to inconsistencies in the rainfall forecast produced by the CCF routine. When rainfall is forecast to occur in one section of the catchment, with a given intensity, the parameters are set appropriately. If the next forecast changes the rainfall coverage and intensity markedly, the model response is similarly altered. In order to counteract this

problem, two approaches may be possible. Firstly, and most obviously, a more accurate rainfall forecasting procedure should produce more stable model tuning parameter settings. The desire for a highly accurate forecast of rainfall movement is not confined to this investigation. In a real world context, however, the use of some form of parameter restraint may help reduce the effect of forecast fluctuation. Here the rate of change of the PRTF parameters may be restricted in order to avoid large changes at any one time step. On this way, parameters would take longer to attain extreme values, but persistence in direction of change over a number of time steps would reflect genuine rainfall / catchment characteristics, rather than a single intermittent forecast error.

Comparison with a GBDM developed by Yu (1989) for the Blackford Bridge catchment showed the knowledge based approach to be less 'data hungry', and produce more accurate forecasts in most cases, especially in terms of runoff peak timing. Despite the improvements in hydrograph forecasting using parameter tuning, the technique is far from perfect. In every event used there is still room for improvement, as can be seen by comparing the RAMPART forecasts with those for the manually optimised PRTF simulation. The answer to better forecasting using a knowledge based approach may lie in refining the knowledge already gained, such as the use of seasonal loss and ERT values. Alternatively progress may be possible in investigating different factors which which affect the runoff hydrograph, and are available in real-time. In this study no account was taken of infiltration excess flow generation, that is transformation of precipitation into flow when rainfall intensity is greater than infiltration rate. At a given rainfall intensity this would lead to hydrograph rise, regardless of catchment antecedent status. Another possible factor for investigation is catchment snow coverage. As stated in Chapter 2, snow cover may completely absorb a rainfall event and release it some time later with a significantly increased volume. This may be important on rural upland catchments such as Blackford Bridge and other similar rapid response areas.

8.15 Conclusion

This chapter details the the development of a simple knowledge based system, using cognition of rainfall extent, movement and intensity induced on a synthetic drainage area, together with loss rate and effective rainfall threshold from real catchment data. The information gained was encoded as production rules within a knowledge base. A current status memory was fed with information about storm dynamics and catchment API from a rainfall forecasting program, at five minute intervals. In order to maintain rainfall forecast accuracy a forecast time of two hours was used, giving reliable results with the frontal events used.

Using RAMPART for PRTF parameter estimation gave encouraging results, producing improved flow forecasts in 14 of the 23 events evaluated, providing greatest accuracy in runoff peak estimation, but suffering significant errors in peak timing. Fluctuation of forecast hydrograph response also proved to be a problem in some forecasts. This is due to inconsistencies in the forecast rainfall input to the system. The effects of response fluctuation may be modified by improved forecasting techniques, or the use of restraint of parameter rate of change. Improvements to the system are possible, as shown by the optimised PRTF errors. Further investigation may be useful in refining the knowledge in the system at present, or in analysing other variables which influence the rainfall-runoff process.

A further area for investigation may be the application of some form of 'learning' technique. Here the storm and catchment characteristics may be used to to update the knowledge base automatically. When the model is found to perform badly, the characteristics of the event are added to the knowledge base, along with the optimum model parameters which should have been used. Thus, next time a similar situation occurs, the system should recognise it and, hopefully, perform better.

CHAPTER 9

CASE STUDIES

9.1 Introduction

Flood forecasting may be thought of as one type of information system. Such structures have been described by Jordan (1990) as an integration of five major components; people, procedures, hardware, software and data, as shown in Figure 9.1.

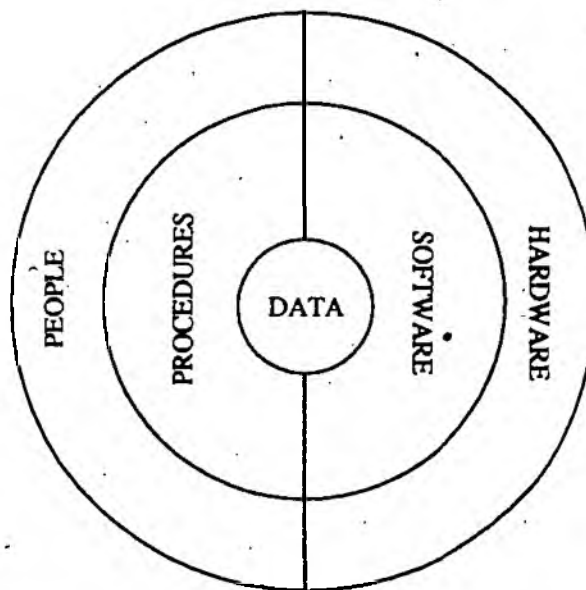


Figure 9.1 *Five Components Of An Information System (After Jordan, 1990)*

Within this representation, the centre line denotes the symmetrical split between people and computer hardware. Data is the central component of the system, consisting of information about rainfall, from radar and raingauges, and river flows, from measuring outstations. The procedures and software provide instructions for people and computers respectively. These are then sources of 'activity' in processing and handling the data.

Throughout this thesis a number of software analyses and techniques have been developed using a knowledge based approach to improve warning of fast response events. In this chapter, three case studies are presented to illustrate how these techniques may be applied in the setting of a real-world flood warning system. Within the case studies, displays and forecasts are generated as they may be seen by a flood forecasting officer monitoring one catchment during an event.

For each event, an overview of the climatic situation around the British Isles is given with the use of synoptic charts. Storm movement over the North West area is shown with the use of radar rainfall data. From this, the return period of the event is calculated and displayed in distributed form as the storm progresses. Flow hydrograph forecasts are produced and displayed using the RAMPART program, along with standard transfer function model forecasts, as a comparison.

9.2 Methodology

9.2.1 Synoptic Overview

For each of the three case studies a synoptic overview leading up to the event is presented. The synoptic charts were sourced from the Royal Meteorological Society Monthly Weather Log in 'Weather' magazine, and provide an outline of the wider synoptic conditions. The four charts shown for each storm show the conditions on the day of the event, along with the two days leading up to it and the day which followed. A short description of the synoptic condition is also given, describing rainfall movement, pressure variation and temperature changes during the period of interest. This information is again quoted from the Monthly Weather Log.

9.2.2 Radar Rainfall Movement

At a more detailed scale than the synoptic charts, information about rainfall movement is provided by radar data. The radar images presented are those produced by the Hameldon Hill device, and are similar to those sent in near real-time to NRA Flood Forecasting Offices and the Meteorological Office.

The radar data comes from archive magnetic tapes, decoded and displayed using FORTRAN and UNIRAS code developed by the author. The radar images proved visual information about storm progression, and changes in rainfall intensity with time. The time step of each of the radar images is not equal, being chosen to show storm movement most effectively within the duration of the event.

9.2.3 Rainfall Return Period

In order to allow an assessment of rainfall recurrence interval, the intensity-duration-frequency analysis developed in Chapter 4 was applied to the rainfall as it took place over the catchment. The rainfall duration for each radar pixel was taken as that time since the start of precipitation on that area. The radar rainfall data for each pixel was then converted into frequency information using the Probability Weighted Moments distribution estimates, as outlined in section 4.8.

In assigning a return period to each rainfall square, the artificial rainfall database was used. As such, the return period values shown in each three dimensional image should only be regarded as visual examples of the type of plot produced. The plots themselves are displayed using UNIRAS graphics, designed and implemented by the author.

9.2.4 Flow Forecasts

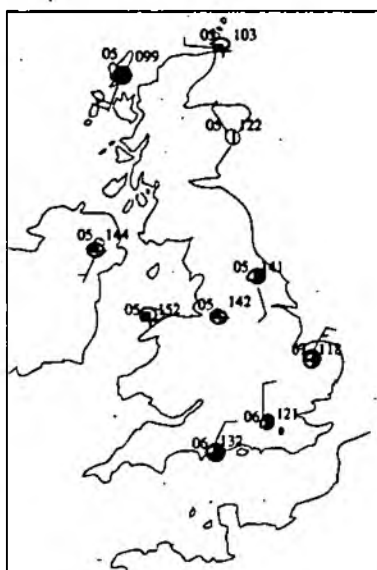
As well as providing information about event recurrence interval, radar rainfall data was also used to produce flow forecasts for the catchment with the RAMPART system. In response to the problems encountered with forecast hydrograph fluctuation due to forecast rainfall errors, precipitation forecasts were not used as inputs to the system. In carrying out the three case studies here, several alternative scenarios were considered, including no more rain, past average rain and perfect foresight. The influence of differing rainfall forecast scenarios has been discussed in detail by Owens (1986).

In order to rule out the effects of inaccuracies in rainfall forecasts perfect foresight was chosen as input to the parameter tuning system. Using this method, the actual rainfall two hours ahead was used to calculate catchment status and storm direction, coverage and intensity instead of the cross correlation forecasting routine discussed in Chapter 8. The perfect rainfall 'forecasts' were then used to provide inputs to the RAMPART system, as outlined in sections 8.8 and 8.9. By way of a comparison, the same perfect foresight rainfall was used as input to a non-adaptive transfer function model, percentage runoff scaling being carried out using delta, as discussed by Owens (1986). The hydrograph plots show the flow forecasts produced for each of the models used along with the actual catchment response for comparison.

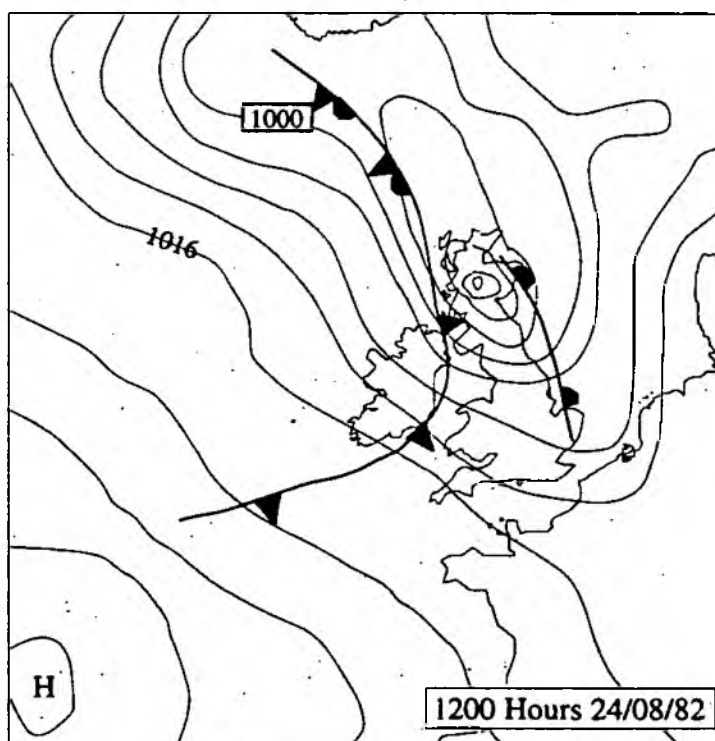
9.3 Event of 24th August 1982

9.3.1 Synoptic Conditions

August began with a spell of warm thundery weather, with high pressure between Iceland and Norway and a light easterly air-stream over much of Britain. On the 8th a much more unsettled westerly regime began. A series of depressions moved north near Iceland and associated troughs moved eastwards across northern areas, accompanied by rain between the 11th and 18th. On the 19th, brighter showery weather moved in, with some heavy thunderstorm activity. The showery weather continued in the North throughout the 20th and 21st, unsettled conditions being maintained. The event of the 24th took place during a further low, when the North suffered severe gales and rainfall occurred over most parts of Britain. This low moved away slowly northwards, leaving a cool, showery air-stream.



Surface Observations at 1200 Hours 24/08/82



Synoptic Weather Charts



Rainfall Ending 2100

Figure 9.2 Synoptic Conditions For The United Kingdom 24th August, 1982

9.3.2 Radar Data

The rainfall field which caused the event of the 24th of August may be seen in Figure 9.3. The radar plots show the storm movement from the west, becoming apparent as a significant event at about 9:28. As the event progressed, it increased in intensity moving rapidly eastwards. The event became most severe between 9:37 and 9:52. During the next twenty minutes it died out quite considerably, both in extent and intensity. By 10:32 the storm had greatly reduced in severity and continued its movement eastwards, out of radar range.

9.3.3 Event Return Period

Figure 9.4 shows the distributed radar return period analysis for the 24th of August event as it took place. The rainfall durations under each plot refer to the duration since the beginning of rainfall on any part of the catchment. The intensity of the first part of the storm to cross the catchment was quite low. After ten minutes, recurrence intervals of between <0.5 years and 1 year are indicated. One hour into the event, the northern part of the catchment shows relatively rarer rainfall than the southern parts, the highest return period being at the northern tip of the catchment, showing a 1 in 8 year event.

After two hours, the more extreme rainfall is still concentrated in the upper catchment area, showing recurrence intervals of up to 8 years. The plot of 4 hour return period shows rarer precipitation spreading southwards over the catchment, with recurrence intervals in the 1 to 15 year range. Examination of the 8 hour return period plot shows a change in rainfall severity distribution. Here, the northern section of the catchment shows a fairly uniform recurrence interval of 1 to 2 years, whereas the southern areas show return periods of upto 1 in 8 years. At the end of the event (8 hours 35 minutes in total) the 'true' return period of the event may be found. Overall

Figure 9.3 Radar Rainfall Movement



Time 9:28



Time 9:32



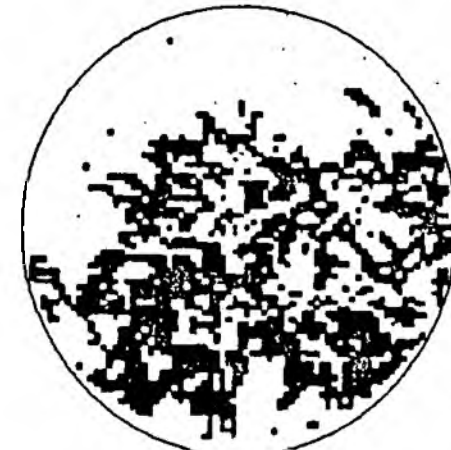
Time 9:37



Time 9:52



Time 10:12



Time 10:32

Hameldon Hill Radar

Event Date : 24-08-82

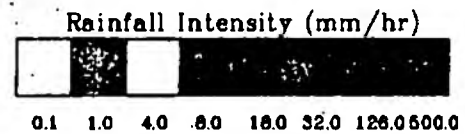
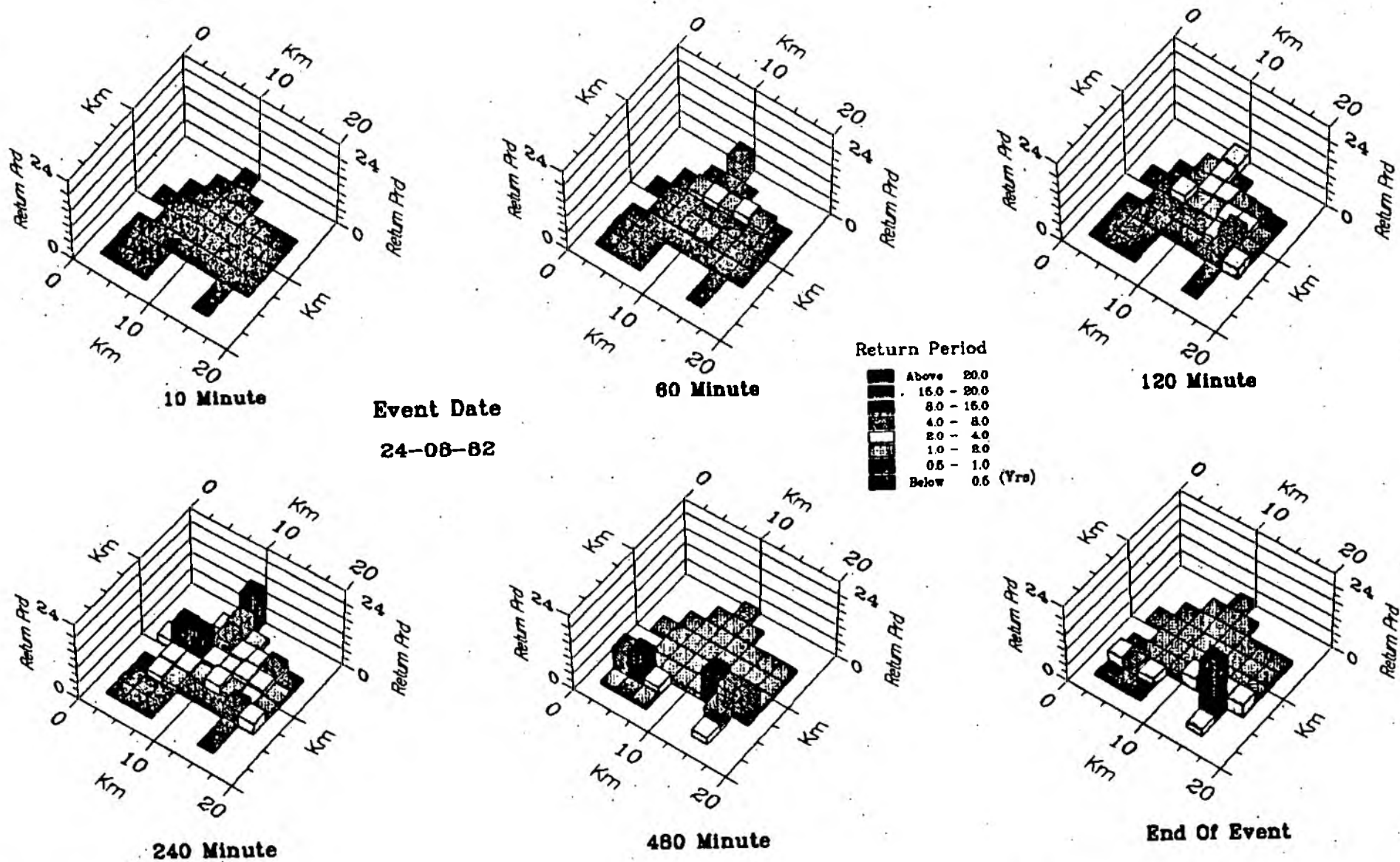


Figure 9.4 Blackford Bridge Storm Return Period Analysis



the distribution analysis shows the event to have been between an annual and 1 in 4 year storm, in relation to Blackford Bridge. The presence of very high intensity rainfall input at the southeast corner of the catchment has raised the return period of one radar pixel considerably. The overall catchment wide return period at the end of the event labels it as a 1 in 4 year storm.

9.3.4 Hydrograph Forecast

The comparison of actual and forecast flow hydrographs for the August 24th event is shown in Figure 9.5.

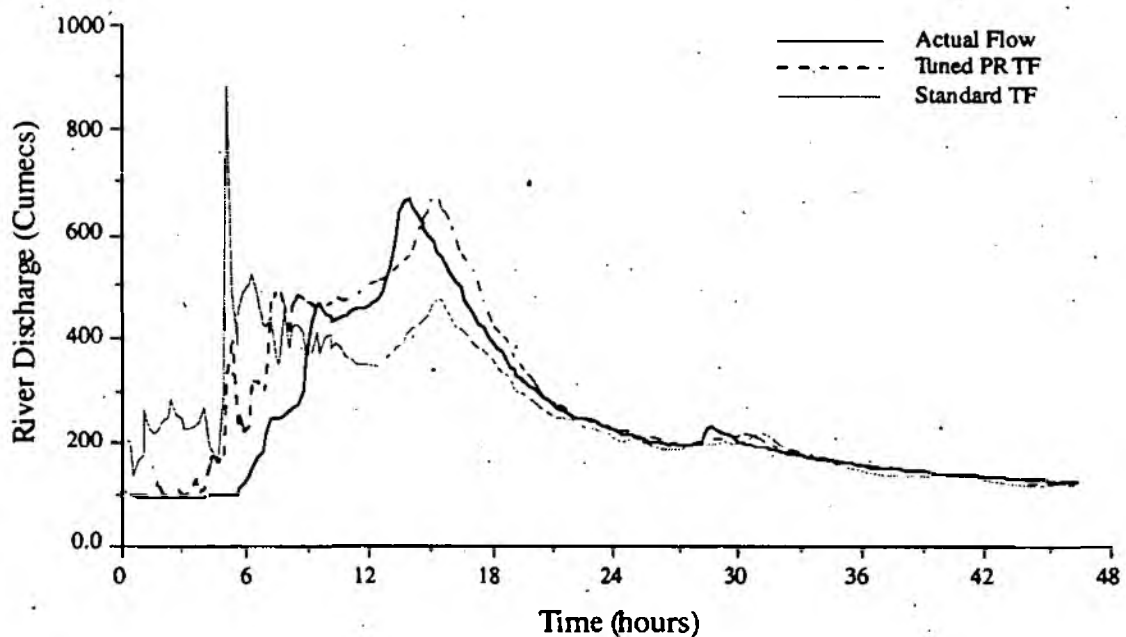


Figure 9.5 24th August, 1982 Forecast and Actual Flow Hydrographs

The non-adaptive transfer function model responds quickly to the rainfall input, causing a peak at three hours into the event, and further fluctuating peaks up to 6 hours, all higher than the true catchment response. The main hydrograph peak takes place at approximately 14 hours. The non-adaptive model misses this both in timing

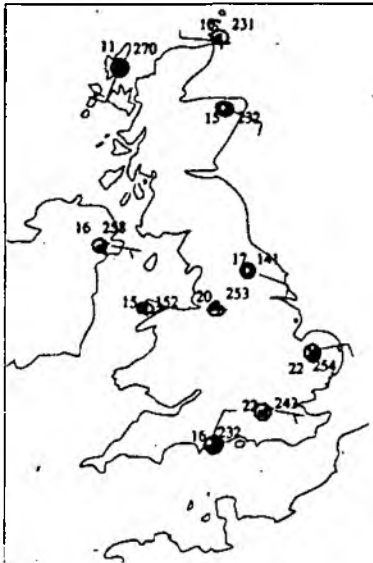
and flow, the timing being forecast around four hours late, and the flow being 40 cumecs below the actual. The recession part of the hydrograph is well represented, although this is of little interest in comparison with flow peak.

The tuned PRTF model output, from RAMPART, shows some volumetric errors on the rising limb of the hydrograph, specifically between three and eight hours into the event. The errors appear to be due to an over-estimate of soil moisture status, leading to a higher level of forecast runoff than actually took place. The main hydrograph peak is represented well in terms of flow magnitude. However, a timing error is present of approximately two hours, representing the flow peak as occurring later than was actually the case. As with the static forecast, the recession limb of the hydrograph was quite well modelled, but again this is of less importance than the timing and extent of the flow peak.

Overall, the tuned model produced a more accurate forecast of both the rising limb and peak discharge than did the static transfer function. The flow volume was well represented, but a timing error was evident in the hydrograph peak.

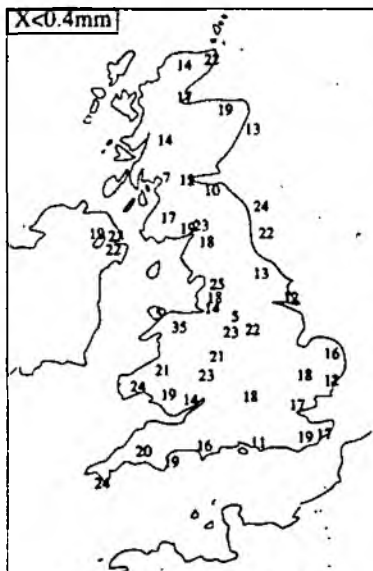
9.4 Event of 21st November 1982

9.4.1 Synoptic Conditions

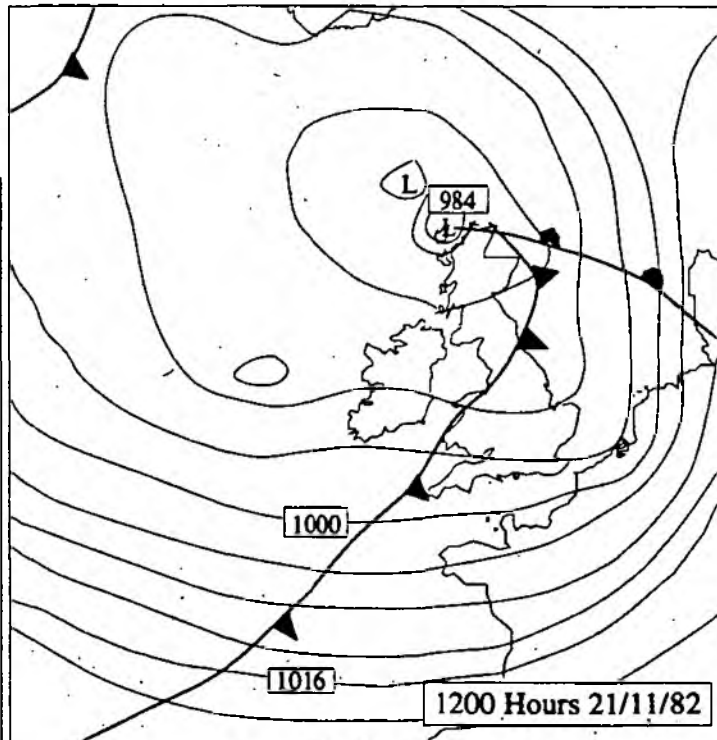


Surface Observations at 1200 Hours 21/11/82

November began with a high pressure belt over south east Europe, a slow moving front causing rain in central Britain. A succession of troughs moved north east, bringing large amounts of cloud and some rain. Between the 6th and 10th a series of depressions moved over the Atlantic, maintaining unsettled conditions as their associated fronts moved across the country. The 11th and 12th brought a vigorous cold front with heavy rain and squalls. Following this was a brief cold spell, bringing snow showers in the north, and a depression in the south east on the 14th. In the the north this lead to snow, especially on high ground. The event of the 21st took place after a short respite of milder weather, but formed part of a period of strong winds and incursions of cold air from the north west. This lead to rain in many areas, and was followed on the 23rd by show falls.



Rainfall Ending 2100



Synoptic Weather Charts

Figure 9.6 Synoptic Conditions For The United Kingdom 21st November, 1982

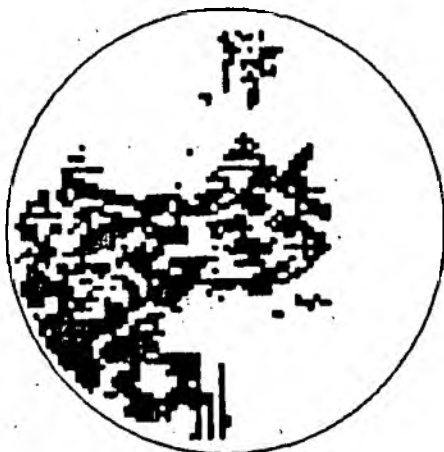
9.4.2 Radar Data

Figure 9.7 shows the radar coverage of the precipitation which caused the event of 21st November, 1982. The rainfall first appeared at 7:10, and moved eastwards across the radar field. By 7:52 the event had reached the west side of the Pennines and began to intensify. Over the following 30 minutes it continued to move eastwards, becoming heavier and more widespread. From 9:52 the storm began to decrease and proceeded to move eastwards with much lower intensity.

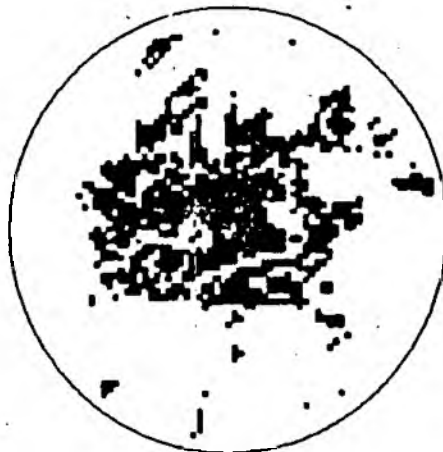
9.4.3 Event Return Period

The distributed return period analysis shown in Figure 9.8, relates the changes in rainfall over time to the intensity duration frequency relationships for each radar pixel within the Blackford catchment. The rainfall during the first hour is very low, with recurrence intervals of a maximum 1 in 2 year event. The two hour analysis shows that the northern area of the catchment has begun to receive rainfall up to 8 year return period on some of the pixels. The following two hours sees the rarest of the precipitation, a band of high recurrence interval rain being registered across the middle of the catchment. Here, return periods of 15 to 20 years are attributed to the four year rainfall. To the north and south of this line are lower return period falls, maximum values being in the 4 to 8 year range. As the storm continues, the rainfall becomes more frequent, with confined pixels recording up to 8 or 15 years precipitation. The end of the storm shows distributed rainfall return periods of 0.5 or less, to a maximum of 8 years for the event. The overall catchment rainfall return period was found to be the 1 in 6 year storm.

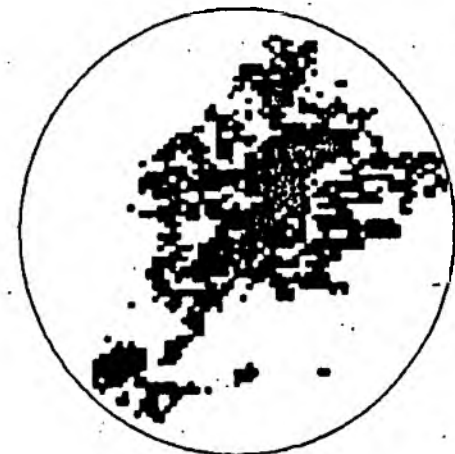
Figure 9.7 Radar Rainfall Movement



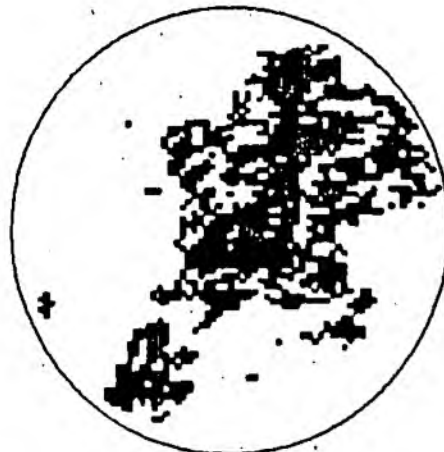
Time 7:32



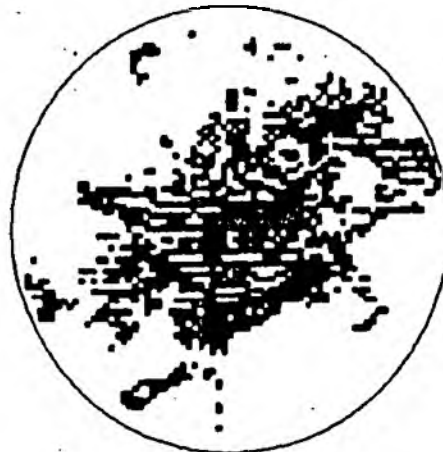
Time 7:52



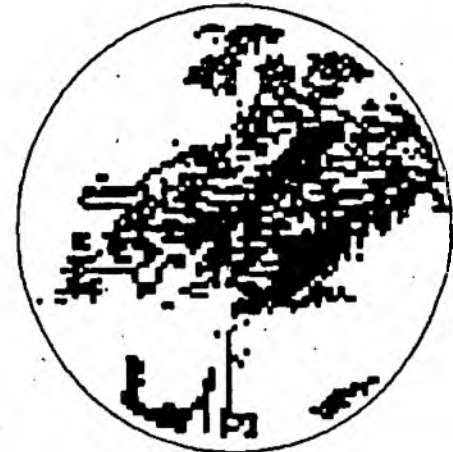
Time 8:12



Time 8:22



Time 9:22



Time 9:52

Hameldon Hill Radar
Event Date : 21-11-82

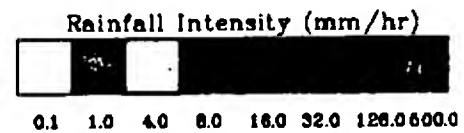
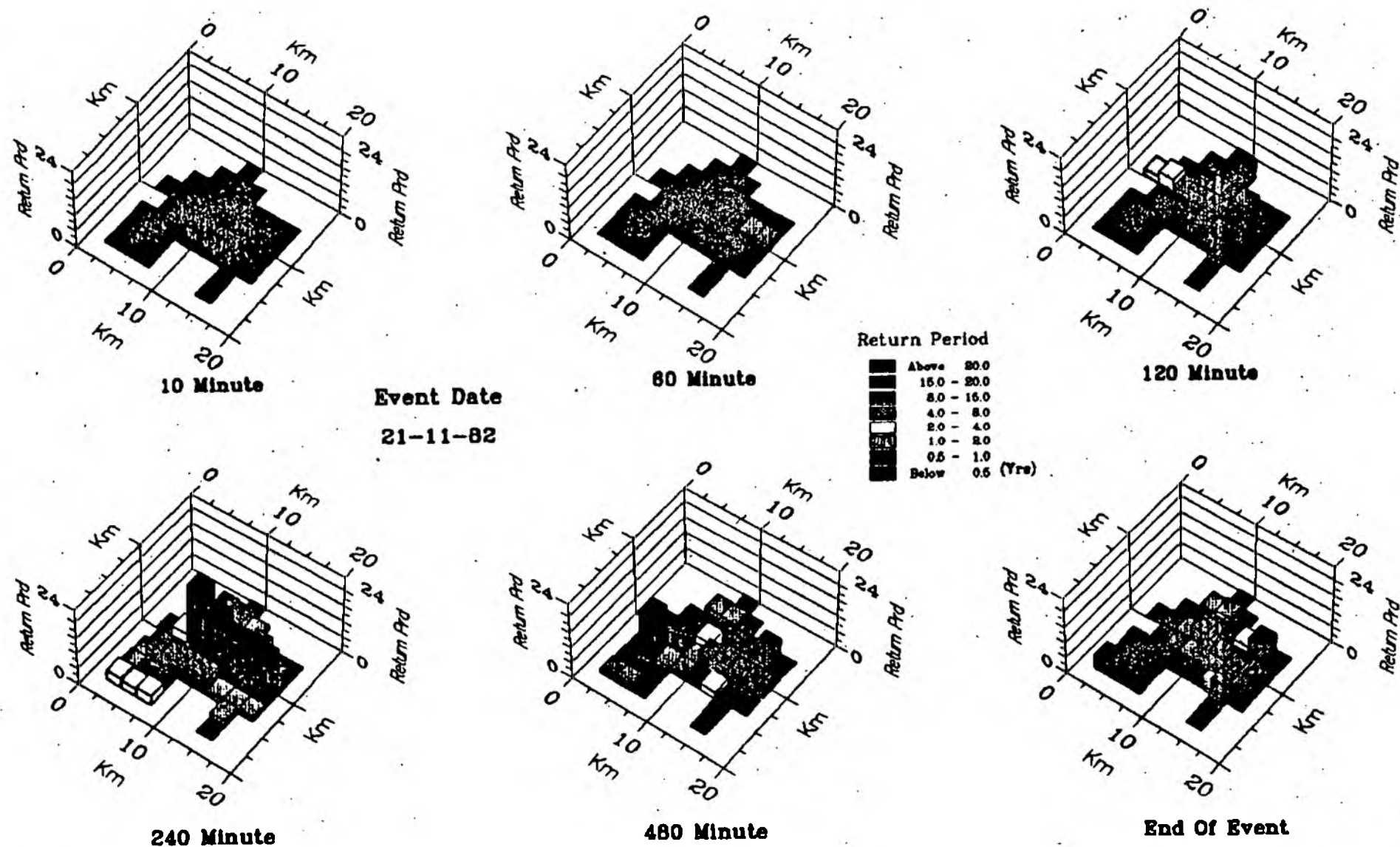


Figure 9.8 Blackford Bridge Storm Return Period Analysis



9.4.4 Hydrograph Forecast

Figure 9.9 shows the flow hydrographs for the tuned PRTF and standard transfer function forecasts, together with the true runoff for the event. The standard TF model shows timing errors from the start of hydrograph rise. These problems worsen as river flow increases, and results in a timing error at peak flow of around two hours. The shape of the rising, peak and falling sections of the hydrograph are quite accurately forecast by the TF model. However, the discharge at time of peak flow is forecast as lower than was actually produced by the event.

The RAMPART flow forecast has a late hydrograph rise and delayed peak flow when compared with the actual catchment runoff. However, these are not as severe as the standard TF model, showing a maximum timing error of just under one hour. The hydrograph shape is well reproduced by the tuned model on both rising and falling sections. Runoff volume is also well represented, with a slight under-estimate of peak flow discharge.

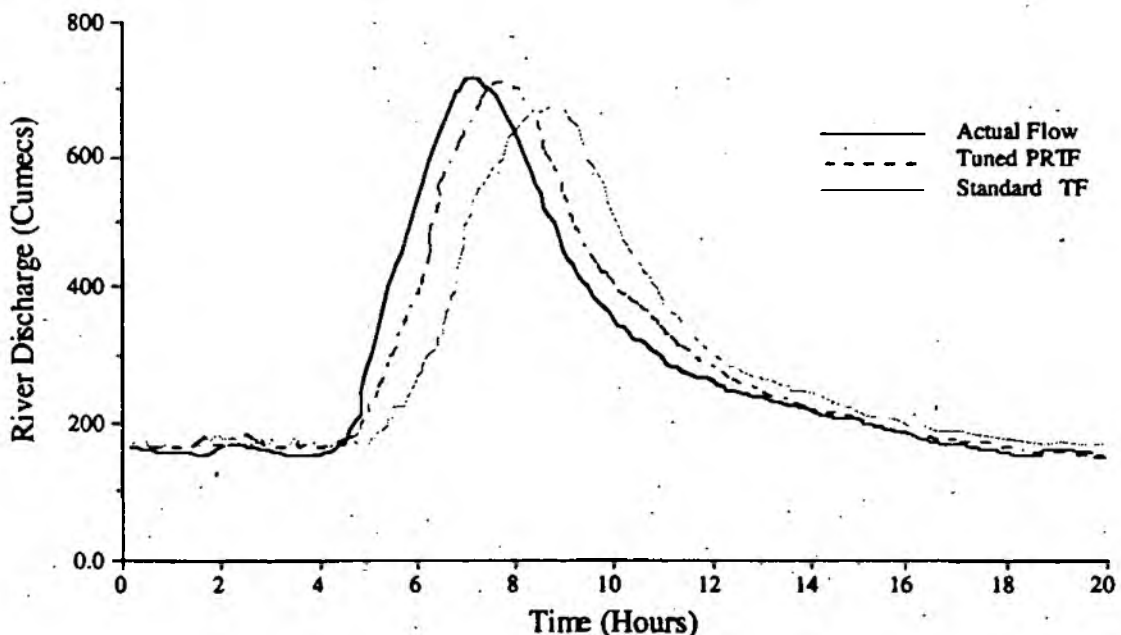
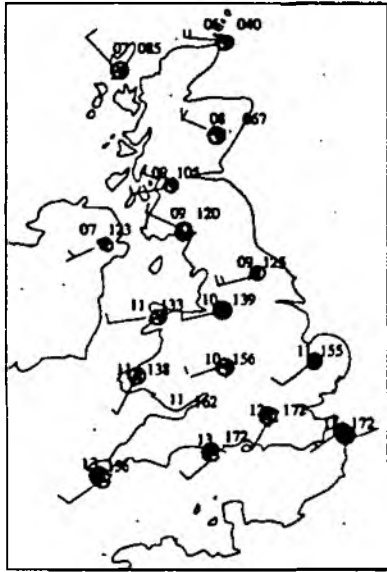


Figure 9.9 21st November, 1982 Forecast and Actual Flow Hydrographs

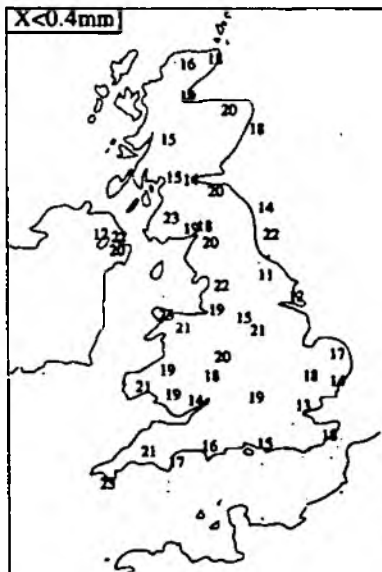
9.5 Event of 31st October 1986

9.5.1 Synoptic Conditions

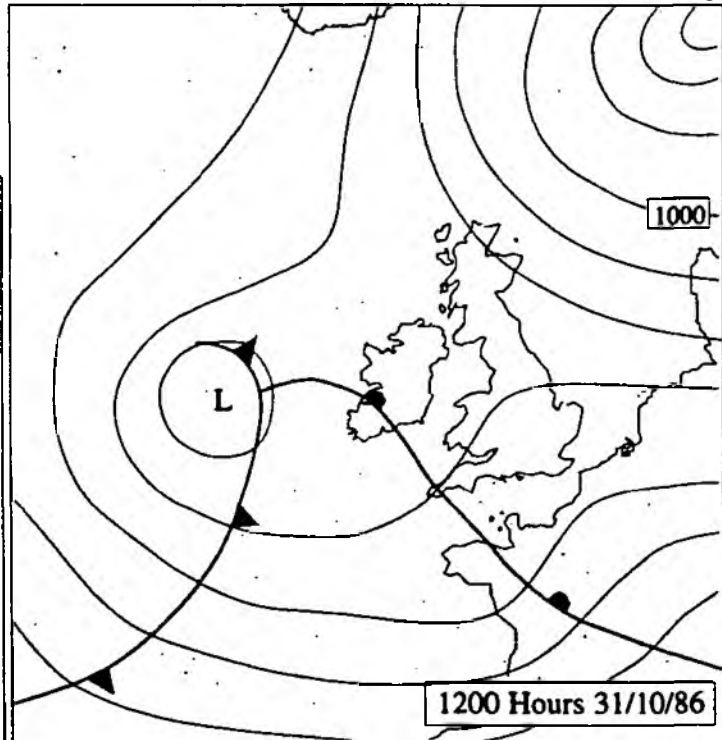
October 1986 began with dry, sunny weather across southern Britain, with fog and cloud at the start and end of the day. The north of the country was less settled, weak Atlantic fronts producing cloud and rain. A cold front moved across the south-east on the 9th and 10th, with showers falling in the north. A further cold front crossed the country on the 14th, giving up to 25mm of rainfall in some areas. The extending influence of depressions near Iceland lead to falling pressure over the British Isles, and a very unsettled spell. On the 20th an intense secondary depression moved east across central areas, bringing rain and gales. Snow showers followed on high ground in the north, and further fronts between 24th and 26th produced severe rain and gales. The event of the 31st took place in this series of depressions, and was part of a period of heavy rain and severe winds.



Surface Observations at 1200 Hours 31/10/86



Rainfall Ending 2100



Synoptic Weather Charts

Figure 9.10 Synoptic Conditions For The United Kingdom 31st October, 1986

9.5.2 Radar Data

Figure 9.11 shows the radar images produced by the October 31st, 1986 event. The storm which hit the Blackford Bridge area was part of a series of fronts and fierce gales which moved across the country. The main rainfall began to move in from the southwest at around 22:17. By 22:47 it was beginning to intensify, moving northeast over the field of radar coverage. A further intense rainfall belt may also be identified at the northern extent of the radar image. The intensification of the event continued through midnight, and into the first day of November, maintaining its northeasterly direction and high intensity levels.

9.5.3 Event Return Period

The distributed rainfall return period analysis is shown in Figure 9.12. The first ten minutes of the event show relatively low severity rainfall in relation to the Blackford area. After one hour the northwest section of the drainage basin shows rainfall between 8 and 20 year recurrence interval. This contrasts with the eastern radar pixels, which register a maximum of 4 years return period. At the end of two hours the events' west / east division is still evident across the centre of the catchment, although the rarer precipitation has spread further to the east. The 240 minute plot show a general reduction in the storm 'risk'. Over the majority of the area the rainfall lies in the 1 to 8 year return period range, with only a single pixel at the southwest corner showing significantly higher rainfall rarity. The eight hour graph indicates lower recurrence interval precipitation west to east across the centre of the catchment, with higher return period rain to the northern and southern reaches. The split in precipitation severity appears quite large, the north and south areas recording return periods in the 15 to 20 year range whereas the centre section shows only a 1 to 4 year fall. The event ended after nine hours 35 minutes, when precipitation had stopped on all catchment pixels. The final distributed return periods for the storm showed overall

Figure 9.11 Radar Rainfall Movement



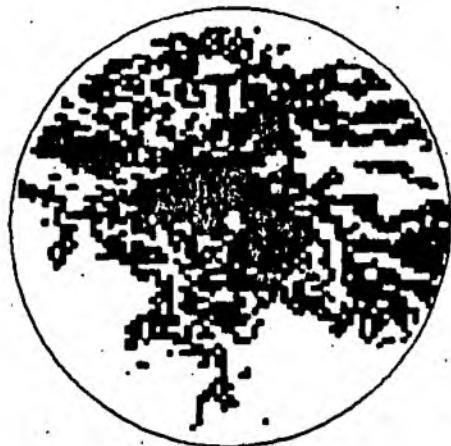
Time 22:17



Time 22:47



Time 23:07



Time 1:07



Time 1:47



Time 2:17

Hameldon Hill Radar

Event Date : 31-10-86

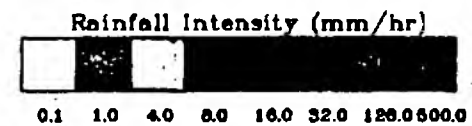
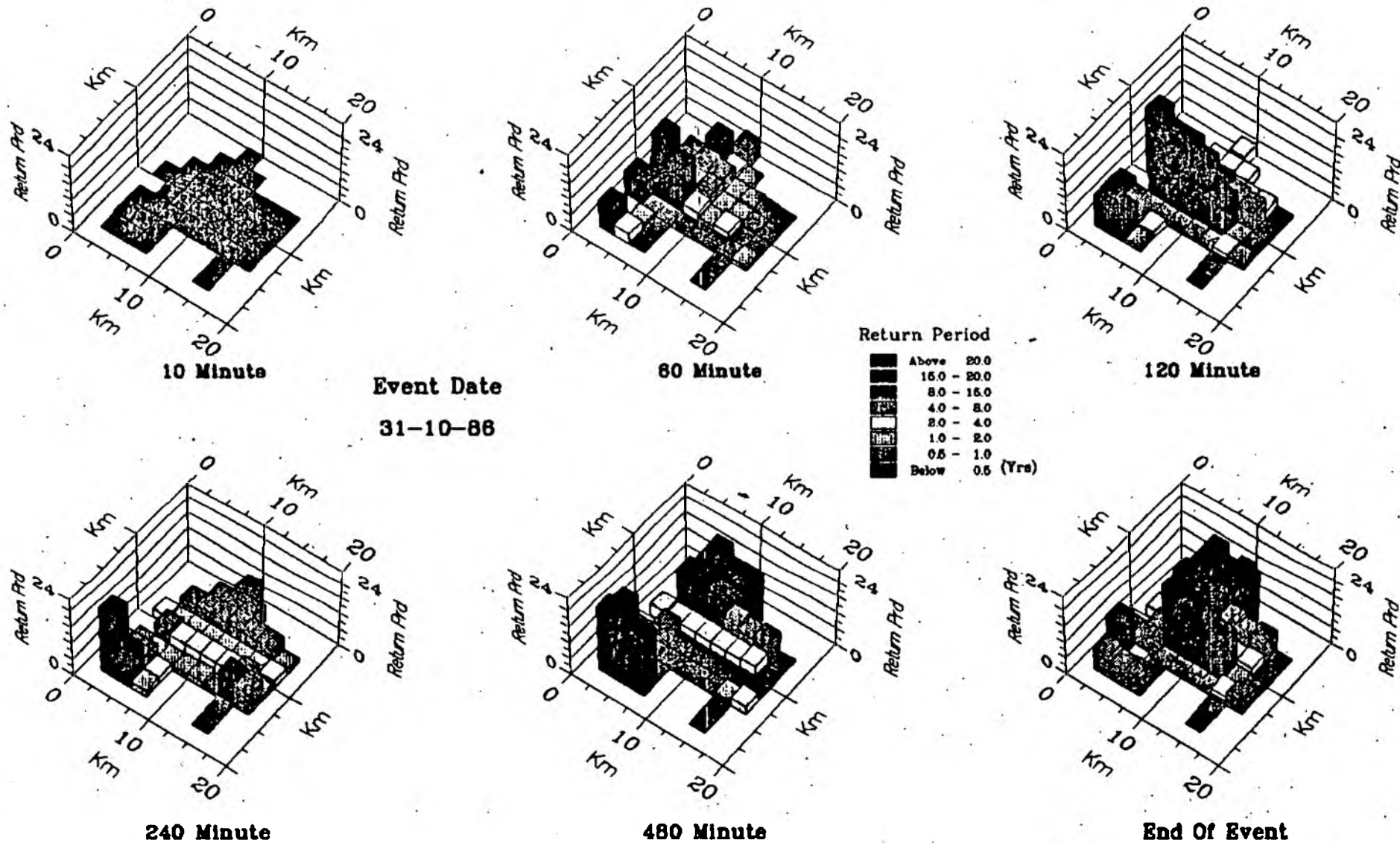


Figure 9.12 Blackford Bridge Storm Return Period Analysis



rarer rainfall in the centre and northern catchment and more 'common' rain at the west, east and southern edges of the area.

9.5.4 Hydrograph Forecast

The forecast flow hydrographs for the 31st October 1986 event may be seen in Figure 9.13. Here the standard transfer function model performs significantly better than the knowledge based tuning approach. The TF forecast shows a minor timing error, rising just before the actual hydrograph, and the peak flow is marginally underestimated. The recession limb, although less important than the rising and peak sections of the hydrograph, is well represented by the standard TF model. The PRTF forecast shows a significant error after the rising limb of the flow hydrograph. This timing problem becomes worse as the runoff moves to peak flow. The maximum forecast flow is also incorrect, being significantly lower than the actual flow level.

The main problem with the RAMPART forecast is the inaccurate shape and timing parameter settings, causing late rising and regression limbs and a low runoff peak. The incorrect parameter estimation may be due to the identification of the majority of rainfall as occurring in the upper section of the catchment in the early stages of the event. This would cause the system to delay and reshape the flow forecast. The action of more intense rain in the middle and lower catchment sections, later in the event, appears to have counterbalanced any timing and shape changes, but this was not accounted for in the PRTF forecast. The standard TF model, by contrast, only responded to rainfall input and consequently produced a more accurate response for this event.

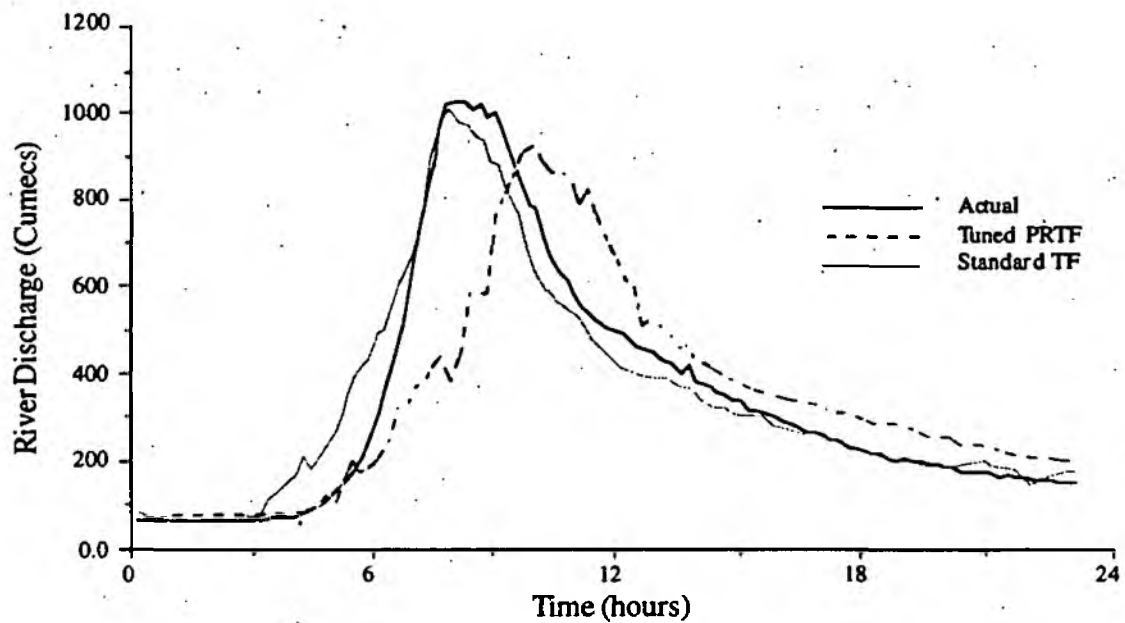


Figure 9.13 31st October, 1986 Forecast and Actual Flow Hydrographs

9.6 Conclusions

This chapter has given a demonstration of the potential uses of some of the techniques and analyses developed throughout the rest of the thesis. Three events have been investigated with distributed return period analysis and runoff hydrograph forecasting, using a knowledge based approach. The assessment of return period allowed identification of storm development as it took place in relation to the rainfall regime of the catchment.

The knowledge based parameter tuning system gave improved forecasts over a standard delta transfer function model in two of the three cases investigated. Where the RAMPART system produced a poorer forecast the problems may be due to inappropriate timing and shape parameter settings, related to the position of rainfall concentration over the catchment. This highlights the system as a first application of the knowledge based approach in real-time forecasting. The opportunities for further research into this type of technique are discussed in Chapter 10.

CHAPTER 10**CONCLUSIONS AND RECOMMENDATIONS****10.1 Introduction**

This thesis has detailed research into the use of a knowledge based approach in extending lead time and improving forecasting accuracy of rapid response flooding within a real-time environment. Traditional knowledge engineering, eliciting knowledge from a domain expert, proved to be unsatisfactory due largely to the number and complexity of catchments in a region as a whole. As a result, the relevant 'expertise' had to be established, and a wider approach was sought to the sourcing and application of knowledge. Cognizance of catchment rainfall regime and machine induction techniques were used, based around radar rainfall input, to assess storm risk, catchment status and forecast flow hydrograph. This chapter outlines the main conclusions of the research, applications of the techniques evolved and recommendations for future work which the investigation raised.

10.2 Conclusions and Recommendations**10.2.1 Rapid Response Flooding**

Rapid inundation, whether from flash flooding or rapid response catchments has proved to be one of the most unpredictable and devastating forms of flood response. The short time between the causal event and resultant runoff means that warning lead time is at a premium. In forecasting a rapid response event, the extension of this lead time, either by information about storm risk or accurate storm flow forecasting, may allow short term warnings to be issued in time for evacuation, amelioration or control of the flood flows.

10.2.2 Radar

In providing prior information about an event, or a combination of factors likely to cause rapid response flooding, information about the rainfall input to the system, and current catchment status are vital. Remote sensing of the atmosphere using radar provides rainfall information updated at five minute intervals over a large area. As well as the real-time catchment input, radar also allows monitoring and forecasting of the precipitation before it reaches the area of interest, using storm or catchment transposition techniques. Quantitative estimation of rainfall using radar is not without its problems, but in providing the foresight needed in fast response situations it is unique. It was these aspects of detailed wide-scale coverage and frequent updating that lead to the use of radar derived rainfall measurements in this investigation.

10.2.3 Radar Derived IDF Analysis

Intensity-Duration-Frequency analysis has been used to establish the severity of a given return period event since before the turn of the century. Many methods of rainfall analysis have been developed since then, using various statistical techniques, but all have based on raingauge information for design purposes or post-event appraisal. The use of such point data necessitates some form of areal averaging or interpolation, and leaves very large areas completely unsampled.

- A new technique has been evolved using distributed radar analysis and General Extreme Value distribution fitting using Probability Weighted Moments.
- Frequent radar updating, combined with a knowledge based approach to the potential of return periods provides knowledge of catchment rainfall history to be used in assigning risk to events as they occur. This allows the conversion of radar rainfall 'data' into 'information' using knowledge of catchment rainfall regime in real-time.

- The technique also provides a new basis for the effective comparison of different storm events.
- A simple catchment transposition procedure was developed, allowing forecast event return period to be calculated before the storm reaches the catchment. This technique provides a new way of classifying an event before it occurs, in terms of the area of interest.
- The return period procedure is quick to run in real-time due to the reduction of each IDF distribution to a small number of PWM parameters.
- The analysis routine may be easily integrated into the existing radar processing system, and it is recommended that this or a similar distributed IDF procedure be included in the radar network system, in order to fully utilise the potential of this form of data.

10.2.4 Rainfall

In an attempt to find detailed knowledge of the rainfall runoff process, analysis was carried out to determine the effect of rainfall characteristics in flood production. In a flood forecasting context, all of the rainfall characteristics analysed could be obtained from weather radar measurements.

- Investigation was carried out of the rainfall input as experienced by the drainage area, by examination of the catchment rainfall hyetograph, to allow direct forecast of runoff characteristics. Various rainfall features were assessed; maximum rainfall intensity sustained for durations from 15 to 90 minutes, rainfall volume, duration, temporal centre of gravity, variance and skew.

- The rainfall hyetograph characteristics were related to the flow hydrograph properties of peak flow, time-to-peak, flow volume and percentage runoff for the ensuing events.

- An optimised transfer function model was applied to each rainfall runoff sequence in order to test the possibility of model selection based on rainfall characteristics, the model impulse responses again being related to the rainfall features outlined above.

- The investigation produced information about several useful links between the rainfall and runoff characteristics analysed, related to runoff time-to-peak and volume. Unfortunately, however, none of the knowledge was sufficiently well defined or linkages strong enough to be included in a knowledge base for direct forecasting of flow.

- In the present study, investigation was moved away from attempting the direct forecasting of flow from rainfall to a model parameter tuning approach. It is recommended that if future work is pursued in this direction then consideration be included of other factors such as catchment vegetation cover and land use.

10.2.5 Knowledge Based Flow Forecasting

No modelling system procedure is perfect, and the problems in the hydrological utilisation of transfer function models has been addressed by Han (1991). An outline of these difficulties has been presented along with a description of a physically realisable transfer function model form.

- In order to allow model parameter tuning, a study was undertaken to gain knowledge of parameter dynamics in relation to storm rainfall, intensity, direction and coverage.

- The study into these model variable relationships was carried out using machine induction, synthetic rainfall runoff sequences being produced from a Kinematic Wave Model, for differing storm movement, coverage and intensity characteristics. A PRTF model was fitted manually to each event, and the optimum parameter values recorded and related to the causal storm characteristics.

- Linkages between the rainfall features and model parameters were summarised in the form of relationships and thresholds, in a suitable form for use in a knowledge based system.

- In order to include the influence of catchment status a new technique was evolved to estimate antecedent precipitation index using radar rainfall inputs. Due to the relatively low number of calibration events available, however, only a single loss factor was determined rather than seasonally variable values.

- Catchment representation was carried out using a reservoir approach, work being undertaken to define the threshold API value at which rainfall began to contribute to runoff (the Effective Rainfall Threshold or ERT).

- The catchment reservoir and effective rainfall concepts were combined to produce a physically based system to determine event runoff contribution, analogous to the 'initial plus continuing loss' mechanism.

- The rainfall runoff parameters and catchment status-threshold relationships established were built into a simple knowledge based system. Knowledge representation followed a production rule format, and rainfall and catchment information came from a cross correlation forecasting routine, a dynamic database

being updated every time a new forecast become available. Model parameter values were set using this rainfall information, with reference to the appropriate production rules, using a forward chaining system.

- When tested with actual rainfall runoff events the model tuning system gave improved forecasts over 60% of the time.
- Detailed examination of the runoff peak magnitude and timing showed that the extent of flow was well forecast, but problems were identified relating to peak timing. Inconsistent rainfall input to the system led to variation in parameter values chosen, and consequent fluctuation in forecast catchment outflow.
- Comparison with a grid based distributed model showed the RAMPART system to be more efficient and produce more accurate flow forecasts, specifically in the area of peak runoff timing.

The investigation procedure outlined above raised several recommendations for further research :

- Firstly, machine induction performs well when 'expert' knowledge is lacking or in identification of relationships where sufficient data would otherwise be unavailable. It also allows control over multi-variable systems, in order to identify links which may be confused by 'noise' from other factors.
- When such techniques are applied, care must be taken to match the induction system to reality as far as possible. Following from this, the rules and relationships established should be tested in a real-world context rather than immediately being taken as fact. This allows identification of weaknesses, essential when the system is used in a high risk application, and the possibility of post-induction optimisation.

Although far from perfect, the knowledge based approach to flow forecasting produced encouraging results. Future work along these lines may be recommended, following a similar rule based representation, or some more complex methodology.

- Research to improve the system in its present form may be focused on refining the current knowledge, or establishing new rules. Refinement may involve tuning the relationships to relate more closely to the drainage area of interest. System testing indicated that the thresholds used to define the timing parameter (τ) may not be exactly matched to the Blackford Bridge catchment. Precipitation index and effective rainfall parameters may also be improved, the definition of seasonally variable loss rates perhaps providing a more accurate representation of catchment status. Alternatively, a device such as the Institute of Hydrology HYDRA may be used to provide point loss calibration, in a similar way to raingauge calibration of radar rainfall data.

- The investigation of new rules and relationships may concentrate on the role of-rainfall or catchment variables. The definition of an infiltration excess runoff value may prove useful in extremely intense events, in contrast to the soil saturation method used in the catchment reservoir representation. Detailed investigation may reveal differing rainfall values required to stimulate infiltration excess runoff, related to prolonged dry period ground surface sealing, or other factors. Further catchment characteristics which may be investigated relate to land use or vegetation cover which may change seasonally.

- The system developed in this thesis uses simple, rule based knowledge representation, the only source for new information being from outside programming. An alternative is the introduction of more complex representation techniques and/or a learning capability. The implementation of some form of 'learning' procedure may be extremely useful in such a variable and important area as rapid response flood

forecasting. Research may be aimed at a system that will 'learn' from its mistakes, forming new rules and associations as time progresses. Thus, if a forecast proves to be inaccurate, the sources of error should be identified, and the circumstances 'remembered'. A similar event in the future should not cause the same mistakes again, but should be better forecast, based on what has been learned.

- In answer to the problems experienced with model forecast fluctuation, a further area of investigation may lie in the use of model parameter restraint. The creation of a completely accurate and reliable rainfall forecasting system would be an alternative solution, benefiting many other applications.

10.3 Summary

Overall, the use of a knowledge based approach has proved to be encouraging, at least in this first study, and is thought to be worthy of further investigation in the future.

In a real-time rapid response flood event, the new analyses and procedures developed here may be used to increase warning of a severe event and improve flow forecast accuracy. With a storm upwind of the catchment the intensity-duration-frequency analysis and catchment transposition techniques allow forecasting of the event risk. This is repeatable as the event approaches and passes over the area of interest, to gain information about increasing or decreasing storm severity. The direct forecasting of runoff characteristics from rainfall analysis proved to be too vague, but model parameter tuning was more successful. Forecast rainfall may be input to the knowledge based system and combined with knowledge of catchment status and thresholds to produce a forecast flow hydrograph. The severity of the runoff anticipated may then be used as a basis to disseminate warnings or call the relevant authorities to 'stand-by' or action.

REFERENCES

- Abramowitz, M. and Stegun, I.A. (1972) **Handbook Of Mathematical Functions**. Dover, New York.
- Acreman, M. (1989) **Extreme Rainfall In Calderdale, 19 May 1989**. *Weather*, Vol.44, pp438-447.
- Alim, S. (1987) **A Prolog-Based Expert System for Encoding Seismic Design Provisions**. *Civil Engineering Systems*, Vol. 4(1), pp39-44.
- Anderson, J.R. (1985) **Cognitive Psychology And Its Implications**. Freeman, New York.
- Atlas, D (1964) **Advances In Radar Metereology**. *Advances in Geophysics*, Vol. 10. Academic Press, London and New York. pp317-478.
- Austin, G.L. and Bellon, A. (1982) **Accuracy Of Short-Term Radar Rainfall Forecasts**. *Journal of Hydrology*, 70, pp 35-49.
- Baffaut, C. and Delleur, J.W. (1989) **Expert System for Calibrating SWMM**. *ASCE Journal of Water Resources Planning and Management*, Vol. 115(3), pp278-298.
- Battan, L. J. (1973) **Radar Observations Of The Atmosphere**. The University of Chicago Press.
- Bedient, P.B & Springer, N.K. (1979) **The Effect Of Rainfall Timing On Design Floods**. *Journal of Civ. Eng. Des.*, 1, No. 4, pp 311-323.
- Belville, J. et al. (1978) **A Flash Flood Aid - The Limited Area QPF**. Preprints. Conf. on Flash Floods, Hydrometeorological Aspects, AMS, Boston, pp 21-28.
- Bergeron, T. (1967) **Meteorological Studies Of Precipitation**. Final Report 1964-1966. Meteorologiska Institutionen, Uppsala, Sweden.
- Best, A.C., Booker, H.G. and Sheppard, P.A. (1948) **Radio Meteorology In The United Kingdom 1939-1947**. Resume Mem. Ass. Met. Un geod Geophys., int, Oslo, Los Angeles, Calif.

- Bevan, K.J. & Homberger, G.M. (1982) **Assessing The Effect Of The Spatial Pattern Of Precipitation In Modelling Stream Flow Hydrographs.** *Water Res. Bull.*, 18, No. 5, pp 823-829.
- Beven, K.J. (1985) **Distributed Models.** In *Hydrological Forecasting*, ed. M.G.Anderson and T.P.Burt, Wiley, pp405-435.
- Beven, K.J. (1989) **Changing Ideas In Hydrology : The Case of Physically Based Models.** *Journal of Hydrology*, Vol. 195, pp157-172.
- Beven, K.J. (1991) **Spatially Distributed Modelling : Conceptual Approach to Runoff Prediction.** In *Recent Advances in the Modelling Of Hydrological Systems*, ed. D.S.Bowles and P.E.O'Connell, NATO -ASI Series, Kluwer Academic Publishers, Netherlands.
- Beynon-Davies, P. (1991) **Expert Database Systems, A Gentle Introduction.** *International Series in Software Emgineering*, McGraw-Hill, New York.
- Bilham, E.G. (1935) (Republished 1962) **Classification of Heavy Falls of Rain in Short Periods.** *British Rainfall*, HMSO, London.
- Biswas, A. K. and Chatterjee, S. (1971) **Dam Disasters - An Assessment.** *Engineering Journal*. March.
- Bootman, A.P. and Willis, A. (1977) **Extreme Two-Day Rainfall In Somerset.** *Wessex Water Authority*, Bristol.
- Bootman, A.P. and Willis, A. (1981) **Discussion In Papers 4-6.** In *FSR Five Years On*, Thomas Telford, London.
- Box, G.E. and Jenkins, G.M. (1970) **Time Series Analysis.** Revised Ed., Holden-Day, San Fransisco.
- Brice, C.R. and Fennerma, C.L. (1970) **Scene Analysis Using Regions.** *Artificial Intelligence I*, pp205-226
- Brooks, C.P.E. & Glasspool, J. (1928) **British Floods And Droughts.** Benn, London.

Browning, K.A. (1977) **The Short-Period Weather Forecasting Pilot Project**. Research Report No. 1, Meteorological Office Radar Research Lab.

Browning, K.A. (1979) **The FRONTIERS Plan : A Strategy For Using Radar And Satellite Imagery For Very-Short-Range Precipitation Forecasting**. Meteorol. Mag., 108, pp 161-184.

Browning, K.A. (1987) **Weather Radar and FRONTIERS**. Schools Supplement No.5, Met. Off. Radar Research Lab.

Browning, K.A. and Collier, C.G. (1982) **An Integrated Radar Satellite Nowcasting System In The U.K.** Nowcasting, ed. K.A. Browning, Academic Press, London, pp47-61.

Bulman, P.J. and Browning, K.A. (1971) **National Weather Radar Network**, Royal Radar Establishment Report, Malvern.

Central Water Planning Unit (1977) **Dee Weather Radar and Real-Time Hydrological Forecasting Project**. Report by the Steering Committee, Reading, Berkshire.

Changnon, S.A. (1981) **Metromex: A review An Summary**. American Meteorological Society Monograph No. 40, Vol. 18, pp 181.

Chatfield, C. (1984) **An Analysis Of Time Series**. Chapman and Hall, London.

Chow, V. T. (1951) **A General Formula For Hydrologic Frequency Analysis**. Trans. Am. Geophys. Union, Vol. 32, pp231-237.

Chow, V. T., Maidment, D.R. and Mays, L. M. (1988) **Applied Hydrology**. McGraw-Hill, New York.

Clark, C. (1991) **A Four-Parameter Model For The Estimation Of Rainfall In South-West England**. Meteorol. Mag., Vol. 120, No. 1423, pp21-31.

Clarkson, C. and Hartigan, J. (1989) **Expert Systems Approach to Water Supply Management Decisions**. 6th Conference on Computing in Civil Engineering, Computing in Civil Engineering, New York, pp 100-107

- Clift, G.A. (1985) **Use Of Radar In Meteorology.** WMO Technical Note No. 181, World Met. Organisation, Geneva.
- Cluckie, I.D. and Ede, P.F. (1985) **End-Point Use As A Criterion For Model Assessment.** 7th IFAC/IFORS Symp. on Identification and System Parameter Estimation, York.
- Cluckie, I.D. and Harpin, R. (1982) **A Real-Time Simulator Of The Rainfall Runoff Process.** Mathematics and Computers in Simulation, Vol. 14, pp131-139.
- Cluckie, I.D. and Owens, M.D. (1986) **Real-Time Rain Runoff Models And Use Of Weather Radar Information.** In Weather Radar and Flood Forecasting ed. V.K. Collinge and C. Kirby, J. Wiley, Chichester.
- Cluckie, I.D. and Smith, F.J.B. (1980) **Flood Forecasting Project For Wessex Water Authority (Avon and Dorset Division).** Report, Dept. of Civil Engineering, University of Birmingham, (Unpublished).
- Collier, C.G., Szejwach, G. and Testud, J. (1988) **Measurement Of Global Precipitation From Space.** Europe Space Agency.
- Collier, C.G. (1980) **Data Processing In The Meteorological Office Short Period Weather Forecasting Pilot Project.** Meteorol. Mag., 109, pp161-177.
- Collier, C.G. (1989) **Applications Of Weather Radar Systems - A Guide To Uses Of Radar Data In Meteorology And Hydrology.** Ellis Horwood Ltd., Chichester.
- Collier, C.G. (1990) **Assessing And Forecasting Extreme Rainfall In The United Kingdom Weather.** Royal Met. Soc., Vol.45, No.4.
- Collinge, V.K. (1961) **Heavy Rainfalls In The British Isles.** Civil Engineering and Public Works Review, Vol. 56, No. 656.
- Collins, A.G., Searleman, J. and Collins K.J. (1991a) **Aspects of Intelligent Tutoring Systems Applied to Small Water Treatment Plant Expert Systems.** Water Science and Technology, Vol. 24(6), pp307-314.

- Collins, A.G., Ellis, G.W., Ford, C. and Bristol, L.E. (1991b) **Coupling Expert Systems to Databases for Water Treatment Plant Control**. Proceedings of the 1991 AWWA Annual Conference, American Water Works Assoc., Denver, CO., pp507-522.
- Conway B.J. (1989) **Expert Systems And Weather Forecasting**. Met. Mag. 118.
- Cotton, D.E. & Burnash, J.C. (1978) **A Flash Flood Warning System**. American Meteorological Society/American Geophysical Union.
- Cunnane, C. (1977) **Unbiased Plotting Positions - A Review**. J. Hydrol., Vol. 37, pp205-222.
- Dales, M.Y. and Reed, D.W. (1989) **Regional Flood And Storm Hazard Assessment**. Report No. 102, Institute of Hydrology, Wallingford.
- Dandy, G.C. and Simpson, A.R. (1991) **Development of Expert Systems for a Water Filtration Plant**. Civil Engineering Systems, Vol. 8(2), pp63-70.
- Davidson, D. D. & McCartney, B.L. (1975) **Water Waves Generated By Landslides In Reservoirs**. J. Hydraul. Div., ASCE, 101, HY12, pp 1489-1501.
- De Wiest, R.J.M. (1965) **Geohydrology**. J. Wiley, New York.
- DeFatta, D., Lucas, J. and Hodgkiss, W. (1988) **Digital Signal Processing**. J. Wiley and Sons, Chichester.
- Delderfield, E.R. (1953) **The Lynmouth Flood Disaster**. David and Charles Ltd, Newton Abbott.
- Doraiswami, R. & Jiang, J. (1989) **Performance Monitoring In Expert Control Systems**. Automatica, 25, No.6, pp 799-81.
- Drew, C. (1993) **Personal Communication**. Emergency Planing Officer, NRA North-West.
- Duda, R.O. and Blackmer, R.H. (1972) **Application Of Pattern Recognition Techniques of Digitised Weather Radar**. Final Report covering 25 May 1971 - 31 March 72, Stanford Research Inst.

Duda, R.O., Gaschnig, J.G. and Hart, P.E. (1979) **Model Design In The PROSPECTOR Consultant System For Mineral Exploration.** In D. Michie (ed) *Expert Systems In The Micro Electronic Age.* Edinburgh: Edinburgh Press.

Duda, R.O. and Shortliffe, E.H. (1983) **Expert Systems Research.** Science, Vol. 220(4594), pp261-268.

Eagleson, P.S. (1970) **Dynamic Hydrology.** McGraw-Hill, New York.

Eccles, P.J. (1978). **Automatic Flash Flood Warnings From Dual Wavelength Radar, Are They Worth It?** Preprints, Conference on Flash Floods, AMS, Boston.

Engman, E.T. (1988) **Diagnostic Strategies of and Expert System for Simulating Snowmelt Runoff.** In *Planning Now for Irrigation and Drainage in the 21st Century*, ASCE, New York, pp 242-249.

Fair, C.A., James, P.K. and Larke, P. (1989) **The U.K. Weather Radar Network.** Seminar on COST Project 73, Brussels. In *Weather Radar Networking* ed. C.G. Collier and M. Chapuins, Kluwer Academic Pub., London.

Fedra, A.D. and Russel, S.O. (1986) **An Expert System for Flood Estimation.** In *Expert Systems in Civil Engineering.* American Society of Civil Engineers, New York, pp174-180.

Fisher, R.A. and Tippett, L.H.C. (1928) **Limiting Forms Of The Frequency Distribution Of The Largest Or Smallest Member Of A Sample.** Proc. of the Cambridge Phil. Soc., 24, pp180-190

Floris, V., Simons, D.B. and Simons, R.K. (1989) **Knowledge Based Expert System for the Real Time Operation of Reservoir Systems.** Proceedings of the International Conference on Hydropower, ASCE, New York pp1170-1780.

Folland, K.C., Kelway, P.S. and Warrilow, D.A. (1981) **The Application Of Meteorological Information To Flood Design.** In *FSR Five Years On*, Thomas Telford, London.

Fox, J. (1979) **Making Decisions Under The Influence Of Memory.** Psychological Review, 87, pp190-211

Frechet, M. (1927) **Sur La Loi De Probabilite De L'ecart Maximum (On the Probability Law Of Maximum Values)**. Annales de la Societe Polonaise de Mathematique, Vol. 6, pp93-116.

Frenzel, L.E. (1987) **Understanding Expert Systems**. Howard W. Sams & Co.

Gashing, J., Reboh, R. and Reitter, J (1981) **Development of a Knowledge Based Expert System for Water Resource Problems**. Final Report, Project 1619, SRI International, Manlo Park, CA.

Georgakakos, K.P.(1986) **A Generalised Stochastic Hydrometeorological Model For Flood And Flash Flood Forecasting**. Water Resources Research, 22, pp 2083.

Goudie, A. (1986) **The Human Impact**. Basil Backwell Ltd.

Greenwood, J.A., Landwehr, J.M., Matalas, N.C. and Wallis J.R. (1979) **Probability Weighted Moments : Definition And Relation To Parameters Of Several Distributions Expressible In Inverse Form**. Water Res. Res., 15, pp1049-1054.

Gray, D (1970) **Handbook On The Principles Of Hydrology**. Water Information Centre, INC.

Gumbel, E.J. (1941) **The Return Period Of Flood Flows**. The Annals of Mathematical Statistics, Vol. 12, No. 2, pp163-190.

Haggett, C.M. (1988) **Thunderstorms Over North-West London - 8 May 1988**. Weather, 43, No. 7, pp 266-267.

Haggett, C.M. (1989) **Weather Radar For Flood Warning**. BHS Occasional Paper No. 2, pp 56-64.

Hall, A.J. (1981) **Flash Flood Forecasting**. World Meteorological Organisation.

Hamlin, M.J. (1983) **The Significance Of Rainfall In The Study Of Hydrological Processes At Basin Scale**. J. Hydrology, 65, pp73-94.

Han, D. (1991) **Weather Radar Information Processing And Real-Time Flood Forecasting**. PhD Thesis. University of Salford, (Unpublished).

- Harpin, R. (1982) **Real-Time Flood Routing With Particular Emphasis On Linear Methods And Estimation Techniques.** PhD Thesis, University of Birmingham, (Unpublished).
- Harrold, T.W., English, E.J. and Nicholass, C.A. (1974) **The Accuracy Of Radar Derived Rainfall Measurements In Hilly Terrain.** Quart. J. Royal Met. Soc., 100, pp331-350.
- Hart, A. (1986) **Knowledge Acquisition For Expert Systems.** Kogan Page Ltd.
- Hershfield, D.M. (1961) **Estimating the Probable Maximum Precipitation.** Journal of Hydraulics Div., Proc. ASCE 87, pp99-116.
- Hewlett, J.D. (1961) **Watershed Management.** U.S.F.S., Southeast For. Exp. Sta. Rept., pp 61-66.
- Hill, F.F. (1984) **The Development Of Hail Storms Along The South Coast Of England On 5 June 1983.** Meteorol. Mag., 113, pp345-363.
- Hill and Robertson (1987) **The Establishment And Operation Of An Unmanned Weather Radar.** In Weather Radar and Flood Forecasting, ed. V.K. Collinge and C. Kirby, J. Wiley, Chichester.
- Holland, D.J. (1961) **Rain Intensity-Frequency Relations In Britain.** British Rainfall, HMSO, London.
- Hollis, G.E. (1975) **The Effects Of Urbanisation On Floods Of Different Recurrence Intervals.** Water Resources Research, 11, pp 431-435
- Horton, R.E. (1933) **The Role Of Infiltration In The Hydrological Cycle.** Trans. Amer. Geophys. Union, 14, pp 446-460.
- Hosking, J.R.M., Wallis, J.R. and Wood, E.F. (1985) **Estimation Of The GEV Distribution By The Method Of Probability-Weighted Moments.** Journal Hydrological Soc., Vol. 30(1), pp85-109.
- Hosking, J.R.M. (1986) **The Theory Of Probability-Weighted Moments.** IBM Math. Research Report RC12210, Yorktown Heights, New York.

- Hoyt, W. G. & Langbein, W. B. (1955) **Floods**. Princeton University Press.
- Hudleston, F. (1933) **The Cloud Bursts On Stainmore, Westmorland, June 18th, 1930**. British Rainfall, 1930, pp 287-292.
- Hudlow, M.D., Smith, J.A., Walton, M.L. and Shedd, R.C. (1989) **NEXRAD Technical Requirements for Precipitation Estimation and Accompanying Economic Benefits**. Hydro Tech. Note 4. National Weather Service, NOAA. Dec.
- Huff, F.A. & Changnon, S.A. (1986) **Potential Urban Effects On Precipitation In The Winter and Transition Seasons At St Louise, Missouri**. J. Climate Appl. Meteorol. , 25, pp 1887-1907.
- ICE (Institute of Civil Engineers) (1978) **Floods And Reservoir Safety : An Engineering Guide**. Working Party on Floods and Reservoir Safety. London.
- Istok, J.D. & Boersma, L. (1986) **Effect Of Antecedent Rainfall On Runoff During Low-Intensity Rainfall**. J. Hydrol., 88, pp 329-342.
- Jenkins, W.O. and Lowitt, P.W. (1987) **Expert Systems in River Basin Managment**. Civil Engineering Systems, Vol. 4(1), pp31-38.
- Jenkinson, A.F. (1955) **The Frequency Distribution Of The Annual Maximum (or Minimum) Values Of Meteorological Elements**. Quart. J. Royal Met. Soc., vol. 81, pp158-171.
- Jordan, E. (1990) **Information Systems Design**. Prentice-Hall Inc.
- Joss, J.K. and Waldvogel, A. (1989) **Precipitation Measurement And Hydrology - A Review**. Battan Memorial and 40th Anniversary Conference on Radar Meteorology. USA.
- Keers, J.F. and Westcott, P. (1977) **A Computer Based Model for Design Rainfall In The U.K.** Met. Office Scientific Paper No. 36.
- Kelway, P.S. (1977) **Rare Or Not So Rare? The Vital Question**. Weather, 32, pp358-363.
- Kidd, C.H.R. and Packman, J.C. (1980) **Selection Of Design Storm And Antecedent Condition For Urban Drainage Design**. Inst. of Hydrology, Rep. N. 61 Wallingford.

Kite, G.W. (1977) (Second Edition 1987) **Frequency And Risk Analysis In Hydrology**. Water Resources Publications : Fort Collins; Colo.

Kottegoda, N.T. (1980) **Statistical Water Resources Technology**. Macmillan, London.

Langdon, J. (1984) **An Investigation Of Percentage Runoff-Antecedent Baseflow Relationship For Catchments In The North West UK**. Msc. Thesis, University of Birmingham. (Unpublished)

Larkin, J.H., McDermott, J., Simon, D.P. and Simon, H.A. (1980) **Expert And Novice Performance In Solving Physics Problems**. *Science*, 208, pp1335-1342.

Lawler, K.P. (1989) **Weather Radar System Design**. BHS Occasional Paper No. 2, pp14-23.

Ligda, M.G.H. (1951) **Radar Storm Observations**. *Compendium of Meteorology*. Am. Met. Soc. Boston, pp1265-1282.

Linsey, R.K., Kohler, M.A. and Paulhus, J.H. (1958) **Hydrology For Engineers**. McGraw-Hill, New York.

Linsley, R.K., Kohler, M.A. and Paulhus, J.L.H. (1982) (Third Edition) **Hydrology For Engineers**. McGraw-Hill, New York.

Loague, K.M. and Freeze, R.A. (1985) **A Comparison of Rainfall-Runoff Modelling Techniques on Small Upland Catchments**. *Water Res. Research*, Vol. 21, pp221-248.

Lovejoy, S. and Austin, G.L. (1979) **The Delineation Of Rain Areas From Visible And Infrared Satellite Data**. *Atmosphere and Ocean*. 17. pp77-92

Lyons, W.A. & Henz, J.F. (1978) **CREAS And SWAT: Inovative Uses Of Radar, Spotter Networks And The Media To Nowcast Local Flash Floods**. American Meteorological Society/American Geophysical Union.

Madox *et al.* (1979) **Synoptic And Mesoscale Aspects Of Flash Flood Events**. *Bull AMS*, Vol 60:, No. 2, pp 115-123.

Madox, R. & Campbel, C. (1978) **Meteortological Aspects Of 20 Significant Flash Flood Events**. American Meteorological Society/American Geophysical Union.

- Males, R.M., Coyle, J.A. Grayman, W.M., Clark, R.M., Borchers, H.J. and Hertz, B.G. (1992) **Knowledge Aquisition for an Expert System for Handling Customer Inquiries on Water Quality.**
- Marshall, J.S. (1957) **The Constant-Altitude Presentation Of Radar Weather Patterns.** Proc. Sixth Weather Radar Conference. Am. Met. Soc. Boston, pp321-324.
- Marshall, J.S. and Palmer, W.M. (1948) **The Distribution Of Raindrops With Size.** J. Meteorology (5), pp165-166.
- Martens, L.A. (1968) **Flood Inundation And The Effects Of Urbanisation In Metropolitan Charlotte, North Carolina.** United States Geological Survey Water Supply Paper.
- Matalas, N.C. and Wallis, J.R. (1973) **Eureka! It Fits A Pearson Type III Distribution.** Water Resources, No. 9, Vol. 2.
- McCullagh and Nelder (1983) **Generalised Linear Models.** Chapman and Hall, London.
- Michalski, R.S. and Chilauski, R.L. (1980) **Knowledge Aquisition By Encoding Expert Rules Versus Computer By Induction from Examples : A Case Study Involving Soybean Pathology.** Int. J. of Man-Machine Studies, 12, pp63-87.
- Michie, D (1980) **Expert Systems.** Computer Journal, 23, pp369-376.
- Mie, G. (1908) **Beitrage Zur Optik Truber Medien, Speziell Kolloidaler Metallosungen (Contribution To The Optics Of Suspended Media, Specifically Colloidal Metal Suspensions).** Ann. Pyhs. (Leipzig), 25, pp377-445.
- Mill (1908), in Bilham (1935) **Classification Of Heavy Falls Of Rain in Short Periods.** British Rainfall, HMSO, London.
- Mogil *et al.* (1978). **NWS's Flash Flood Warning And Preparedness Programs.** Bull. AMS. Vol. 79, No.6, pp 690-699.
- Montgomery, D.C. (1984) **Design And Analysis Of Experiments.** J. Wiley and Sons, Chichester.

Moore, R.J. and O'Connell, P.E. (1978) **Real-Time Forecasting Of Flood Events Using Transfer Function Noise Models.** Report on work for the Water Research Centre at the Institute of Hydrology, Wllingford.

Moore, R.J. (1980) **Transfer Functions, Noise Predictors And The Forecasting Of Flood Events In Real-Time.** In Statistical Analysis of Rainfall and Runoff by V.P. Singh, Water Resources Pub., Colorado, pp229-250.

Moriyama, T. and Hirano, M. (1991) **Short-Term Forecasting For Water Level Of A Flash Flood By Radar Hyetometer.** 1st Symp. on Hydrological Applications of Weather Radar. In Hydrological Application of Weather Radar, ed. I.D. Cluckie and C.G. Collier, Ellis Horwood, London.

Muller, B.M. & Madox, R.A. (1979) **A Climatological Comparison Of Heavy Precipitaion And Flash Flooding.** Preprints, 11th Conf. on Severe Local Storms, (Kansas City), AMS, Boston.

Nash, J.E. (1957) **The Form Of The Instantaneous Unit Hydrograph.** Int. Assoc. of Scientific Hydrologists, General Assembly, Toronto, Vol. III, pp114-121.

Naylor, C. (1985) **Build Your Own Expert System.** Sigma Technical, Wilmslow.

Neff, E.L. (1977) **How Much Rain Does A Raingage Gauge?** Journal of Hydrology, 35, pp 213.

NERC (National Environment Research Council) (1975) **Flood Studies Report.** Five Volumes, London.

Newell, A. and Simon, H.A. (1972) **Computer Science As Empirical Enquiry: Symbols And Search.** Communications of the ACM, 19 (3), pp113-126.

Newsome, D.H. (1987) **COST-72 And Weather Radar In Western Europe.** In Weather Radar and Flood Forecasting ed. V.K. Collinge and C. Kirby. J Wiley, Chichester.

NOAA (1972) Final report of the disaster survey team on the events of Agnes. Natural Disaster Survey Rept. 73-1, NOAA, Rockville, Md.

- NOAA (1976) **Big Thompson Canyon Flash Flood Of July 31 - August 1, 1976.** Natural Disaster Survey Rept. 76-1, NOAA, Rockville, Md.
- Noonan, G.A. (1987) **An Operational Flood Warning System.** In *Weather Radar and Flood Forecasting*, ed. V.K. Collinge and C. Kirby, J. Wiley, Chichester.
- North West Radar Project (1977) **Report of the Steering Group**, North West Water Authority, Warrington.
- NWC (1983) **Report to the Working Group on National Weather Radar Coverage**, National Water Council/Meteorological Office.
- NWS Office of Hydrology, The radar Group (1984) **Proposal To Develop And Validate "A Flash Flood Potential Algorithm" For The Next Generation Weather Radar (NEXRAD).** The radar Group, NWS Office of Hydrology.
- O'Connell, P.E. and Clark, R.T. (1986) **Adaptive Hydrological Forecasting - A Review.** Hyd. Sci. Bulletin, 26(2) pp179-205.
- Oke, T.R. (1982) **The Energetic Basis Of The Urban Heat Island.** Quart J. Royal Met. Soc., 108, pp 1-24.
- Overton, D.E. and Meadows, M.E. (1976) **Stormwater Modelling.** Academic Press, New York.
- Owens, M.D. (1986) **Real-Time Flood Forecasting Using Radar Data.** PhD Thesis, University of Birmingham, (Unpublished).
- Oya, M. and Hamyama, S. (1987) **Flooding And Urbanisation In The Lowlands Of Tokyo And Vicinity.** Natural Disaster Sci., Vol. 9, No.2, pp1-21.
- Palmer, J. (1992) **Personal Communication.** Head of British Soil Survey, York.
- Pearse, I.H. (1992) **Personal Communication.** Flood Warning Manager, NRA North-West Region.
- Potyondy, J.P. (1987) **Some Techniques For Using Frequency Analysis And Real-Time Data To Interpret Flood Potential Data.** Water Res. Bull., Vol. 23, No.1, pp139-145.

Probert-Jones, J.R. (1962) **The Radar Equation In Meteorology.** Quart. J. Royal Met. Soc. (88), pp485-495.

Reed, D.W. (1984) **A Review of British Flood Forecasting in Practice.** Institute of Hydrology Technical Report, 90.

Reed, D.W. and Dales, M.Y. (1988) **Regional Rainfall Risk, A Study of Dependence.** IAHR Symp. of Stochastic Hydraulics, Paper B2, University of Birmingham, (Unpublished).

Reed, D.W. and Stewart, E.S. (1989) **Focus On Rainfall Growth Estimation.** Proc. of 2nd National Hydrology Symp., Sheffield.

Rehak, D.R. (1983) **Expert Systems In Water Resources. Emerging Techniques In Stormwater and Flood Management.** American Society of Civil Engineers.

Rushton, R. (1990) Personal Communication. Senior Hydrometric Officer, NRA North-West Region.

Sargent, G.P. (1984) **Haddington Flood Warning Scheme.** Jour. of Inst. of Water Eng. and Sci., Vol. 38, pp 108-118.

Sargent, G.P. (1987) **The FRONTIERS Project.** Weather Radar and Flood Forecasting, Ed. Collinge & Kirby.

Schnick, A.P. (1970) **Desert Floods.** Symposium on the results of research on representative and experimental basins, IASH/UNESCO, pp 479-493.

Shanholtz, V.O., Ross, B.B. and Carr, J.C. (1981) **Effect Of Spatioal Variability On The Simulation Of Overland And Channel Flows.** Trans. of ASAE, pp124-133.

Shaw, E.M. (1983) **Hydrology In Practice.** Van Nostrand Reinhold, Wokingham.

Shedd, R.C., Smith, J.A. and Walton, M.L. (1989) **Sectorised Hybrid Scan Strategy Of The NEXRAD Precipitation Processing System.** Proc. Int. Symp. on Hydrological Applications of Weather Radar, Salford. (In Hydrological Applications of Weather Radar, ed. I.D. Cluckie and C.G. Collier. Ellis Horwood).

Shepherd, G.W. (1987) **On The Utilisation Of Weather Radar In The Simulation Of Urban Drainage Networks.** PhD Thesis, University of Birmingham, (Unpublished).

Sherman, L.K. (1932), **Streamflow From Rainfall By Unit-Graph Method.** Engineering News Record, Vol. 108, pp501-505.

Shortliffe, E.H. (1976) **Computer Based Medical Consultations: MYCIN.** New York: American Elsevier

Simonovic, S.P. (1991) **Knowledge-Based Systems and Operational Hydrology.** Canadian Journal of Civil Engineering, Vol. 18, pp1-11.

Simonovic, S.P. and Savic, D.A. (1989) **Intelligent Decision Support and Reservoir Management and Operations.** ASCE Journal of Computing in Civil Engineering, Vol. 3(4), pp367-385.

Simons, G.L. (1983) **Towards Fifth-Generation Computers.** NCC Pub., Manchester.

Slatter, P.E. (1987) **Building Expert Systems : Cognitive Emulation.** Ellis Horwood Ltd., Chichester.

Smith, C.J. (1986) **The Reduction Of Errors Caused By Bright-Bands In Quantitative Rainfall Measurements Made Using Radar.** J. of Atmospheric and Oceanic Tech., Vol. 3, pp129-131.

Stephenson, D. and Meadows, M.E. (1986) **Kinematic Hydrology And Modelling.** Developments in Water Science Pub., Elsevier, Amsterdam.

Strzepek, K.M., Berkowitz, L. and Eaton, L. (1988) **Expert Systems Water Management : A Demonstration.** In Planning Now for Irrigation and Drainage in the 21st Century, ASCE, New York, pp544-552.

Symons (1888) in Bilham (1935) **Classification Of Heavy Falls Of Rain in Short Periods.** British Rainfall, HMSO, London.

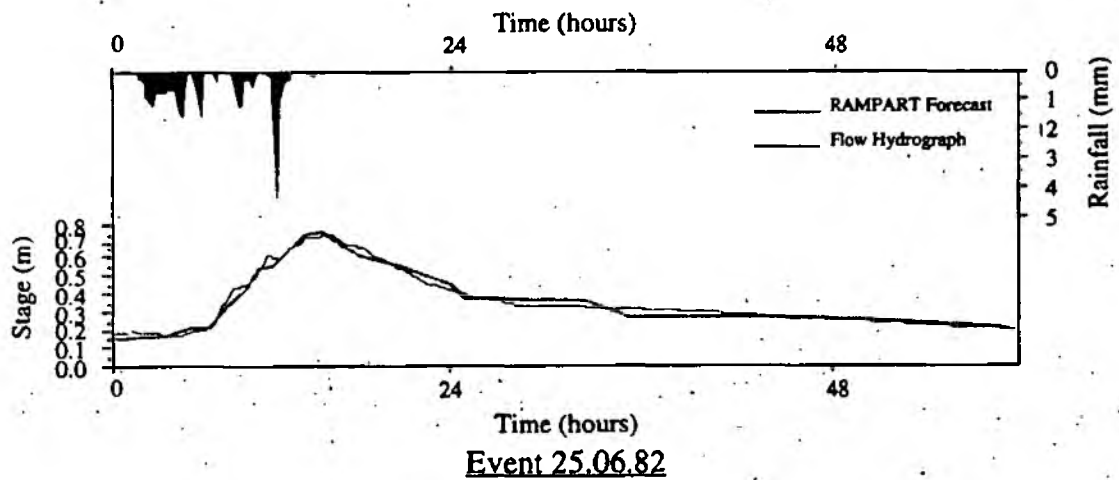
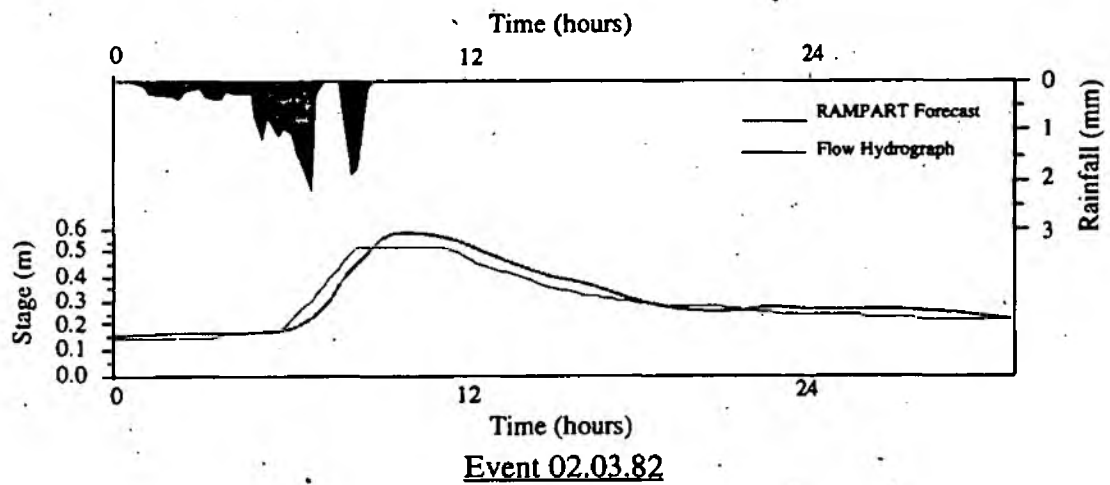
Taylor B.C. and Browning K.A. (1974) **Towards An Automated Radar Weather Network.** Weather 29. pp202-216

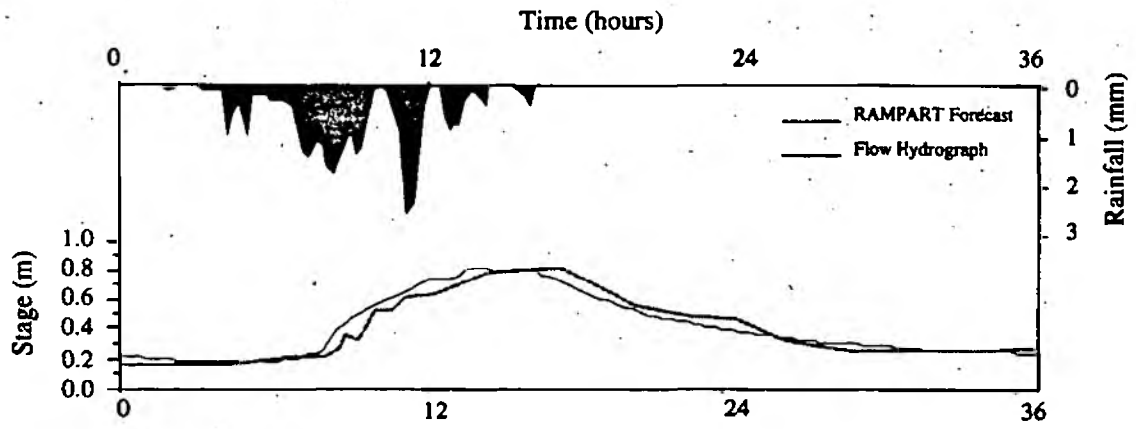
- Taylor B.C. (1975) **A Mini Network Of Weather Radars**. Preprints, 16th Conf. On Radar Meteorology, Houston, Texas. American Met. Soc. Boston, Mass. pp361-363
- Tilford, K.A. (1990) **TFCal User Manual**. Water Resources Research Group, Internal Technical Report, University of Salford, (Unpublished).
- Tilford, K.A. (1992) **Weather Radar Data For Operational Hydrology**. PhD Thesis, University of Salford, (Unpublished).
- Trovati, L.R. and Mattos, A. (1990) **A Radar Reflectivity-Runoff Model For Use In Flood Warning**. In Weather Radar Networking Seminar on COST Project 73, Brussels, Kluwer Publ.
- US Army Corps of Engineers (1975) **Lincoln, Nebraska Flood Study**. Report Prepared For Federal Insurance Administration By Corps Of Engineers, Omaha.
- van Gorp, J.J. (1989) **Ground Clutter Reduction During Rain Measurement By A Non-Coherent Radar System**. Proc. COST-73 Seminar on Weather Radar Networking in Weather Radar Networking ed C.G. Collier et al. Kluwer Academic Pub.
- Viner, D. (1992) **The Hydrological Utilisation Of The FRONTIERS System**. PhD Thesis, University of Salford, (Unpublished).
- Viner, D. and Cluckie, I.D. (1990) **Hydrological Utilisation Of FRONTIERS Data**. Presented at Remote Sensing of Precipitation with Hydrological Applications, Sao Paulo, Brazil.
- Viner, D., Cluckie, I.D., Collier, C.G. (1991) **A Preliminary Analysis Of The Hydrological Utilisation of FRONTIERS System**. COST-73 Seminar, Yugoslavia.
- Walker, S. and Bunch, A.H. (1991) **Development of a Decision Support System for Drought Management Within North West Water**. IWEM North Western and North Wales Branch, Internal Report.
- Ward, R. (1978) **Floods. A Geographical Perspective**. Macmillan Press Ltd.
- Weibull, W. (1939) **A Statistical Theory of the Strength of Materials**. Ingeniors Vetenskaps Akademien (The Royal Swedish Institute for Engineering Research), proc. 51, pp5-45.

- Welbank, M. (1983) **A Review Of Knowledge Aquisition Techniques For Expert Systems.** Martlesham Consultancy Services, British Telecom Research Labs, Martlesham Heath, Ipswich.
- Wheater, H.S., Shaw, T.L. & Rutherford, J.C. (1982). **Storm Runoff From Small Lowland Catchments in South West England.** *J. Hydrol.*, 55, pp 321-337.
- White, E.L. and Reich, B.M. (1970). **Behaviour Of Annual Floods In Limestone Basins In Pennsylvania** *J. Hydrology*, Vol. 10, pp193-198.
- Willeke, G.E. (1979) **Foreward to the Second Conferance on Flash Floods.** Preprints, Second Conference on Flash Floods, AMS, Boston.
- Wilson C.B., Valdes J.B., Rodriguez-Iturbe I. (1979) **On The Inffence Of The Distribution Of Rainfall On Storm Runoff.** *Water Resour. Res.*, 15, No. 2, pp 321-328.
- Wolf, P.O. (1952) **Forecasts And Records Of Floods In Glen Cannich In 1947.** *Journal Inst. Wat. Engrs.*, 6, pp 298-324.
- Wood, E.F., Sivapalan, M., Beven, K. and Band, L. (1988) **Effects of Spatial Variability and Scale with Implications to Hydrological Modelling.** *Journal of Hydrology*, Vol. 102, pp29-47.
- Woodley, W.L. et al. (1978) **Satellite Rain Estimation In The Big Thompson And Johnson Flash Floods.** American Meteorological Society/American Geophysical Union.
- WRIP (**Weather Radar Information Processor**) (1992) Water Resources Research Group, Internal Technical Report, University of Salford.
- WRRG 23 (Water Resources Research Group) (1992) **MATH : Model Analytical Tool for Hydrology.** Internal Technical Report, University of Salford.
- Yarnell, D.L. (1935) **Rainfall Intensity-Frequency Data.** U.S. Dept. of Agriculture, Mis. Pub. 204.
- Yu, P.S. (1989) **Real-Time Grid Based Distributed Rainfall Runoff Model for Flood Forecasting With Weather Radar.** PhD Thesis. University of Birmingham, (Unpublished).
- Zevin, S.F. (1986) **A Probabalistic Approach To Flash Flood Forecasting.** Phd, University of Arizona, (Unpublished).

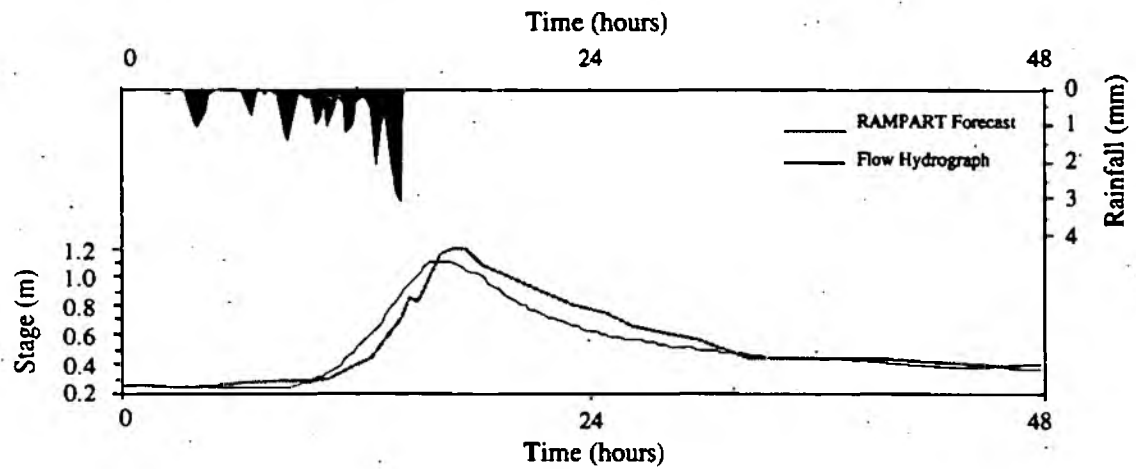
APPENDIX A

Rainfall Hyetographs And Runoff Hydrographs Used In The Catchment Rainfall - Flow Analysis (Chapter 5) And KBS Testing (Chapter 8)

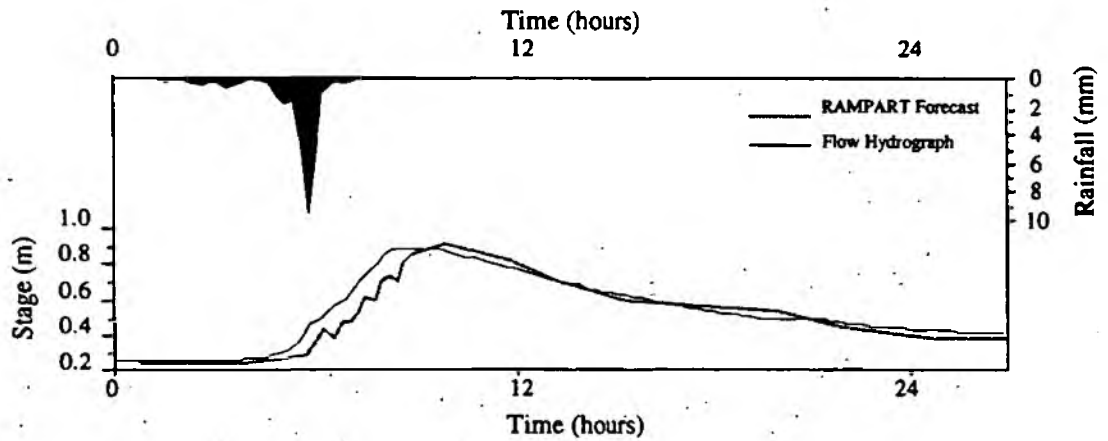




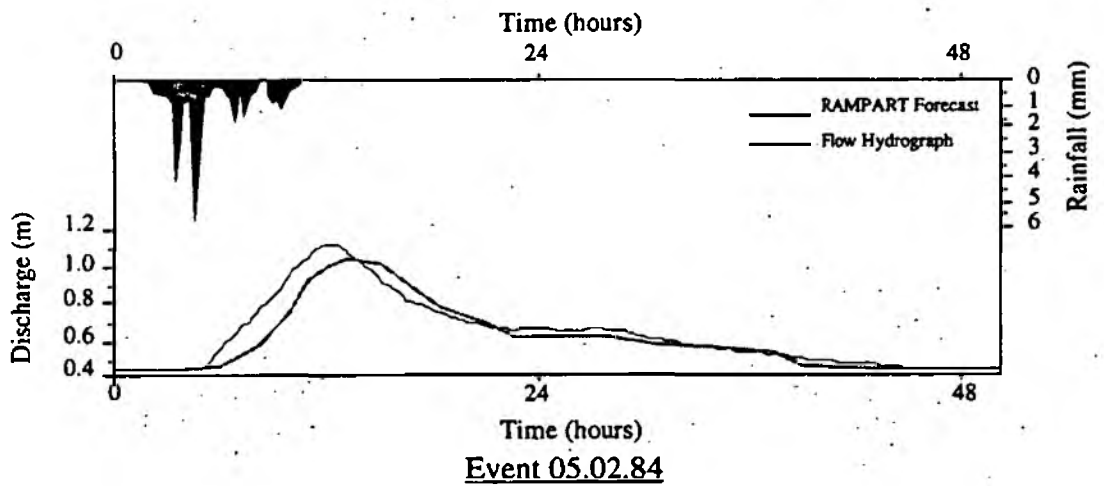
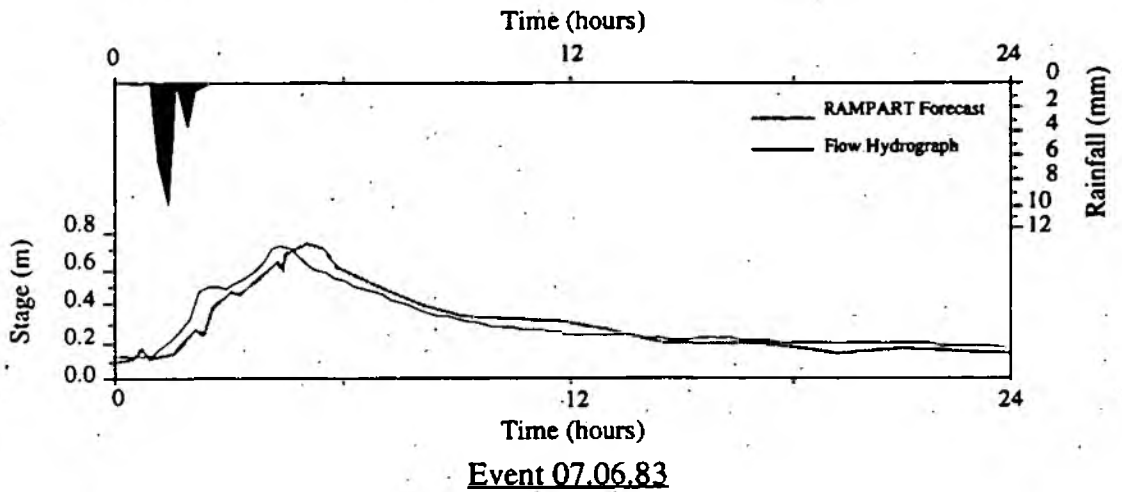
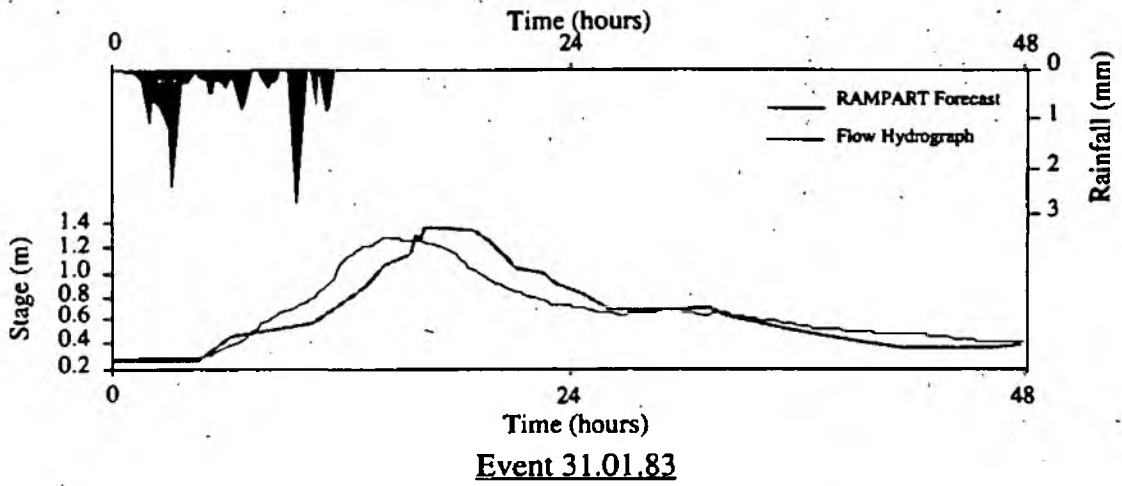
Event 17.08.82

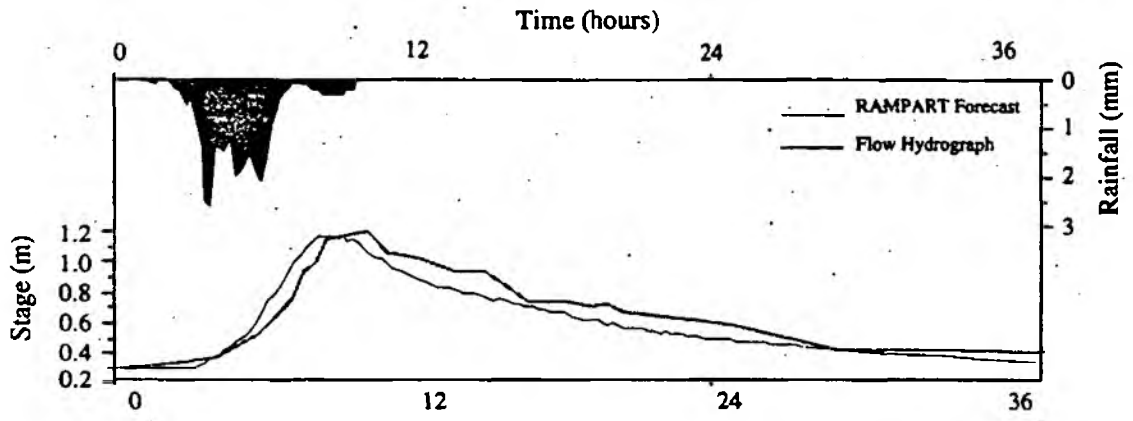


Event 18.12.82

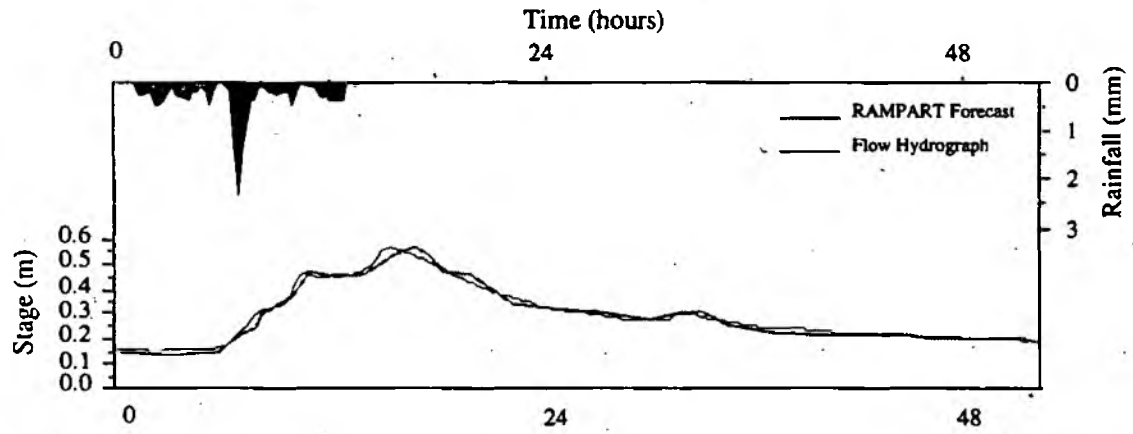


Event 14.01.83

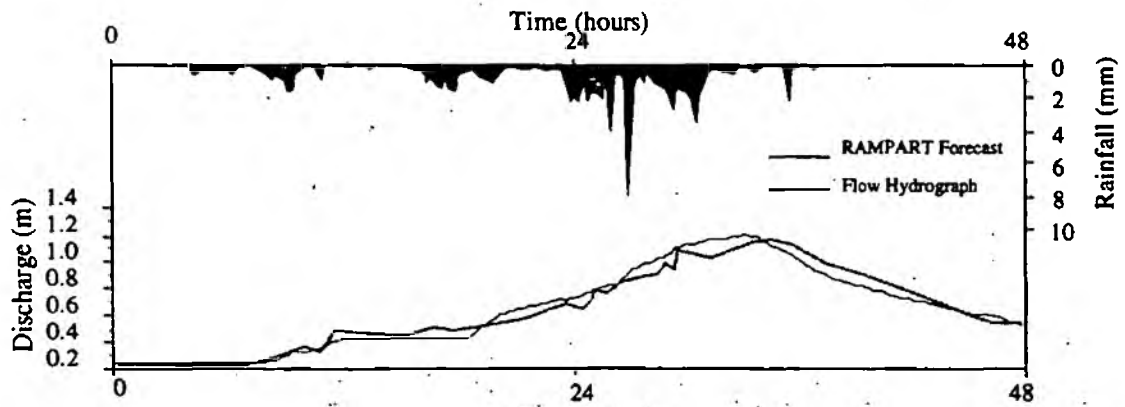




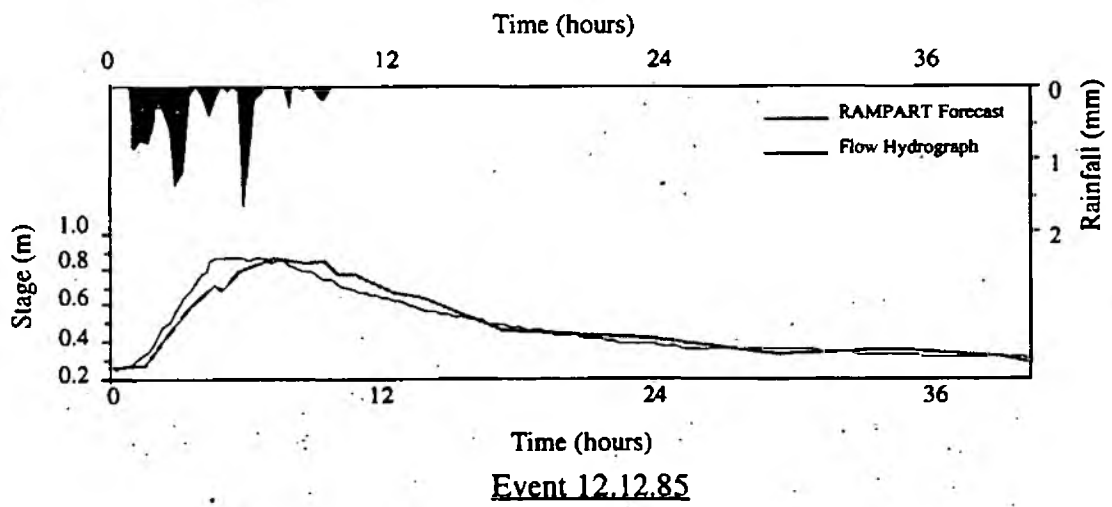
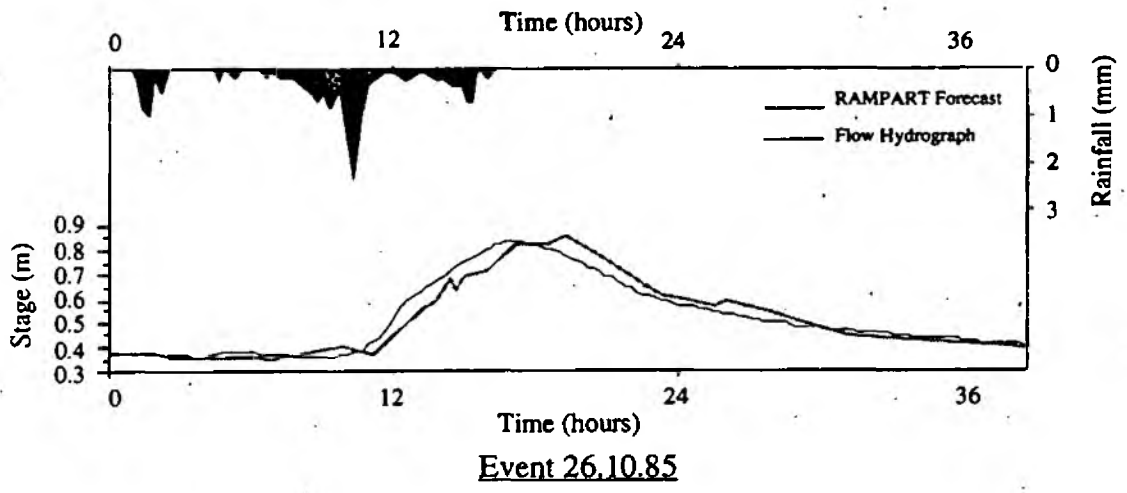
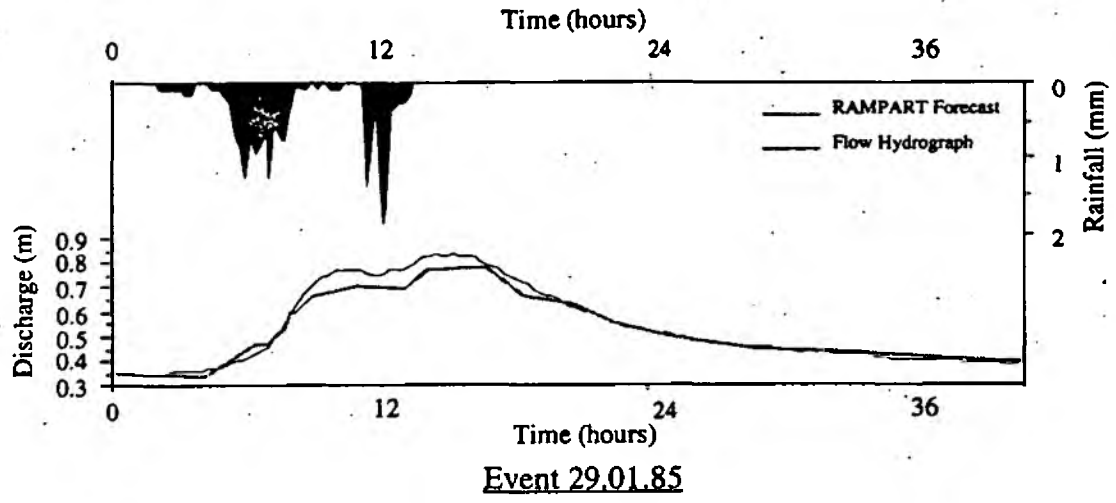
Event 16.03.84

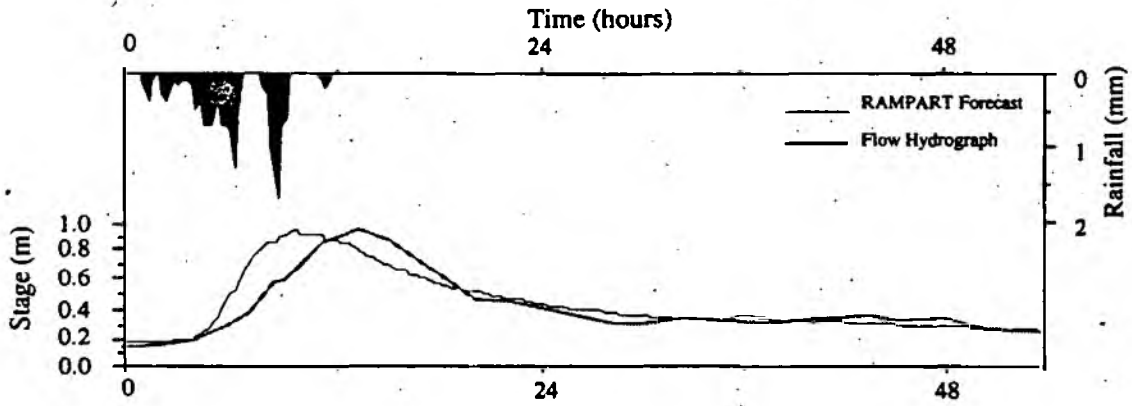


Event 17.10.84

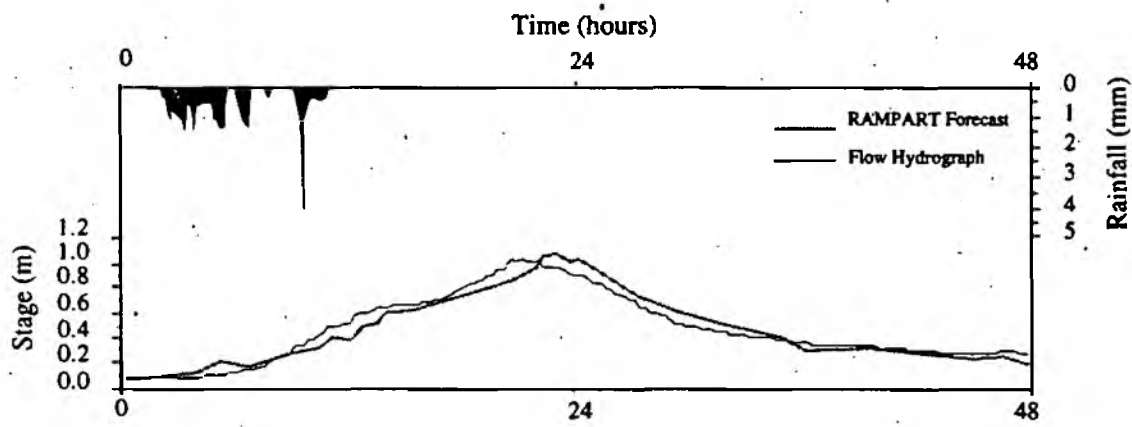


Event 02.11.84

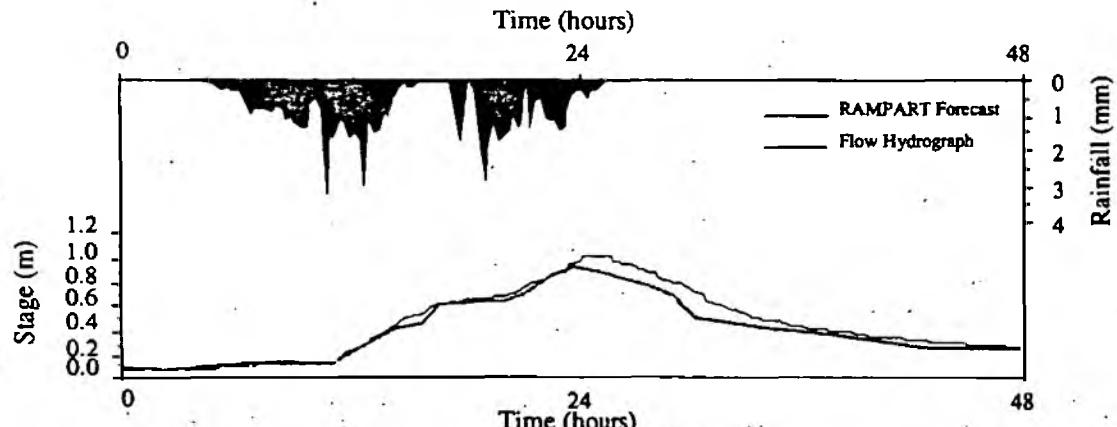




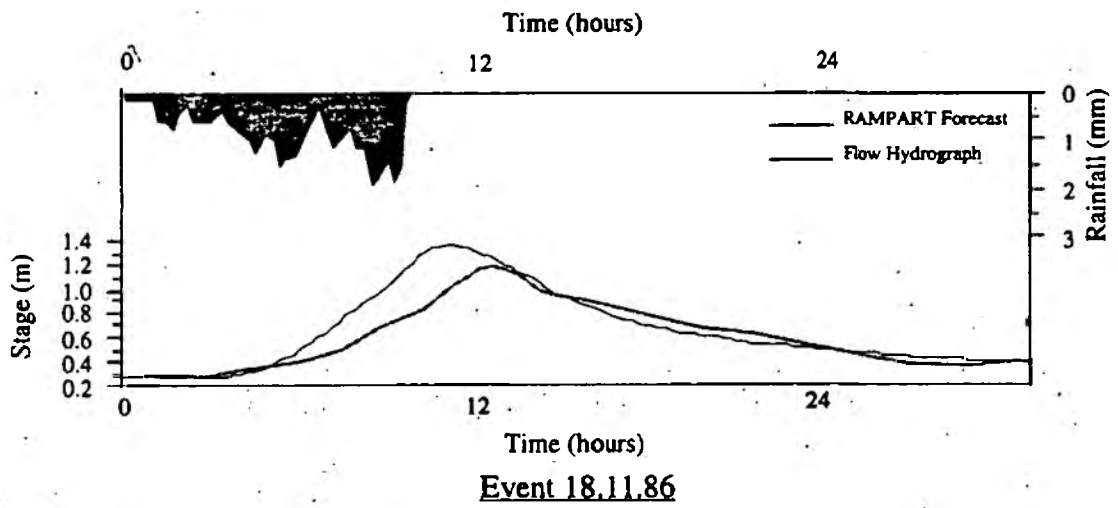
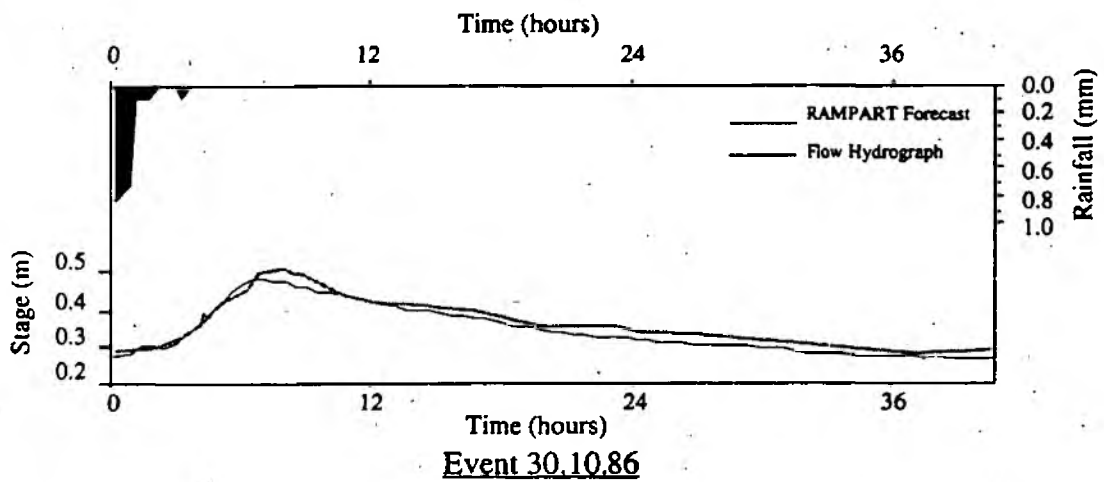
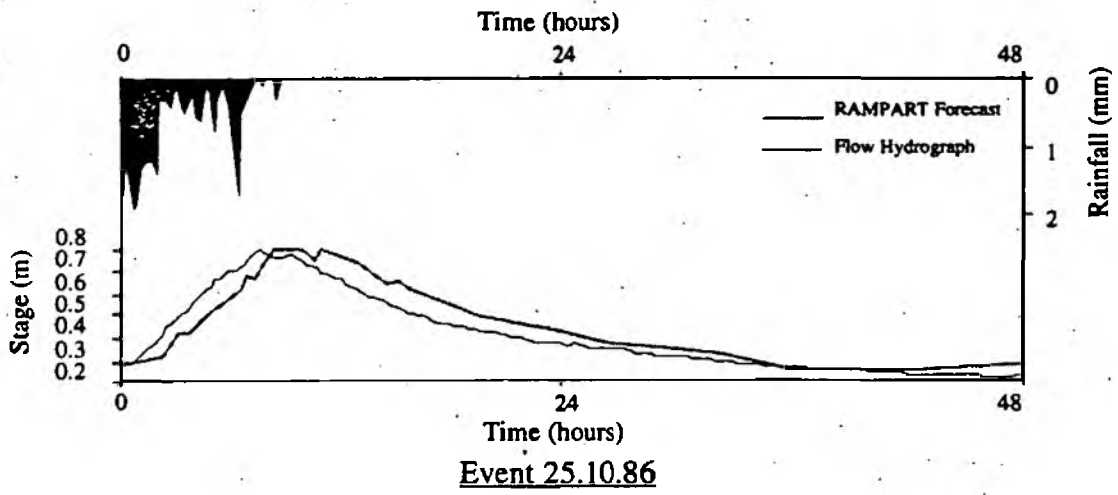
Event 09.01.86

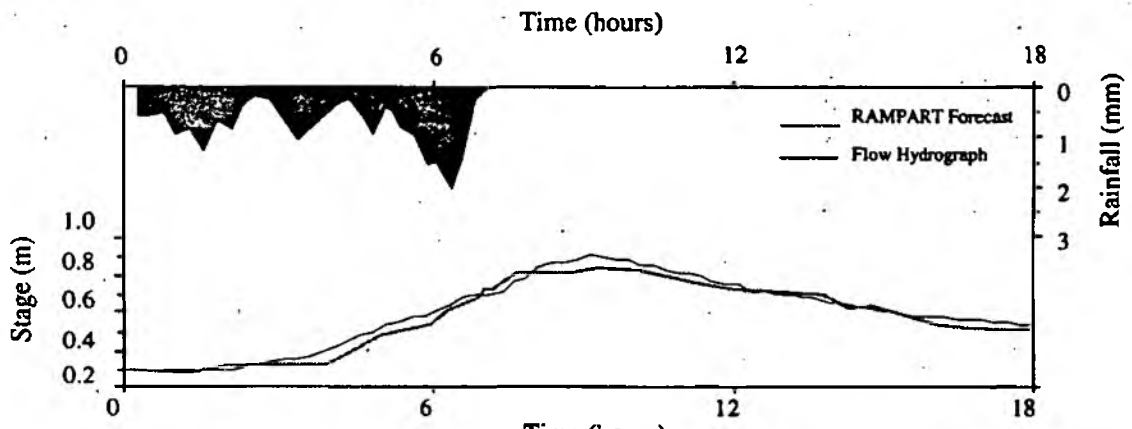


Event 25.08.86

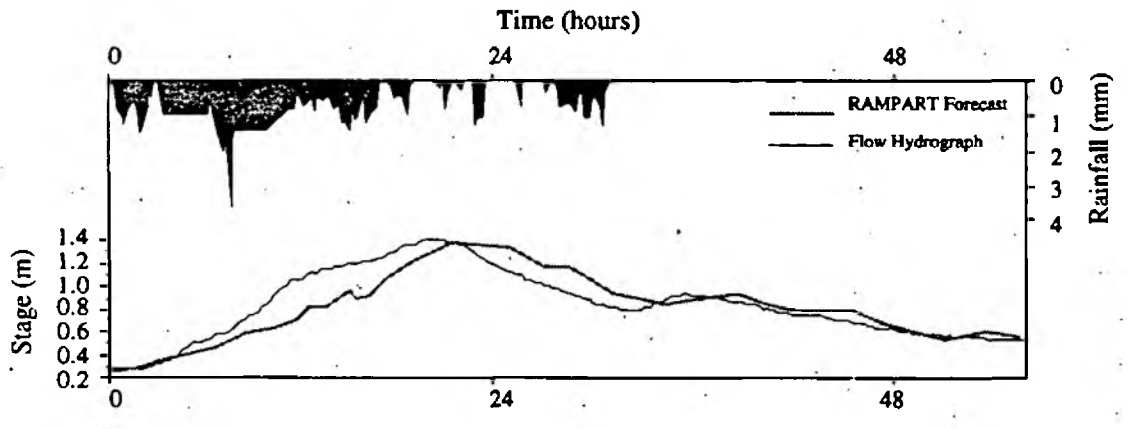


Event 26.08.86

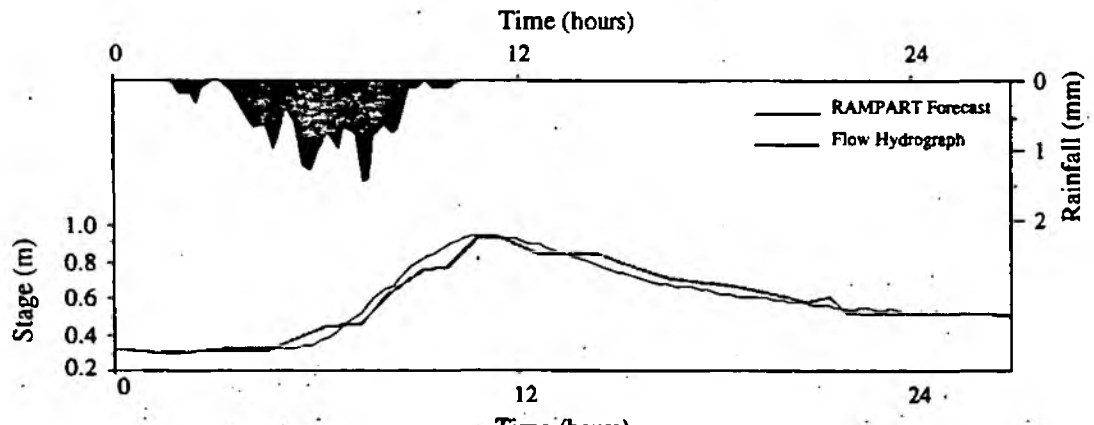




Event 14.12.86



Event 29.12.86



Event 03.01.87

APPENDIX B

**Values And Errors From The Synthetic Catchment
Kinematic Wave Model Investigation
(Chapter 7).**

**Physically Realisable Transfer Function (PRTF) Model Parameter
Dynamics In Relation To Rainfall Direction, Position,
Coverage And Intensity.**

Results Of Rainfall Moving Down The Catchment

Average Rain Intensity (mm/hr)	Optimum Gamma Value	Optimum Tao Value	PRTF RMS Error	Static TF RMS Error
2	100	10	0.35	8.64
4	100	10	0.31	8.97
8	100	10	0.42	9.32
12	94	10	0.41	13.93
16	82	10	0.37	18.46
20	73	10	0.33	22.83
24	43	10	0.37	27.19
28	29	9	0.72	31.26
32	20	9	0.85	35.43
36	15	8	1.06	39.48
40	18	7	1.35	43.42
44	10	7	1.63	47.32
48	18	6	1.74	50.10
52	10	6	2.12	54.92
56	2	6	2.36	58.74
60	7	5	2.97	62.56
64	3	5	3.19	66.15
68	-2	5	3.72	69.84
72	-3	5	3.81	73.52
76	-6	5	4.65	77.00
80	-8	5	4.24	80.74
84	-10	5	4.33	84.20
88	-12	5	4.52	87.23
92	-16	5	5.31	91.73
96	-19	5	5.45	94.72
100	-22	5	6.13	98.24
104	-23	5	6.26	101.75
108	-25	5	6.72	105.62
112	-27	5	7.33	108.46
116	-28	5	7.51	112.31
120	-30	5	8.22	115.46
124	-30	5	8.13	118.23
128	-31	5	8.42	122.63
132	-32	5	8.76	125.92
136	-33	5	9.14	129.67
140	-33	5	8.92	132.43
144	-34	5	9.37	135.54
148	-35	5	9.75	139.72
152	-23	4	9.83	142.14
156	-26	4	11.21	146.28
160	-28	4	11.06	149.92
164	-30	4	11.74	152.01
168	-31	4	12.23	156.50
172	-31	4	12.17	159.78
176	-32	4	12.63	163.22
180	-33	4	13.32	166.64
184	-34	4	13.97	169.16
188	-34	4	13.81	173.70
192	-35	4	14.52	176.44
196	-35	4	14.46	179.29
200	-35	4	15.23	183.81

Results Of Rainfall Moving Up The Catchment

Average Rain Intensity (mm/hr)	Optimum Gamma Value	Optimum Tao Value	PRTF RMS Error	Static TF RMS Error
2	100	10	0.12	7.44
4	100	10	0.14	8.96
8	100	10	0.16	9.19
12	100	4	0.19	13.41
16	71	4	0.26	17.58
20	56	3	0.31	21.44
24	52	2	0.35	25.33
28	53	2	0.51	29.27
32	46	1	0.56	32.82
36	39	1	0.65	36.66
40	44	0	1.37	40.31
44	28	1	1.48	43.99
48	33	1	1.41	47.61
52	29	1	1.55	51.37
56	28	0	1.55	54.96
60	25	0	1.67	58.52
64	24	0	1.72	62.16
68	20	0	1.91	65.72
72	18	0	2.03	69.38
76	16	0	2.12	72.95
80	17	0	2.14	76.53
84	15	0	2.25	80.24
88	14	0	2.36	83.66
92	12	0	2.46	87.29
96	11	0	2.57	90.02
100	-1	1	2.35	94.19
104	-2	1	2.47	97.94
108	-3	1	2.62	101.27
112	-4	1	2.74	105.34
116	-5	1	2.84	108.45
120	-6	1	2.96	112.25
124	-7	1	3.19	115.89
128	-8	1	3.21	119.34
132	-8	1	3.37	122.45
136	-10	1	3.47	126.13
140	-11	1	3.63	129.26
144	-11	1	3.73	133.37
148	-11	1	3.85	137.61
152	-13	1	3.99	140.49
156	-13	1	4.12	144.24
160	-14	1	4.25	147.66
164	-14	1	4.39	151.23
168	-15	1	4.52	154.81
172	-15	1	4.67	158.34
176	-16	1	4.79	162.24
180	-17	1	4.95	165.47
184	-17	1	5.14	169.18
188	-17	1	5.22	172.33
192	-18	1	5.35	176.52
196	-18	1	5.52	179.97
200	-19	1	5.64	183.02

Results Of Rainfall On The Lower Catchment Area

Average Rain Intensity (mm/hr)	Optimum Gamma Value	Optimum Tao Value	PRTF RMS Error	Static TF RMS Error
2	18	0	0.27	3.18
4	14	0	0.32	3.54
8	-2	0	0.65	6.21
12	-10	0	0.98	8.63
16	-13	0	1.22	11.07
20	-18	0	1.73	13.55
24	-19	0	1.92	16.03
28	-22	0	2.38	18.61
32	-25	0	2.96	21.26
36	-25	0	3.14	23.87
40	-26	0	3.62	26.53
44	-27	0	3.90	29.37
48	-27	0	4.61	32.15
52	-28	0	5.03	34.82
56	-30	0	5.82	37.73
60	-30	0	5.94	40.61
64	-31	0	6.41	43.57
68	-32	0	7.18	46.44
72	-32	0	7.13	49.42
76	-33	0	7.72	52.38
80	-33	0	7.85	55.31
84	-33	0	7.93	58.39
88	-34	0	8.67	61.37
92	-35	0	9.55	64.45
96	-35	0	9.63	67.53
100	-36	0	10.78	70.55
104	-37	0	11.96	73.60
108	-36	0	11.94	76.64
112	-36	0	10.90	79.81
116	-38	0	12.77	83.07
120	-38	0	13.53	86.10
124	-35	0	12.42	89.35
128	-35	0	12.63	92.52
132	-35	0	12.82	95.26
136	-36	0	13.75	98.83
140	-35	0	13.43	102.02
144	-37	0	15.22	105.31
148	-37	0	15.27	108.53
152	-38	0	14.27	111.75
156	-37	0	15.59	114.96
160	-39	0	15.83	118.28
164	-39	0	15.91	121.49
168	-39	0	16.02	124.74
172	-39	0	16.13	127.93
176	-39	0	16.28	131.39
180	-39	0	19.23	134.55
184	-39	0	19.35	137.82
188	-40	0	19.52	141.19
192	-41	0	19.67	144.44
196	-41	0	19.72	147.72
200	-41	0	19.79	151.11

Results Of Rainfall On The Middle Catchment Area

Average Rain Intensity (mm/hr)	Optimum Gamma Value *	Optimum Tao Value	PRTF RMS Error	Static TF RMS Error
2	84	10	0.17	7.42
4	79	10	0.20	8.72
8	79	10	0.23	9.14
12	44	9	0.28	13.30
16	24	8	0.58	17.11
20	12	7	0.99	20.75
24	3	7	1.18	24.32
28	2	6	1.42	27.50
32	-5	6	1.81	30.76
36	-8	6	2.40	33.84
40	-2	5	1.93	36.81
44	0	4	2.36	39.86
48	-2	4	2.54	42.72
52	-7	4	2.92	45.62
56	-14	4	3.68	48.41
60	-18	4	4.29	51.25
64	-21	4	4.85	54.16
68	-24	4	5.86	56.48
72	-12	3	5.44	59.45
76	-17	3	5.65	62.24
80	-19	3	6.15	65.25
84	-20	3	5.94	67.94
88	-21	3	6.58	70.67
92	-22	3	6.72	73.82
96	-23	3	6.94	76.31
100	-24	3	7.28	78.27
104	-28	3	8.82	81.43
108	-30	3	9.61	84.24
112	-19	2	9.94	87.15
116	-19	2	9.76	89.27
120	-21	2	10.81	92.34
124	-21	2	10.63	95.26
128	-22	2	11.13	98.12
132	-23	2	10.97	100.51
136	-24	2	12.26	103.44
140	-25	2	12.50	106.80
144	-25	2	12.76	109.31
148	-25	2	12.67	111.96
152	-26	2	13.36	114.23
156	-26	2	13.21	117.22
160	-27	2	13.92	120.74
164	-27	2	13.86	123.22
168	-27	2	13.79	125.56
172	-28	2	14.59	128.29
176	-28	2	14.44	131.61
180	-30	2	16.43	134.13
184	-31	2	17.51	137.55
188	-31	2	17.45	140.08
192	-32	2	16.66	142.34
196	-32	2	16.81	145.63
200	-33	2	17.67	148.65

Results Of Rainfall On The Upper Catchment Area

Average Rain Intensity (mm/hr)	Optimum Gamma Value	Optimum Tao Value	PRTF RMS Error	Static TF RMS Error
2	100	10	0.31	2.32
4	100	10	0.53	9.3
8	93	10	0.85	11.64
12	84	10	1.24	13.97
16	70	10	1.45	18.5
20	56	10	1.63	20.8
24	39	10	1.72	25.19
28	33	10	1.68	29.4
32	22	10	1.47	33.5
36	24	9	1.37	35.5
40	16	9	1.56	39.5
44	14	8	1.92	43.83
48	12	8	2.02	47.15
52	12	7	2.61	48.97
56	11	7	2.62	50.81
60	7	7	2.63	52.6
64	6	7	3.09	57.8
68	4	6	2.96	63.02
72	3	6	3.44	68.04
76	2	6	4.32	72.9
80	1	6	4.53	77.73
84	1	6	4.56	82.47
88	0	6	4.64	87.04
92	-2	5	6.62	89.42
96	-1	5	5.95	91.65
100	-3	5	7.52	95.30
104	-7	5	7.87	96.04
108	-3	5	7.89	100.52
112	-4	5	9.85	104.91
116	-6	5	9.66	109.27
120	-8	5	10.98	111.05
124	-9	4	11.56	113.14
128	-10	4	11.68	113.69
132	-10	4	11.22	117.84
136	-11	4	11.46	120.31
140	-12	4	12.13	122.12
144	-14	4	13.24	126.23
148	-14	4	12.94	127.02
152	-15	4	13.02	130.43
156	-16	4	13.46	134.60
160	-16	4	13.66	138.76
164	-16	4	13.72	139.94
168	-17	4	14.45	142.97
172	-18	4	14.35	145.90
176	-19	4	15.26	147.61
180	-19	4	15.22	151.24
184	-20	4	15.85	154.01
188	-22	4	16.20	155.33
192	-22	4	16.11	159.45
196	-23	4	16.87	161.29
200	-23	4	17.14	163.52

Results Of Rainfall Covering The Whole Catchment

Average Rain Intensity (mm/hr)	Optimum Gamma Value	Optimum Tao Value	PRTF RMS Error	Static TF RMS Error
2	70	0	0.07	2.59
4	50	0	0.63	6.82
8	26	0	1.31	8.47
12	15	0	2.39	7.79
16	8	0	3.92	5.73
20	0	0	5.32	5.81
24	-2	0	7.54	9.50
28	-4	0	8.17	10.8
32	-5	0	8.76	12.19
36	-6	0	9.29	13.69
40	-9	0	9.84	15.25
44	-10	0	10.38	16.87
48	-12	0	10.93	18.55
52	-13	0	11.51	20.29
56	-13	0	12.05	22.07
60	-14	0	12.61	23.89
64	-14	0	13.22	25.75
68	-15	0	13.75	27.65
72	-15	0	14.92	29.59
76	-15	0	15.58	31.56
80	-15	0	16.06	35.61
84	-16	0	16.62	37.66
88	-17	0	17.86	39.76
92	-17	0	18.42	44.02
96	-18	0	19.01	46.12
100	-18	0	20.19	50.59
104	-18	0	21.42	55.09
108	-19	0	21.97	59.68
112	-19	0	22.6	69.07
116	-20	0	23.78	73.88
120	-20	0	24.99	78.75
124	-21	0	26.26	83.68
128	-21	0	27.39	88.67
132	-22	0	29.79	93.73
136	-23	0	31.04	98.83
140	-22	0	32.21	103.98
144	-23	0	33.44	109.18
148	-24	0	34.64	114.44
152	-24	0	35.91	119.74
156	-24	0	37.04	125.07
160	-25	0	38.25	130.45
164	-25	0	39.44	135.87
168	-25	0	40.67	141.33
172	-26	0	41.89	146.83
176	-26	0	43.04	152.36
180	-26	0	44.32	157.93
184	-26	0	45.42	163.53
188	-27	0	47.86	174.82
192	-27	0	49.03	180.51
196	-27	0	50.14	186.24
200	-27	0	52.59	191.99

APPENDIX C

**Examples Of Decision Making Code From The RAMPART
(Real-Time Automatic Model PARAMeter Tuning)
System (Chapter 8).**

**Program Written In FORTRAN With VAX Extensions
To Run On DEC VMS Machines, Using
Radar Rainfall Inputs.**

Rainfall Direction Assessment :

```

If (DIRN.GE.193.AND.DIRN.LE.253)THEN
  Type*,'Rainfall Movement Is With The Direction Of Flow'
  CALL DOWNCAT (RFINT)
Else If (DIRN.GE.12.AND.DIRN.LE.72)THEN
  Type*,'Rainfall Movement Is Against The Direction Of Flow'
  CALL UPCAT (RFINT)
Else
  CALL ACROSSCAT(PCTCOVA,PCTCOVB,PCTCOVC,RFINT)
End If

```

Rainfall Across The Catchment :

```

SUBROUTINE ACROSSCAT(PCTCOVA,PCTCOVB,PCTCOVC,RFINT)

If (PCTCOVA.GT.65)THEN
  Type*,'The Rainfall Is Concentrated On The Upper Catchment Reach'
  CALL UPPERSECTION (RFINT)
Else If (PCTCOVB.GT.65)THEN
  Type*,'The Rainfall Is Concentrated On The Middle Catchment Reach'
  CALL MIDDLESECTION (RFINT)
Else If (PCTCOVC.GT.65)THEN
  Type*,'The Rainfall Is Concentrated On The Lower Catchment Reach'
  CALL LOWERSECTION (RFINT)
Else
  CALL CATWIDE (RFINT)
End If

Return
End

```

Rainfall Movement With Flow :

```

SUBROUTINE DOWNCAT(RFINT)

Gamma=184.76-99.903*LOG(RFINT)

If (RFINT.LT.24)THEN
  Tau=10.
Else If (RFINT.GE.24.AND.RFINT.LT.36)THEN
  Tau=9
Else If (RFINT.GE.36.AND.RFINT.LT.40)THEN

```

```
Tau=8
Else If (RFINT.GE.40.AND.RFINT.LT.48)THEN
Tau=7
Else If (RFINT.GE.48.AND.RFINT.LT.60)THEN
Tau=6
Else If (RFINT.GE.60.AND.RFINT.LT.152)THEN
Tau=5
Else If (RFINT.GT.152)THEN
Tau=4
End If

Return
End
```

Rainfall Movement Against Flow :

SUBROUTINE UPCAT(RFINT)

```
Gamma=178.97 + -87.373 * LOG(RFINT)
```

```
tau = 0
```

```
Return
End
```

Rainfall-Flow Contribution :

```
If (FAPI.GT.29.79)THEN
Type*,'Catchment Is Wet, Rainfall Contributes To Flow'
IFLAG=1
Else
IFLAG=0
End If
```